TERNARY ION EXCHANGE
IN ZEOLITES

BY

RAVI PARAKRAMA

Kiṃsu uppatataṃ seṭṭhā ?
Vijjā uppatataṃ seṭṭhā.

Which of all things uprising is the best ?
Knowledge, of things uprising is the best.

— Buddha
Saṃyutta Nikāya, Vol.1, p.42

A THESIS SUBMITTED FOR THE DEGREE OF

DOCTOR OF PHILOSOPHY

OF

THE CITY UNIVERSITY
LONDON.

The Department
of
Chemistry.

November 1983.

Kiṃsu uppatataṃ seṭṭhā ?

Vijjā uppatataṃ seṭṭhā.

Which of all things uprising is the best ?

Knowledge, of things uprising is the best.

- The Buddha
  Saṃyutta Nikāya, Vol.I, p.42

I grant powers of discretion to the University Librarian to allow this thesis to be copied in whole or in part without further reference to me. This permission covers only single copies made for study purposes, subject to normal conditions of acknowledgement.

ABSTRACT

This work comprises a study of ternary ion exchange behaviour of zeolite X in exchange systems involving the cations Na^+, K^+ and Li^+ or Ag^+. Also reported are investigations into binary exchange systems involving pairs of the same cations, and methods of preparation of the K-X and Li-X zeolites. Methods of separating the phases after exchange are also discussed, together with the methods of analyses employed.

The ternary equilibria have been treated thermodynamically using a recently developed phenomenological model, and at the same time, the model has been tested for validity and ease of application. In particular, the computer procedures used in the model have been discussed, and their validity established. The work has shown that the inclusion of data from the conjugate binary exchanges increases the validity of the results from the ternary treatment. These binary data have also been treated separately.

Data from appropriate pairs of binary exchange systems have been used to predict standard free energies of conjugate binary systems and also of the corresponding ternary systems by means of the 'triangle rule'. Binary data have also been used to test the applicability to zeolites of the Elprince-Babcock model originally developed for clays.

C O N T E N T S

LIST OF TABLES

- 11 -

LIST OF PRINCIPAL SYMBOLS

A	Ingoing cation (Binary Ion Exchange)
a	Activity
B	Outgoing cation (Binary Ion Exchange)
A,B	Debye-Hückel Constants
a,b	Debye-Hückel Parameters
c	Crystal (zeolite) Phase
e	Charge on One Electron (C)
f	Crystal Phase Activity Coefficient (Binary Ion Exchange)
$\Delta G^\ominus$	Standard Free Energy of Reaction
g^E	Excess Gibbs Free Energy
I	Ionic Strength of Solution ($mol\ dm^{-3}$)
K_a	Thermodynamic Equilibrium Constant
K_c	(Kielland Quotient) Corrected Selectivity Quotient
K_m	Mass Action Quotient
k	Boltzmann Constant (JK^{-1})
m	Solution Concentration ($mol\ dm^{-3}$)
N	Solution Concentration ($g\ equiv.\ dm^{-3}$)
N	Avogadro's Constant (mol^{-1})
n	Number of Moles of any component
n_T	Total Number of Moles
p	Pressure
R	Gas Constant ($8.314\ JK^{-1}\ mol^{-1}$)
r	Ionic Radius
S	Entropy
s	Solution Phase
T	Absolute Temperature (K)
T_N	Total Solution Concentration ($g\ equiv.dm^{-3}$)

v	Vapour Phase
V	Volume
z	Valence of Ion
α, α'	Separation factor
Γ	Ratio of Solution Phase Activity Coefficients raised to the respective powers
γ	Solution Phase Activity Coefficient
$\gamma_{\pm}$	Mean Molal Stoichiometric Activity Coefficient
Δ	Crystal Phase Water Activity Term
ε	Permittivity of Medium ($CV^{-1} m^{-1}$)
Λ	Elprince-Babcock Interaction Energy Terms
λ	Characteristic Constants of Single Electrolytes
μ	Chemical Potential
ν	Molar Volume
ν_w	Water Content of One "Exchange Equivalent" of Zeolite
Φ	Ratio of Crystal Phase Activity Coefficients raised to the respective powers
ϕ	Crystal Phase Activity Coefficient (Ternary Ion Exchange)

- 13 -

CHAPTER ONE INTRODUCTION

1.1. GENERAL INTRODUCTION

Sodium tri polyphosphate (STP) and before that sodium
di polyphosphate (SDP) have been used in detergent formu-
lations throughout the world for over 45 years. STP fulfils
a dual function in the washing process (i) by contributing to
the washing efficiency of the detergent and (ii) by protecting
the textiles and the washing machine against damage caused by
the deposition of insoluble salts arising from calcium and
magnesium ions which are initially present in the wash water.
Phosphates are toxicologically harmless and do not interfere
either in the preparation of drinking water or in waste-water
purification processes. Phosphates are, however, ecologically
harmful by promoting the growth of algae in stagnant or slow-
flowing waters. This over-fertilisation of water with inorganic
salts is known as eutrophication, and is clearly different
from pollution of the water by waste substances. The
accelerated algal growth in turn damages other water life
(plant and micro-organic) by reducing the oxygen content of the
immediate environment, leading to the formation of waters
devoid of flora and fauna.

In addition to the phosphates naturally present in spring
water, soil erosion and agricultural sources (i.e. fertilizers)
contribute towards the phosphate loading in water. This
loading increases when municipal waste-waters (within which
about 60% of the phosphate content comes from detergents and
around 40% from faeces) are added. Though the eutrophication

- 14 -

problem cannot be solved by changes in detergent formulation only, possible future legislation and some existing legislation in several countries restricting the use of phosphates in detergents, has caused research studies to be carried out to find suitable substitutes for phosphates in detergents.

The overall search for phosphate substitutes has included studies of organic and inorganic substances, both water soluble, and water insoluble, and zeolite ion exchangers have shown promise during preliminary studies. Several patents have been filed[p1-p5] by leading detergent manufacturers, where the phosphate content in the formulations has been partially or totally replaced by zeolites of various types. There are many publications which review or report the situation regarding the possible use of zeolites as phosphate substitutes[1-6].

1.2. ZEOLITES

Zeolites are crystalline aluminosilicates, either occurring naturally (e.g. mordenite or faujasite) or prepared synthetically (e.g. Linde A, Linde X). Zeolite minerals were discovered and named as early as 1756, and it became known that they were capable of reversibly exchanging their metal cations on treatment with aqueous solutions of various salts. Amorphous, gel-type, aluminosilicates like 'Permutite' have been used for years in water treatment. Zeolites, also known in literature as molecular sieves, have been defined as "aluminosilicates with a framework structure enclosing cavities occupied by large ions and water molecules both of which have considerable freedom of movement, permitting ion exchange and reversible

- 15 -

dehydration."[7]

Zeolite crystals were reversibly dehydrated without any change
in external crystal form occurring as early as 1840[8]. It
was later found that dehydrated crystals would reversibly sorb
certain inorganic vapours[8]. In 1925, it was reported that
the zeolitic mineral chabazite adsorbed water vapour, methanol
and ethanol while benzene and acetone were largely excluded[8].
Since then, the use of zeolites as molecular sieves has grown
enormously, the shapes and sizes of various molecules being
the criteria of exclusion, as dictated by channel and pore
sizes within the zeolite. This selectivity can be changed by
exchanging the cations originally present in the zeolite by
other cations of different ionic radii. The resulting change
in channel size affects the molecular-sieving characteristics.
For example, Na-A zeolite (known in industry as 4A molecular
sieve because of its 8-oxygen window aperture dimensions of 4 $\overset{o}{A}$
units), does not sorb propane, but if the Na^+ ions are replaced
with Ca^{2+} ions to give zeolite 5A, then propane is no longer
excluded[9]. Exchanging with potassium ions gives zeolite 3A,
reducing the sieve size to less than that in Na-A, and essent-
ially stopping the sorption of oxygen[9].

Another major use of zeolites is in the field of catalysis[10-12].
Ion exchange of the zeolite (usually with transition metals or
rare earths) often forms the first stage of the catalyst
preparation, but the nature of the zeolite itself plays an
essential part in catalytic activity by providing reaction sites
and a shape-selective substrate. For example, on calcination,
the exchanged forms produce Brønsted and Lewis acid sites which

act as the catalyst centres, producing reaction through a carbonium ion mechanism[13-15]. Since these acid centres occur within the zeolite, its molecular sieving properties can also be used productively by allowing selective cracking. Thus in catalysts based upon erionite n-paraffins can enter the zeolite and reach the intracrystalline acid centres but not branched chain or cycloparaffins, or aromatics. Therefore the n-paraffins can be selectively cracked while the other hydrocarbons are relatively unchanged. Similar effects can be observed in isomerization reactions[14].

Other zeolites which are used in catalysis - mainly in cracking or hydrocracking processes - are ZSM5, synthetic mordenite, Y and erionite[16-18].

There are many other important uses of zeolites. Some of these applications are briefly described below.

Zeolites are stable to ionizing radiation and to high temperatures, and therefore can be used in the separation and purification of radioisotopes. Their low solubility over a wide pH range especially at high alkalinity together with their attrition resistant, dimensionally stable and rigid framework make zeolites particularly useful in this field. The zeolites investigated and used in this respect, and in terms of storage of radioisotopes safely, include chabazite, clinoptilolite, synthetic mordenite and Linde AW-500[16-18].

In an application of ion exchange in pollution abatement, zeolites - particularly clinoptilolite - have been used to remove NH_4^+ ions from effluents. Several processes have been

reported[16-18] that are now used commercially to purify
wastewaters, and some of these even involve regeneration of
the zeolite.

Ammonia removal by zeolites is also practised in aquatic animal
systems such as aquariums and fish farms, where the ammonia,
released directly by the fish along with other nitrogenous
wastes, and from bacterial deamination of protein in food and
wastes, can reach toxic concentrations if not removed in time[16].

In the feeding of ruminant animals, zeolites may be introduced
into the rumen prior to feeding of non-protein nitrogen(NPN)
compounds so that NH_4^+ ions are partially exchanged into the
mineral zeolite and thereafter slowly released by the regen-
erant action of saliva, entering the rumen. It is reported
that feeding efficiency improves this way[16,17].

Other agricultural and horticultural applications of zeolites
include the feeding of zeolites to pigs and chickens, use in
odour control in poultry farms, use as soil conditioners, in
fertilizers, as carriers of fungicides and pesticides, and
even as NH_4^+ ion exchangers to prolong the life of cut
flowers[16,17].

Many zeolites have also been used for separating and recover-
ing metals because of their high selectivity for various heavy
metals. The applications include removal of heavy metals from
industrial effluents and metal processing wastewaters and in
the recovery of precious and semi-precious metals[16-18].

It is obvious therefore that zeolites are a most interesting
and versatile set of materials, and extensive studies of most

of the 30-odd types of zeolite minerals and 100-odd types of synthetic zeolites have been carried out since the discovery of their properties. A vast number of technical papers, describing the characteristic ion exchange behaviour of various zeolites, have been written.

Although the synthesis of zeolites has been reported in the literature of the last 50 years, the majority of the accounts must be disallowed on the basis of improper identification[19,20]. The advent of X-ray diffraction techniques, however, has resulted in more positive identification of complete structures and compositions.

Credit for early successes in zeolite syntheses goes to R.M. Barrer and co-workers at Imperial College, who prepared synthetic mordenite and several others[19-21], and to the Linde Research Division of the Union Carbide Corporation[22,p6] who prepared many different species of zeolites, some of which had no naturally occurring analogues. Zeolites A and X are two of the most important zeolites prepared by Linde, of which the former has no mineral analogue.

A literature survey of phosphate substitution studies and ion exchange work related to that field showed that zeolites A and X were the most promising substitutes, while zeolite Y was the next most widely studied[1-6,13,16-46]. The reasons for concentrating on these zeolites had been their open structures and high exchange capacities. The primary function of a detergent 'builder' is as a water softener. The 'builder' removes the free Ca^{2+} and Mg^{2+} ions present in the water by

sequestering them (e.g. STP) or ion-exchanging them (e.g. Na-X). For a zeolite to be a good phosphate substitute it must have a high capacity for storing the exchanged Ca^{2+} and Mg^{2+} ions, and must also be highly selective for the same two ions in the presence of very large excess concentrations of monovalent cations, especially sodium. This is because in addition to the Na^+ ions normally present in water, modern detergent powders are made up of several components which include surfactants, bleaches, anti-redeposition agents and foam inhibitors, nearly all of which contain sodium.

Literature suggests that zeolite A has a very high selectivity for Ca^{2+} ions but a much lower selectivity for Mg^{2+} ions, while zeolite X has a high selectivity for both Mg^{2+} and Ca^{2+} ions[16,17]. It must, however, be remembered that a detergent 'builder' has functions other than that as a water softener[4], and a final selection of a phosphate substitute must take all these into account.

1.3. <u>STRUCTURE OF ZEOLITES</u>

The aluminosilicate portion of the zeolite structure is a three-dimensional open framework consisting of an infinitely extending network of AlO_4 and SiO_4 tetrahedra which are linked to each other by sharing all of the oxygen atoms. The aluminium ion is small enough to achieve tetrahedral coordination with an Al-O bond length of 1.73 $\overset{o}{A}$, compared to the Si-O bond length of 1.63 $\overset{o}{A}$; however, each isomorphous substitution of Al^{3+} for Si^{4+} in the framework silicate leads to a charge deficiency of -1, resulting in the distribution throughout the framework

of an overall delocalised negative charge. In order to
maintain electrical neutrality, the presence of an electro
chemical equivalent of loosely-bound cations, normally of
an alkali metal or alkaline earth metal, is required within
the framework[46].

$$
\left[
\begin{array}{c}
O \\
\mid \\
O - Al - O - Si - O \\
\mid \qquad\quad \mid \\
O \qquad\quad O
\end{array}
\right]^{-} \quad Na^{+}
$$
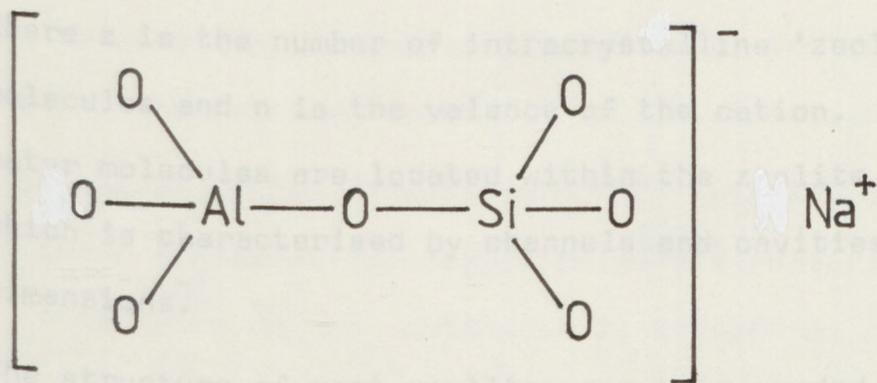
The ion exchange property results from the charge imbalance
found in the lattice being neutralised by the exchangeable
cations mentioned above. The number of charged sites (i.e.
the extent of Si^{4+} replacement by Al^{3+}) is normally limited
according to the so-called Loewenstein's rule[47], which states
that the maximum ratio of tetrahedrally coordinated aluminium
to silicon is 1:1, since the linkage of two AlO_4 tetrahedra
is energetically highly unfavourable.

Generally, a zeolite may be represented by an empirical oxide
formula of the form[14,46],

$$
M_{2/n} O . Al_2 O_3 . xSiO_2 . yH_2 O
$$
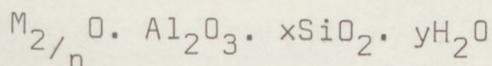
where n is the valence of cation M, and x is either equal to
or greater than two.

Because of the crystalline structure of zeolites it is also possible to express their composition using a unit cell formula[14,46], viz:

$$M_{x/n} \left[(AlO_2)_x . (SiO_2)_y \right] . zH_2O$$
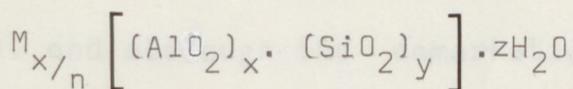
where z is the number of intracrystalline 'zeolitic' water molecules and n is the valence of the cation. The cations and water molecules are located within the zeolite framework, which is characterised by channels and cavities of molecular dimensions.

The structure of most zeolites can be regarded as consisting of simple arrangements of polyhedra, each polyhedron being a three-dimensional array of SiO_4, AlO_4 tetrahedra in a definite geometric form. The sodalite group of zeolites, to which zeolites A,X and Y belong, are all based on frameworks which consist of simple arrangements of truncated octahedra. The tetrahedra are arranged at the corners of a truncated octahedron which, in keeping with Euler's theorem, contains six square faces, eight hexagonal faces, twenty-four vertices and thiry-six edges[14,19]. In the sodalite structure, the truncated octahedra share all their square and hexagonal faces[8,46]. Although sodalite is more usually classified as a felspathoid, the framework structure is based on similar units.

It is worth noting here that there are other naturally occurring or synthetic crystalline aluminosilicates made up of three-dimensional framework structures which exhibit ion

exchange properties, and which may retain salts or guest molecules irreversibly occluded in the interstices of the framework lattice, but are generally not classified as zeolites. These are the aluminosilicates which are known as felspathoids, and although the demarkation between zeolites and felspathoids is not clearly defined, the main character- istics of a zeolite are considered to be the existence and size of channels and voids within the structure.

Zeolites have been classified[14,46] into seven groups based on their framework topology. Meier's structural classification [48] is based on the continuous re-occurrence of subunits, which are specific arrangements of SiO_4 or AlO_4 tetrahedra within the structure of the framework. These subunits, known as "secondary building units" (SBU) are shown in figure 1.1.

The classification used by Breck[9] is also based on the seven SBU's where zeolites are categorised in terms of the SBU that comprises the framework. However, other structural blocks chains and plates of tetrahedra exist which express the inter- relationships between the tetrahedra equally well, or more readily than the use of SBU's. Thus, most zeolites can be classified on the basis of linked polyhedra built up from combinations of some of the SBU's, or from chain layer structures[14] based on SBU's.

1.4. STRUCTURE OF ZEOLITE X

The arrangement of the tetrahedra in the framework in synthetic zeolites X and Y, and in naturally occurring faujasite is basically the same. Differences among them arise from

composition and composition-related physical property
differences. Zeolite X differs from zeolite Y only by the
degree of isomorphous substitution of aluminium for silicon
within the framework. Thus the two zeolites have identical
aluminosilicate framework structures, slightly different unit
cell dimensions but quite different ion-site distributions.
The silicon to aluminium ratio can vary with both these
zeolites (especially Y), and typical unit cell formulae are
given below together with the corresponding Si/Al ratios[46].

for zeolite X,

$$Na_{86}\left[(AlO_2)_{86} (SiO_2)_{106}\right] \cdot 264H_2O \qquad Si/Al = 1 \text{ to } 1.5$$

for zeolite Y,

$$Na_{56}\left[(AlO_2)_{56} (SiO_2)_{136}\right] \cdot 250H_2O \qquad Si/Al \Rightarrow 1.5 \text{ to } 3$$
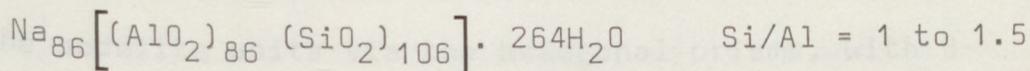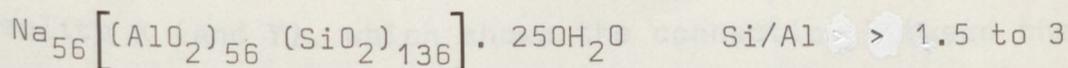
The framework of zeolite X (and zeolite Y and faujasite)
consists of a tetrahedral arrangement of the distorted
truncated octahedra (sodalite units); i.e. the octahedra are
linked at the octahedral faces by hexagonal prisms containing
12 SiO_4 or AlO_4 tetrahedra, formed by linking (not sharing)
two six-oxygen windows, one from each sodalite unit (see
figure 1.2). The centres of the truncated octahedra occupy
the same relative positions as the carbon atoms in a diamond.
Alternatively, the structure can also be described in terms of
linked hexagonal prisms (6-6 units in SBU nomenclature). Thus
zeolite X (and Y) can be considered to have two independent
but inter-connecting three-dimensional networks of cavities
because of the way the linked sodalite units are arranged

topologically. One such network consists of the so-called 26-hedra type II[14] voids (sometimes also known as "super-cages") - (see figure 1.3). These voids are created when sodalite units are tetrahedrally joined, and are themselves joined to each other by the sharing of 12-oxygen windows which have free dimensions of about 0.74 nm. The void spaces in the structure of Na-X consist of elliptical shaped cavities 13 $\overset{\circ}{A}$ (1.3 nm) in length, giving rise to the name 13-X zeolite. The gross impression of the structure is that of a densely packed structure of oxygen atoms surrounding relatively large interstitial voids[8,14,17]. The other network is the linking of the sodalite units via the hexagonal prisms, with 6-oxygen windows which have free dimensions of 0.25 nm. Figure 1.4 is a simple diagrammatic representation of the cavities in zeolite X (and Y), which shows the connection between the sodalite units and the main channels (i.e. the 26-hedra type II cages). In order to enter a sodalite unit or a hexagonal prism, an ion must pass through an orifice which is only 0.25 nm diameter.

1.5. CATION SITINGS IN ZEOLITES

Zeolites normally consist of several crystallographically distinct yet intimately mixed sets of sublattices each of which have associated with them a proportion of exchangeable cations. The sites depend both on the nature of the alumino-silicate structure and on the positions of tetrahedrally co-ordinated oxygens. The number of electrochemical equivalents required to neutralise the negative charge within the frame-

- 25 -

work may be smaller than the total number of available cation sites. Since the cations tend to disperse among the sites so as to minimise the overall free energy of the system, there may be several sets of partially occupied or unoccupied sites. The factors which decide the cation distribution pattern within the framework are complex and involve properties of the cationic species such as valency, ionic radius, hydration energy, electronic structures, as well as properties of the zeolite such as water content, temperature and framework charge. Due to these complexities ion site distribution data from different samples and investigators are not always consistent. These variations may be caused by the Si/Al ratio as well as fundamental differences in the histories and morphologies of the samples studied.

Studies on the available ion sites and the degrees of occupancy of these sites in differently exchanged faujasite-type zeolites has been summarised by Barrer[14], Breck[46] and more recently, Mortier[49]. The different approaches and findings of various scientists are illustrated well by these discussions. Figure 1.5 illustrates Breck's classification of cation sites[46].

Barrer's classification of cation sites in faujasite[14].

This classification is based on the work done by Smith[50].

Site I - In the centre of hexagonal prisms (16 sites per
            unit cell)
Site I' - In sodalite cages, i.e. 14-hedra, adjacent to six-
            oxygen windows leading to hexagonal prisms (32 sites
            per unit cell)

Site U - In the centre of sodalite cages (8 sites per
            unit cell)

Site II - In the plane of the six-oxygen windows linking the
            sodalite cages and 26-hedra type II cages (32 sites
            per unit cell)

Site II' - Near site II but inside sodalite cages (32 sites
            per unit cell)

Site II* - Near site II but inside type II cages (32 sites
            per unit cell)

Site III - Against four-oxygen rings on the walls of type II
            cages (48 sites per unit cell)

Site IV - In the centre of 26-hedra type II cages (8 sites
            per unit cell)

Site V - In the 12-oxygen rings of the type II cages (16
            sites per unit cell)

Breck's classification of cation sites in faujasite[46].

In this widely-used classification, Breck uses a slightly
different nomenclature.

Site I - In the centre of hexagonal prisms

Site I' - In sodalite cages, adjacent to six-oxygen windows
            leading to hexagonal prisms

Site II' - In sodalite cage , adjacent to six-oxygen windows
            leading to type II cages.

Site II - Near site II' but inside type II cages (i.e. out-
            side sodalite cage)

Site III - Near the walls of the large cavities next to the
            4-rings

Site IV - In the 12-oxygen rings between the large
           cavities

Mortier's classification of cation sites in faujasite[49].

Mortier has done an extensive rationalization of site classi-
fication, and has allocated 16 different sites for faujasite
based on site symmetry and coordination distances[49]. This
site classification is tabulated below, where the conventional
site nomenclature is given in parentheses.

site	type	coordination distances (Å)	
A (I)	I	6 × 2.8	
B	II6	3 × 2.2	
C (I')	II6	3 × 2.6	
D (U)	V6	-	
E (II')	II6	3 × 2.6	
F	II12	3 × 2.2	
G (II)	II12	3 × 2.6	
H (III)	IV12	2 × 2.7	
I (III')	IV12	2 × 2.7	2 × 2.7
J	IV12	2.3	2 × 2.9
K	IV12	2.8	
L (V)	V12	-	
M	IV12	2 × 3.1	3.2
N	IV12	2.5	3.1
O	V12	-	
P	IV12	2.6	2.9

N.B. The coordination distances which are underlined are fixed
by symmetry. The others are indicated in the stereo plots
shown in Mortier's atlas[49].

The atlas, which has been published on behalf of the Structure Commission of the International Zeolite Association, also contains information of site symmetry and site occupancies.

As noted earlier, the various studies that have been carried out to allocate different exchanged cations into particular cation sites have given results that are often not in agreement. Many publications reporting on cation siting investigations are available in literature[18,36,49,51-58].

Figure 1.1

Secondary Building Units (SBU's)

T4

T6

T8

4-4

6-6

8-8

5-1

4-4-1

4-1
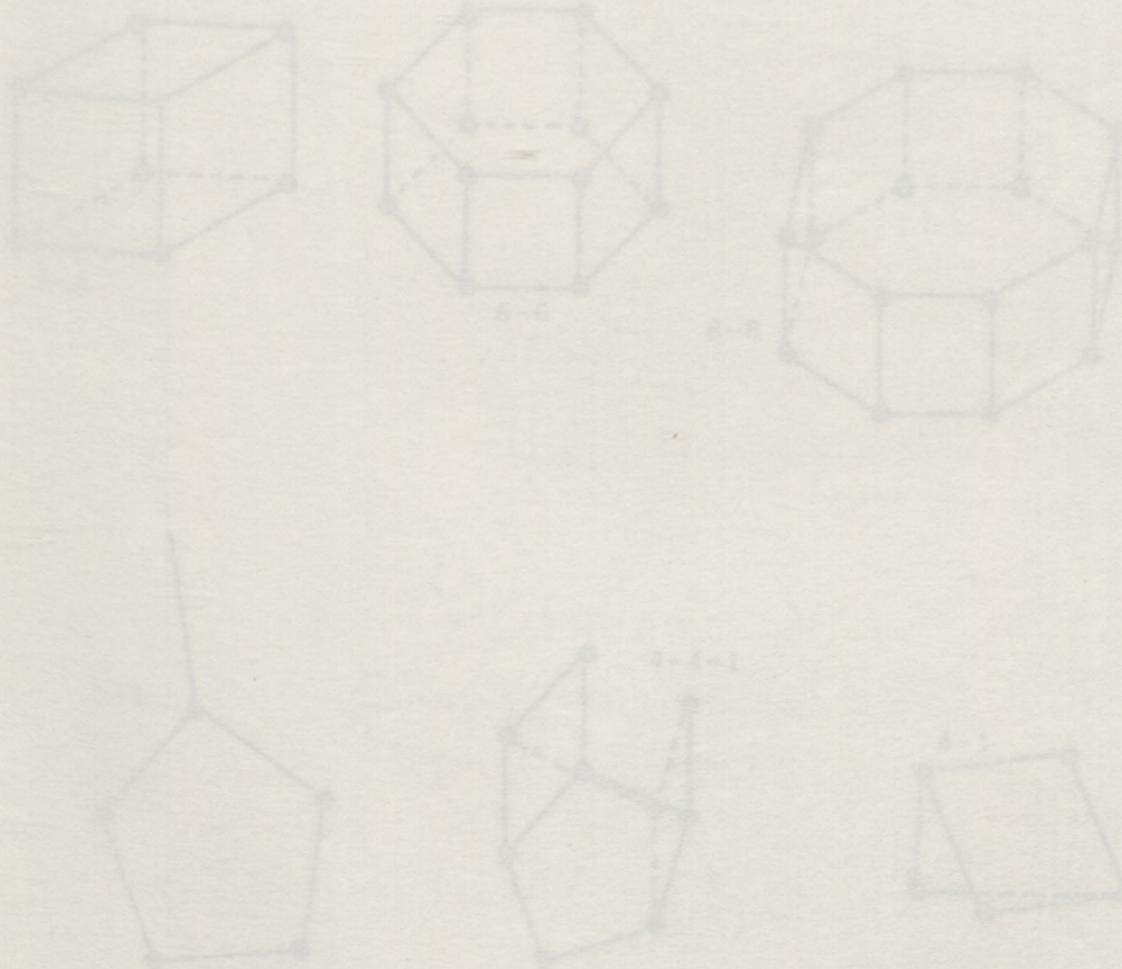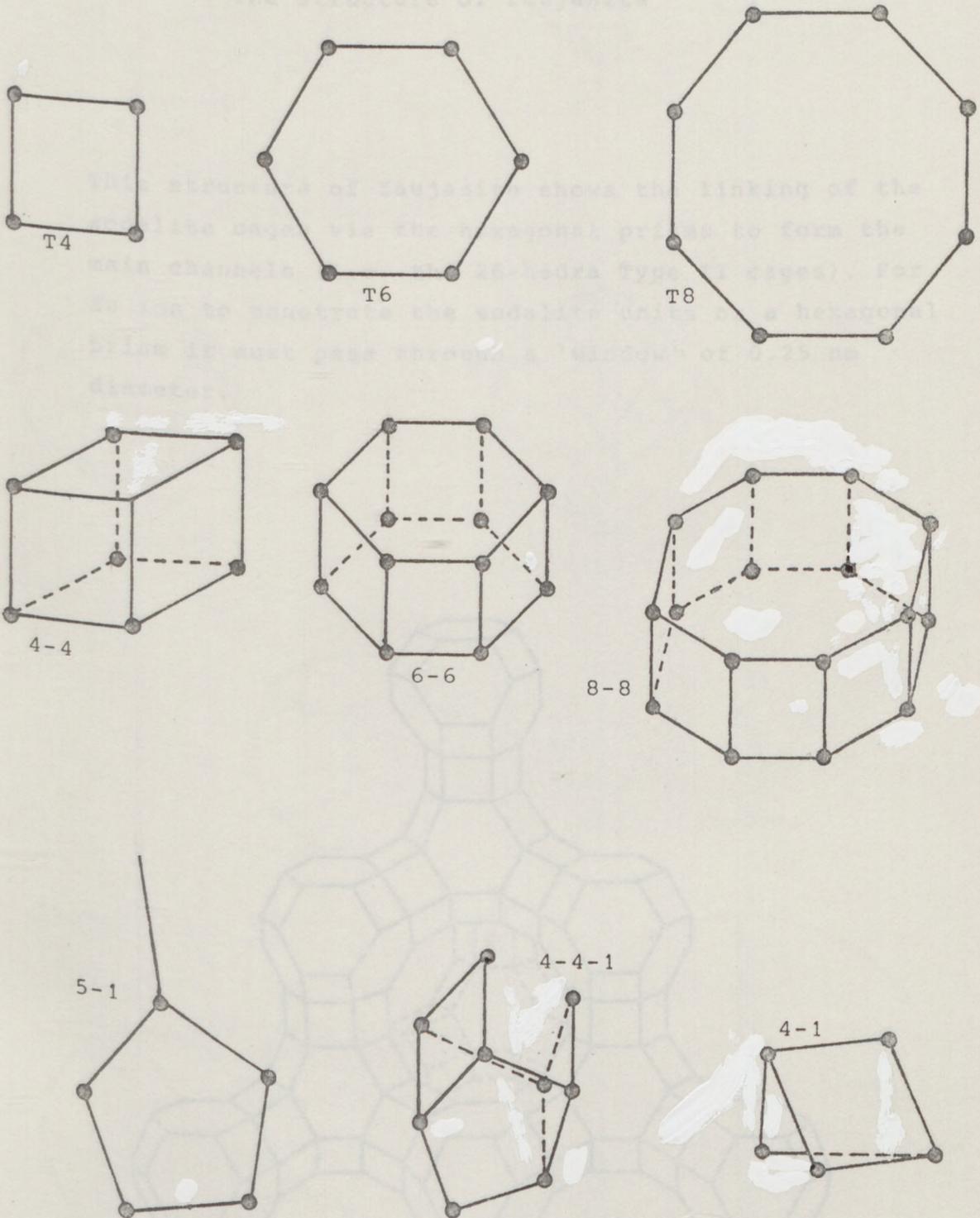
These finite units can contain up to 16 tetrahedral atoms
per unit. The unit cells of framework silicates, based on
the secondary building units, contain an integral number
of SBU's. Many of the frameworks encountered can be built
up from several different SBU's.

Figure 1.2

The structure of faujasite

This structure of faujasite shows the linking of the
sodalite cages via the hexagonal prisms to form the
main channels (i.e. the 26-hedra Type II cages). For
an ion to penetrate the sodalite units or a hexagonal
prism it must pass through a 'window' of 0.25 nm
diameter.
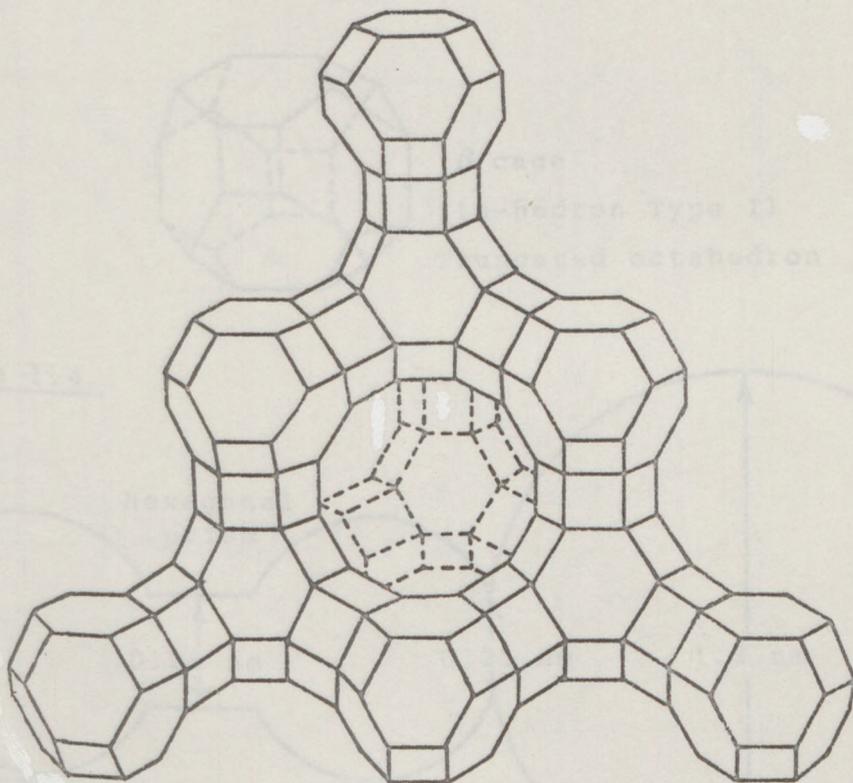
Figure 1.3   Polyhedral voids
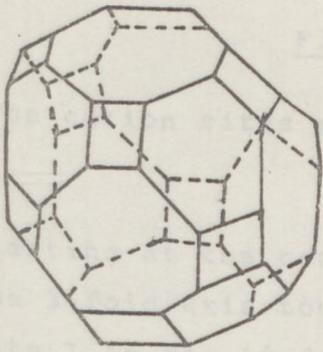
α cage

(26-hedron Type I)

Truncated cuboctahedron

γ cage
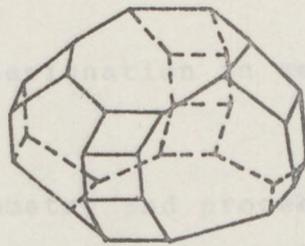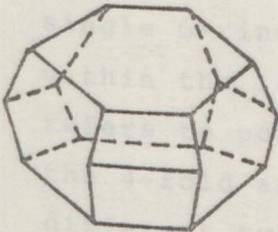
(18-hedron)

ε cage
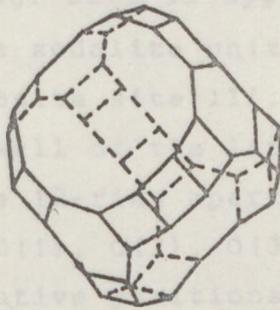
(11-hedron)

(26-hedron Type II)
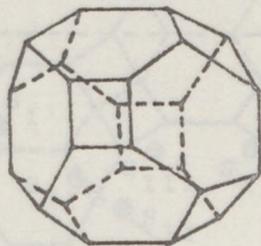
β cage

(14-hedron Type I)

Truncated octahedron

Figure 1.4

hexagonal
prism

0.25 nm   0.25 nm   1.3 nm   0.75 nm

β cage   β cage

26-hedron Type II
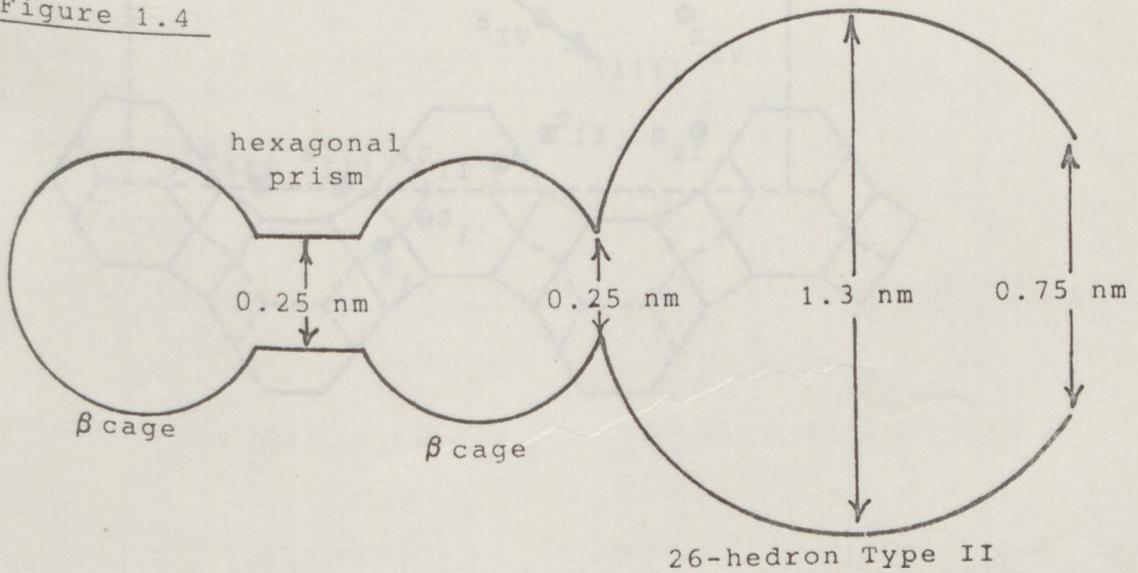
Figure 1.5

The cation sites and their designation in zeolite X

Starting at the centre of symmetry and proceeding along
the 3-fold axis toward the centre of the unit cell,
site I is the 16-fold site located in the centre of the
double 6-ring (hexagonal prism). Site I' is on the
inside of the sodalite unit adjacent to the double
6-ring. Site II' is on the inside of the sodalite unit
adjacent to the single 6-ring. Site II approaches the
single 6-ring outside of the sodalite unit and lies
within the large cavity opposite site II'. Site III
refers to positions in the wall of the large cavity, on
the 4-fold axis in the large 12-ring aperture. The four
different types of oxygens O(1), O(2), O(3), O(4) are
also indicated in their relative positions.

CHAPTER TWO   ION EXCHANGE
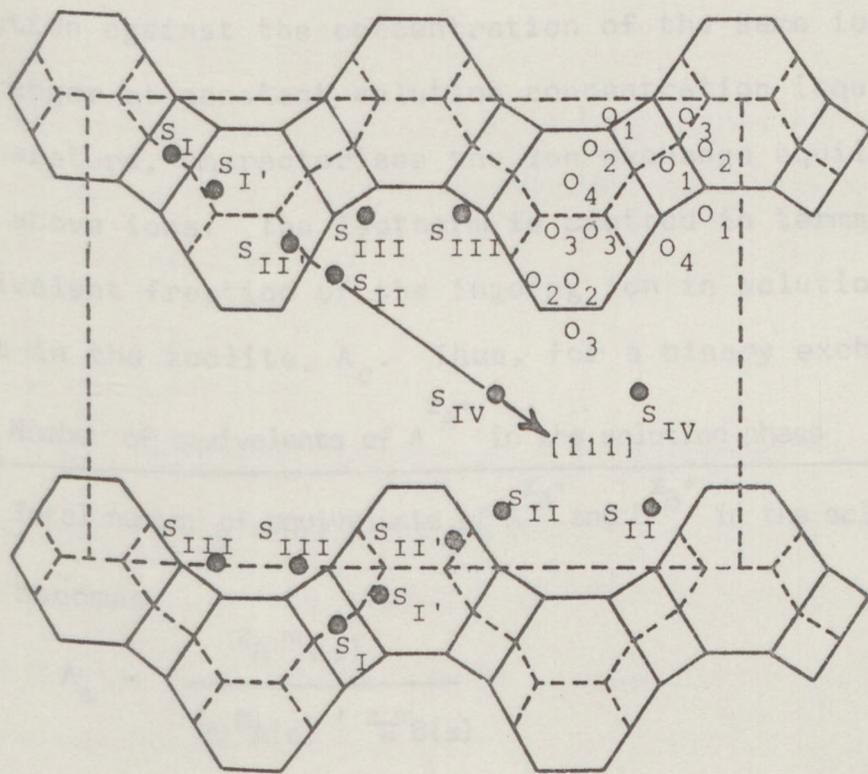
2.1.   BINARY ION EXCHANGE

Ion exchange can be defined as the reversible interchange of

ions between two phases occurring such that there is no gross

change in the solid. For a binary exchange, the reaction may

be written as

$$z_A B^{z_B^+}_{(c)} + z_B A^{z_A^+}_{(s)} \rightleftharpoons z_A B^{z_B^+}_{(s)} + z_B A^{z_A^+}_{(c)} \qquad \dots (2.1.)$$
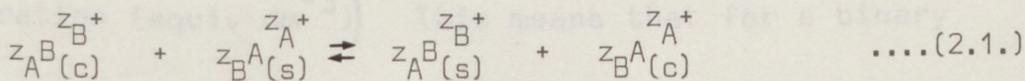
where z_A, z_B are the valences of ions $A^{z_A^+}$, $B^{z_B^+}$ respectively,

and subscripts (c) and (s) refer to the crystal and solution

phases respectively.

The ion B, initially in the zeolite, is frequently referred to

as the counter ion. An ion exchange isotherm, which is an

equilibrium plot of the concentration of an exchanging ion in

solution against the concentration of the same ion in the

exchanger at constant solution concentration (equiv dm^{-3}) and

temperature, characterises the ion exchange equilibrium for

the above ions. The isotherm is plotted in terms of the

equivalent fraction of the ingoing ion in solution, A_s, against

that in the zeolite, A_c. Thus, for a binary exchange,

$$A_s = \frac{\text{Number of equivalents of } A^{z_A^+} \text{ in the solution phase}}{\text{Total number of equivalents of } A^{z_A^+} \text{ and } B^{z_B^+} \text{ in the solution phase}}$$

This becomes

$$A_s = \frac{z_A \, m_{A(s)}}{z_A \, m_{A(s)} + z_B m_{B(s)}} \qquad \dots (2.2.)$$

where m(s) is the concentration (mol kg^{-1}) of the species in solution.

- 34 -

Similarly

$$A_c = \frac{z_A m_{A(c)}}{z_A m_{A(c)} + z_B m_{B(c)}} \qquad \ldots.(2.3.)$$

(The total concentration (equiv dm^{-3}) of the solution is kept constant because the selectivity of the zeolite for the ingoing ion is not only a function of A_c, but also of the total concentration (equiv dm^{-3})) This means that for a binary system

$$B_s = 1 - A_s \qquad \text{and}$$

$$B_c = 1 - A_c$$

the preference of a zeolite for one cation over another is expressed as a separation factor, $\alpha^`$

$$\alpha^` = \frac{A_c/A_s}{B_c/B_s} = \frac{A_c B_s}{B_c A_s} \qquad \ldots.(2.4.)$$

Isotherms are usually plotted with A_s on the ordinate and A_c on the abscissa, and the value of $\alpha^`$ can be graphically obtained as shown in Figure 2.1, as the ratio

$$\alpha^` = \frac{\text{Area I}}{\text{Area II}} \qquad \ldots.(2.5.)$$

In an ion exchange system where the zeolite shows equal preference for both ions, A_c equals B_c, and the isotherm is linear, following the diagonal in the diagram (Figure 2.1).

Ion exchange preferences can be summarised in terms of the separation factor as follows:

$\alpha^` > 1$ — zeolite exhibits preference for ingoing ion

$\alpha^{\textbf{`}} < 1$ - zeolite exhibits preference for outgoing ion

$\alpha^{\textbf{`}} = 1$ - zeolite exhibits equal preference

For the thermodynamics of ion exchange in zeolites, the ionic concentrations are normally given in mol dm^{-3} for the solution phase, and therefore another separation factor α, is defined as

$$\alpha = \frac{A_c/m_A}{B_c/m_B} = \frac{A_c \, m_B}{B_c \, m_A} \qquad \ldots.(2.6.)$$

An isotherm is obtained experimentally by equilibrating solutions of constant total concentration (equiv dm^{-3}), T_N, but containing different proportions of cations A and B, with known weights of either the homoionic A or homoionic B zeolite. The experiments are carried out over a period of time sufficient for equilibrium to be effected. Following this the equilibrium compositions of the zeolite and solution phases are found. Thus, for a particular value of A_c, A_s might vary in value from 0 to 1 depending on the magnitude of T_N; each of these values of A_s belongs to a different isotherm plot. For the zeolite phase, the exchange capacity of the zeolite determines the number of equivalents per unit mass; the exchange capacity is normally defined in terms of the wet zeolite which has taken up a known quantity of water by equilibration at constant temperature under a known and constant water vapour pressure.

For aqueous solutions,

$$T_N = z_A m_A + z_B m_B \qquad \ldots.(2.7.)$$

Therefore

$$m_A = \frac{A_s \cdot T_N}{z_A} \qquad \qquad ....(2.8)$$

and

$$m_B = \frac{(1 - A_s) \cdot T_N}{z_B} \qquad \qquad ....(2.9)$$

Thus,

$$\alpha = \left[\frac{z_A}{z_B}\right]\alpha` \qquad \qquad ....(2.10)$$

For ion exchange systems where $z_A = z_B$, $\alpha = \alpha`$; and the

criteria for a zeolite to be selective are as above. When

$z_A \neq z_B$, then

$$\alpha = \left[\frac{z_A}{z_B}\right] \cdot \frac{Area\ I}{Area\ II} \qquad \qquad ....(2.11)$$

in Figure 2.1,

and the requirements for selectivity become

$\alpha > {}^{z_A}/z_B$ - zeolite shows preference for ingoing ion

$\alpha < {}^{z_A}/z_B$ - zeolite shows preference for outgoing ion

$\alpha = {}^{z_A}/z_B$ - zeolite shows equal preference

2.1.1. Classification of Binary Isotherms

The ion exchange isotherm shown in Figure 2.1 is not the only

type of isotherm encountered in zeolite studies. As shown in

Figures 2.2. - 2.7., there are six different kinds of isotherms

as follows:

(i) Isotherms of the first kind (Figure 2.2.)

When the valences of the ingoing and outgoing cations are

equal, the figures represent the following preferences.

- 37 -

a - zeolite shows preference for outgoing cation

            b - zeolite shows equal preference

            c - zeolite shows preference for ingoing cation

If the exchanging ions have different valences, the select-
ivity is not visually obvious since

$$\alpha = \left[\frac{z_A}{z_B} \right] \cdot \frac{Area\ I}{Area\ II} \quad in\ Figure\ 2.1. \quad \dots(2.11)$$

Examples of this are Li/Na-X[23,30], Sr/Na-phillipsite[59],
Ag/Na-X[30] and Tl/Na-X[30].

(ii) Isotherms of the second kind (Figure 2.3.)

These are characterised by a sigmoid curve and are often
observed when the selectivity is strongly dependent upon cation
composition and the selectivity is reversed during the course of
exchange. These sigmoidal curves have been explained in terms
of the presence of two or more different types of exchange
sites[30] but other factors[18,60,61] may also give rise to
curves of this form.

Examples of this are K/Na-X[23,30] and Li/Na-basic cancrinite[62].

(iii) Isotherms of the third kind (Figure 2.4.)

These are less commonly seen, and are found to be partially
irreversible in the region of the "plateau", leading to the
formation of "hysteresis loops" between forward and reverse
isotherms. An exchange system where recrystallisation (i.e.
change of structure and framework) of the zeolite phase occurs
during exchange characterises this type of isotherm. The
"plateau" region, where the two crystal phases co-exist can

also be reversible if the zeolite framework is flexible and readily recrystallises. The "hysteresis loops" arise when the growth of the new phase is hindered by an energy barrier caused by strain and interfacial free energy contributions[61,63], and these isotherms are thus said to be characteristic of meta-stable conditions[61]. Examples of these are Ag/Na and Ag/Li exchange in basic cancrinite[62].

(iv) Partial exchange (Figures 2.5. - 2.7.)

Often in zeolite ion-exchange processes at a given temperature, the ingoing cation fails to attain 100% of the exchange capacity of the zeolite. The isotherms shown in Figures 2.5, 2.6 and 2.7, all of which apply to partial ion-exchange processes, correspond to the respective total ion-exchange isotherms so shown as the first, second and third kinds (Figures 2.2. - 2.4).

The reasons for partial ion-exchange are complex, and not fully understood. The cause may be the rigid, crystalline structure of the zeolite, rendering certain sites within the zeolite inaccessible to the ingoing ion. Entering ions larger than the channel size within a crystal are excluded, and the zeolite acts as a sieve. This sieving effect is often observed when the entering ion is hydrated because the ionic radii of the hydrated species may be much larger than the ionic radii of the non-hydrated ion. This sieve effect may be total[64,65], when the ingoing ion is completely excluded, or partial, leading to incomplete exchange[23,30,31,66,67]. Partial exchange may also be caused through the filling of all the intra-crystalline passages before complete exchange is reached, and

thereby limiting the level of exchange. This phenomenon is known as a volume-steric exclusion mechanism[64,65,68]. It must be stated, however, that ion-sieve effects and volume-steric effects are not necessarily adequate to explain partial exchange, and a more comprehensive explanation, involving statistical mechanics, has been put forward[18,61,69]. Examples of partial exchange are Na/Ba, Na/Rb and Na/Cs exchanges in zeolite X and Y[23,25,30,31], Na/Ca and Na/Sr exchanges in Y[25,31], transition metal exchanges in X and Y[18,67], alkaline earth metal exchange in sodium mordenite[66], transition metal exchange in sodium mordenite[71], amminated zinc exchange in ammonium phillipsite[72] and amminated silver exchange in X,Y and mordenite[73]. An example of total exclusion by the ion-sieve effect is the case of $(CH_3)_4N^+$ and $(C_2H_5)_4N^+$ ions and zeolite A[64,65].

2.1.2. Thermodynamics of Binary Ion-Exchange

Only a brief discussion of the principles involved is given here as more detailed accounts are readily available elsewhere[18,61,74].

An adequate model for the rigorous thermodynamic treatment of the ion-exchange reaction was formulated by Gaines and Thomas[75], for ion exchange in clay minerals. This treatment covered the exchange of cations between the exchanger and solution and also considered possible changes in not only the quantity of solvent occluded within the exchanger but also in the extent of salt imbibition by the exchanger. Of the two cases considered, the first model comprised an exchanger capable of exchanging cations and sorbing solvent molecules

but which was incapable of imbibing anions, while the
second case took all three factors into account. It is
accepted practice to use the model corresponding to the first
case because it has been experimentally shown[76] that salt
imbibition effects are negligible at low external electrolyte
concentrations in solution.

In the Gaines and Thomas treatment, the exchanger phase is
taken as the *wet* solid. This is because the exchanger sorbs
water and the extent of sorption varies for different ion
exchanged forms of the same exchanger. This definition also
incorporates the free energy of hydration of each homoionic
form, which would otherwise complicate calculations arising
from the model. The Gaines and Thomas treatment involves
considering all three phases, vapour, solution and exchanger,
as a closed system. The standard states are defined initially
in terms of water as a reference so that the activity of water
is the same in each phase. The chemical potential of the water
is therefore regarded as equal to the standard chemical poten-
tial $\mu_W^\ominus(s)$ when the solution phase is pure solvent and the
activity of water in the solution phase, $a_W(s)$, is unity.
Then,

$$\mu_W^\ominus(c) = \mu_W^\ominus(s) = \mu_W^\ominus(v) \qquad \qquad ....(2.12)$$

where subscripts (c) and (v) indicate crystal and vapour phases
respectively.

By choosing the standard state for the exchanger as being the
homoionic form in equilibrium with an infinitely dilute
solution of the relevant ion (i.e. pure water) the imbibed
water is also involved in the definition of the standard state.

Then, for ion A^{z_A+}, $A_c = a_A(c) = f_A = 1$ in the standard state

where $a_A(c)$ is the activity of the ion in the crystal phase

and f_A is the activity coefficient of ion A^{z_A+} in association

with its equivalent of zeolite[75]. The standard states for

the ions in the solution phase are defined in terms of the

hypothetical ideal molal (concentration mol kg^{-1}) solutions of

the salts[77,78]. Then, for ion A^{z_A+}, $m_A = a_A(s) = \gamma_A = 1$ in

the standard state, where $a_A(s)$ is the activity of the ion in

solution and γ_A is the activity coefficient in solution.

For the binary ion exchange given by

$$z_A B(c)^{z_B+} + z_B A(s)^{z_A+} \rightleftharpoons z_A B(s)^{z_B+} + z_B A(c)^{z_A+} \qquad ....(2.1)$$
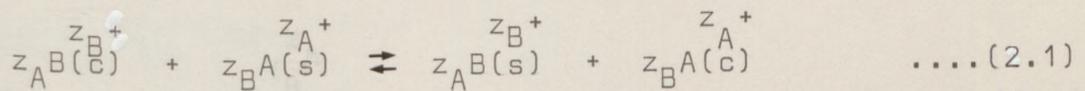
the thermodynamic equilibrium constant is defined as

$$K_a = \frac{a_A(c)^{z_B} \cdot a_B(s)^{z_A}}{a_B(c)^{z_A} \cdot a_A(s)^{z_B}} \qquad ....(2.13)$$

where a_A and a_B are the activities of ions A^{z_A+} and B^{z_B+} in

each phase. In terms of concentrations and activity coefficients

this becomes

$$K_a = \frac{A_c^{z_B} \cdot f_A^{z_B} \cdot m_B^{z_A} \cdot \gamma_B^{z_A}}{B_c^{z_A} \cdot f_B^{z_A} \cdot m_A^{z_B} \cdot \gamma_A^{z_B}} \qquad ....(2.14)$$

The mass action quotient is thus defined as

$$K_m = \frac{A_c^{z_B} \cdot m_B^{z_A}}{B_c^{z_A} \cdot m_A^{z_B}} \qquad ....(2.15)$$

Therefore, K_a and K_m are related by

- 42 -

$$K_a = K_m \cdot \frac{f_A^{z_B} \cdot \gamma_B^{z_A}}{f_B^{z_A} \cdot \gamma_A^{z_B}} \qquad \ldots\ldots(2.16)$$

The equilibrium is also described by a third quotient, K_c which includes only the solution phase activity correction. For this reason it is sometimes known as the corrected selectivity coefficient. For historical reasons, it has usually been known as the Kielland quotient[79] but this latter terminology is disappearing in favour of the former.

$$K_c = K_m \Gamma \qquad \ldots\ldots(2.17)$$

where
$$\Gamma = \frac{\gamma_B^{z_A}}{\gamma_A^{z_B}} \qquad \ldots\ldots(2.18)$$

and
$$K_a = K_c \frac{f_A^{z_B}}{f_B^{z_A}} \qquad \ldots\ldots(2.19)$$

This leads to

$$\ln K_a = \ln K_c + z_B \ln f_A - z_A \ln f_B \qquad \ldots\ldots(2.20)$$

The determination of K_a from isotherm data involves two steps. Firstly, K_c is obtained by the solution activity correction, and secondly, the activity coefficients of the ions in the zeolite are determined to obtain K_a.

The standard free energy per equivalent of ion exchange is then found from

$$\Delta G^{\ominus} = \frac{-RT}{z_A z_B} \cdot \ln K_a \qquad \ldots\ldots(2.21)$$

2.1.3. Determination of Solution Phase Activity Coefficients

An expression for the mean molal stoichiometric activity coefficients may be derived theoretically using a modified Debye-Hückel approach[61,77] but the values of individual ion activity coefficients cannot be separately determined, since ions in solution are necessarily accompanied by an equivalent number of oppositely charged ions. The *ratio* of single ion activity coefficients, however, can be determined from empirical mean molal stoichiometric activity coefficients $\gamma_{\pm AX}$ and $\gamma_{\pm BX}$; the subscripts AX and BX refer to the salts where X is the common anion.

The relationship between $\gamma_{\pm AX}$ and the individual ion activity coefficients γ_A and γ_X is[77]

$$\ln \gamma_{\pm AX} = \frac{1}{z_A + z_X} \left[z_X \ln \gamma_A + z_A \ln \gamma_X \right] \qquad \dots (2.22)$$

and similarly

$$\ln \gamma_{\pm BX} = \frac{1}{z_B + z_X} \left[z_X \ln \gamma_B + z_B \ln \gamma_X \right] \qquad \dots (2.23)$$

Multiplying these two equations by $z_B(z_A + z_X)/z_X$ and $z_A(z_B + z_X)/z_X$ respectively, and subsequent subtraction gives[18,61]

$$\ln \Gamma = \ln \frac{\gamma_B^{z_A}}{\gamma_A^{z_B}} = \frac{1}{z_X} \left[z_A(z_B + z_X) \ln \gamma_{\pm BX} - z_B(z_A + z_X) \ln \gamma_{\pm AX} \right]$$

$$\dots (2.24)$$

This expression yields Γ in terms of the mean molal stoichiometric activity coefficients of *pure* solutions, and therefore, does not relate to the experimental situation. What is

- 44 -

required is an expression for Γ in terms of activity coefficients of AX and BX in mixed solution; i.e. $\gamma_{\pm AX}^{(BX)}$ and $\gamma_{\pm BX}^{(AX)}$, where the superscripts denote the other salt present in the binary solution. Expressions were derived by Glueckauf[80] to represent this particular situation, and are shown below:

$$\log \gamma_{\pm AX}^{(BX)} = \log \gamma_{\pm AX} - \frac{m_B}{4I}\left[k_1 \log\gamma_{\pm AX} - k_2 \log\gamma_{\pm(BX)} - \frac{k_3}{I+I^{-\frac{1}{2}}}\right]$$

$$....(2.25)$$

and

$$\log \gamma_{\pm BX}^{(AX)} = \log \gamma_{\pm BX} - \frac{m_A}{4I}\left[k_4 \log\gamma_{\pm BX} - k_5 \log\gamma_{\pm AX} - \frac{k_6}{I+I^{-\frac{1}{2}}}\right]$$

$$....(2.26)$$

where
$$k_1 = z_B(2z_B - z_A + z_X)$$
$$k_2 = z_A(z_B + z_X)^2(z_A + z_X)^{-1}$$
$$k_3 = \tfrac{1}{2}z_A z_B z_X(z_A - z_B)^2(z_A + z_X)^{-1}$$
$$k_4 = z_A(2z_A - z_B + z_X)$$
$$k_5 = z_B(z_A + z_X)^2(z_B + z_X)^{-1}$$
$$k_6 = \tfrac{1}{2}z_A z_B z_X(z_B - z_A)^2(z_B + z_X)^{-1}$$

and I is the ionic strength of the solution.

The procedure is therefore to determine $\gamma_{\pm AX}^{(BX)}$ and $\gamma_{\pm BX}^{(AX)}$ in terms of $\gamma_{\pm AX}$ and $\gamma_{\pm BX}$ over the ionic strength range covered by the isotherm solutions. Then, by analogy with equation (2.24),

$$\ln \Gamma = \frac{1}{z_X}\left[z_A(z_B + z_X)\ln\gamma_{\pm BX}^{(AX)} - z_B(z_A + z_X)\ln\gamma_{\pm AX}^{(BX)}\right] \quad ....(2.27)$$

- 45 -

2.1.4. Determination of Zeolite Phase Activity Coefficients

In the rigorous formulation by Gaines and Thomas[75], for the three phase system to be at equilibrium, it must be true first that

$$\mu_W(v) = \mu_W(s) = \mu_W(c) = \mu_W^{\ominus}(c) + RT \ln a_W(c) \qquad ....(2.28)$$

Also, in addition to the temperature and pressure being equal,

$$\mu_A(s) = \mu_A(c) = \mu_A^{\ominus}(c) + RT \ln a_A(c) = \mu_A^{\ominus}(c) + RT \ln(A_c f_A)$$

$$....(2.29)$$

and

$$\mu_B(s) = \mu_B(c) = \mu_B^{\ominus}(c) + RT \ln a_B(c) = \mu_B^{\ominus}(c) + RT \ln(B_c f_B)$$

$$....(2.30)$$

At constant temperature and pressure, the Gibbs-Duhem equation is

$$\sum_i n_i \, d\mu_i = 0 \qquad\qquad ....(2.31)$$

where n_i is the number of moles of the ith component of a particular phase. The equation becomes applicable to the exchanger phase if,

(i) all the components in the exchanger which affect the equilibrium are included in the summation

(ii) salt imbibition is negligible

(iii) the exchanger contains a constant number of exchange sites.

Combining the equations (2.28), (2.29), (2.30) and (2.31),

$$n_W RT \, d\ln a_W(c) + n_A RT d\ln A_c f_A + n_B RT d\ln B_c f_B = 0 \qquad ....(2.32)$$

Cancelling the RT terms and multiplying throughout by $z_A z_B /$ $(z_A n_A + z_B n_B)$, subject to the condition that $A_c + B_c = 1$ where

$A_c = z_A n_A / (z_A n_A + z_B n_B)$ and $B_c = z_B n_B / (z_A n_A + z_B n_B)$ gives

an expression in terms of equivalent fractions of ions in the

zeolite as shown below;

$$\nu_w \cdot z_A z_B \, dlna_w(c) + z_B A_c \, dlnA_c f_A + z_A B_c \, dlnB_c f_B = 0$$

$$\ldots (2.33)$$

simplification and separation of logarithmic terms gives

$$\nu_w \cdot z_A z_B \, dlna_w(c) + z_B dA_c + z_A dB_c + A_c dlnf_A^{z_B} + B_c dlnf_B^{z_A} = 0$$

$$\ldots (2.34)$$

where $\quad \nu_w = n_w / (z_A n_A + z_B n_B)$

From equation (2.20)

$$dlnK_c + dlnf_A^{z_B} - dlnf_B^{z_A} = 0 \qquad \ldots (2.35)$$

By combining equations (2.34) and (2.35), explicit expressions

for f_A and f_B can be derived by eliminating either f_A or f_B.

$$dlnf_A^{z_B} = (z_B - z_A)dB_c - B_c dlnK_c - \nu_w z_A z_B dlna_w(c) \qquad \ldots (2.36)$$

$$dlnf_B^{z_A} = (z_A - z_B)dA_c + A_c dlnK_c - \nu_w z_A z_B dlna_w(c) \qquad \ldots (2.37)$$

Gaines and Thomas evaluated these expressions by integrating

between standard states and a value of A_c. For f_A, the

integration is between $f_A^{z_B} = A_c = 1$ and $f_A^{z_B}$ at A_c. It has

been shown that the water activity term is negligible for the

zeolite phase[60], and this means that $f_A^{z_B} = 1$ at $A_c = 1$ even

when the concentration of ions in the solution phase is not

zero. This simplifies the integration path[61], and equation

(2.36) becomes

- 47 -

$$\int\limits_{f_A = A_c = 1}^{f_A(A_c)} d\ln f_A^{z_B} = (z_B - z_A) \int\limits_{1,0}^{A_c, B_c} dB_c - \int\limits_{K_c(A_c=1)}^{K_c(A_c)} (1-A_c)d\ln K_c$$

$$....(2.38)$$

giving

$$\ln f_A^{z_B} = (z_B - z_A)B_c - \int\limits_{K_c(A_c=1)}^{K_c(A_c)} (1-A_c)d\ln K_c \qquad ....(2.39)$$

This integral can be transformed since

$$\int (1 - A_c)d\ln K_c = (1 - A_c)\ln K_c - \int \ln K_c d(1-A_c) \qquad ....(2.40)$$

If $\ln K_c^{(A_c)}$ is the value of $\ln K_c$ at A_c, then

$$\ln f_A^{z_B} = (z_B - z_A)B_c - (1 - A_c)\ln K_c^{(A_c)} + \int\limits_{A_c}^{1} \ln K_c dA_c$$

$$....(2.41)$$

and

$$\ln f_B^{z_A} = (z_A - z_B)A_c + A_c\ln K_c^{(A_c)} - \int\limits_{0}^{A_c} \ln K_c dA_c \qquad ....(2.42)$$

substituting equations (2.41) and (2.42) in equation (2.20) gives

$$\ln K_a = (z_B - z_A) + \int\limits_{0}^{1} \ln K_c dA_c \qquad ....(2.43)$$

This equation allows the thermodynamic equilibrium constant to be evaluated from isotherm data by integration of the plot of $\ln K_c$ against A_c over the complete range of A_c values from 0 to 1.

2.1.5. Dielectric Theory

Dielectric theory has been used to rationalize ion-exchange affinities[18,23,25,73,81]. The reversible work w necessary to create a charge z_e on a sphere of radius r placed in a medium of permittivity ε is[82]

$$w = \frac{z^2 . e^2}{8\pi r \varepsilon} \qquad \qquad ....(2.44)$$

where e is the charge of one electron (1.602×10^{-18} As), and ε is obtained from the relationship $\varepsilon = \varepsilon_r . \varepsilon_o$ where ε_r is the relative permittivity (previously known as the "dielectric constant") and ε_o is the permittivity of free space (8.854×10^{-12} $A^2 s^4 kg^{-1} m^{-3}$ = $CV^{-1} m^{-1}$).

The Helmholtz free energy of charge formation may be equated to the reversible work function and since for a condensed phase reaction the work of expansion tends to zero (i.e. $pV \longrightarrow 0$),

$$w = G \sim F \qquad \qquad ....(2.45)$$

from the relationships

$$G = H - TS \qquad \qquad ....(2.46a)$$
$$F = U - TS \qquad \qquad ....(2.46b)$$
$$H = U + pV \qquad \qquad ....(2.46c)$$

where G is the Gibbs free energy of charge formation. For the ion-exchange equilibrium represented by the equation

$$z_B A^{z_A +}_{(s)} + z_A B^{z_B +}_{(c)} \rightleftharpoons z_B A^{z_A +}_{(c)} + z_A B^{z_B +}_{(s)} \qquad ....(2.1)$$
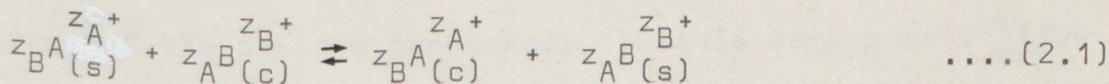
$$\Delta G = \left[z_B G_A(c) + z_A G_B(s) \right] - \left[z_B G_A(s) + z_A G_B(c) \right] \qquad ....(2.47)$$

If the values of G in the equation correspond to the work of

charge formation of the individual ions $A^{z_A^+}$ and $B^{z_B^+}$ in their standard states in both the crystal and solution phases, then ΔG becomes a standard free energy change. Then, per mole of exchange,

$$G^{\ominus} = \frac{N z^2 e^2}{8\pi r \varepsilon} \qquad \qquad \dots(2.48)$$

where N is the Avagadro constant (6.023×10^{-23} molecules).

Thus, for the above binary exchange

$$\Delta G^{\ominus} = \left[z_B G_A^{\ominus}(c) + z_A G_B^{\ominus}(s) \right] - \left[z_B G_A^{\ominus}(s) + z_A G_B^{\ominus}(c) \right] \qquad \dots(2.49)$$

$$= \frac{N e^2}{8\pi} \left[\frac{z_B z_A^2}{r_A \varepsilon_A(c)} + \frac{z_A z_B^2}{r_B \varepsilon_B(s)} - \frac{z_B z_A^2}{r_A \varepsilon_A(s)} - \frac{z_A z_B^2}{r_B \varepsilon_B(c)} \right]$$

$$\dots(2.50)$$

Therefore, per equivalent of exchange,

$$\Delta G^{\ominus} = \frac{N e^2}{8\pi} \left[\frac{z_A}{r_A \varepsilon_A(c)} + \frac{z_B}{r_B \varepsilon_B(s)} - \frac{z_A}{r_A \varepsilon_A(s)} - \frac{z_B}{r_B \varepsilon_B(c)} \right]$$

$$\dots(2.51)$$

Certain ion-exchange phenomena can be explained in terms of simple parameters by using dielectric theory. For example, Barrer, Rees and Shamsuzzoha[23] explained the selectivity sequence for the Ca/Na, Sr/Na and Ba/Na uni-divalent exchanges in zeolite X in terms of the influence of ionic radii and charge of the cations concerned. In this semi-quantitative sequence they assumed that

(i) $\varepsilon_A(c) \sim \varepsilon_B(c) = \varepsilon(c)$ $\qquad \qquad \dots(2.52a)$

(ii) $\varepsilon_A(s) \sim \varepsilon_B(s) = \varepsilon(s)$ $\qquad \qquad \dots(2.52b)$

Then, for uni-divalent exchange where the divalent ion A^{2+} is the ingoing ion,

$$\Delta G^{\ominus} = \frac{Ne^2}{8\pi} \left[\left(\frac{2}{r_A} - \frac{1}{r_B} \right) \left(\frac{1}{\varepsilon(c)} - \frac{1}{\varepsilon(s)} \right) \right] \qquad ...(2.53)$$

For all experimentally determined values it was true that[23]

$$\varepsilon(c) < \varepsilon(s)$$

and therefore,

$$\left(\frac{1}{\varepsilon(c)} - \frac{1}{\varepsilon(s)} \right) > 0 \qquad ....(2.54)$$

For the zeolite to be selective for ion A^{2+} over ion B^+, $\Delta G^{\ominus}$ should be negative, and therefore,

$$\left(\frac{2}{r_A} - \frac{1}{r_B} \right) < 0 \qquad ....(2.55)$$

or

$$r_A > 2r_B$$

Thus, the radius of the divalent entering ion should be at least twice that of the outgoing univalent to meet the above requirement. If the same argument is applied to uni-univalent exchange, the condition for $\Delta G^{\ominus}$ to be negative is

$$r_A > r_B .$$

The observed cation affinity sequence for zeolite X, based on $\Delta G^{\ominus}$ values is[23],

$$Li^+ < Na^+ < Ca^{2+} = K^+ < Sr^{2+} = Cs^+ < Ba^{2+} < Rb^+$$
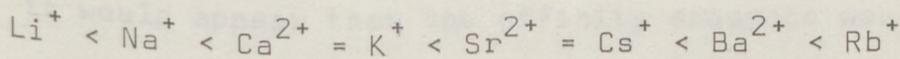
The ionic radii of these ions and Ag are shown in Table 2.1[83]. Therefore, the ion size sequence is

- 51 -

$$Li^+ < Na^+ < Ca^{2+} < Sr^{2+} < K^+ < Ba^{2+} < Rb^+ < Cs^{2+}$$
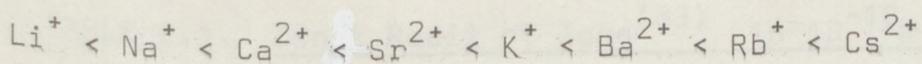
and it is apparent that the affinity sequence is in close agreement with the ion size sequence. It must be noted, however, that selectivity sequences based on standard free energy changes should be used only as a guide towards understanding the ion exchange behaviour because in a real system selectivities may very well be reversed as actual ΔG values depend on prevalent conditions, which in turn are a function of the non-ideality of the system. The above treatment was also used by Barrer and Townsend[72] to rationalize the thermodynamic affinity sequence for the exchange of Mn^{2+}, Co^{2+}, Ni^{2+}, Cu^{2+} and Zn^{2+} in synthetic ammonium mordenite.

In another use of the dielectric theory, Barrer and Klinowski[81] discussed uni-univalent and uni-divalent ion-exchange patterns for two isostructural zeolites in terms of their different framework charge densities. Earlier observations which gave rise to the general conclusion that "the ion of larger crystallographic radius is preferred by the zeolite of lower charge density over the entire range of exchanger composition" were justified by the dielectric approach.

Considering the ion size sequence for the univalent ions under investigation in this project, *viz*

$$Li^+ < Na^+ < Ag^+ < K^+,$$
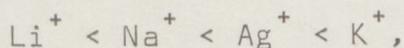
it would appear that the affinity sequence would follow a similar pattern. However, factors like the polarisability and the hydrated radii of cations could significantly alter this affinity sequence. Fletcher and Townsend[73,84] discuss the

TABLE 2.1. Ionic Radii of Ions[83] in 10^{-10}m

Ion	Goldschmidt radius	Pauling radius	Ladd radius	Hydrated radius
Li$^+$	0.78	0.60	0.86	3.40
Na$^+$	0.98	0.95	1.12	2.76
K$^+$	1.33	1.33	1.44	2.32
Rb$^+$	1.49	1.48	1.58	2.28
Cs$^+$	1.65	1.69	1.84	2.28
Ag$^+$	1.13	1.26	1.27	
Ca^{2+}	1.06	0.99	1.18	
Sr^{2+}	1.27	1.13	1.32	
Ba^{2+}	1.43	1.35	1.49	

effect of the high polarisability of the silver (I) ion on
the permittivity of the medium and argue that the assumption
$\varepsilon_{Na}(c) \sim \varepsilon_{Ag}(c)$ and $\varepsilon_{Na}(s) \sim \varepsilon_{Ag}(s)$ (See equations (2.52a &
b)) are unjustified for exchange involving sodium and silver.
Rearranging equation (2.51) to give

$$\Delta G^{\ominus} = \frac{N_3^2}{8\pi r_{Ag} r_{Na}} \left[\left(\frac{r_{Na}}{\varepsilon_{Ag}(c)} - \frac{r_{Ag}}{\varepsilon_{Na}(c)} \right) - \left(\frac{r_{Na}}{\varepsilon_{Ag}(s)} - \frac{r_{Ag}}{\varepsilon_{Na}(s)} \right) \right]$$

$$....(2.51)'$$

Since the polarisability of silver is higher than that of
sodium, it follows that

$\varepsilon_{Ag}(c) > \varepsilon_{Na}(c)$ and $\varepsilon_{Ag}(s) > \varepsilon_{Na}(s)$.   Therefore since
$r_{Ag} > r_{Na}$, the terms within the parentheses are negative.   This

means that the criterion for $\Delta G^{\ominus}$ to be negative is not simply the relative magnitudes of the radii, but the relative magnitudes of the terms in parentheses; *viz*

if

$$\left(\frac{r_{Na}}{\epsilon_{Ag}(c)} - \frac{r_{Ag}}{\epsilon_{Na}(c)} \right) > \left(\frac{r_{Na}}{\epsilon_{Ag}(c)} - \frac{r_{Ag}}{\epsilon_{Na}(s)} \right), \quad \text{then } \Delta G^{\ominus} < 0$$

This would easily explain why the real cation affinity sequence might be in the opposite direction to that suggested by the ionic radii.

2.2. TERNARY ION EXCHANGE

Exchange involving three ions is the main concern of this research project. The experimental procedure was to begin with two types of ions initially present in the solution phase and the third type alone present in the zeolite phase. For the theoretical treatment, however, the opposite case is taken as the starting point for the ion exchange reaction (the choice is of course immaterial only affecting the sign but not the magnitude of the standard free energy of exchange). Three equations may then be written for the three ion exchange situations involving ions $A^{z_A^+}$, $B^{z_B^+}$ and $C^{z_C^+}$, which are

$$2z_B z_C A^{z_A^+}_{(s)} + z_A z_C B^{z_B^+}_{(c)} + z_A z_B C^{z_C^+}_{(c)} \rightleftharpoons 2z_B z_C A^{z_A^+}_{(c)} + z_A z_C B^{z_B^+}_{(s)} + z_A z_B C^{z_C^+}_{(s)}$$

$$....(2.56)$$

$$z_B z_C A^{z_A^+}_{(c)} + 2z_A z_C B^{z_B^+}_{(s)} + z_A z_B C^{z_C^+}_{(c)} \rightleftharpoons z_B z_C A^{z_A^+}_{(s)} + 2z_A z_C B^{z_B^+}_{(c)} + z_A z_B C^{z_C^+}_{(s)}$$

$$....(2.57)$$

$$z_B z_C A^{z_A^+}_{(c)} + z_A z_C B^{z_B^+}_{(c)} + 2z_A z_B C^{z_C^+}_{(s)} \rightleftharpoons z_B z_C A^{z_A^+}_{(s)} + z_A z_C B^{z_B^+}_{(s)} + 2z_A z_B C^{z_C^+}_{(c)}$$

$$....(2.58)$$
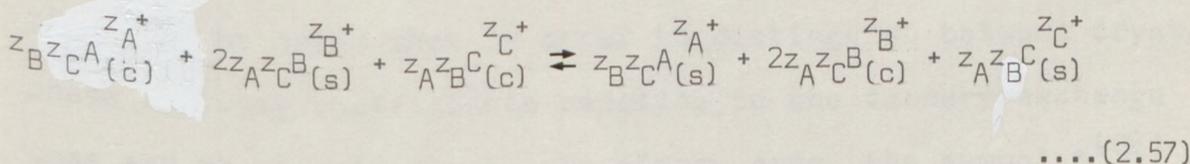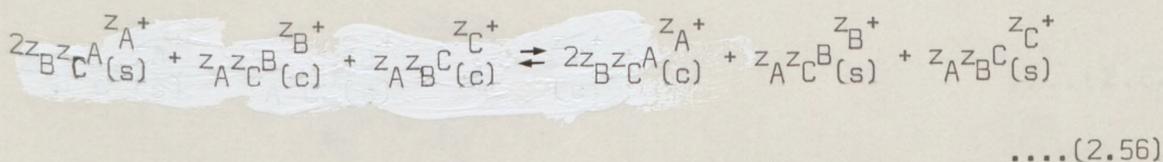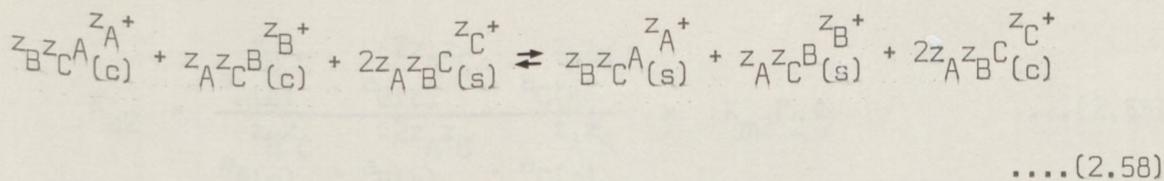
If the thermodynamic equilibrium constants corresponding to the above three equations are K_{a1}, K_{a2} and K_{a3} respectively, then [85]

$$K_{a1} = \frac{a_{A(c)}^{2z_B z_C} \cdot a_{B(s)}^{z_A z_C} \cdot a_{C(s)}^{z_A z_B}}{a_{A(s)}^{2z_B z_C} \cdot a_{B(c)}^{z_A z_C} \cdot a_{C(c)}^{z_A z_B}} = K_{m1} \Gamma_1 \Phi_1 \qquad ....(2.59)$$

where the mass action quotient is

$$K_{m1} = \frac{A_c^{2z_B z_C} \cdot m_B^{z_A z_C} \cdot m_C^{z_A z_B}}{m_A^{2z_B z_C} \cdot B_c^{z_A z_C} \cdot C_c^{z_A z_B}} \qquad ....(2.60)$$

Γ_1 is the ratio of individual ion activity coefficients in the solution phase:

$$\Gamma_1 = \frac{\gamma_B^{z_A z_C} \cdot \gamma_C^{z_A z_B}}{\gamma_A^{2z_B z_C}} \qquad ....(2.61)$$

Similarly, Φ_1 is the ratio of ion activity coefficients in the crystal phase:

$$\Phi_1 = \frac{\phi_A^{2z_B z_C}}{\phi_B^{z_A z_C} \cdot \phi_C^{z_A z_B}} \qquad ....(2.62)$$

It should be noted that in order to distinguish between crystal phase activity coefficients relating to the ternary exchange case and those relating to the binary case, the symbol ϕ [85] is used for the former case instead of f.

Similar equations are obtained to define K_{a2} and K_{a3}:

$$K_{a2} = \frac{a_{A(s)}^{z_B z_C} \cdot a_{B(c)}^{2z_A z_C} \cdot a_{C(s)}^{z_A z_B}}{a_{A(c)}^{z_B z_C} \cdot a_{B(s)}^{2z_A z_C} \cdot a_{C(c)}^{z_A z_B}} = K_{m2} \Gamma_2 \Phi_2 \qquad \qquad ....(2.63)$$

and

$$K_{a3} = \frac{a_{A(s)}^{z_B z_C} \cdot a_{B(s)}^{z_A z_C} \cdot a_{C(c)}^{2z_A z_B}}{a_{A(c)}^{z_B z_C} \cdot a_{B(c)}^{z_A z_C} \cdot a_{C(s)}^{2z_A z_B}} = K_{m3} \Gamma_3 \Phi_3 \qquad \qquad ....(2.64)$$

Then, for example, the free energy change per equivalent of
exchange corresponding to the reaction depicted in equation
(2.56) is

$$\Delta G^{\ominus} = -\left(\frac{RT}{z_A z_B z_C}\right) \ln K_{a1} \qquad \qquad ....(2.65)$$

2.2.1. Prediction of Equilibria

To use a zeolite as a water softening "builder" in a detergent,
it is necessary to know the equilibrium exchange properties of
the system over a range of differing conditions. Of particular
interest are the effects on the equilibrium of changing (i) the
total concentration of salts in solution, (ii) the relative
amounts of different exchangeable cations originally present in
the solution (Na^+, Ca^{2+} and Mg^{2+} in the "builder" context), and
(iii) the temperature.

To reliably predict ion exchange equilibria, it is essential that
an adequate knowledge of the activities of the components
involved in the exchange over the relevant range of conditions
exists; these data may only be supplied with a suitable thermo-
dynamic model.

For binary ion exchange involving zeolites and dilute solutions,

- 56 -

such prediction of ion exchange equilibria is well known[85].
Based on Barrer and Klinowski's conclusions that, at solution
concentrations less than 0.5 mol dm^{-3}, salt imbibition and
the effect of water activities on the value of the thermody-
namic equilibrium constant are negligible[60], and therefore,
that the ratio of zeolite phase activity coefficients should
be invariant with external solution concentrations at any
particular A_c value[60], a means of predicting equilibrium
composition can be established by transforming equations
(2.15) and (2.16) to give (for a particular value of A_c),

$$\left[\frac{m_B^{z_A}}{m_A^{z_B}}\right]r = K_a \left[\frac{f_B^{z_A}}{f_A^{z_B}}\right]\left[\frac{(1 - A_c)^{z_A}}{A_c^{z_B}}\right] = \text{constant} \quad ....(2.66)$$

For binary exchange, the total concentration (equiv.dm^{-3}) of
the solution, T_N is related to m_A and m_B by the equation

$$z_A m_A + z_B m_B = T_N \quad ....(2.7)$$

Fletcher and Townsend demonstrated how these two equations can
be used to graphically predict values of m_A in solution for any
given A_c value over a range of T_N values for which activity
coefficient data are known[85]. Using the same approach for
ternary ion exchange where salt imbibition and water activity
terms are ignored, equations (2.59) and (2.60) can be trans-
formed to give (for particular values of A_c and B_c),

$$\left[\frac{m_B^{z_A z_C} \cdot m_C^{z_A z_B}}{m_A^{2 z_B z_C}} \right] \Gamma_1 = K_{a1} \cdot \frac{1}{\phi_1} \left[\frac{B_c^{z_A z_C} (1-A_c-B_c)^{z_A z_B}}{A_c^{2 z_B z_C}} \right] = \text{constant}$$

$$....(2.67)$$

Also, for ternary ion exchange,

$$z_A m_A + z_B m_B + z_C m_C = T_N \qquad ....(2.68)$$

Unlike the binary case, however, these two equations are not adequate to predict the equilibrium solution phase composition even though the zeolite phase composition has been fully defined by the chosen values of A_c and B_c. This is because several solutions may coexist that can satisfy the two equations. In order to determine the correct solution, therefore, a third equation is necessary, and Fletcher and Townsend provide the additional constraints by utilising equations defined in terms of K_{a2} and K_{a3}[85]. For example

$$\left[\frac{m_A^{z_B z_C} \cdot m_C^{z_A z_B}}{m_B^{2 z_A z_C}} \right] \Gamma_2 = K_{a2} \cdot \frac{1}{\phi_2} \left[\frac{A_c^{z_B z_C} (1-A_c-B_c)^{z_A z_B}}{B_c^{2 z_A z_C}} \right] = \text{constant}$$

$$....(2.69)$$

Fletcher and Townsend discuss the requirements for successfully predicting ternary equilibrium compositions, and emphasise the need to use a thermodynamic model which allows reliable values for ϕ_A, ϕ_B and ϕ_C to be evaluated solely from experimental measurements[85]. These values of ϕ_A, ϕ_B and ϕ_C could then be used to determine K_{a1}, K_{a2} and K_{a3} values. The phenomenological model recently put forward by Fletcher and

Townsend[85-88], applicable directly to ternary ion exchange in zeolites, attempts to provide this information.

2.2.2. Dissimilarities to the Binary Treatment

In order to rationalise the treatment of ion exchange systems, attempts have been made to predict ternary ion exchange equilibria using the corresponding binary equilibrium data. The difficulty here is that ternary systems involve parameters which are dissimilar to the binary ones on account of the presence of the extra ions in the system, and the resulting inter-ion effects. To examine this aspect closely, one can use equations (2.59) and (2.63) which define K_{a1} and K_{a2}, two of the thermodynamic equilibrium constants for ternary exchange. Dividing K_{a1} by K_{a2},

$$\frac{a_{B(s)}^{3z_A z_C} \cdot a_{A(c)}^{3z_B z_C}}{a_{B(c)}^{3z_A z_C} \cdot a_{A(s)}^{3z_B z_C}} = \frac{K_{a1}}{K_{a2}} \quad \ldots (2.70)$$

Therefore,

$$\frac{a_{B(s)}^{z_A} \cdot a_{A(c)}^{z_B}}{a_{B(c)}^{z_A} \cdot a_{A(s)}^{z_B}} = \left[\frac{K_{a1}}{K_{a2}}\right]^{1/3z_C} \quad \ldots (2.71)$$

A comparison with equation (2.13) for the binary exchange shows that the ratios of activities in the two equations are identical.

$$\frac{a_{B(s)}^{z_A} \cdot a_{A(c)}^{z_B}}{a_{B(c)}^{z_A} \cdot a_{A(s)}^{z_B}} = K_a \quad \ldots (2.13)$$

On expanding these two equations, however, it becomes apparent why the equilibrium constants may not be equated.

$$K_a = \left[\frac{a_{B(s)}^{z_A}}{a_{A(s)}^{z_B}} \right] \left[\frac{A_c^{z_B} \cdot f_A^{z_B}}{B_c^{z_A} \cdot f_B^{z_A}} \right] \qquad \ldots.(2.72)$$

$$\left[\frac{K_{a1}}{K_{a2}} \right]^{1/3z_C} = \left[\frac{a_{B(s)}^{z_A}}{a_{A(s)}^{z_B}} \right] \left[\frac{A_c^{z_B} \cdot \phi_A^{z_B}}{B_c^{z_A} \cdot \phi_B^{z_A}} \right] \qquad \ldots.(2.73)$$

The crystal phase activity coefficients in these two equations are not identical. For the ternary case, the activity coefficient of one cation is influenced by *two* other cations (i.e. $A_c = 1 - B_c - C_c$), while for the binary case, each cation activity coefficient is influenced by only *one* other cation. Thus ϕ_A may not be similar to f_A for the same A_c value. The same rationale applies to the solution phase activity coefficients where the influence of the third cation and the accompanying anions in solution must be accounted for in the ternary case. Thus, for a given A_s value, γ_A for a ternary system may be different from γ_A for a corresponding binary system.

The Fletcher-Townsend thermodynamic model avoids these problems by applying theory directly to the ternary ion exchange system, in a similar fashion to that used by Gaines and Thomas when formulating their treatment for binary ion exchange. The model derives directly the crystal phase activity coefficients ϕ_A,

- 60 -

ϕ_B, ϕ_C using the Gibbs-Duhem equations and experimental data that are determined from the ternary exchange equilibrium at a given temperature.

2.2.3. The Equilibrium Conditions

The basis for the treatment[86] is similar to that of the binary case. The exchange system, consisting of the three phases vapour, liquid and crystal (zeolite), is taken as closed. By neglecting salt imbibition (see section 2.1.2), the exchange capacity of the zeolite may be assumed to be constant:

$$z_A dn_{A(c)} + z_B dn_{B(c)} + z_C dn_{C(c)} = 0 \qquad \ldots\ldots(2.74)$$

and because the system is closed

$$dn_{A(s)} + dn_{A(c)} = 0 \qquad \ldots\ldots(2.75a)$$

$$dn_{B(s)} + dn_{B(c)} = 0 \qquad \ldots\ldots(2.75b)$$

$$dn_{C(s)} + dn_{C(c)} = 0 \qquad \ldots\ldots(2.75c)$$

and

$$dn_{w(v)} + dn_{w(s)} + dn_{w(c)} = 0 \qquad \ldots\ldots(2.75d)$$

where n refers to the number of moles of the respective component and (v), (s) and (c) refer to vapour, solution and crystal phase respectively.

In Barrer and Klinowski's work[60] on the effect of variations in exchanger composition on water activity terms, they showed that, although the values of the individual integrals that

make up the water term in the expression for the equilib-
rium constant may be large, "because their signs are opposite,
their sums are therefore small"[60]. It is very likely there-
fore, that these findings for the binary case would be equally
valid for ternary ion exchange in zeolites, and the water
activity terms could be ignored. However, for completeness
and because the zeolite phase reference states are defined so
as to conform with Gaines and Thomas' treatment for binary
exchange[75], the water terms were included in the thermodyn-
amic model.

From equations (2.74) - (2.75c), it follows that

$$z_A dn_{A(s)} + z_B dn_{B(s)} + z_C dn_{C(s)} = 0 \qquad \dots (2.76)$$

Subject to the constraints defined by equations (2.75a) -
(2.75d), changes in the Gibbs free energy of the system is
governed by[78,89]

$$dG = dG(v) + dG(s) + dG(c) = Vdp - SdT + \sum_{\substack{all \\ phases}} (\sum_i \mu_i dn_i)$$

$$\dots (2.77)$$

where V and S refer to the volume and entropy of the closed
system and μ_i and n_i refer to the chemical potential and number
of moles of the ith independent component.

For the equilibria described by equations (2.56), (2.57) and
(2.58), at constant temperature and pressure, the relationships
between the chemical potentials in the respective phases are
therefore[86]

$$\mu_{w(v)} = \mu_{w(s)} = \mu_{w(c)} \qquad \dots (2.78)$$

and

$$z_B(\mu_{A(c)} - \mu_{C(c)}) + (z_C - z_A)\mu_{B(c)} = z_B(\mu_{A(s)} - \mu_{C(s)}) + (z_C - z_A)\mu_{B(s)}$$

$$\dots\dots(2.79)$$

Considering for example, ion A$^{z_A+}$, the chemical potentials were then defined in conformity with the Gaines and Thomas approach (75) as,

$$\mu_{A(s)} = \mu^{\ominus}_{A(s)} + RT \ln\left[m_{A(s)}\gamma_A\right] \qquad \dots\dots(2.80)$$

and

$$\mu_{A(c)} = \mu^{\ominus}_{A(c)} + RT \ln\left[A_c\phi_A\right] \qquad \dots\dots(2.81)$$

For water, at equilibrium

$$\mu_{w(v)} = \mu_{w(s)} = \mu_{w(c)} = \mu^{\ominus}_{w(c)} + RT \ln a_{w(c)} \qquad \dots\dots(2.82)$$

where a_w is the activity of water.

The conditions for equilibrium within one phase are defined by the Gibbs-Duhem equation

$$SdT - Vdp + \sum_i n_i d\mu_i = 0 \qquad \dots\dots(2.83)$$

For the crystal (zeolite) phase, at constant temperature and pressure,

$$\sum_i n_i d\mu_i = n_w d\mu_w + n_A d\mu_A + n_B d\mu_B + n_C d\mu_C = 0 \qquad \dots\dots(2.84)$$

Therefore

$$n_w d\ln a_w + n_A d\ln A_c\phi_A + n_B d\ln B_c\phi_B + n_C d\ln C_c\phi_C = 0 \dots\dots(2.85)$$

Multiplication of this equation throughout by

$$z_A z_B z_C/(z_A n_A + z_B n_B + z_C n_C) \qquad \dots\dots(2.86)$$

gives

$$z_A z_B z_C \nu_w d\ln a_w + z_B z_C A_c d\ln A_c \phi_A + z_A z_C B_c d\ln B_c \phi_B + z_A z_B C_c d\ln C_c \phi_C = 0$$

....(2.87)

where

$$\nu_w = \frac{n_w}{\sum\limits_{i=A}^{C} z_i n_i} \quad \text{(i.e. water content of one "exchange equivalent" of zeolite}^{(75)}\text{)}$$

since by definition

$$\frac{z_A n_A}{\sum\limits_{i=A}^{C} z_i n_i} = A_c \quad \text{etc.} \qquad \text{....(2.88)}$$

It therefore follows from

$$A_c + B_c + C_c = 1 \qquad \text{....(2.89)}$$

that

$$dC_c = -dA_c - dB_c \qquad \text{....(2.90)}$$

Furthermore, from

$$d\ln C_c = \frac{1}{C_c} dC_c \quad \text{etc.} \qquad \text{....(2.91)}$$

it follows that

$$C_c d\ln C_c = dC_c \quad \text{etc.} \qquad \text{....(2.92)}$$

Therefore, equation (2.87) becomes after simplification and substitution

$$z_A z_B z_C \nu_w d\ln a_w + z_B z_C (dA_c + A_c d\ln\phi_A) + z_A z_C (dB_c + B_c d\ln\phi_B)$$

$$+ z_A z_B (dC_c + C_c d\ln\phi_C) = 0 \qquad \text{....(2.93)}$$

and then eliminating the dC_c terms,

$$z_A z_B z_C \nu_w d\ln a_w + z_B (z_C - z_A) dA_c + z_A (z_C - z_B) dB_c + A_c d\ln\phi_A{}^{z_B z_C}$$

$$+ B_c d\ln\phi_B{}^{z_A z_C} + C_c d\ln\phi_C{}^{z_A z_B} = 0$$

....(2.94)

- 64 -

For the three ion exchange equilibria depicted by equations (2.56), (2.57) and (2.58), it is possible to define a set of quotients, which contain activity corrections only for the solution phase. These corrected selectivity quotients, also known as Kielland quotients[79], are[86]

$$K_{c1} = \frac{A_c^{2z_B z_C} \cdot a_{B(s)}^{z_A z_C} \cdot a_{C(s)}^{z_A z_B}}{a_{A(s)}^{2z_B z_C} \cdot B_c^{z_A z_C} \cdot C_c^{z_A z_B}} \qquad \ldots(2.95)$$

$$K_{c2} = \frac{a_{A(s)}^{z_B z_C} \cdot B_c^{2z_A z_C} \cdot a_{C(s)}^{z_A z_B}}{A_c^{z_B z_C} \cdot a_{B(s)}^{2z_A z_C} \cdot C_c^{z_A z_B}} \qquad \ldots(2.96)$$

$$K_{c3} = \frac{a_{A(s)}^{z_B z_C} \cdot a_{B(s)}^{z_A z_C} \cdot C_c^{2z_A z_B}}{A_c^{z_B z_C} \cdot B_c^{z_A z_C} \cdot a_{C(s)}^{2z_A z_B}} \qquad \ldots(2.97)$$

From equations (2.59),(2.63) and (2.64) which define the thermo-dynamic equilibrium constants it follows that

$$\ln K_{a1} = \ln K_{c1} + 2\ln\phi_A^{z_B z_C} - \ln\phi_B^{z_A z_C} - \ln\phi_C^{z_A z_B}$$
$$\ldots(2.98)$$

$$\ln K_{a2} = \ln K_{c2} + 2\ln\phi_B^{z_A z_C} - \ln\phi_A^{z_B z_C} - \ln\phi_C^{z_A z_B}$$
$$\ldots(2.99)$$

$$\ln K_{a3} = \ln K_{c3} + 2\ln\phi_C^{z_A z_B} - \ln\phi_A^{z_B z_C} - \ln\phi_B^{z_A z_C}$$
$$\ldots(2.100)$$

On differentiating these equations we obtain[86]

$$d\ln K_{c1} + d\ln\phi_A^{2z_B z_C} - d\ln\phi_B^{z_A z_C} - d\ln\phi_C^{z_A z_B} = 0$$
$$\ldots(2.101)$$

$$\text{dlnK}_{c2} + \text{dln}\phi_B{}^{2z_A z_C} - \text{dln}\phi_A{}^{z_B z_C} - \text{dln}\phi_C{}^{z_A z_B} = 0 \qquad \ldots.(2.102)$$

$$\text{dlnK}_{c3} + \text{dln}\phi_C{}^{2z_A z_B} - \text{dln}\phi_A{}^{z_B z_C} - \text{dln}\phi_B{}^{z_A z_C} = 0 \qquad \ldots.(2.103)$$

These three equations, used in conjunction with equation (2.94) give explicit expressions for the three crystal phase activity coefficients ϕ_A, ϕ_B and ϕ_C.

2.2.4. Determination of Zeolite Phase Activity Coefficients

Subtracting equation (2.101) from equation (2.102), and re-arranging gives

$$\text{dln}\phi_A{}^{3z_B z_C} = \text{dlnK}_{c2} - \text{dlnK}_{c1} + \text{dln}\phi_B{}^{3z_A z_C} \qquad \ldots.(2.104)$$

Similar procedures yield

$$\text{dln}\phi_B{}^{3z_A z_C} = \text{dlnK}_{c3} - \text{dlnK}_{c2} + \text{dln}\phi_C{}^{3z_A z_B} \qquad \ldots.(2.105)$$

and

$$\text{dln}\phi_C{}^{3z_A z_B} = \text{dlnK}_{c1} - \text{dlnK}_{c3} + \text{dln}\phi_A{}^{3z_B z_C} \qquad \ldots.(2.106)$$

Substituting equations (2.105) and (2.106) into equation (2.94) gives explicit expression for ϕ_A:

$$\text{dln}\phi_A{}^{z_B z_C} = \frac{1}{3} \left[(A_c - 1)\text{dlnK}_{c1} + B_c \text{dlnK}_{c2} + C_c \text{dlnK}_{c3} \right] - \Psi$$

$$\ldots.(2.107)$$

where $\Psi = z_B(z_C - z_A)dA_c + z_A(z_C - z_B)dB_c + z_A z_B z_C \nu_w \text{dln}a_w$

$$\ldots.(2.108)$$

Similar procedure leads to

- 66 -

$$d\ln\phi_B{}^{z_A z_C} = \frac{1}{3}\left[A_c d\ln K_{c1} + (B_c - 1)d\ln K_{c2} + C_c d\ln K_{c3}\right] - \Psi$$

$$....(2.109)$$

$$d\ln\phi_C{}^{z_A z_B} = \frac{1}{3}\left[A_c d\ln K_{c1} + B_c d\ln K_{c2} + (C_c - 1)d\ln K_{c3}\right] - \Psi$$

$$....(2.110)$$

In order to integrate equations (2.107) - (2.110) the standard states must be specified. In keeping with Gaines and Thomas definitions for binary exchange[75], Fletcher and Townsend define the reference states for the zeolite phase in terms of the homoionic forms[86]. This results in *three* reference states for ternary exchange, involving either pure A-, or pure B-, or pure C- zeolite. They specify the state of the water in the homoionic zeolites as follows[86]: For the external solution phase, the activity of the water is defined as being unity when only pure solvent is present; in order for the activity of the water also to be unity in the standard states for the zeolite phase, each of the pure zeolites in their standard states must therefore be immersed in infinitely dilute solutions of the corresponding ion.

Fletcher and Townsend define the *three* reference states for the solution phase in terms of Henry's law as the hypothetical ideal molar (mol dm^{-3}) solutions of pure salts of the three cations.

Ion exchange equilibria are experimentally measured by immersing the zeolite in a solution of known constant concentration (equiv.dm^{-3}) in which the activities of the ions and the water are not equal to one. For example, ϕ_A (for pure A-zeolite) will not be unity if the water activity is also not unity in

the crystal, even though the zeolite is still in its pure form. Fletcher and Townsend illustrate this point diagramatically (Figure 2.8), where the first step in the integration is from $a_w = 1$ to $a_{w(a)}$ at a *constant* composition of $A_c = 1$, $B_c = C_c = 0$, where $a_{w(a)}$ is the water activity in the pure A-zeolite immersed in a pure A-salt solution at the experimental concentration[86]. This first integration is then followed by a second step across a surface[86] which defines the composition of the zeolite phase (Figure 2.8) to the experimental composition A_c, B_c and $a_{w(A_c,B_c)}$. From equation (2.107) the first integration step is[86]

$$\int_{\phi_A=1}^{\phi_{A(a)}} d\ln\phi_A^{z_B z_C} = \ln\phi_{A(a)}^{z_B z_C} = -z_A z_B z_C \int_{a_w=1}^{a_{w(a)}} (\nu_w^A) d\ln a_w \quad \ldots\ldots(2.111)$$

where the superscript A on ν_w refers to the homoionic A-zeolite. For the more complex next stage the boundary conditions are $\phi_A = \phi_{A(a)}$ at $A_c = 1$, $B_c = 0$, $a_w = a_{w(a)}$ and $0 < \phi_A < \infty$ at $A_c, B_c, a_{w(A_c,B_c)}$ and equation (2.107) gives

$$\int_{\phi_{A(a)}}^{\phi_A(A_c,B_c)} d\ln\phi_A^{z_B z_C} = \int_{K_{c1}(A_c=1)}^{K_{c1}(A_c)} \frac{A_c-1}{3} d\ln K_{c1} + \int_{K_{c2}(B_c=0)}^{K_{c2}(B_c)} \frac{B_c}{3} d\ln K_{c2} + \int_{K_{c3}(C_c=0)}^{K_{c3}(C_c)} \frac{C_c}{3} d\ln K_{c3}$$

$$-z_B(z_C-z_A)\int_1^{A_c} dA_c - z_A(z_C-z_B)\int_0^{B_c} dB_c - z_A z_B z_C \int_{a_w(a)}^{a_{w(A_c,B_c)}} (\nu_w^{ABC}) \, d\ln a_w \quad \ldots\ldots(2.112)$$

- 68 -

where ν_w^{ABC} represents the water content (per exchange equivalent) of the mixed (A,B,C) cationic forms of the zeolite. On adding equations (2.111) and (2.112) and transforming integrals (see Appendix I) we obtain

$$\ln\phi_A^{z_B z_C} = \frac{1}{3}\int_1^{A_c}\left[\ln K_{c3} - \ln K_{c1}\right]dA_c + \frac{1}{3}\int_0^{B_c}\left[\ln K_{c3}-\ln K_{c2}\right]dB_c$$

$$+ \frac{1}{3}\left[(A_c-1)\ln K_{c1} + B_c\ln K_{c2} + C_c\ln K_{c3}\right]-z_B(z_C-z_A)(A_c-1)-z_A(z_C-z_B)B_c$$

$$-z_A z_B z_C\left[\int_{a_w=1}^{a_{w(a)}}(\nu_w^A)d\ln a_w + \int_{a_{w(a)}}^{a_{w(A_c,B_c)}}(\nu_w^{ABC})d\ln a_w\right] \qquad ....(2.113)$$

where the values of K_{c1}, K_{c2} and K_{c3} in the third set of square brackets immediately after the two integral terms are the values of these functions at A_c, B_c [86] (see Appendix I).

For the evaluation of ϕ_B, the boundary conditions are (i) $\phi_B=1$ at $B_c=1, A_c=0, a_w=1$, (ii) $\phi_B=\phi_{B(b)}$ at $B_c=1, A_c=0, a_w=a_{w(b)}$ and (iii) $0<\phi_B<\infty$ at $A_c, B_c, a_{w(A_c,B_c)}$ and integration gives

$$\ln\phi_B^{z_A z_C} = \frac{1}{3}\int_0^{A_c}\left[\ln K_{c3}-\ln K_{c1}\right]dA_c + \frac{1}{3}\int_1^{B_c}\left[\ln K_{c3}-\ln K_{c2}\right]dB_c$$

$$+ \frac{1}{3}\left[A_c\ln K_{c1} + (B_c-1)\ln K_{c2} + C_c\ln K_{c3}\right]-z_B(z_C-z_A)A_c-z_A(z_C-z_B)(B_c-1)$$

$$-z_A z_B z_C\left[\int_{a_w=1}^{a_{w(b)}}(\nu_w^B)d\ln a_w + \int_{a_{w(b)}}^{a_{w(A_c,B_c)}}(\nu_w^{ABC})d\ln a_w\right] \qquad ....(2.114)$$

Similarly, ϕ_C is evaluated by integrating with boundary conditions

(i) $\phi_C = 1$ at $C_c = 1$, $A_c = 0$, $a_w = 1$,

(ii) $\phi_C = \phi_{C(c)}$ at $C_c = 1$, $A_c = 0$, $a_w = a_{w(c)}$ and

(iii) $0 < \phi_C < \infty$ at $A_c, B_c, a_{w(A_c,B_c)}$

$$
\ln\phi_C^{z_A z_B} = \frac{1}{3}\int_0^{A_c}\left[\ln K_{c3} - \ln K_{c1}\right]dA_c + \frac{1}{3}\int_0^{B_c}\left[\ln K_{c3} - \ln K_{c2}\right]dB_c
$$

$$
+ \frac{1}{3}\left[A_c \ln K_{c1} + B_c \ln K_{c2} + (C_c - 1)\ln K_{c3}\right] - z_B(z_C - z_A)A_c - z_A(z_C - z_B)B_c
$$

$$
-z_A z_B z_C\left[\int_{a_w=1}^{a_{w(c)}}(\nu_w^C)d\ln a_w + \int_{a_{w(c)}}^{a_{w(A_c,B_c)}}(\nu_w^{ABC})d\ln a_w\right] \qquad \ldots\ldots(2.115)
$$

The determination of ϕ values is greatly simplified if the water terms can be excluded. It has already been shown that they are insignificant for binary exchanges[60], and Fletcher and Townsend discuss and conclude[86] that the inclusion of water terms only complicate the procedures but do not alter the principles behind the experimental determination of K_a values.

The evaluation of ϕ_A at a particular zeolite composition (A_c, B_c) is therefore achieved by solving integrals. For binary exchange a polynomial of some order[90] has been used to represent the logarithm of the Kielland quotient. Fletcher and Townsend adopt the same approach for ternary exchange, but, for convenience, express the *difference* between the logarithms of two of the

- 70 -

Kielland quotients as a polynomial in both A_c and B_c[86]. The
equations defining the crystal phase activity coefficients may
then be solved in parts. For example, the first integral
term in equation (2.113) becomes[86]

$$\ln\left[\frac{K_{c3}}{K_{c1}}\right] = \ln\left[\frac{K_{c3}}{K_{c1}}\right]_{C_c=1} + \sum_{i=1}^{m} \alpha_i A_c^i + \sum_{j=1}^{n} \beta_j B_c^j \qquad \ldots.(2.116)$$

where α_i, β_j are coefficients in A_c^i, B_c^j respectively. On
integration between the appropriate limits,

$$\int_{1}^{A_c} \ln\left[\frac{K_{c3}}{K_{c1}}\right] dA_c = \int_{0}^{A_c} \ln\left[\frac{K_{c3}}{K_{c1}}\right]_{C_c=1} dA_c + \int_{1}^{A_c} \sum_{i=1}^{m} \alpha_i A_c^i dA_c + \int_{0}^{A_c} \sum_{j=1}^{n} \beta_j B_c^j dA_c$$

$$\ldots.(2.117)$$

$$= (A_c - 1)\alpha_0 + \sum_{i=1}^{m} \frac{\alpha_i}{i+1} \left(A_c^{i+1} - 1^{i+1} \right) + A_c\left[\sum_{j=1}^{n} \beta_j B_c^j\right] \qquad \ldots.(2.118)$$

where $\alpha_0 = \ln(K_{c3}/K_{c1})$ at $C_c=1$. If α_0 is incorporated into the second
term we obtain,

$$\int_{1}^{A_c} \ln\left[\frac{K_{c3}}{K_{c1}}\right] dA_c = \sum_{i=0}^{m} \frac{\alpha_i}{i+1} \left(A_c^{i+1} - 1 \right) + A_c\left[\sum_{j=1}^{n} \beta_j B_c^j\right]$$

$$\ldots.(2.119)$$

Diagramatically, Fletcher and Townsend represent the integral
in this equation by the difference between two surface areas[86]
as shown in Figure 2.9 . By a similar procedure, the second
integral in equation (2.113) is

$$\int_0^{B_c} \ln\left[\frac{K_{e3}}{K_{c2}}\right] dB_c = B_c\left[\sum_{i=1}^{p} \gamma_i A_c^i\right] + \sum_{j=0}^{q}\left[\frac{\delta_j}{j+1}\right] B_c^{j+1}$$

....(2.120)

where γ_i and δ_j are the coefficients of a polynomial describing $\ln(K_{c3}/K_{c2})$ as a function of A_c and B_c, respectively, and $\delta_0 = \ln(K_{c3}/K_{c2})$ at $C_c = 1$.

The procedure for evaluating crystal phase activity coefficients for ternary ion exchange is, therefore simply a matter of taking experimental isotherm data to calculate mass action quotients, and then applying the appropriate solution phase activity corrections to obtain sets of values of $\ln(K_{c3}/K_{c1})$ and $\ln(K_{c3}/K_{c2})$ as functions of both A_c and B_c. Fletcher and Townsend then use a least-squares method to deduce the poly-nomials expressing the dependencies of these functions on A_c and B_c and from there obtain values for the activity coeffic-ients[86]. The convenience of using this model for treating ternary data is that *only* these two polynomial equations are necessary to determine *all* the activity co-efficients and thermodynamic equilibrium constants (see equations (2.113) - (2.115) and (2.166) - (2.168)); the computation procedure for ternary ion exchange is not there-fore greatly more complicated than for its binary counter-part[86].

2.2.5. Determination of Solution Phase Activity Coefficients

For binary ion exchange in zeolites, the ratio of single-ion activity coefficients in solution is evaluated using Glueckauf's

method[80] to calculate the mean molal stoichiometric activity
coefficients of the relevant salts in mixed solution followed
by a subsequent manipulation of these salt activity co-
efficients to obtain the required ratio[74]. For the ternary
case the same approach may be used to calculate the activity
coefficient ratios in solutions containing all three salts.

For the ion exchange equilibria depicted by equations (2.56),
(2.57) and (2.58), the relationship between the mass action
quotient and corrected selectivity (or Kielland) quotient
is given by

$$K_c = K_m \cdot \Gamma \qquad \qquad ....(2.121)$$

where Γ is the appropriate ratio of solution phase single ion
activity coefficients. For example, equation (2.61) gives
the Γ value for the ion exchange equilibrium represented by
equation (2.56).

$$\Gamma_1 = \frac{\gamma_B^{z_A z_C} \cdot \gamma_C^{z_A z_B}}{\gamma_A^{2 z_B z_C}} \qquad \qquad ....(2.61)$$

In the previous section it was shown that crystal phase
activity coefficients ϕ_i were derived in terms of the approp-
riate Kielland coefficients. Therefore, when the water terms
are excluded,

$$\ln\phi_A^{z_B z_C} = \frac{1}{3} \int_1^{A_c} (\ln K_{c3} - \ln K_{c1}) dA_c + \frac{1}{3} \int_0^{B_c} (\ln K_{c3} - \ln K_{c2}) dB_c$$

$$+ \frac{1}{3} \left[(A_c - 1)\ln K_{c1} + B_c \ln K_{c2} + C_c \ln K_{c3} \right] - z_B(z_C - z_A)(A_c - 1) - z_A(z_C - z_B)B_c$$

$$....(2.122)$$

On substituting for K_c values this yields

$$\ln\phi_A{}^{3z_Bz_C} = \int_1^{A_c} \left[\ln\frac{K_{m3}}{K_{m1}} + \ln\frac{\Gamma_3}{\Gamma_1} \right] dA_c + \int_0^{B_c} \left[\ln\frac{K_{m3}}{K_{m2}} + \ln\frac{\Gamma_3}{\Gamma_2} \right] dB_c$$

$$+ (1-A_c)\ln\frac{\Gamma_3}{\Gamma_1} - B_c \ln\frac{\Gamma_3}{\Gamma_2} + (1-A_c)\left[\ln\frac{K_{m3}}{K_{m1}} + 3z_B(z_C-z_A) \right]$$

$$- B_c \left[\ln\frac{K_{m3}}{K_{m2}} + 3z_A(z_C-z_B) \right] \qquad ....(2.123)$$

Therefore , only two ratios, i.e. Γ_3/Γ_1 and Γ_3/Γ_2, are necessary to evaluate solution phase activity coefficients at any particular zeolite phase composition A_c, B_c[87]. Corresponding expressions for ϕ_B, ϕ_C, K_{a1}, K_{a2} and K_{a3} also involve only *the same two* Γ ratios[87]. The evaluation of these Γ ratios is not straight-forward, however, because the single-ion activity coefficients, which are used to define the Γ ratios, cannot be measured experimentally. Only mean values for the *salts* in solution can be so measured; thus mean stoichiometric activity coefficients are used to define the departure from ideality of a salt in solution (with the standard state defined in terms of the hypo-thetical ideal molal (mol kg^{-1}) solution[77]). The Γ ratios can however, be expressed in measurable quantities. Fletcher and Townsend discuss several cases[87] depending on whether the salts share a common anion or not.

2.2.5.1. Three salts with a common anion

Considering the simplest case first, where three salts share the same anion X, the mean activity coefficients and their corresponding single-ion activity coefficients are related by[87]

$$\ln\gamma_{\pm AX} = \frac{1}{z_A + z_X}(z_X \ln\gamma_A + z_A \ln\gamma_X) \qquad \text{....(2.22)}$$

$$\ln\gamma_{\pm BX} = \frac{1}{z_B + z_X}(z_X \ln\gamma_B + z_B \ln\gamma_X) \qquad \text{....(2.23)}$$

and

$$\ln\gamma_{\pm CX} = \frac{1}{z_C + z_X}(z_X \ln\gamma_C + z_C \ln\gamma_X) \qquad \text{....(2.125)}$$

Multiplying these three equations by $z_B z_C (z_A + z_X)$, $z_A z_C (z_B + z_X)$ and $z_A z_B (z_C + z_X)$ respectively, and effecting appropriate subtractions, we obtain

$$z_B z_C (z_A + z_X)\ln\gamma_{\pm AX} - z_A z_B (z_C + z_X)\ln\gamma_{\pm CX} = z_B z_C z_X \ln\gamma_A - z_A z_B z_X \ln\gamma_C$$

$$\text{....(2.126)}$$

and

$$z_A z_C (z_B + z_X)\ln\gamma_{\pm BX} - z_A z_B (z_C + z_X)\ln\gamma_{\pm CX} = z_A z_C z_X \ln\gamma_B - z_A z_B z_X \ln\gamma_C$$

$$\text{....(2.127)}$$

These two equations are then simplified as[87]

$$\ln\xi_{AX} - \ln\xi_{CX} = z_X\left[\ln\gamma_A^{\,z_B z_C} - \ln\gamma_C^{\,z_A z_B}\right] \qquad \text{....(2.128)}$$

and

$$\ln\xi_{BX} - \ln\xi_{CX} = z_X\left[\ln\gamma_B^{\,z_A z_C} - \ln\gamma_C^{\,z_A z_B}\right] \qquad \text{....(2.129)}$$

where
$$\xi_{AX} = \gamma_{\pm AX}^{\,z_B z_C (z_A + z_X)} \quad , \quad \xi_{BX} = \xi_{\pm BX}^{\,z_A z_C (z_B + z_X)}$$

and
$$\xi_{CX} = \gamma_{\pm CX}^{\,z_A z_B (z_C + z_X)}$$

From the definitions of Γ ratios given below

$$\Gamma_1 = \frac{\gamma_B^{z_A z_C} \cdot \gamma_C^{z_A z_B}}{\gamma_A^{2z_B z_C}} \qquad\qquad ....(2.61)$$

$$\Gamma_2 = \frac{\gamma_A^{z_B z_C} \cdot \gamma_C^{z_A z_B}}{\gamma_B^{2z_A z_C}} \qquad\qquad ...(2.130)$$

and

$$\Gamma_3 = \frac{\gamma_A^{z_B z_C} \cdot \gamma_B^{z_A z_C}}{\gamma_C^{2z_A z_B}} \qquad\qquad ....(2.131)$$

$$\ln \Gamma_{3/\Gamma_1} = \ln \gamma_A^{3z_B z_C} / \gamma_C^{3z_A z_B} = 3\ln\gamma_A^{z_B z_C} - 3\ln\gamma_C^{z_A z_B} \qquad ....(2.132)$$

and

$$\ln \Gamma_{3/\Gamma_2} = \ln \gamma_B^{3z_A z_C} / \gamma_C^{3z_A z_B} = 3\ln\gamma_B^{z_A z_C} - 3\ln\gamma_C^{z_A z_B} \qquad ....(2.133)$$

By combining equations (2.132) and (2.133) with (2.128) and (2.129) respectively

$$\ln \Gamma_{3/\Gamma_1} = \frac{3}{z_X} \ln \xi_{AX}/\xi_{CX} \qquad\qquad ....(2.134)$$

$$\ln \Gamma_{3/\Gamma_2} = \frac{3}{z_X} \ln \xi_{BX}/\xi_{CX} \qquad\qquad ....(2.135)$$

2.2.5.2. <u>Three salts with three different anions</u>

This most complex case of a ternary ion exchange situation, may be found in a typical detergent wash solution where in addition to the calcium and magnesium salts from the water, the detergent may release into solution several sodium salts (for

example, silicates, perborates) together with the zeolite component. Combining equations (2.61), (2.130) and (2.131) with the appropriate definitions of $\gamma_{\pm AX}$, $\gamma_{\pm AY}$, $\gamma_{\pm AZ}$, $\gamma_{\pm BX}$, $\gamma_{\pm BY}$, $\gamma_{\pm BZ}$, $\gamma_{\pm CX}$, $\gamma_{\pm CY}$ and $\gamma_{\pm CZ}$ and treating as before, two expressions involving Γ ratios are obtained[87].

For example, equation (2.22) can be rearranged as

$$(z_A + z_X)\, \ln\gamma_{\pm AX} = z_A \ln\gamma_X + z_X \ln\gamma_A \qquad \ldots\ldots(2.22)'$$

Multiplication of this equation by $z_B z_C$ gives

$$\ln\gamma_{\pm AX}^{z_B z_C (z_A + z_X)} = \ln\gamma_X^{z_A z_B z_C} + \ln\gamma_A^{z_X z_B z_C} \qquad \ldots\ldots(2.136)$$

Therefore

$$\xi_{AX} = \gamma_{\pm AX}^{z_B z_C (z_A + z_X)} = \gamma_A^{z_B z_C z_X} \cdot \gamma_X^{z_A z_B z_C} \qquad \ldots\ldots(2.137)$$

Altogether, nine such expressions are obtained in terms of all the combinations of the three cations and the three anions. These expressions in ξ are then manipulated to obtain the required Γ ratios.

For example,

$$\xi_{AX/\xi_{CX}} = \gamma_A^{z_B z_C z_X} / \dfrac{\gamma_A^{z_A z_B z_X}}{\gamma_C} \qquad \ldots\ldots(2.138)$$

whence

$$\left(\xi_{AX/\xi_{CX}}\right)^{2 z_Y z_Z} = \left(\gamma_A^{2 z_B z_C} / \dfrac{\gamma_A^{2 z_A z_B}}{\gamma_C}\right)^{z_X z_Y z_Z} \qquad \ldots\ldots(2.139)$$

Similarly,

$$\left(\xi_{AY/\xi_{BY}}\right)^{z_X z_Z} = \left(\gamma_A^{z_B z_C} / \dfrac{\gamma_A^{z_A z_C}}{\gamma_B}\right)^{z_X z_Y z_Z} \qquad \ldots\ldots(2.140)$$

and

$$\left(\xi_{BZ/\xi_{CZ}}\right)^{z_X z_Y} = \left(\gamma_B^{z_A z_C} / \dfrac{\gamma_C^{z_A z_B}}{}\right)^{z_X z_Y z_Z} \qquad \ldots\ldots(2.141)$$

- 77 -

Multiplication of equations (2.139), (2.140) and (2.141) together yield

$$\left(\xi_{AX}/\xi_{CX}\right)^{2z_Y z_Z} \left(\xi_{AY}/\xi_{BY}\right)^{z_X z_Z} \left(\xi_{BZ}/\xi_{CZ}\right)^{z_X z_Y} = \gamma_A^{3z_B z_C} / \gamma_C^{3z_A z_B}$$

Therefore, ...(2.142)

$$= \Gamma_3/\Gamma_1$$

$$\ln \frac{\Gamma_3}{\Gamma_1} = \frac{1}{z_X z_Y z_Z} \ln\left[\left(\frac{\xi_{AX}}{\xi_{CX}}\right)^{2z_Y z_Z} \left(\frac{\xi_{AY}}{\xi_{BY}}\right)^{z_X z_Z} \left(\frac{\xi_{BZ}}{\xi_{CZ}}\right)^{z_X z_Y}\right] \quad ....(2.143)$$

Similar procedures lead to

$$\ln \frac{\Gamma_3}{\Gamma_2} = \frac{1}{z_X z_Y z_Z} \ln\left[\left(\frac{\xi_{BX}}{\xi_{CX}}\right)^{2z_Y z_Z} \left(\frac{\xi_{AY}}{\xi_{CY}}\right)^{z_X z_Z} \left(\frac{\xi_{BZ}}{\xi_{AZ}}\right)^{z_X z_Y}\right] \quad ....(2.144)$$

2.2.5.3. Values of Γ functions in mixed solutions

It is apparent, however, that all the preceding equations involving Γ ratios hold for the *pure* solutions. In practice, however, values derived in terms of activity coefficient data for the *mixed* salt solutions are required.

Thus, considering equation (2.134) for the common anion case, the required value is

$$\ln(\Gamma_3/\Gamma_1) = \frac{3}{z_X} \ln\left[\xi_{AX}^{(B,C,X)} / \xi_{CX}^{(A,B,X)}\right] \quad ....(2.145)$$

where (for example)

$$\ln\xi_{AX}^{(B,C,X)} = z_B z_C (z_A + z_X) \ln\gamma_{\pm AX}^{(B,C,X)} \quad ....(2.146)$$

and $\gamma_{\pm AX}^{(B,C,X)}$ is the mean stoichiometric activity coefficient

- 78 -

for salt AX in the presence of known concentrations of salts BX and CX and therefore a known total ionic strength I[87]. To evaluate these functions Fletcher and Townsend have adapted and extended existing solution phase models as shown below[87].

The most basic model for the solution phase was developed by Guggenheim as early as 1935[91] in which the (decadic) logarithm of the rational salt activity coefficient was equated to an electrostatic term (i.e.the Debye-Hückel formulation[92]) plus a series of terms which took into account specific interactions between ions of opposite charge. In subsequent years, many workers have expanded and modified the Guggenheim approach which allowed the required activity coefficients in single-salt solutions to be accurately predicted, but unfortunately this resulted in the introduction of many further complexities into the equations[93-97].

Since the Fletcher-Townsend model for ternary ion exchange ignores salt imbibition[85-88], it is applicable only to systems where the total electrolyte concentration is less than about 0.5 mol dm^{-3}[76]. Most of the above-mentioned modifications to the Debye-Hückel model are therefore unnecessarily complex for the Fletcher-Townsend model, as many of the terms become operative only at higher concentrations[96] and it is possible to derive equations for the Γ functions in terms of older, less complicated models[87]. The method followed here is an extension of Glueckauf's approach[80], whose results, as were those of Guggenheim, were derived with respect to *rational* activity coefficients.

Generally, mean molal (mol kg^{-1}) stoichiometric activity

coefficients ($\gamma_\pm$) are used in ion exchange work instead of
the rational (mole fraction) functions, and the relation
between these are, when water is solvent[77],

$$\log \gamma_{\pm AX} = \log f_{AX} - \log(1+0.018 \Sigma \nu_s m_s) \qquad ....(2.147)$$

where f_{AX} is the mean rational activity coefficient of the salt
AX, ν_s is the number of moles of ions formed when one mole of
salt s ionises, and m_s is the concentration (mol kg^{-1}) of salt.
The summation is over all solute species (i.e. salts). If the
solution contains more than one salt, this correction may be
significant even at relatively low concentrations.

Similarly, $\gamma_\pm$ is related to the mean molar (mol dm^{-3}) activity
coefficient $y_\pm$ by[77]

$$\log y_\pm = \log \gamma_\pm - \log \left[d/d_o (1+0.001 \Sigma m_s W_s) \right] \qquad ....(2.148)$$

where d and d_o are the densities of the solution and pure water
respectively, and W_s is the molecular weight (g mol^{-1}) of salt
s. It follows, therefore that $\gamma_\pm \rightarrow y_\pm$ in dilute aqueous
solutions.

Generally, the Guggenheim equation is[91],

$$\log f_{A_1X_1} = \frac{-A z_{A1} z_{X1} \sqrt{I}}{1 + \sqrt{I}} + \frac{z_{A1}}{z_{A1}+z_{X1}} \sum_{\substack{i=1 \text{ all} \\ \text{cations}}}^{m} (\lambda_{Aix1} m_{Ai})$$

$$+ \frac{z_{X1}}{z_{A1}+z_{X1}} \sum_{\substack{j=1 \text{ all} \\ \text{anions}}}^{n} (\lambda_{A1Xj} m_{Xj}) \qquad ....(2.149)$$

where f_{A1X1} is the mean rational activity coefficient of the
salt A_1X_1 in solution at an ionic strength I; the λ terms are

- 80 -

characteristic constants of the single electrolytes. $\mathbf{A}$ is the
Debye-Hückel constant[77] defined by

$$A = \frac{1}{2.303} \sqrt{\left[\frac{500\ N}{16\ \pi^2}\right] \left[\frac{e^2}{\epsilon kT}\right]^{3/2}} \quad dm^{3/2} mol^{-\frac{1}{2}} \qquad ....(2.150)$$

where N is Avogadro's constant, k Boltzmann constant, e the
charge of a proton, ϵ the permittivity of the solution
$(CV^{-1}m^{-1})$ and T the absolute temperature. Implicit in the
formulation of equation (2.149) is the assumption that the
product of the Debye-Hückel constants $\mathbf{B}$ a [usually found in the
denominator of the first term of equation (2.149)] is unity[87].

If the solution contains only one salt, equation (2.149) reduces
to

$$\log f_{AX} = \frac{-A z_A z_X \sqrt{I}}{1 + \sqrt{I}} + \frac{\lambda_{AX}}{z_A + z_X} (z_X m_X + z_A m_A) \qquad ....(2.151)$$

Since $z_X m_X = z_A m_A$ and $I = (m_A z_A^2 + m_X z_X^2)/2$,

$$2 z_A m_A (z_A + z_X) = 2(m_A z_A^2 + m_A z_A z_X) = 2(m_A z_A^2 + m_X z_X^2) = 4I$$

$$....(2.152)$$

and therefore

$$\log f_{AX} = \frac{-A z_A z_X \sqrt{I}}{1 + \sqrt{I}} + \frac{\lambda_{AX}}{(z_A + z_X)^2} 4I \qquad ....(2.153)$$

Glueckauf[80] removed the assumption that λ values were constant
in relation to I, and expressed λ as a function of the ionic
strength of the solution:

$$\lambda_{AX} = \frac{(z_A + z_X)^2}{4I} \left[\log f_{AX} + \frac{A z_A z_X \sqrt{I}}{1 + \sqrt{I}}\right] \qquad ....(2.153)'$$

- 81 -

For a ternary solution with a common anion, equation (2.149) becomes

$$\log f_{AX}^{(B,C,X)} = \frac{-A z_A z_X \sqrt{I}}{1 + \sqrt{I}} + \frac{z_X}{z_A + z_X} (\lambda_{AX} m_X) + \frac{z_A}{z_A + z_X} (\lambda_{AX} m_A + \lambda_{BX} m_B + \lambda_{CX} m_C)$$

$$....(2.154)$$

The three λ terms are then expressed with respect to I to give

$$\log f_{AX}^{(B,C,X)} = \frac{-A z_A z_X \sqrt{I}}{1 + \sqrt{I}} + \frac{1}{4I} \left[\alpha_1 \log f_{AX} + \alpha_2 \log f_{BX} + \alpha_3 \log f_{CX} + \frac{\alpha_4 \sqrt{I} A}{1 + \sqrt{I}} \right]$$

$$....(2.155)$$

where

$$\alpha_1 = (z_A + z_X)(z_A m_A + z_X m_X)$$

$$\alpha_2 = z_A m_B (z_B + z_X)^2 / (z_A + z_X)$$

$$\alpha_3 = z_A m_C (z_C + z_X)^2 / (z_A + z_X)$$

and

$$\alpha_4 = z_X (z_A \alpha_1 + z_B \alpha_2 + z_C \alpha_3)$$

For this system

$$z_X m_X = z_A m_A + z_B m_B + z_C m_C \qquad ....(2.156)$$

and

$$I = (m_A z_A^2 + m_B z_B^2 + m_C z_C^2 + m_X z_X^2)/2 \qquad ....(2.157)$$

Therefore,

$$z_X m_X - z_A m_A = z_B m_B + z_C m_C \qquad ....(2.156)'$$

and

$$m_A z_A^2 + m_X z_X^2 = 2I - m_B z_B^2 - m_C z_C^2 \qquad ....(2.157)'$$

Now, in this case an allowance is made for the presence of

$$\alpha_1 = (z_A + z_X)(z_X m_X + z_A m_A)$$

$$= (z_A - z_X)(z_X m_X - z_A m_A) + 2(m_A z_A^2 + m_X z_X^2)$$

$$= (z_A - z_X)(z_B m_B + z_C m_C) + 4I - 2m_B z_B^2 - 2m_C z_C^2$$

$$= z_B m_B (z_A - 2z_B - z_X) + z_C m_C (z_A - 2z_C - z_X) + 4I$$

and

$$\alpha_4 = z_X \left[z_A z_B m_B (z_A - 2z_B - z_X) + z_A z_C m_C (z_A - 2z_C - z_X) + 4I . z_A + z_B \alpha_2 + z_C \alpha_3 \right]$$

$$= \frac{z_X z_A}{(z_A + z_X)} \left[z_B m_B (z_A - z_B)^2 + z_C m_C (z_A - z_C)^2 + 4I(z_A + z_X) \right]$$

Substitution in equation (2.155) to eliminate m_A and m_X terms and subsequent rearrangement gives

$$\log f_{AX}^{(B,C,X)} = \log f_{AX} + \frac{1}{4I(z_A + z_X)} \left[m_B \left\{ \beta_1 \log f_{AX} + \beta_2 \log f_{BX} + \beta_3 A(1 + I^{-\frac{1}{2}})^{-1} \right\} \right.$$

$$\left. + m_C \left\{ \beta_4 \log f_{AX} + \beta_5 \log f_{CX} + \beta_6 A(1 + I^{-\frac{1}{2}})^{-1} \right\} \right]$$

....(2.158)

where

$$\beta_1 = z_B (z_A + z_X)(z_A - 2z_B - z_X)$$

$$\beta_2 = z_A (z_B + z_X)^2$$

$$\beta_3 = z_A z_B z_X (z_A - z_B)^2$$

$$\beta_4 = z_C (z_A + z_X)(z_A - 2z_C - z_X)$$

$$\beta_5 = z_A (z_C + z_X)^2$$

$$\beta_6 = z_A z_C z_X (z_A - z_C)^2$$

Equation (2.158) is similar in form to the one derived by Glueckauf[80] for a binary solution with a common anion except

that in this case an allowance is made for the presence of the third cation and that Glueckauf had given a value of 0.5 to the temperature dependent constant **A**. Both Glueckauf's equation (80) and equation (2.158) are special cases of a general relationship valid for a multicomponent solution system, which may be expressed in terms of mean molal (mol kg^{-1}) stoichiometric activity coefficients[87]:

$$
\log \gamma_{\pm A_1 X_1}^{(A_2 \ldots A_m / X_2 \ldots X_n)} = \log \gamma_{\pm A_1 X_1} + \frac{1}{4I(z_{A_1}+z_{X_1})} \left[\sum_{i=2}^{m} m_{A_i} \left\{ \zeta_{i1} \log \gamma_{\pm A_1 X_1} \right. \right.
$$

$$
\left. + \zeta_{i2} \log \gamma_{\pm A_i X_1} + \zeta_{i3} A(1+I^{-\frac{1}{2}})^{-1} + (\zeta_{i1}+\zeta_{i2}) \log Q \right\}
$$

$$
+ \sum_{j=2}^{n} m_{X_j} \left\{ \zeta_{j1} \log \gamma_{\pm A_1 X_1} + \zeta_{j2} \log \gamma_{\pm A_1 X_j} + \zeta_{j3} A(1+I^{-\frac{1}{2}})^{-1} \right.
$$

$$
\left. \left. + (\zeta_{j1}+\zeta_{j2}) \log Q \right\} \right] \quad \ldots\ldots(2.159)
$$

where
$$
\zeta_{i1} = z_{A_i}(z_{A_1}+z_{X_1})(z_{A_1}-2z_{A_i}-z_{X_1})
$$

$$
\zeta_{i2} = z_{A_1}(z_{A_i}+z_{X_1})^2
$$

$$
\zeta_{i3} = z_{A_1} z_{A_i} z_{X_1}(z_{A_1}-z_{A_i})^2
$$

$$
\zeta_{j1} = z_{X_j}(z_{A_1}+z_{X_1})(z_{X_1}-2z_{X_j}-z_{A_1})
$$

$$
\zeta_{j2} = z_{X_1}(z_{X_j}+z_{A_1})^2
$$

$$
\zeta_{j3} = z_{X_1} z_{X_j} z_{A_1}(z_{X_1}-z_{X_j})^2
$$

$$
Q = 1 + 0.018 \, \Sigma \nu_s m_s
$$

and $\gamma_{\pm A_1 X_1}^{(A_2 \ldots A_m / X_2 \ldots X_n)}$ is the mean molal stoichiometric coefficient of salt $A_1 X_1$ in a solution also containing (m-1) and (n-1) other cations and

anions , respectively.

For ternary ion exchange, it was shown earlier that the required ratios Γ_3/Γ_1 and Γ_3/Γ_2 could be conveniently determined from expressions involving ξ functions - see equations (2.134) and (2.135). Thus, for ternary exchange where the anion is common, equation (2.159) becomes[87]

$$\log \xi_{AX}^{(B,C,X)} = \log \xi_{AX} + \frac{z_B z_C}{4I} \left[(m_B \beta_1 + m_C \beta_4) \log \gamma_{\pm AX} \right.$$

$$+ \beta_2 \log \gamma_{\pm BX} + \beta_5 \log \gamma_{\pm CX} + (\beta_3 + \beta_6)(1+I^{-\frac{1}{2}})^{-1} A$$

$$\left. + \left\{ m_B(\beta_1 + \beta_2) + m_C(\beta_4 + \beta_5) \right\} \log Q \right] \quad \ldots\text{(2.160)}$$

and the required Γ ratios are[87]

$$\ln(\Gamma_3/\Gamma_1) = \frac{3}{z_X} \ln(\xi_{AX}/\xi_{CX}) - \frac{1.727}{z_X I} \left[T_1 \log \xi_{AX} + T_2 \log \xi_{CX} \right.$$

$$\left. + T_3 A (1+I^{-\frac{1}{2}})^{-1} + \left\{ z_B z_C (z_A + z_X) \, T_1 + z_A z_B (z_C + z_X) \, T_2 \right\} \log Q \right]$$

$$\ldots\text{(2.161)}$$

where $T_1 = z_A m_A(z_A + z_X) - z_B m_B(z_A - 2z_B - z_X) - z_C m_C(z_A - 2z_C - z_X)$

$T_2 = z_A m_A(z_C - 2z_A - z_X) + z_B m_B(z_C - 2z_B - z_X) - z_C m_C(z_C + z_X)$

$T_3 = z_A z_B z_C z_X(z_C - z_A) \left[(z_A m_A - z_C m_C)(z_C - z_A) + z_B m_B(z_A + z_C - 2z_B) \right]$

and

$$\ln(\Gamma_3/\Gamma_2) = \frac{3}{z_X} \ln(\xi_{BX}/\xi_{CX}) - \frac{1.727}{z_X I} \left[T_4 \log \xi_{BX} + T_5 \log \xi_{CX} \right.$$

$$\left. + T_6 A (1+I^{-\frac{1}{2}})^{-1} + \left\{ z_A z_C (z_B + z_X) T_4 + z_A z_B (z_C + z_X) T_5 \right\} \log Q \right]$$

$$\ldots\text{(2.162)}$$

where $T_4 = z_B m_B(z_B + z_X) - z_A m_A(z_B - 2z_A - z_X) - z_C m_C(z_B - 2z_C - z_X)$

$T_5 = z_B m_B(z_C - 2z_B - z_X) + z_A m_A(z_C - 2z_A - z_X) - z_C m_C(z_C + z_X)$

$T_6 = z_A z_B z_C z_X(z_C - z_B) \left[(z_B m_B - z_C m_C)(z_C - z_B) + z_A m_A(z_B + z_C - 2z_A) \right]$

In their discussion, Fletcher and Townsend[87] compare their model with the rigorous formulation of Pitzer[96], whose equations were similar in form to those of Guggenheim[91], but included extra terms to account for interactions of ions of *like* charge. These interaction terms were related to the logarithm of the activity coefficient as a function of the *products* of the concentrations of the respective ions in solution. For dilute solutions ($\leqslant 0.1$ mol dm^{-3}) this interaction term (being a function of the product of the two concentrations) can only have a small effect on the size of the activity coefficient. Also Glueckauf's modification of Guggenheim's treatment assumes that the λ terms [see equation (2.149)] were functions of ionic strength (thus automatically allowing for some effects of interactions between ions of like charge). Thus Fletcher and Townsend concluded that for many ion exchanges involving zeolites (where the solutions contain only a few different electrolytes and where the solution ionic strength is below 0.5 mol dm^{-3}) the Pitzer approach is over-complicated[87]. Therefore, for a ternary ion exchange system, equations (2.161) and (2.162) should allow the required Γ_3/Γ_1 and Γ_3/Γ_2 ratios to be determined with sufficient accuracy[87].

This assumption has been tested by Townsend and Fletcher by comparing experimental $\gamma_\pm$ values for various binary and ternary systems with the calculated values from equation (2.160), and they found that good agreement occurred between theory and experiment[87]. The deviation was found to be less than 0.5% at I values up to 0.35 mol dm^{-3} for a binary system of HCl and LaCl$_3$, and even smaller deviations were found for binary

systems containing HCl and either $Ca(ClO_4)$ or $Mg(ClO_4)$. For a ternary system comprising of HCl, $BaCl_2$ and CsCl the differences between experimental and theoretical values of $\gamma_{\pm HCl}$ were normally < 1.5%, which is higher than the value of < 0.5% found for the binary system of HCl and $BaCl_2$. Fletcher and Townsend suggest that this larger discrepancy in the ternary system should be attributed to the higher ionic strength of the solutions used (0.5 mol dm^{-3} for the ternary mixture vs < 0.3 mol dm^{-3} for the binary)[87].

They conclude emphatically that the observed small discrepancies should not be solely ascribed to weaknesses of the model because an allowance must be made for experimental error in measuring an activity.

2.2.6. Evaluation of Thermodynamic Equilibrium Constants

The three explicit expressions for ϕ_A, ϕ_B and ϕ_C, derived in section 2.2.4 and depicted by equations (2.113), (2.114) and (2.115) were used to obtain expressions for the three K_a terms by substituting in equations (2.98), (2.99) and (2.100) respectively, viz[86]:

$$\ln K_{a1} = \ln K_{c1} + 2\ln\phi_A^{z_B z_C} - \ln\phi_B^{z_A z_C} - \ln\phi_C^{z_A z_B} \quad \dots (2.98)$$

Substitution for ϕ_A, ϕ_B and ϕ_C yields, after simplification,

$$\ln K_{a1} = z_A(z_B - z_C) - 2z_B(z_A - z_C) - \frac{2}{3} \int_0^1 \left[\ln K_{c3} - \ln K_{c1} \right] dA_c$$

$$+ \frac{1}{3} \int_0^1 \left[\ln K_{c3} - \ln K_{c2} \right] dB_c + \frac{1}{3} \ln(K_{c1} K_{c2} K_{c3}) + \Delta 1$$

$$\dots (2.163)$$

where the water term

$$\Delta_1 = -z_A z_B z_C \left[2 \int_{a_w=1}^{a_{w(a)}} (\nu_w^A)\, d\ln a_w - \int_{a_w=1}^{a_{w(b)}} (\nu_w^B)\, d\ln a_w - \int_{a_w=1}^{a_{w(c)}} (\nu_w^C)\, d\ln a_w \right.$$

$$\left. + \int_{a_{w(a)}}^{a_{w(b)}} (\nu_w^{ABC})\, d\ln a_w + \int_{a_{w(a)}}^{a_{w(c)}} (\nu_w^{ABC})\, d\ln a_w \right] \qquad \ldots.(2.164)$$

From equations (2.95), (2.96) and (2.97), which define the K_c terms, we know that

$$\ln(K_{c1} \cdot K_{c2} \cdot K_{c3}) = 0 \qquad \ldots.(2.\ 165)$$

Therefore,

$$\ln K_{a1} = z_A(z_B - z_C) + 2z_B(z_A - z_C) - \frac{2}{3} \int_0^1 \left[\ln K_{c3} - \ln K_{c1} \right] dA_c$$

$$+ \frac{1}{3} \int_0^1 \left[\ln K_{c3} - \ln K_{c2} \right] dB_c + \Delta_1 \qquad \ldots.(2.166)$$

The elimination of the $\frac{1}{3} \ln(K_{c1} \cdot K_{c2} \cdot K_{c3})$ is in accordance with the fact that, as emphasised by Fletcher and Townsend, the K_{c1}, K_{c2} and K_{c3} values in this term correspond to a particular composition, yet K_{a1} is invariant with the zeolite phase composition[86].

Similarly,

$$\ln K_{a2} = -2z_A(z_B - z_C) + z_B(z_A - z_C) + \frac{1}{3} \int_0^1 \left[\ln K_{c3} - \ln K_{c1} \right] dA_c$$

$$- \frac{2}{3} \int_0^1 \left[\ln K_{c3} - \ln K_{c2} \right] dB_c + \Delta_2 \qquad \ldots.(2.167)$$

and

$$\ln K_{a3} = z_A(z_B - z_C) + z_B(z_A - z_C) + \frac{1}{3} \int_0^1 \left[\ln K_{c3} - \ln K_{c1} \right] dA_c$$

$$- \frac{1}{3} \int_0^1 \left[\ln K_{c3} - \ln K_{c2} \right] dB_c + \Delta_3 \qquad \qquad \ldots\ldots(2.168)$$

where

$$\Delta_2 = -z_A z_B z_C \left[2 \int_{a_w=1}^{a_{w(b)}} (\nu_w^B) \, d\ln a_w - \int_{a_w=1}^{a_{w(a)}} (\nu_w^A) \, d\ln a_w - \int_{a_w=1}^{a_{w(c)}} (\nu_w^C) \, d\ln a_w \right.$$

$$\left. + \int_{a_{w(b)}}^{a_{w(a)}} (\nu_w^{ABC}) \, d\ln a_w + \int_{a_{w(b)}}^{a_{w(c)}} (\nu_w^{ABC}) \, d\ln a_w \right] \qquad \ldots\ldots(2.169)$$

and

$$\Delta_3 = -z_A z_B z_C \left[2 \int_{a_w=1}^{a_{w(c)}} (\nu_w^C) \, d\ln a_w - \int_{a_w=1}^{a_{w(a)}} (\nu_w^A) \, d\ln a_w - \int_{a_w=1}^{a_{w(b)}} (\nu_w^B) \, d\ln a_w \right.$$

$$\left. + \int_{a_{w(c)}}^{a_{w(a)}} (\nu_w^{ABC}) \, d\ln a_w + \int_{a_{w(c)}}^{a_{w(b)}} (\nu_w^{ABC}) \, d\ln a_w \right] \qquad \ldots\ldots(2.170)$$

It is apparent from equations (2.166) - (2.168) that their sum
is zero, and thus fully compatible with the definitions of K_{a1}
K_{a2} and K_{a3} given by equations (2.59), (2.63) and (2.64), where
it is also seen that $\ln(K_{a1} \cdot K_{a2} \cdot K_{a3}) = 0$. This is a useful
check on the correctness and internal consistency of the
integration procedure used above [86].

Considering the studies carried out in this research project,
involving the simplest case of ternary ion exchange where all

three cations are univalent, equation (2.56) becomes

$$2A^+(s) + B^+(c) + C^+(c) \rightleftharpoons 2A^+(c) + B^+(s) + C^+(s) \quad \ldots(2.171)$$
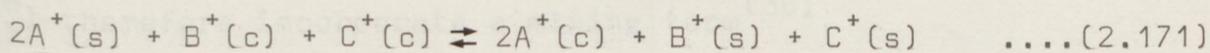
The change in free energy for this reaction is the standard free energy ($\Delta G^\ominus$) if 2 moles of A^+ in solution are mixed with 1 mole each of B-zeolite and C-zeolite and the reaction goes entirely to products, the reactants initially and the products finally all being in their respective standard states[86]. Considering equation (2.166), which enables K_{a1} (and hence, $\Delta G^\ominus_1$) to be evaluated, for the univalent case, the equation simplifies markedly to give

$$\ln K_{a1} = -\frac{2}{3} \int_0^1 \left[\ln K_{c3} - \ln K_{c1} \right] dA_c + \frac{1}{3} \int_0^1 \left[\ln K_{c3} - \ln K_{c2} \right] dB_c + \Delta_1$$

$$\ldots(2.166)'$$

Therefore, the integration is effected from the standard states of appropriate amounts of each homoionic zeolite (A,B and C) to the derived zeolite phase composition defined by A_c, B_c, $a_{w(Ac,Bc)}$. Figure 2.10 shows how such a situation may be depicted visually, where the points a,b and c represent each pure zeolite in contact with a solution at experimental concentration (T_N) and point d represents an equal mixture of B- and C-zeolites. The experimental point Q (A_c,B_c) can be arrived at by many paths, but because $\Delta G^\ominus$ is a state function, the paths by which the three ions pass from their standard states to the experimental point are of no significance, subject to the restraints imposed by equations (2.74) - (2.76)[86]. The depicted path corresponds to an extreme situation, since complete mixing of ions B^+ and C^+ occurs (point d) within

the zeolite prior to any exchange with ion A$^+$; K_{a1} (and hence $\Delta G_1^\ominus$) therefore incorporate a mixing term[86].

Fletcher and Townsend discuss the question of whether the ion exchange in zeolites is ideal or not and conclude that[86] "since the zeolite is made up of sets of sub-lattices[98] into which the ions can exchange, and therefore, even if exchange into each of the sub-lattice sets is ideal (which is unlikely), the overall behaviour of the zeolite can be highly non-ideal[90]". Thus the mixing of homoionic B- and C- zeolites is probably non-ideal, and likely to contain both entropic and enthalpic terms[86]. It therefore follows from equation (2.171) that, after ion exchange, ions B$^+$ and C$^+$ must be "un-mixed" in solution before they can proceed to their respective standard states, implying that K_{a1} must also contain the entropic and enthalpic terms relating to this process.

2.2.7. Ternary Isotherms

Data from ternary ion exchange equilibria are used to derive the Kielland-type plots described in section 2.2.4.

Presenting this equilibrium data in an isotherm, however, involves some problems. Usually, the measured equilibrium compositions of *both* zeolite and solution phase compositions are plotted on *one* triangular coordinate diagram and the corresponding compositions of the two phases are joined by tie-lines[99,100]. But, as Fletcher and Townsend point out, one needs to be careful about the use of such graphs for two reasons[86]. First, though each tie-line joins together two points representing experimentally determined equilibrium compositions of the two

phases, the *prediction* of any corresponding two-phase equilibrium compositions by interpolation between any two tie-lines must be ambiguous. Secondly, unlike the binary isotherm case, lines linking the equilibrium compositions in one particular phase at a given total solution concentration (equiv dm^{-3}) have no particular significance in themselves because the ternary isotherm actually consists of two inter-linked *surfaces*, one for each phase[86]. Other investigators have by-passed these problems by representing ternary isotherms by superimposing the triangular coordinate diagrams for the two phases, but with the solution phase coordinates distorted so that equilibrium compositions for the two phases coin-cided[101,102].

Considering the case of reversibility, the usual direct methods of testing reversibility for binary exchange[71] cannot be used in the ternary case because the isotherm consists of two joined-together surfaces, and there are many paths (each made up of equilibrium points) over these surfaces by which the original composition of the zeolites can be restored[86]. Fletcher and Townsend conclude that[86] "the best test for reversibility in ternary exchange is that of prediction of different equilibrium positions from experimental data".

2.2.8. The Elprince and Babcock Model

As mentioned earlier (section 2.2), there have been attempts by some workers to utilise binary data to predict ternary ion exchange behaviour. The procedure used by Elprince and

Babcock[102] for the prediction of multi-ion exchange equili-
bria in clays involved expressing the activity coefficients
in terms of sets of constants Λ, which were exponential
functions of the differences in interaction energies between
pairs of *like* and *unlike* ions. They then used experimentally
determined activity coefficient values for the inter-related
binary systems Na $\rightleftarrows$ Cs, Na $\rightleftarrows$ Rb and Rb $\rightleftarrows$ Cs in montmorillonite
to iteratively determine the Λ values. These Λ values were
then used in expressions for activity coefficients correspond-
ing to the ternary system Na-Cs-Rb, enabling exchanger-phase
composition to be predicted[102].

Thus [102],

$$\Lambda_{AB} = (\nu_B/\nu_A) \exp\left[-(\lambda_{AB} - \lambda_{AA})/RT\right] \quad ....(2.172)$$

for binary systems, where ν_B, ν_A are the molar volumes of the
pure components and the $(\lambda_{AB} - \lambda_{AA})$ term represents the
difference in interaction energy between unlike (AB) and like
(AA) ion pairs. The emphasis in the above definitions should
be noted because the binary activity coefficient f is defined
on the basis of the exchanger being a non-ideal solid solution
(75,103) and therefore according to Gaines and Thomas[75]
"f does not have the character of an individual ion activity
coefficient but refers to the combination of that ion with the
exchanger in a definite composition of the whole mass".

The derivation of the Elprince and Babcock model is carried out
as follows:

For a univalent binary ion exchange given by,

$$I^+_{(s)} + J^+_{(c)} \rightleftarrows I^+_{(c)} + J^+_{(s)} \quad ....(2.173)$$
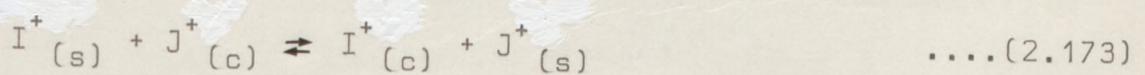
the thermodynamic equilibrium constant is given by [102]

$$K_{ij} = \left[\frac{A_i \ X_j \ f_i \ \gamma_j}{A_j \ X_i \ f_j \ \gamma_i} \right]_M \qquad \qquad ....(2.174)$$

where X is the mole fraction of the component in the solution
phase, A is the equivalent fraction of the component in the
crystal phase and M refers to a multicomponent system.
Therefore

$$\sum_{i=1}^{m} X_i = 1 \qquad \text{and} \qquad \sum_{i=1}^{m} A_i = 1 \qquad ....(2.175a/b)$$

Elprince and Babcock assume [102] that the γ_j / γ_i ratio is equal
to unity when the ionic strength is low and that the thermo-
dynamic equilibrium constant (being independent of composition,
by definition) has the same numerical value for the ion pair
i-j at constant temperature and pressure regardless of the
number of ions present in the system. If the solid phase
activity coefficients can be determined in the multicomponent
phase and (m-1) independent K_{ij} values are available, it
follows that with m number of X values known, the m number of
corresponding A values (or vice-versa) could be found by the
simultaneous solution of (m-1) independent i-j combinations
for equations (2.174), (2.175a) and (2.175b). The means of
estimating solid phase activity coefficients in the multi-
component phase involves properties which have "molecular
significance" [102].

Considering the thermodynamic relationship between activity
coefficients and the excess Gibbs energy g^E in terms of the
mole fractions of all components, where g^E=G (actual mixture

- 94 -

$T,P,A_i)-G$ (ideal mixture $T,P,A_i)$[102], then

$$\left[\partial n_T g^E / \partial n_i\right]_{n_j,T,P} = RT \ln f_i \qquad \ldots (2.176)$$

$$g^E = RT \sum_{i=1}^{m} N_i \ln f_i = RT \sum_{i=1}^{m} n_i/n_T \ln f_i \qquad \ldots (2.177)$$

where n_T is the total number of moles, n_i is the number of moles of component i and N_i is the mole fraction in the exchanger phase. Elprince and Babcock use a solution model suggested by Wilson[104] (where the Wilson equation is a semi-empirical general form of the Flory-Huggins' equation[105]), suitable for a large variety of non-ideal mixtures[102]. The Wilson equation is[102,104],

$$\frac{g^E}{RT} = -\sum_{i=1}^{m} N_i \ln \left[\sum_{j=1}^{m} \Lambda_{ij} N_j\right] \qquad \ldots (2.178)$$

where the excess Gibbs energy is defined in terms of an ideal solution in the sense of Raoult's law (i.e. $f_i \to 1$ as $N_i \to 1$).

Therefore

$$n_T \cdot g^E = -n_T RT \sum_{i=1}^{m} \frac{n_i}{n_T} \ln \left[\sum_{j=1}^{m} \Lambda_{ij} N_j\right] \qquad \ldots (2.179)$$

Thus

$$RT \ln f_i = \left[\frac{\partial n_T g^E}{\partial n_i}\right]_{n_j,T,P} = -n_T RT \left[\frac{\partial}{\partial n_i}\left(\sum_{i=1}^{m} \frac{n_i}{n_T} \ln \sum_{j=1}^{m} \Lambda_{ij} N_j\right)\right]$$

$$\ldots (2.180)$$

$$\ln f_i = -n_T \frac{\partial}{\partial n_i}\left(\sum_{i=1}^{m} \frac{n_i}{n_T} \ln \sum_{j=1}^{m} \Lambda_{ij} N_j\right) \qquad \ldots (2.181)$$

This leads to[102]

$$\ln f_i = 1 - \ln\left[\sum_{j=1}^{m} N_j \Lambda_{ij}\right] - \sum_{k=1}^{m} \frac{N_k \Lambda_{ki}}{\sum_{j=1}^{m} N_j \Lambda_{kj}} \qquad \ldots (2.182)$$

- 95 -

(Note that $\Lambda_{ii} = \Lambda_{jj} = \Lambda_{kk} = 1$). Thus, only binary constants (Λ_{jk}, Λ_{kj} etc) appear on this equation, and therefore activity coefficients in a multicomponent system can be determined if, for each i-j combination, a table of activity coefficients as a function of surface composition is available.

For a binary exchange system, the equations (2.178) and (2.182) reduce to[102]

$$-g^E/RT = N_1 \ln\left[N_1 + N_2\Lambda_{12}\right] + N_2 \ln\left[N_2 + N_1\Lambda_{21}\right] \quad \dots(2.183)$$

$$\ln f_1 = -\ln(N_1 + N_2\Lambda_{12}) + N_2\left[\frac{\Lambda_{12}}{N_1+N_2\Lambda_{12}} - \frac{\Lambda_{21}}{N_1\Lambda_{21}+N_2}\right] \quad \dots(2.184)$$

and

$$\ln f_2 = -\ln(N_2+N_1\Lambda_{21}) - N_1\left[\frac{\Lambda_{12}}{N_1+N_2\Lambda_{12}} - \frac{\Lambda_{21}}{N_1\Lambda_{21}+N_2}\right] \quad \dots(2.185)$$

(note that eqn. (2.185) is wrong in ref. 102) where the left hand side of equation (2.183) can be calculated from

$$g^E/RT = N_1 \ln f_1 + N_2 \ln f_2 \quad \dots(2.186)$$

To fit the non-linear equation (2.183) to the points $(N_i, g^E/RT)$ an iterative procedure, using a computer, is necessary[102]. Thus the corresponding λ values can be found for any set of binary systems.

For a ternary system, equation (2.182) reduces to

$$\ln f_1 = 1 - \ln A - \left[N_1/A + N_2\Lambda_{21}/B + N_3\Lambda_{31}/C\right] \quad \dots(2.187)$$

$$\ln f_2 = 1 - \ln B - \left[N_1\Lambda_{12}/A + N_2/B + N_3\Lambda_{32}/C\right] \quad \dots(2.188)$$

and

$$\ln f_3 = 1 - \ln C - \left[N_1\Lambda_{13}/A + N_2\Lambda_{23}/B + N_3/C\right] \quad \dots(2.189)$$

where
$$A = N_1 + N_2 \Lambda_{12} + N_3 \Lambda_{13}$$
$$B = N_1 \Lambda_{21} + N_2 + N_3 \Lambda_{23}$$
$$C = N_1 \Lambda_{31} + N_2 \Lambda_{32} + N_3$$

Therefore, for a given exchanger phase composition (N_1, N_2, N_3) these equations can be used to calculate the appropriate activity coefficients for the ternary system[102] from binary data alone.

From equation (2.174), expressions can be obtained for *binary* equilibrium constants in a *multicomponent system*. Thus,

$$K_{12} = \left[\frac{N_1 \ X_2 \ f_1 \ \gamma_2}{N_2 \ X_1 \ f_2 \ \gamma_1} \right]_M = \left[\frac{N_1 \ X_2 \ f_1}{N_2 \ X_1 \ f_2} \right]_M \quad \ldots (2.190)$$

and

$$K_{32} = \left[\frac{N_3 \ X_2 \ f_3 \ \gamma_2}{N_2 \ X_3 \ f_2 \ \gamma_3} \right]_M = \left[\frac{N_3 \ X_2 \ f_3}{N_2 \ X_3 \ f_2} \right]_M \quad \ldots (2.191)$$

assuming that $\gamma_2/\gamma_1 = 1$ etc.[102], and where all N,X,f values relate to *binary* exchanges. These two expressions are rearranged to give

$$X_1 = X_2 \left[N_1 f_1 / K_{12} N_2 f_2 \right]_M \quad \ldots (2.192)$$

and

$$X_3 = X_2 \left[N_3 f_3 / K_{32} N_2 f_2 \right]_M \quad \ldots (2.193)$$

Elprince and Babcock then applied these two equations to a ternary system where all N,X,f values relate to the corresponding ternary exchanges. Furthermore, for a ternary system, $X_1 + X_2 + X_3 = 1$, and therefore

$$1 - X_2 = X_1 + X_3 = X_2 \left[N_1 f_1 / K_{12} N_2 f_2 \right] + X_2 \left[N_3 f_3 / K_{32} N_2 f_2 \right]$$

$$\ldots (2.194)$$

Therefore,

$$X_2 = 1/\left[1 + \frac{N_1 f_1}{K_{12} N_2 f_2} + \frac{N_3 f_3}{K_{32} N_2 f_2}\right] \qquad \ldots(2.195)$$

By a similar procedure,

$$X_1 = 1/\left[1 + \frac{N_2 f_2}{K_{21} N_1 f_1} + \frac{N_3 f_3}{K_{31} N_1 f_1}\right] \qquad (2.196)$$

Thus, when N_1 and N_2 (where $N_3 = 1 - N_1 - N_2$) and the three ternary exchanger phase activity coefficients f_1, f_2 and f_3 are known, Elprince and Babcock claim to be able to use the above relationships to calculate the corresponding X_1 and X_2 (where $X_3 = 1 - X_1 - X_2$) values[102]. They present their results by showing contour lines on a triangular coordinate diagram[102]. The model was tested successfully by Elprince and Babcock on the interrelated exchange system of Na-Cs-Rb on Wyoming montmorillonite, and subsequently used also to predict ternary equilibrium in the systems Na-Rb-Cs on Chambers montmorillonite and Na-K-Cs on attapulgite[102].
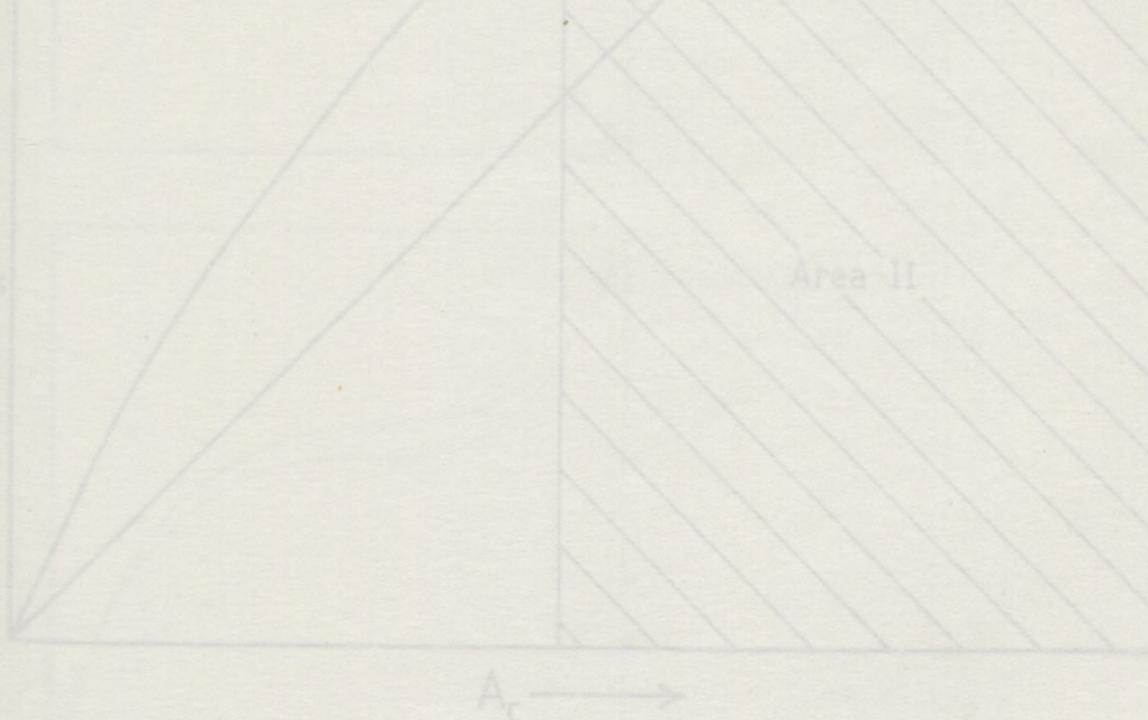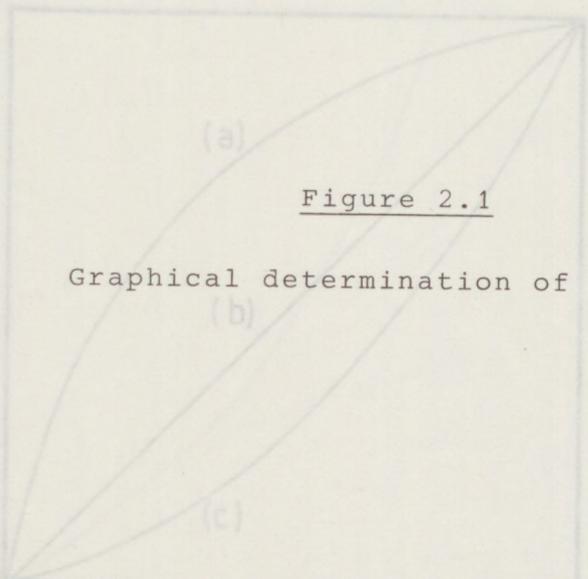
Figure 2.1

Graphical determination of α and α'

Figure 2.2

Isotherms of the 1st kind

(a) Outgoing ion preferred
(b) Equal preference
(c) Ingoing ion preferred
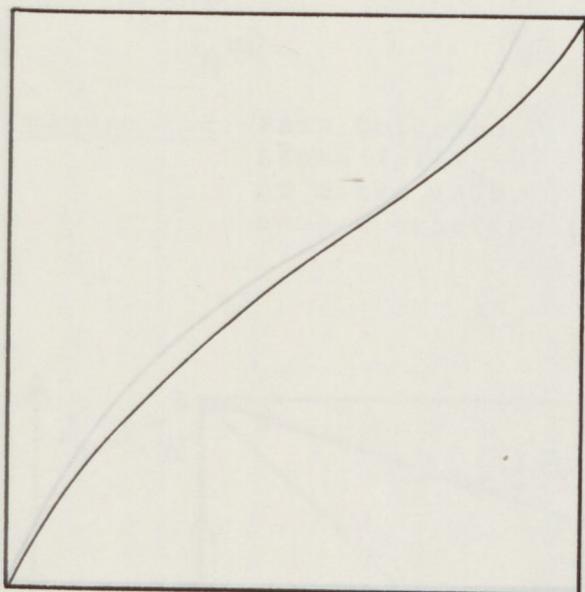
Figure 2.3

Isotherm of the 2nd kind
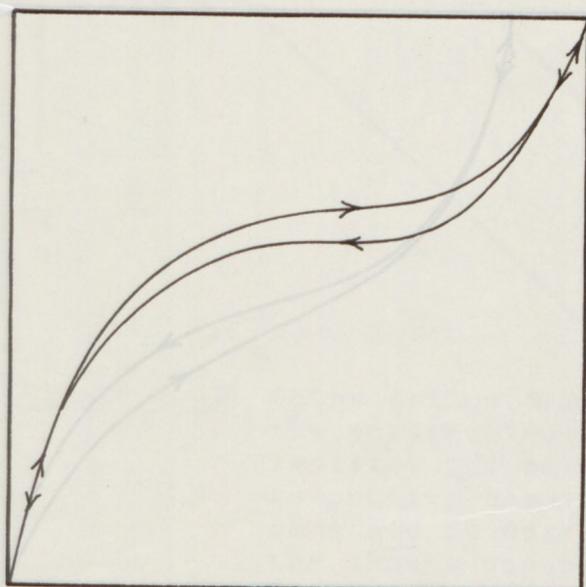
Figure 2.4

Isotherm of the 3rd kind
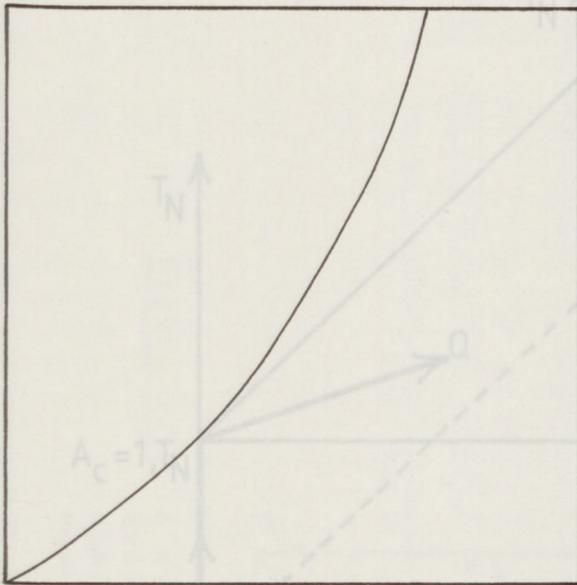
Figure 2.5

Isotherm of the 4th kind
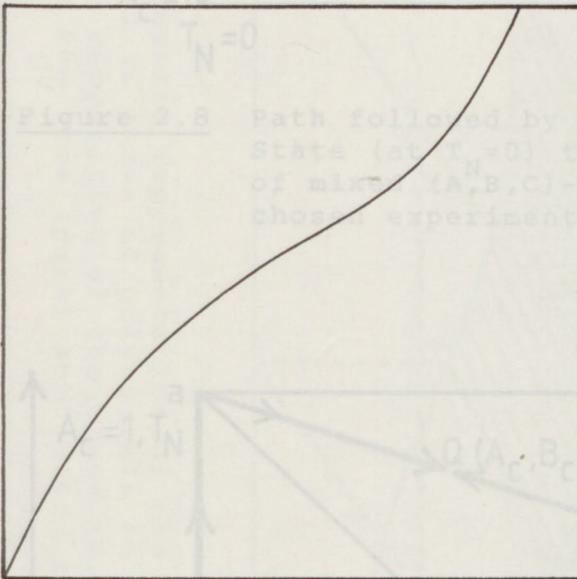
Figure 2.6

Isotherm of the 5th kind
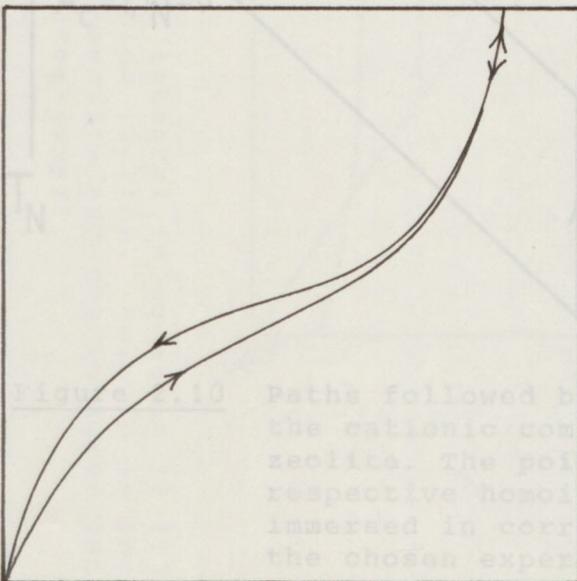
Figure 2.7

Isotherm of the 6th kind

Figure 2.8 Path followed by ions A$^{z_A+}$ from the Standard State (at $T_N \to 0$) to the cationic composition of mixed (A,B,C)-zeolite (point Q) at the chosen experimental concentration (T_N).

Figure 2.10 Paths followed by ions A$^{z_A+}$, B$^{z_B+}$ and C$^{z_C+}$ to the cationic composition Q of mixed (A,B,C)-zeolite. The points a, b and c refer to the respective homoionic forms of the zeolite immersed in corresponding solutions at the chosen experimental concentration T_N.

Figure 2.8   Path followed by ions $A^{z_A^+}$ from the Standard State (at $T_N=0$) to the cationic composition of mixed (A,B,C)-zeolite (point Q) at the chosen experimental concentration (T_N).

Figure 2.10   Paths followed by ions $A^{z_A^+}$, $B^{z_B^+}$ and $C^{z_C^+}$ to the cationic composition Q of mixed (A,B,C)-zeolite. The points a, b and c refer to the respective homoionic forms of the zeolite immersed in corresponding solutions at the chosen experimental concentration T_N.

3.1. RATIONALE OF EXPERIMENTAL WORK

An ideal ternary ion exchange system to be studied in the context of detergents would be a sodium-calcium-magnesium system. Since the testing of a new thermodynamic model was one of the first objects of this work it was however desirable to work on a simple system initially where the treatment of results would be straightforward, and without the additional complications of allowing for partial exchange which is a characteristic of the Na-Ca-Mg zeolite systems. It was therefore decided to study two examples of the simplest possible ternary systems — a uni-uni-univalent system with a common co-anion. Using the findings from these simple systems it would then be possible to progressively add the valencies of the cations and anions and hence increasingly complicate the analysis of the system. The results obtained on the simple systems could hopefully be used to test thermodynamic models to predict ternary ion exchange behaviour under different conditions.

It was decided to work on zeolite X on account of the much published binary work on it and its easy solubility in nitric acid (see Radiation Analyses section).

Regarding the choice of exchanging cations, sodium and potassium were chosen because of the stability in solution of their salts in aqueous. Binary ion exchange data had showed that 100% exchange was possible with zeolite X [16,29]. As the third ionic species, silver and lithium were both

Figure 2.9 A diagrammatic representation of the first integral in equation (2.113) evaluated in terms of polynomials in equation (2.116). Point Q is the cationic composition of the mixed (A,B,C)-zeolite and the integral is equal to the area (pqrs) subtracted from area (wxyz).

CHAPTER THREE   EXPERIMENTAL
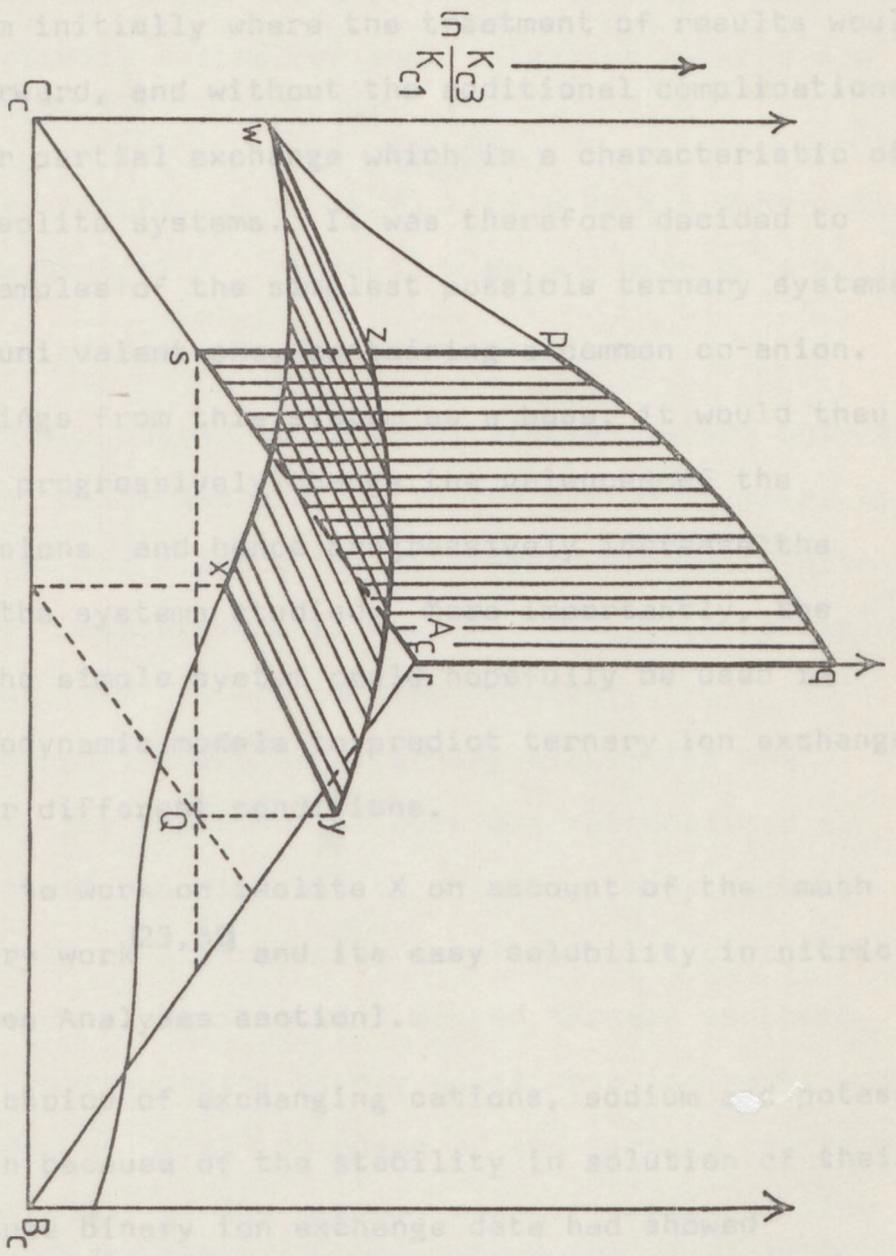
3.1. <u>RATIONALE OF EXPERIMENTAL WORK</u>

The ideal ternary ion exchange system to be studied in the
context of detergents would be a sodium-calcium-magnesium system.
Since the testing of a new thermodynamic model was one of the
first objects of this work it was however desirable to work on
a simple system initially where the treatment of results would
be straight forward, and without the additional complications
of allowing for partial exchange which is a characteristic of
the Na/Ca/Mg zeolite systems. It was therefore decided to
study first examples of the simplest possible ternary systems
viz a uni-uni-uni valent one, containing a common co-anion.
Using the findings from this system as a base, it would then
be possible to progressively change the valences of the
cations and anions and hence progressively increase the
complexity of the systems studied. More importantly, the
results from the simple system could hopefully be used in
suitable thermodynamic models to predict ternary ion exchange
behaviour under different conditions.

It was decided to work on zeolite X on account of the much
published binary work[23,30] and its easy solubility in nitric
acid (see Cation Analyses section).

Regarding the choice of exchanging cations, sodium and potass-
ium were chosen because of the stability in solution of their
salts and because binary ion exchange data had showed
previously that 100% exchange was possible with zeolite X[16,23].
For the third ionic species, silver and lithium were both

considered.

Reported binary work had shown that both ions were capable of being fully exchanged into zeolite X[16,23,30,46]. Furthermore, literature studies also showed that silver and lithium represented the extremes of selectivity patterns shown by zeolite X for univalent metal cations, in that silver was a highly preferred ion while lithium was the least preferred. Published selectivity series for some univalent cations are as follows[16,23,30,46]:

    Up to 40% exchange: Ag >> Tl > Cs ≥ Rb > K > Na > Li
    After 40% exchange: Ag >> Tl > Na > K > Rb ≥ Cs > Li

Both lithium and silver were therefore studied.

The nitrate ion was chosen for initial studies, where only a single univalent anion was present in the system, because it was reported that the nitrate ion interfered minimally with the flame photometric measurement of mixtures of sodium potassium and lithium ions (see Cation Analyses section).

Having selected the Li/Na/K(NO_3) ternary system for the initial studies, the experimental work was rationalized as follows. The first priority was to obtain as many exchange equilibrium points at a particular total solution concentration as were necessary to obtain a well mapped ternary isotherm. Then the three corresponding binary equilibria isotherms were obtained in order to "fix" the edges of the ternary isotherm. Next, other variables of the system, viz (i) total solution concentration (equiv dm^{-3}), (ii) exchange period, (iii) one of the cations, and (iv) choice of anion, were altered system-

atically in order to study separately the effects.

3.2. THE ION EXCHANGE SYSTEMS STUDIED

A total solution concentration of 0.1 equiv. dm^{-3} was used for
most of the work. Ion exchange was effected by placing a known
weight of zeolite in a known volume of solution for a
particular period of time. The ratio of cations in the
exchange solutions was varied to obtain different equilibrium
points. The period of exchange used was 6 days, and all the
measurements were carried out at $25^{o}C$.

The total solution concentration was varied as follows. A
limited isotherm was obtained at a lower concentration of
0.04 equiv. dm^{-3} for comparison with the work at 0.1 equiv.
dm^{-3}. Progressively higher concentrations (from 0.25 to 2.0
equiv. dm^{-3}) were investigated to compare exchange character-
istics and more importantly to look for significant changes
which could not necessarily be corrected for using the new
thermodynamic model[86,87], such as salt imbibition and/or
activity coefficient corrections.

A limited amount of isotherm data were obtained (at the lower
total solution concentration of 0.04 equiv. dm^{-3}) after
exchanging for a lengthy period of $12\frac{1}{2}$ weeks in order to look
for hydrolysis and structural breakdown.

An isotherm consisting of binary as well as ternary data was
obtained for the Ag/Na/K(NO_3)-X system at 0.04 equiv. dm^{-3}
in order to establish the applicability of the model to highly
selective systems.

Finally, a Li/Na/K(NO_3/SO_4/Fe(CN)$_6$)-X multi anion ternary
system was investigated, together with a Na/K(NO_3/Fe(CN)$_6$)- X
binary system; the bulk of this work was done at a concentra-
tion of 0.1 equiv. dm^{-3}. Ternary data were also obtained for
some compositions at a lower concentration of 0.04 equiv. dm^{-3},
and further binary points were obtained at 0.25 and 0.5 equiv.
dm^{-3}.

3.3. PREPARATION OF HOMOIONIC ZEOLITES

Starting materials used were high grade commercial Na-X powder
supplied by B.D.H. Chemicals. 240 g of this powder were
washed for 20 hours in 2 dm^3 of 1 mol dm^{-3} NaNO$_3$ solution.
The zeolite was filtered using a Büchner funnel, and the
procedure repeated with a fresh batch of NaNO$_3$ solution.
After filtering, the filter cake was washed in 1 dm^3 of dist-
illed water, and filtered, and two further washings of 15
minutes each were made with fresh distilled water. The final
filter cake was dried overnight in an oven at 60°C. The solid
mass was then broken up into a powder and placed on a large
clock glass. The zeolite was then left to equilibrate in a
large desiccator containing a saturated solution of sodium
chloride for two weeks to allow the sample to take up an
equilibrium quantity of water.

Due to the difficulty of obtaining homoionic forms of the
zeolite exchanged with potassium and lithium (especially the
latter) six consecutive exchanges were carried out in each
case, and then the washing, drying and equilibrating operations
were accomplished. On analysis, however, it was found that

both the K-X and Li-X samples contained a significant amount of Na ion impurity. (6.8% and 13.8% of exchange capacity respectively). The whole operation was repeated in order to obtain purer samples of K-X and Li-X.

The method of preparing K-X and Li-X was amended so as to obtain a zeolite in as homoionic a form as possible. As many as 15 consecutive exchanges (14 for K-X) were carried out up to several hours at a time, and each time after separation, the wash liquor was analysed for sodium by flame photometry in order to monitor the decrease in Na$^+$ concentration, and this criterion was used to decide when the exchange was near-complete. Also, after some of the exchanges, instead of filtering the total solution to separate the zeolite, the solids were allowed to settle for about 30 minutes, the top liquor decanted off and only the residual sludge filtered.

Appendix II gives details of the process, i.e. exchange periods used, solution concentration, Na$^+$ concentration in wash liquor etc.

3.4. CHEMICAL ANALYSES OF ZEOLITES

Each zeolite was analysed for water, silica, iron, aluminium and the exchanged metals. Three samples of each zeolite were analysed on each occasion and such analyses were carried out frequently. The methods involved in each analysis are described below. Platinum crucibles, where used, were always heated to constant weight before use.

<u>Water</u> - Samples of 0.3 g of the zeolite were placed in pre-heated pre-weighed platinum crucibles, and ignited for two hours to $1000^{\circ}C$ using Meker burners. After cooling in a desiccator for 15 minutes, the crucibles and contents were weighed. The crucibles and contents were then returned to the Meker burners and heated for 30 minutes, then allowed to cool and weighed again. The operation was repeated, and if on this third weighing constant weights were observed, then the procedure was stopped. If not, the procedure was repeated until constant weights were reached. The water content of the zeolite was thus found thermogravimetrically by subtraction.

<u>Silicon</u> - Two methods were originally used to determine the silica content. One of them (in which an HF solution was used to react with silica and form gaseous SiF_4) was soon discarded as being insufficiently accurate. The preferred method, using an equimolar mixture of the anhydrous carbonates of sodium and potassium ("Fusion mixture") was not only more reliable but was also a step in the method for aluminium analysis. Here, samples of 0.3g of zeolite were placed in pre-heated, pre-weighed platinum crucibles, and the crucibles were about two-thirds filled with the fusion mixture. The zeolite was well mixed into the fusion mixture and the crucibles were covered and ignited slowly at first and then to $1000^{\circ}C$ using Meker burners. After about two hours the crucibles were allowed to cool below red-heat and until the salt melt solidified, and then quenched rapidly

in porcelain dishes containing about 25 cm^3 of water. Then
about 75 cm^3 of concentrated HCl solution were added, slowly
at first until the reaction ceased. The resultant solution
was then tested for acidity, and on confirmation of this,
each dish was heated on a steam bath. Once all the solid
matter had ceased evolving carbon dioxide, the platinum
crucible and lid were removed after cleaning carefully with
a 'policeman'; all residues were washed back into the
dishes. The dishes were heated until the contents had dried
to whiteness. During evaporation, the crust had to be
broken several times with a glass rod in order to expose the
solution underneath.

Once dry, about 50 cm^3 of 1:1 HCl solution was added and the
dishes left on the steam bath to evaporate to dryness. This
procedure was repeated with a second batch of 1:1 HCl
solution. Finally, 50 cm^3 of 5% HCl solution were added to
the residue, and the suspension was allowed to digest for
15 minutes on a steam bath. The hot suspension was filtered
through a number 40 Whatman ashless filter paper, and the
precipitate washed thoroughly with hot 5% HCl solution, and
then with hot water. The filtrate was made up to 250 cm^3
with water and used for analysis of iron and aluminium.

Each filter paper was placed in a pre-heated pre-weighed
platinum crucible, taking great care not to loose any of the
precipitate, and each crucible was covered and placed over
a small bunsen burner giving a low non-oxidising flame.
The filter papers were thus warmed very slowly in order to
drive out the liquid without disturbing the residue. Over

a period of hours, the gas flow to the burners was increased

slowly to raise the height of the flame, and after reaching

maximum height, the flame temperature was gradually raised.

The operation so far took about 10 hours, and the filter

paper turned from white to brown to black. Great care was

taken to prevent the filter papers from catching fire. The

crucibles were stored overnight in a desiccator then the

operation was repeated on the following day using tall

bunsen burners. By the end of this operation, only a white

residue remained. Next the crucibles were transferred to

Meker burners and ignited at a very high temperature (1000°C)

for about 2 hours. The crucibles were then removed from the

flame, cooled in a desiccator for 15 minutes and weighed.

Thus the weight of the silica residue was determined by

difference. As a verification, however, the crucibles were

then two-thirds filled with 40% HF solution, and placed on a

hot-plate to allow the volatile SiF_4 so formed to escape.

On complete evaporation, more HF was added and the procedure

repeated. The dry crucibles were then ignited over Meker

burners, cooled and weighed. A consistency of weights before

and after this operation indicated that the previous weight

difference was indeed due to the presence of silica only.

Aluminium - A 100 cm^3 aliquot of filtrate from the fusion

was pipetted into a beaker and just neutralised with 1:1

ammonia solution, using an on-line pH meter. Then 4 cm^3

of 1:1 HCl solution were added and the solution made up to

200 cm^3 and warmed for 15 minutes on a steam bath. To this

an excess of (i.e. about 18 cm^3) 5% 8-Hydroxyquinoline

solution was added. The solution was further warmed to 50°C

and 40 cm^3 of 40% ammonium acetate solution were added slowly,

while stirring. The suspension was heated to 70°C (and no

higher), and left at this temperature for 10 minutes. The

precipitate was then allowed to cool and checked for colour

(any green colouration is an indication of contamination by

iron).

The cool suspension was vacuum filtered through a pre-weighed

P4 sintered crucible, washed thoroughly with hot water and

dried in an oven at 140°C for two hours, then cooled and

weighed.

For determination of aluminium content, the stoichiometry

was assumed to be $(H_6C_9ON)_3Al$. If f grammes of iron were

present in the aliquot of filtrate used, the iron present

(as the oxime compound) was allowed for as follows:

$$(H_6C_9ON)_3Fe = \frac{488.31}{55.85} \times f \qquad \text{(in grammes)}$$

$$\therefore \ Al = \left[W - \frac{488.31}{55.85} \times f \right] \times \frac{26.9815}{459.44} \qquad \text{(in grammes)}$$

where W is the weight of precipitate in grammes. The weight

of iron, f, is found as described below.

Iron - 10 cm^3 samples of the filtrate from the fusion were

transferred into 50 cm^3 volumetric flasks. To each flask,

5 cm^3 of 0.5 mol dm^{-3} sodium acetate solution and 4 cm^3

of a 0.25% solution of 1:10 phenanthroline were added. The
solutions were made up to 50 cm^3 with water and read against
a reagent blank using an EEL absorptiometer to determine
the iron content colorimetrically.

All the zeolites prepared were analysed for iron in this
manner, but it became apparent that the level of iron was
undetectably small in each case.

Attempts were also made to measure the iron content using
atomic absorption spectroscopy, but again no iron could be
detected. Thus, the iron levels in the X zeolites used in
the studies were taken to be negligible.

Alkali Metal Content - Samples of 0.3 g of each zeolite were
treated with HF as if for a silica determination, but the
crucibles were not ignited as this rendered the residue
insoluble. The crucibles were immersed in a 1:1 HCl solution
on a steam bath, and after all of the residue had dissolved,
the crucibles were thoroughly cleaned with a 'policeman',
washed and removed from the solution. The solutions were
then evaporated to dryness, and the residues dissolved in
dilute nitric acid and re-evaporated to dryness. The
residues were then dissolved in dilute nitric acid and made
up to 250 cm^3 with water. The sodium, potassium and lithium
contents were determined using the appropriate standards and
filters in a Corning 400 flame photometer. The potassium
and lithium samples were also checked for any sodium contam-
ination.

Solutions for cation determination were also prepared in a

different way as follows: 0.4 g samples of zeolite were weighed in small plastic vials, shaken up with a little water, and the contents were emptied into beakers containing some 50% nitric acid solution. After washing out the plastic vials several times with more water and nitric acid, the beakers were covered and left for 24 hours. Then the solutions were made up to 250 cm^3 with water, and after suitable dilutions checked for their sodium potassium and lithium contents by flame photometry.

3.5. THERMOGRAVIMETRIC ANALYSES (T.G.A.) AND DIFFERENTIAL

THERMAL ANALYSES (D.T.A.)

25 milligramme samples of each zeolite were subjected to both T.G.A. and D.T.A. and a recording of weight change against the rise in temperature, was obtained. The analyses were normally carried out in an atmosphere of air, supplied at 70 cm^3 per minute, and with a rate of heating of 5°C per minute. All the instruments used were ones manufactured by Metler.

3.6. X-RAY ANALYSES

The crystallinities of the zeolite samples were examined by powder X-ray diffraction using CuK$_\alpha$ radiation and a Guinier camera. Initially, a molybdenum target was used but this was later replaced by the copper target in order to increase the resolution of the diffraction pattern. Samples subjected to T.G.A. were also ground and examined to ascertain whether the intense heat treatment had affected the structure in any way.

- 114 -

3.7. PREPARATION OF ION EXCHANGE SOLUTIONS

First, master solutions of the required salts were made up
by dissolving the appropriate amounts (AnalaR Grade,
supplied by BDH Chemicals) in fresh distilled water whose
pH value was never less than 6. Then different amounts of
these master solutions were added via burettes into volum-
etric flasks and diluted accordingly to give mixed (binary
or ternary) solutions of varied cation compositions at the
selected constant total concentration (equivalents dm^{-3}).
For example, master solutions of $LiNO_3$ $NaNO_3$ and KNO_3, all
at a concentration of 0.25 $equiv.dm^{-3}$, were used to mix
respectively 60, 20 and 20 cm^3 of solution and diluted to
250 cm^3 to obtain a ternary solution of 0.1 $equiv. dm^{-3}$
concentration with a cation composition of 3:1:1 of Li:Na:K.
For the very first batch prepared, the cation ratios were
varied by decreasing the amount of one cation (say Na^+)
and increasing the other two (K^+, Li^+) equally while main-
taining the same total number of cations in solution. The
solutions where the Na^+ composition was varied from 100%
to 0% (with K^+ and Li^+ compositions rising equally from 0%
to 50% each) were identified as "Nalik" solutions. As shown
in Table 3.1, there were eleven Nalik solutions, and simil-
arly eleven each of "Klina" and "Linak" solutions. These 33
solutions were known as the primary solutions because the
equilibrium points obtained by exchanging these solutions
with the corresponding zeolite (i.e. Na-X with "Nalik"
solutions, K-X with "Klina" solutions and Li-X with "Linak"
solutions), formed the basis of the comparison work carried

TABLE 3.1. "NALIK" PRIMARY SOLUTIONS USED FOR ION EXCHANGE

Identity code of primary solution used	Concentrations of mixed primary solution (fractions)			Amount of master solutions used (cm^3)		
	Na	K	Li	Na	K	Li
Nalik 1	1.0	0.00	0.00	100	0	0
Nalik 2	0.9	0.05	0.05	90	5	5
Nalik 3	0.8	0.10	0.10	80	10	10
Nalik 4	0.7	0.15	0.15	70	15	15
Nalik 5	0.6	0.20	0.20	60	20	20
Nalik 6	0.5	0.25	0.25	50	25	25
Nalik 7	0.4	0.30	0.30	40	30	30
Nalik 8	0.3	0.35	0.35	30	35	35
Nalik 9	0.2	0.40	0.40	20	40	40
Nalik 10	0.1	0.45	0.45	10	45	45
Nalik 11	0.0	0.50	0.50	0	50	50

The concentration of the (nitrate) master solution was either 0.25 or 0.1 equiv. dm^{-3}.

The 100 cm^3 mixed solution prepared was diluted to 250 cm^3 to obtain the required solutions.

out. For the major isotherm (total solution concentration of 0.1 equiv. dm^{-3}, exchange period of 6 days), in order to obtain the many other equilibrium points, a substantial number of intermediate ternary solutions of various cation compositions were made up; for example, there were solutions where the cation ratio ranged from 7:2:1 to 4:5:1 (i.e. one cation remaining constant) and others where the ratio ranged from 3:1:6 to 5:4:1 (i.e. all three cations being changed). Furthermore, some of the binary solutions, which were made up for the binary exchange work, when used with a zeolite of the third cation (say, a K/Li solution with Na-X) gave rise to an 'in situ' ternary exchange, resulting in equilibrium points which also contributed towards the major ternary isotherm.

For the Ag/Na/K (NO$_3$) system, fewer primary solutions were prepared, because the isotherm was obtained by using only K-X and Na-X zeolites; a fully exchanged Ag-X zeolite was not prepared. For the binary work, the required binary solutions were prepared.

Numerous other solutions were made up in a similar manner for the examination of the effect of total concentration and co-anion concentrations on the selectivity.

3.8. THE ION EXCHANGE EXPERIMENTS

Ion exchange was effected by accurately weighing out a small amount of zeolite into a clean dry plastic vial, and then carefully pipetting in 50 cm^3 of the appropriate solution. The vial mouth was sealed with PTFE tape and then the cap

was screwed on tightly. The vials were then shaken hard

and allowed to equilibrate at 25°C for the exchange period

selected. They were shaken by hand many times during that

period to maintain good exchange contact. In the case of

exchanges involving silver, all samples were kept in the dark

as light reduces the silver ion in the zeolite to the metal.

For most of the exchanges, the amount of zeolite used was

0.4g, but for a few exchanges greater or lesser amounts were

used in order to obtain an equilibrium point at an

extremum of an isotherm.

3.9. SEPARATION AND TREATMENT OF PHASES

Basic background studies had to be effected first before a

suitable method of separation and subsequent treatment could

be established. Since it was intended that both phases

should be analysed for all cations, it was important that

adequate amounts of each phase were recovered. It was also

important that contamination of one phase by the other could

be minimised (especially the presence of zeolite "fines" in

the centrifugate). After separation, it was necessary to

dissolve the solid phase for analysis which was by flame

photometry for sodium, potassium and lithium ions, and by

titration or atomic absorption spectroscopy for silver.

This meant that the solid phase had to be fully decomposed,

followed by dissolution in a suitable medium. In previous

work done in this research group, mainly on highly siliceous

mordenite, however, the zeolite had been dissolved in aqua

regia[18]. For this project aqua regia was inadvisable

because the presence of chloride ions would (obviously) cause the precipitation of silver and also give rise to interference problems when using the flame photometer. Because of its high aluminium content, X is soluble in nitric acid, and the best concentration of acid solution was found to be one made up using AnalaR Grade (sp.gr.1.42) nitric acid, and water in a ratio of 1:1; hereafter, this will be referred to as 50% nitric acid.

It was not necessary to recover all of each phase as only the ratio of the cations was required in order to obtain equilibrium points. The method used, however, allowed all of the solid phase to be recovered. The procedure involved in separating and treating the phases is described below.

Each vial was thoroughly shaken, and about 50 cm^3 of the contents were poured into a separation tube. (The pyrex glass tubes of 50 cm^3 capacity were treated with 50% nitric acid initially to leach out any surplus sodium ions. Glass tubes were chosen instead of cheaper plastic ones because it was necessary to examine the solutions by visual inspection during the separation work.) Tubes containing the zeolite suspension were spun in a MSE minor's' centrifugal separator for about 10 minutes at a speed of 3500 min^{-1}. Then, approximately 45 cm^3 of each solution were collected, leaving behind some of the solution, taking great care not to disturb the solid at the bottom of the tube. This 45 cm^3 of solution represented the solution phase, and was set aside for subsequent analyses. The solid at the bottom of the tube was then broken up by squirting water from a wash bottle, and to this was added the

remainder of the exchange mixture from the vial. The vial
was then washed out, and the washings added to the tube. The
solution was made up to the height mark on the tube (about
50 cm^3), and the tubes were spun again for 10 minutes at the
previous speed. The zeolite was thus washed to remove the
superficial cations which otherwise would be carried away
with the solids and erroneously add to the ion content. The
liquid was then carefully poured out; by leaving behind some
of the wash water it was possible not to lose any solid. The
4-5 cm^3 of liquid thus retained did not affect subsequent
operations. The solid was then broken up as before, and more
water poured in. After a subsequent centrifugal separation,
the wash water was poured out, and the solid phase was ready
for treatment.

The number of washings necessary after the separation of
phases was decided after carrying out a sub-study where small
samples of wash water and zeolite were analysed for cation
content after each of several consecutive washings. From the
zeolite analyses it was apparent that the cation content
remained constant after the second washing, while the wash-
liquor from the second washing contained less than 15 ppm
of total cations. As such, only two washings were made in all
the separations carried out. This additionally minimised
hydrolysis of the zeolite which can accompany excessive
washing[106]. This point was further confirmed during the
multi-anion work, when only a very faint yellow colour (from
the Fe(CN)$_6^{3-}$ ion) was visible after the second washing.

- 120 -

The solid phase was treated next by breaking it up and pouring it into a 400 cm^3 beaker containing about 50 cm^3 of 50% nitric acid. The beaker was shaken slightly to aid dissolution which occurred fairly rapidly. A further 35 cm^3 of 50% nitric acid were poured into each tube and allowed to stand for a few minutes to dissolve any residual zeolite. The vials used for exchange were treated similarly. Any sub-sequent washings of the vials and tubes were added to the beakers. The beakers used had all been treated with nitric acid initially to leach out any surplus sodium ions. About 170 cm^3 of solution was thus collected in each beaker which was then covered and allowed to stand for 24 hours. This 24 hour period too was established after another sub-study where similar solutions that had been allowed to stand for periods ranging from 6 hours to 4 days were analysed to compare cationic composition and total cation content.

After the 24 hour period, the beaker contents were poured into a volumetric flask, and the beaker washed several times by squirting water, the washings being added to the flask each time, and made up to 250 cm^3.

After several batches of solid phase analyses had been carried out, a blockage problem of the flame photometer was traced back to silica particles present in the dissolved solid phase. Therefore, a further stage was added to the procedure whereby after the 24 hour period the beaker was placed on a steam bath and the suspension evaporated to dryness. About 60cm^3 of 5% nitric acid were then added, and warmed, in order to dissolve the soluble matter. After about 1½ hours on the steam bath,

the contents are filtered to remove the silica, and the

solution made up to 250 cm^3 as before.

3.10 CATION ANALYSES

At the start of the project, it was decided that both the
solution and solid phases should be fully analysed for all
cations. A literature survey was carried out to find the most
accurate methods of analysing for the cations used.

3.10.1. Flame Photometry

For the first three cations, which formed the main body of work,
flame photometry was found to be, by far, the best method. A
flame photometric review by Snell[107], suggested that a propane
gas fired flame photometer was best suited for accurate work
on Na, K and Li, and a new Corning 400 machine was purchased
for this purpose. It was fitted with a sliding 3-filter
holder, one for each ion, and this provision facilitated
switching over from analysing for one ion to another. A batch
of calibration standards were carefully prepared for each ion,
of concentrations of 2.5, 3.75, 5.0, 7.5, 10.0, 12.5, 15.0,
17.5, 20.0 and 25.0 ppm. These standards were prepared by
diluting the corresponding standard solutions for atomic
absorption spectroscopy (at 1000 ppm) supplied by B.D.H.
Chemicals. The flame photometer was then calibrated, and the
readings on the 0-100 scale were plotted against the concen-
tration of the standards to obtain the calibration curves
(Appendix III). These calibrations were repeated several
times over a long period of time to confirm reproducibility.

An investigation into possible interference effects was

- 122 -

carried out next. Snell's review[107] suggested that sodium,
lithium and potassium did not significantly interfere with each
other when present together. It also stated[107] that the presence
of silver did not cause interference when measuring sodium
and potassium, but that the presence of anions like chloride
and sulphate affected readings of sodium, potassium and lithium.
The presence of the nitrate anion had no affect towards measure-
ments. The review was inconsistent with regard to the effect
of aluminium stating in some places that it had no effect, and
in others that it had a slight effect. A small sub-study was
then set up to examine possible effects by making up standard
solutions containing 10 ppm of cation to be measured and 10
and 100 ppm each of one or more other cations. (see Section 4.1).

Because of the reported adverse effects of certain anions, it
was decided to carry out all the main ion exchange work in the
nitrate system. It was particularly useful to select the nitrate
ion because all the standard solutions (used to make up standards)
were also available in the nitrate form.

Each of the samples had generated approximately 45 cm^3 of solution
solution and 250 cm^3 of dissolved solid, and therefore,
analyses of the two phases were carried out after diluting
these to suitable levels. Since at first it was not possible
to predict the extent of ion exchange that had occurred with-
in each sample, the initial analyses involved diluting samples
on a trial and error basis. As such, it was decided to
commence the analytical work on the dissolved solid phase
where much more solution was available for experimenting.
The procedure followed was to select several strategic samples

from the sets of samples, make broad estimates regarding
their composition and make appropriate trial dilutions. The
resulting solutions were then analysed for one or more of
the cations. Though at the very beginning there were a few
dilutions which were wildly off-mark, a trend was soon
established, and the gaps within the array of samples were
systematically filled. It should be noted that most samples
contained widely different concentrations (in ppm) of the
cations, necessitating two or three levels of dilutions for
many of the samples so that all cations could be read on the
instrument.

The ion exchange studies were carried out in batches (usually
of up to 10 samples each), and the analyses of one phase of
each batch was carried out in one session. This meant that,
after preparing and checking the trial dilutions, all the
intermediate dilutions were carried out prior to the final
analyses. Before and after analysing one batch of dilutions
for a particular cation, the calibration for that ion was
checked by using several standard solutions. Furthermore,
before and after each individual reading, a standard solution
of concentration near that of the sample was read to check
for any variation. Thus the analytical procedure consisted
of alternatively reading samples and standards, and where
necessary, continually re-adjusting the flame photometer scale
settings to maintain constant calibration readings. Often
three or four readings on the flame photometer per diluted
sample were adequate for an accurate result, but occasionally,
where machine variability was high, up to eight readings were

taken and averaged out. Occasional artefactual readings
occurred, which were normally found to be due to blockages
in the machine (usually in the atomizer or sample feed tube).

These blockages, and the resulting variability of readings
became more and more frequent with time. Several possible
reasons were investigated and the problem was eventually
traced to the presence of small silica particles in the
dissolved solid phase. A sub-study was carried out as
described earlier (section 3.9): In addition to the extra
stage in the dissolution procedure used for the zeolite samples
(section 3.9), it was found that flushing the flame photo-
meter feed system and atomizer regularly with dilute nitric
acid (about 5%) and then with water, cleaned the system
effectively eliminating the problem.

After analysing the solid phase and determining the compos-
ition, the composition of the corresponding solution phase was
estimated by difference before the solution phase samples
were also analysed. This enabled solution phase dilutions
to be estimated in advance of analysis, resulting in minimal
loss of available solution volume (approximately 45 cm^3).
Here again, the differences in concentration levels between
the three cations present usually necessitated more than one
dilution per sample.

3.10.2. Silver Analyses

The first method considered for silver analysis was a 'wet'
method, in which 10 cm^3 of 880 ammonia solution and about
0.2 g of $K_2Ni(CN)_4$ were added to an aliquot of solution to

effect the reaction;

$$2(Ag(NH_3)_2)^+ \; + \; (Ni(CN)_4)^{2-} \; \rightleftharpoons \; 2(Ag(CN)_2)^- + Ni^{2+} + 4NH_3$$

The liberated nickel(II) was then determined by back-titration with ethylenediaminetetraacetic acid (EDTA) using Eriochrome Black T indicator. After a few trial runs this method was abandoned in favour of analysis by the much easier Volhard's method, where about 5 ml of concentrated nitric acid were added to a known volume of the sample and titrated with ammonium thiocyanate solution using a ferric alum (ferric ammonium sulphate) indicator[108]. First, a whitish silver thiocyanate precipitate was produced according to the reaction

$$Ag^+ \; + \; (SCN)^- \; \rightarrow \; AgSCN\downarrow$$

and when all the silver was expended, the slightest excess of thiocyanate produced a reddish-brown coloration caused by the formation of the complex ferri-thiocyanate ion:

$$Fe^{3+} \; + \; (SCN)^- \; \rightleftharpoons \; (FeSCN)^{2+}$$

During the titration, as each drop of thiocyanate was added, a reddish-brown cloud was produced in the liquid which disappeared quickly on shaking. As the end point was approached, the precipitate became flocculent and settled easily; at the end point, the last half drop of thiocyanate produced a faint brown colour which did not disappear when shaken. It is therefore essential to shake vigourously throughout the titration in order to obtain accurate results.

The concentration of the nitric acid used in the procedure had to be around $0.5 - 1.5$ mol dm^{-3} because stronger acid retards the formation of the ferri-thiocyanate complex. As high temperatures tend to bleach the colour of the indicator, the temperature was kept below $25^{o}C$ during the titrations. The solutions also had to be free of nitrous acid, which gives a red colour with thiocyanic acid (and may be mistaken for the end point). Pure nitric acid was prepared by diluting the A.R. grade acid in water and boiling until colourless; this removed the lower nitrogen oxides from the acid.
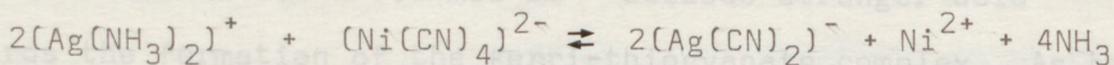
Atomic absorption spectroscopy was used to determine silver when it was present only in very small quantities, usually in the solution phase after exchange. All analyses on the solid phase and the solutions before exchange were effected using Volhard's method. It was only necessary to use atomic absorption spectroscopy on some solutions after exchange due to the high selectivity of the zeolite for silver.

3.11   RADIO -ISOTOPIC ANALYSIS

Early results on the main Na/K/Li system showed that a large uncharted area within the isotherm triangle existed, corresponding to very low concentrations of sodium. This was mainly because the zeolite was less selective for the Li^{+} ion. In order to chart this particular area, it was decided to study a complementary sub-system of Na/K/Li-X where the sodium concentration would be kept extremely low, and a special exercise was set up at Unilever Research Laboratories, Port Sunlight (the collaborating body on this research project).

Although flame photometry had been the method of analysis used for the main work, the very low concentrations of sodium necessitated a more sensitive method of analysis, and this was achieved by the use of radio-isotopic methods.

In the studies carried out on the main Na/K/Li ternary system so far, ion exchange had been arranged between each zeolite sample and solutions containing varying ratios of all three ions. For the radio-isotope work, however, only two ions were present in solution (sodium and one other) while the third ion was present in the zeolite (i.e. K-X was exchanged with solutions containing mostly lithium and very little sodium and Li-X was exchanged with solutions consisting of mainly potassium). This simplification, an 'in-situ' ternary system - allowed the solutions to be made up more easily and quickly (and also more accurately despite the smaller quantities involved). Na-X was not used in this exercise because only low concentrations of sodium were being studied.

For the radio-isotope work, reasons of safety and cost dictated that minimum amounts of ^{22}Na should be present, and thus the quantities used were scaled down to 0.16 g of zeolite exchanging with 20 cm^3 of 0.1 equiv. dm^{-3} solutions in each case. For each zeolite, 5 ratios of sodium to potassium or lithium were used; from 1:99 to 1:19.

Safety aspects complicated the analytical procedure because all three cations were present in each phase after exchange. The sodium was measured using radio-tracer techniques but potassium and lithium could not be analysed in the radio-tracer laboratory because there were no means to do so.

The presence of ^{22}Na dictated that the samples could not
be removed from the laboratory for analysis outside. In
order to overcome this problem, it was decided to duplicate
all experiments, using identical amounts of non-radioactive
Na outside the radio-tracer laboratory, and analyse these
for potassium and lithium using the flame photometer at The
City University. Thus the exercise was set up as follows:-

(1) 5 samples of radioactive Na/K(NO_3) solutions with
ratios 1:99 through 1:19 for exchanging with Li-X zeolite.

(2) Duplicate set of above.

(3) 5 samples of radioactive Na/Li(NO_3) solutions with
ratios 1:99 through to 1:19 for exchanging with K-X zeolite.

(4) Duplicate set of above.

(5)-(8) Duplicate sets of (1) - (4) above using identical
amounts of non-radioactive sodium.

This yielded 40 samples in all.
The amount of ^{22}Na required for the whole exercise (i.e. 20
exchange samples and some preliminary work) was calculated
on a minimum count per sample after exchange basis allowing
for counter inefficiency. For an accurate result, the
machine required at least 10,000 c.p.m. (counts per minute)
per cm^3 of each sample. The preliminary work carried out
showed that the counter efficiency was higher than 70%. This
meant that a count rate of about 14,500 min^{-1} or more were
required for an accurate count. For the lowest initial con-
centration of sodium in a sample (i.e. the 1:99 sample),
20 cm^3 of solution contained 0.02 meq of Na$^+$(and 1.98 meq of

K^+ or Li^+). Assuming that only 30% of this sodium remained
in the solution phase after exchange, in order to satisfy
the minimum count requirement, it followed that the initial
solution should contain enough ^{22}Na to give at least
9.5×10^5 d.p.m.(disintegrations per minute).

The ^{22}Na used was supplied as a 0.5 cm^3 $^{22}NaCl$ solution of
strength 105.7 µCi (where 100 µCi ≡ 1 µg of ^{22}Na).

Therefore,

$$0.5 cm^3 \rightarrow 1.057 \mu g \ ^{22}Na = 4.8 \times 10^{-5} \ m \ eq \ Na^+$$

For NaCl, 1 m eq Na^+ ≡ 1 m eq Cl^-, and therefore

$$0.1 cm^3 \ ^{22}NaCl \equiv 1 \times 10^{-5} \ m \ eq \ Na^+ \ or \ Cl^-$$

The ^{22}Na was diluted in small batches before use, and this
was done as follows:

$$0.1 \ cm^3 \ ^{22}NaCl \ + \ 4.9 \ cm^3 \ NaNO_3 \rightarrow \ 5 \ cm^3 \ *NaNO_3$$
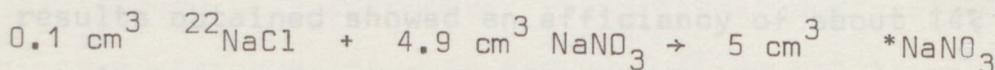
Each 5 cm^3 batch of $*NaNO_3$ had a concentration of 0.1 mol dm^{-3}.
This was achieved by using a bulk $NaNO_3$ solution which had been
made up to a concentration somewhat greater than 0.1 mol dm^{-3},
so that a concentration error was not made on adding the
0.1 cm^3 of NaCl solution. The $^{22}Na^+$ and Cl^- contribution towards
the solution was negligible on a weight basis (i.e. 2×10^{-5} m eq
in 1 m eq).

Four such 5 cm^3 batches of $*NaNO_3$ solution were prepared,
utilizing 0.4 cm^3 of the original $^{22}NaCl$ solution. Using a
0.5 cm^3 Oxford pipette, appropriate aliquots of this solution
were transferred to a 50 cm^3 volumetric flask, and made up to
50 cm^3 with 0.1 mol dm^{-3} KNO_3 (or $LiNO_3$) solution to give the

required mixed solutions of 0.1 mol dm^{-3} concentration.

This procedure used up 15 cm^3 of the 20 cm^3 (i.e. 4x5 cm^3)
*NaNO$_3$ solution prepared, and 1 cm^3 of the remainder was diluted
to 50 cm^3 with water and used for preliminary experiments. These
experiments were conducted to gain experience in dealing with
small quantities of radioactive material, and also to establish
counter efficiency.   The 50 cm^3 of dilute *NaNO$_3$ solution were
used as follows:

       2 x 0.5 cm^3 each in three β vials
       2 x 0.5 cm^3 each in three γ vials

These six vials were counted on both instruments available in the
laboratory (a Packard 3390 and a Packard 460). Each 1 cm^3
sample contained 0.0423 μCi of radiation, and since 1 μCi ≡ 2.2
x 10^6 d.p.m., about 93000 d.p.m. were expected for each vial.
The results obtained showed an efficiency of about 14% for the
γ count (both machines) and about 74% (Packard 460) and 83%
(Packard 3390) for the β count at the settings used. It was
clear that higher accuracy would be obtained - because of the
higher efficiency - for β counts. It was decided however, to
use both instruments for all readings.

The settings on the counters used for the preliminary work,
and the subsequent analytical work, were specifically adjusted
for the ^{22}Na isotope. The channel selected was the ^{14}C
channel, optimised for ^{22}Na. The pulse-height discriminators
used to define the 'window' (i.e. the channel) had a lower
limit of 50 m.V. and an infinite upper limit. The background
count setting used was 30 c.p.m. and for the background a vial
containing only the scintillator solution was used with all
batches measured. The particular scintillator solution used

(usually 10 cm^3 per vial), was Packard 'Instagel', a Xylene based solution which incorporated all the necessary solvents, solutes and additives.

The occurrence of chemical 'quenching' was also investigated as part of the preliminary work. Chemical 'quenching' is caused by the de-excitation of electronically excited molecules which would otherwise give rise to emitted photons, and this reduction in the number of photons emitted from the scintillator solution (for a given radio active decay energy) in turn causes a reduction in the magnitude of the electrical pulse as read by the photomultiplier tube[109,110].

Thus, the counting efficiency for a particular isotope varies with the degree of quenching within the solution. The investigation was carried out by treating β vials containing 'Instagel' and the isotope with increasing amounts of a quenching agent (0, 10,20,50,100,200,500,1000 and 2000 μl of CCl$_4$). These were counted subsequently, and compared with the results obtained when the same β vials were counted prior to the addition of CCl$_4$. The difference in counts was very small, and it was concluded therefore that 'quenching' would not be a problem for the ^{22}Na work planned. It should be noted here that there exists another form of quenching known as 'colour quenching', caused by absorption of emitted photons by materials in the solution (usually a coloured sample)[109,110]. This aspect was not investigated because the 'Instagel' solution used contained agents designed to overcome colour quenching.

Preliminary work complete, the experimental work was begun. 0.16g of equilibrated zeolite (Li-X and K-X) were weighed out into 20 vials, and to each vial, 20 cm^3 of the appropriate

mixed nitrate solution were added. The vials were tightly

sealed, mounted on a shaker and agitated for about 130 hours.

Each of the 50 cm^3 batches of mixed nitrate solutions were

used as follows:

   20 cm^3 solution + 0.16g zeolite } duplicate sets for
   20 cm^3 solution + 0.16g zeolite }   exchange

   5 cm^3 solution }
                      } for the 'before' count (see below)
   1 cm^3 solution }

The procedure followed to measure the sodium exchange into the

zeolite was to 'count' the radioactivity of the solution both

before and after the exchange, so that the difference in counts

gave the extent of exchange. This method was far simpler than

separating the solid zeolite and counting it directly for

sodium. Therefore, 5 cm^3 and 1 cm^3 samples of solution, with

only the appropriate amounts of scintillating liquid added, were

read in the two machines. Each vial was counted five times over

a period of 1 minute each time, and the results were averaged

out. The results showed that the 5 cm^3 samples gave counts which

neared, and sometimes exceeded, the upper limit of accuracy

of the machines (approximately one million c.p.m.) and these

results were discarded in favour of the results for the 1 cm^3

samples.

While the radioactive samples were exchanging, the corresponding

non-radioactive work was started. The procedure was identical

to the above except that a non-radioactive NaNO$_3$ solution was

used to prepare the mixed solutions. The same apparatus was used

as far as possible for both preparations. The exchanging non-

radioactive samples were transferred to the university research

laboratory and left on a shaker for a length of time correspond-

ing to their radioactive counterparts.

After the set time, the radioactive samples were removed from the shaker, allowed to settle, and treated as follows: a syringe was inserted into each vial and about 2.5 cm^3 of liquid (and associated small particles) were drawn out. The syringe nozzle was then placed into a micropore filter and the liquid was forced into a clean vial through the filter. The operation was repeated so that about 4.5 cm^3 of pure solution was collected in the vial. From this vial, 1 cm^3 aliquots of each were transferred using an Oxford pipette to three vials already containing scintillator solution. A new filter and syringe were used for each sample.

Sixty vials were obtained in this way, and after shaking up, each vial was counted five times for 1 minute each time, and the five counts averaged out. These 'after' counts were processed with the corresponding 'before' counts for each machine.

The non-radioactive samples were removed from the shaker after the appropriate length of time, and centrifugally separated (and the solids washed) into the two phases. Each phase was treated and analysed in the manner described earlier (sections 3.9,3.10).

CHAPTER FOUR   RESULTS

The compositions of all the zeolites used for the studies, the measured isotherms and the derived thermodynamic parameters are all reported in this chapter. Also given are the flame photometer calibration plots, and the results of the flame photometer interference studies.

4.1.   FLAME PHOTOMETER CALIBRATIONS

These were carried out for sodium, potassium and lithium using standards prepared in the manner described in section 3.10.1. The calibrations were carried out on several occasions, and the reproducibility of the flame photometer was excellent. The three calibration curves obtained are shown in Appendix III, and these curves were checked and used when analysing experimental solutions.

The interference studies were carried out by making up mixed standards containing 10 ppm of the cation under investigation plus a 10 ppm or 100 ppm background of one or more of the other ions that would be present under experimental conditions (for example, 10 ppm sodium with 100 ppm each of either potassium, aluminium or silver). The higher background of 100 ppm was calculated to simulate experimental conditions but because of the high molecular weight of silver and the large amounts of silver present in the crystal phase, 100 ppm fell somewhat below representative experimental silver concentrations. All the standards used in the interference studies contained only one anion (nitrate) and therefore any interference caused by the presence of other anions was not investigated.

In all cases, the readings on the flame photometer for the pure and mixed 10 ppm cation were compared to determine any

difference, studies being carried out in duplicate at least.
In all cases, the studies confirmed the published informa-
tion[107] that the presence of the other ions in these experi-
mental solutions did not interfere with flame photometric
analyses for sodium, potassium and lithium.

4.2.   ZEOLITE ANALYSES

Complete chemical analyses of all the zeolites used are found in
tables 4.1 and 4.2. It should be noted that the first batch
of Na-X, K-X and Li-X zeolites were used only to obtain the
long-term Na/K/Li (NO_3) ternary isotherm (at a concentration of
0.04 equiv. dm^{-3}). All other ternary work, and all the binary
work, were carried out using the second batch of Na-X, K-X and
Li-X zeolites.

All analytical results show a small deficit, with the components
of the zeolite only summing to approximately 99% by weight.
An examination of each cation to aluminium ratio revealed that
it was always slightly different to the expected value of one.
Exchange capacities have been calculated on the basis of the
cation composition, and are therefore slightly smaller than the
theoretical value based on the aluminium content. These points
are further discussed in section 5.1.

The similarity between the two batches of zeolite is good (except
for the residual sodium in the K-X and Li-X zeolites), and the
small differences can be attributed to batch to batch varia-
bility. No iron was detected in any of the samples analysed.

4.3.   ION EXCHANGE ISOTHERMS

4.3.1.   Binary Isotherms

Figures 4.1 - 4.8 show all the binary equilibria studied in this

TABLE 4.1. <u>Analyses of Zeolites</u>

<u>First batch</u> - used for long-term ternary study

(The number of samples used to determine the

mean value is given in parentheses).

Zeolite	Na-X	K-X	Li-X
Component	%	%	%
SiO_2	35.58(9)	33.94(7)	37.47(8)
Al_2O_3	23.27(10)	22.26(7)	24.56(9)
Na_2O	14.08(6)	0.46(5)	2.05(6)
K_2O	-	19.68(5)	-
Li_2O	-	-	6.17(6)
H_2O	26.01(12)	23.15(10)	29.10(10)
Total	98.94	99.49	99.35
Exchange Capacity (m equiv g^{-1})	4.542	4.327	4.790

<u>Oxide formulae</u>

Na-X :- $0.995\ Na_2O.\ Al_2O_3.\ 2.594\ SiO_2.\ 6.326\ H_2O$

K-X   :- $0.034\ Na_2O.\ 0.957\ K_2O.\ Al_2O_3.\ 2.586\ SiO_2.\ 5.886\ H_2O$

Li-X :- $0.137\ Na_2O.\ 0.857\ Li_2O.\ Al_2O_3.\ 2.588\ SiO_2.\ 6.706\ H_2O$

<u>Unit cell formulae</u>

Na-X :- $83.2Na^{+}(83.6AlO_2.108.4SiO_2)^{83.6-}.264.4H_2O$

K-X   :- $2.9Na^{+}.80.1K^{+}(83.7AlO_2.108.3SiO_2)^{83.7-}.246.4H_2O$

Li-X :- $11.5Na^{+}.\ 71.7Li^{+}(83.7AlO_2.108.3SiO_2)^{83.7-}.280.6H_2O$

TABLE 4.2.   Analyses of Zeolites

Main (second) batch - used for all other work

(The number of samples used to determine the mean

value is given in parentheses)

Zeolite Component	Na-X %	K-X %	Li-X %
SiO_2	35.22(14)	33.36(15)	37.01(14)
Al_2O_3	23.24(15)	22.05(13)	24.36(14)
Na_2O	14.02(9)	0.22(8)	0.95(9)
K_2O	-	19.96(8)	-
Li_2O	-	-	6.65(9)
H_2O	26.67(17)	23.43(15)	29.98(15)
Total	99.15	99.02	98.95
Exchange Capacity (m equiv g^{-1})	4.523	4.308	4.753

Oxide formulae

Na-X   :- 0.992 $Na_2O.Al_2O_3.$ 2.571 $SiO_2.$ 6.490 H_2O

K-X   :- 0.016 $Na_2O.$ 0.979 $K_2O.$ $Al_2O_3.$ 2.568 $SiO_2.$ 6.004 H_2O

Li-X   :- 0.064 $Na_2O.$ 0.931 $Li_2O.$ $Al_2O_3.$ 2.578 $SiO_2.$ 6.972 H_2O

Unit cell formulae

Na-X   :- 83.3Na^+(84.0 $AlO_2.$ 108.0 SiO_2)$^{84-}.$ 272.7 H_2O

K-X   :- 1.4 $Na^+.$ 82.4K^+ (84.1 $AlO_2.$ 107.9 SiO_2)$^{84.1-}.$ 252.4H_2O

Li-X   :- 5.4 $Na^+.$ 78.1 Li^+(83.9 $AlO_2.$ 108.1 SiO_2)$^{83.9-}.$ 292.4H_2O
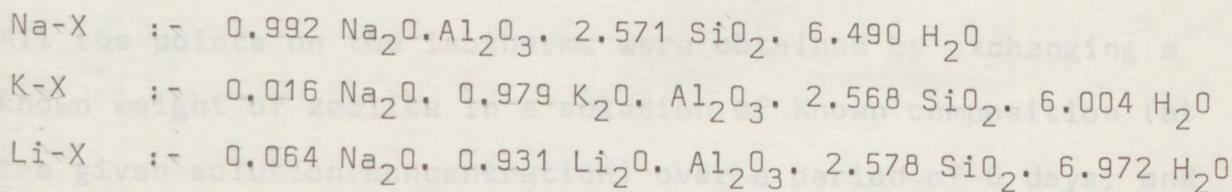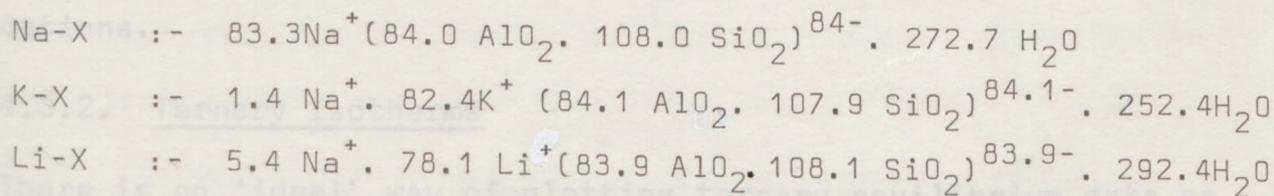
project. The isotherms are plotted with the equivalent fraction
of the ingoing ion in the zeolite (A_c) as the abscissae and
the equivalent fraction of the same ion in solution (A_s) as the
ordinates.

The isotherms are arranged in pairs so that visual comparisons
may be made (figures 4.3 and 4.5 depict the same Na/K equilibria
for this reason). It is obvious from figures 4.1 and 4.2 that
for the case of lithium exchanging into a sodium or potassium
zeolite, the outgoing ion is strongly preferred by the zeolite,
and that the preference for sodium or potassium is similar.
An examination of the sigmoidal shaped Na/K isotherms (figures
4.3 - 4.6) shows that the preference for sodium over potassium
is quite small and that this preference changes from one ion
to the other as the exchange progresses. This trend is seen
at different total solution concentrations, and when one or
two anions were present in solution. Figures 4.7 and 4.8 show
a completely opposite case to Li/K and Li/Na exchange, in that
the zeolite is enormously selective for the ingoing ion (silver)
over the outgoing ion (sodium or potassium).

All the points on the isotherms were obtained by exchanging a
known weight of zeolite in a solution of known composition (at
the given solution concentration) over a period of 6 days, and
then analysing *both* the solution and crystal phases for *all*
cations.

4.3.2. Ternary Isotherms

There is no 'ideal' way of plotting ternary equilibrium data on
triangular coordinate diagrams. Two different methods have
been used here, depending on the total number of data points.
For the two main systems, (i.e. Na/K/Li (NO_3) at a total solution

concentration of 0.1 equiv. dm^{-3} and Na/K/Ag (NO$_3$) at a con-
centration of 0.04 equiv. dm^{-3}) the solution phase points are
plotted on one triangular coordinate diagram and the crystal
phase points on another (figures 4.9 - 4.12), and some corresp-
onding pairs are numbered for visual examination. For all other
ternary studies, both phases are depicted on one ternary
diagram, and the corresponding pairs are numbered or joined by
lines to show the equilibria. Where possible, the correspond-
ing binary equilibrium points (at the same total solution
concentration where available or at a different concentration)
are plotted along the sides of the triangles, as these are
represented by the edges of the triangular diagram (figures
4.13 - 4.17).(Note that in figure 4.12, only some of the Na/K
binary solution phase data are shown because of the high density
of data points in this area).

As with the binary equilibrium points, all the ternary points
for these isotherms were obtained by exchanging a known weight
of zeolite in a solution of known composition (at the given
solution concentration) over a period of 6 days (except for
the long-term study of 3 months), and then analysing *both* phases
for *all* cations.

The results from the ternary radio-chemical work are shown
separately in figure 4.13. These results are part of the main
Na/K/Li system (at 0.1 equiv. dm^{-3}), and are also shown in the
main isotherm(figures 4.9 and 4.10).

4.4. THERMODYNAMIC TREATMENT AND DERIVED RESULTS

The thermodynamic parameters were obtained by using computer
routines (see Appendix IV: Flow diagrams and Programs). The
actual experimental data which were used to plot the isotherms

were used in a program which, for the binary cases calculated
the separation factor α (defined by equation (2.6)) which
describes the selectivity of the zeolite for a cation under
the prevailing conditions, and which for univalent exchange
systems is identical to the mass action quotient, K_m (see
equation (2.15)).

For ternary systems, the computer program calculated the three
mass action quotients, defined by equation (2.60) *et sequens*,
and thence the required ratios of mass action quotients K_{m3}/K_{m1}
and K_{m3}/K_{m2}.

4.4.1. Solution Phase Treatment

Values of the activity coefficient ratio Γ were obtained as
follows. First, the mean molal stoichiometric activity co-
efficients γ± of each pure salt at two different ionic strengths
were obtained from literature[77]. Then, a modified Debye-
Hückel equation of the form

$$\log \gamma\pm \; = \; - \; \frac{A \; z_A \; z_B \; \sqrt{I}}{1 + B.a\sqrt{I}} \quad + \quad bI \qquad \qquad ....(4.1)$$

was used to determine the Debye-Hückel parameters a and b by
simultaneous solution. The parameters A and B are functions
of the temperature and the relative permittivity of the medium;
A is defined in section 2.2.5.3. and B is defined as

$$B = \left(\frac{Ne^2}{5k\epsilon T} \right)^{\frac{1}{2}} dm^{3/2} \; cm^{-1} \; mol^{-\frac{1}{2}} \qquad ....(4.2)$$

where N is Avogadro's constant (mol^{-1}), k the Boltzmann constant
(JK^{-1}), e the charge of a proton (C), ε the permittivity of the
medium $(CV^{-1}m^{-1})$ and T the absolute temperature (K).

TABLE 4.3. <u>Debye-Huckel parameters a and b</u>
(For all the salts used in the project)

Salt	$a \times 10^{-10}$	b
$NaNO_3$	4.40687	-0.07131
KNO_3	4.06436	-0.17662
$LiNO_3$	4.37196	+0.07714
$AgNO_3$	3.49781	-0.15696
Na_2SO_4	3.98674	-0.06257
K_2SO_4	3.29330	-0.02950
Li_2SO_4	4.50366	-0.03751
$Na_3Fe(CN)_6$		
$K_3Fe(CN)_6$	4.41194	-0.02055
$Li_3Fe(CN)_6$		

When the solvent is water, and the temperature is 298K,

$$A = 0.5115 \ dm^{3/2} \ mol^{-\frac{1}{2}}$$

$$B = 3.291 \times 10^{-9} \ dm^{3/2} \ cm^{-1} \ mol^{-\frac{1}{2}}$$

The parameters a and b depend on the properties of both the salt and the solvent (water) and can be taken as near-constant[18] over a wide range of ionic strengths. The parameter a can be regarded as the "radius of the ionic atmosphere" surrounding the particular ion[91], and the parameter b has been included to compensate for interactions at higher concentrations[77].

On solving for a and b, two values of a (and two values of b) were

obtained, and usually one of these roots was positive and the
other negative. The physical significance of a dictated that
the positive value be taken and the corresponding value of b
was taken as the correct value. The values of these parameters
'a' and 'b' are shown in table 4.3.

Once a and b are known, the values of $\gamma_\pm$ for that salt can be
calculated using equation (4.1) for any ionic strength. These
pure salt activity coefficients must then be corrected for the
influence of other ions (cations, and anions where applicable)
which were present in the experimental solutions. These mixed
salt activity coefficients were calculated using modified
Guggenheim expressions[87,88] as described in sections 2.1.3.
and 2.2.5, and these data were substituted into equations which
define Γ as the ratio of the single ion activity coefficients
raised to the powers of the appropriate ion valences.

For the ternary treatment, these Γ values are used to obtain
the required ratios Γ_3/Γ_1 and Γ_3/Γ_2. The appropriate Γ functions
were then used with the corresponding mass action quotients to
obtain the corrected selectivity quotients, K_c (or, the ratios
K_{c3}/K_{c1} and K_{c3}/K_{c2}, for the ternary case).

It should be noted that in solution systems where *all* the ions
(cations *and* anions) are univalent, Γ is invariant with ionic
strength[84].

4.4.2. Fitting K_c data as a function of crystal phase composition

For the binary equilibria, fitting was accomplished using a
polynomial equation to express $\ln K_c$ in terms of the correspond-
ing crystal phase composition A_c (the value of B_c then being
fixed), as shown below.

$$\ln K_c = A_0 + A_1(A_c) + A_2(A_c)^2 + A_3(A_c)^3 + \ldots + A_n(A_c)^n$$

$$\ldots (4.3)$$

Then the polynomial equations were 'best-fitted' to the values of A_c with their corresponding values of $\ln K_c$. This allowed a comparison between calculated and observed $\ln K_c$ values for each A_c value which leads to an equation of the form,

$$R = \sqrt{\left[\left\{(\ln K_c)_{obs} - (\ln K_c)_{calc}\right\}^2 / (N-m-1)\right]} \quad \ldots (4.4)$$

where N is the number of data points and m is the order of the polynomial. The value of the standard deviation of the sum of residuals between the observed value of $\ln K_c$ and the predicted value of $\ln K_c$ (from the polynomial equation) was obtained this way, for each order of polynomial used.

The choice of order of the polynomial equation was made on the basis of the lowest sum of residuals R and a visual inspection of the plot of $\ln K_c$ against A_c (i.e. the Kielland plot). Usually, the value of R decreased with increasing m, so a visual inspection was helpful in deciding on the order of the poly-nomial.

Once the polynomial equation had been selected, a substitution for $\ln K_c$ was made in equations (2.41) and (2.42) (see section 2.1.4), and an analytical integration carried out to obtain the crystal phase activity coefficients f_A and f_B at the correspond-ing values of A_c. Similarly, substitution for $\ln K_c$ in equation (2.43) and subsequent integration gave the thermodynamic equil-ibrium constant K_a. Finally, equation (2.21) was used to obtain the standard free energy change $\Delta G^\ominus$ at the experimental temperature.

- 144 -

Figures 4.18 - 4.24 show plots of A_c vs. $\ln K_c$, f_A and f_B and α for each binary system studied. The derived data used to obtain these plots are shown in Appendix V and the values of K_a, $\Delta G^{\ominus}$, Γ and the chosen order of polynomial for each system are given in table 4.4. The curves given in the Kielland plots are computer fitted while the curves for α, f_A and f_B have been fitted 'by eye' (figures 4.18 - 4.24).

The procedure for fitting ternary data is more complex as the composition of crystal phase has to be defined in terms of *two* cations. As described in section 2.2.4, it is the differences in $\ln K_c$ values that are expressed in the form of a polynomial equation in A_c and B_c. Furthermore, two such equations are necessary to fully define the required thermodynamic parameters as shown below.

$$\ln(K_{c3}/K_{c1}) = A_0 + A_1(A_c) + A_2(B_c) + A_3(A_c)^2 + A_4(B_c)^2 + \ldots$$
$$\ldots A_{2n}(B_c)^n \qquad \ldots (4.5)$$

and

$$\ln(K_{c3}/K_{c2}) = B_0 + B_1(A_c) + B_2(B_c) + B_3(A_c)^2 + B_4(B_c)^2 + \ldots$$
$$\ldots + B_{2n}(B_c)^n \qquad \ldots (4.6)$$

The 'best fitting' procedure leads to obtaining a sum of residuals given by

$$R = \sqrt{\left[\{(\ln K_c)_{obs} - (\ln K_c)_{calc}\}^2 / (N - 2m - 1)\right]} \qquad \ldots (4.7)$$

This is identical to the binary case except that the order of the polynomial m is multiplied by 2 to allow for the extra polynomial coefficients required to describe the crystal phase equivalent fraction of the second cation B_c.

The procedure for choosing the best order of polynomial equation

is more complicated than in the binary case. Several criteria
were considered, and the two 'best' equations were chosen in-
dependently of one another; for example, a 4th order equation
was selected for $\ln K_{c3}/K_{c1}$ and a 1st order for $\ln K_{c3}/K_{c2}$ when
treating the ternary system of Na/K/Li(NO3) at a concentration
of 0.04 equiv.dm⁻³. This aspect is discussed at length in the
next chapter (section 5.3.2.).

After the equations were selected, the integration procedures
were carried out on the computer in the manner described in
sections 2.2.4 and 3.2.3 to obtain values of the crystal phase
activity corrections $a_?$, $a_?$ and $a_?$, and the thermodynamic equi-
librium constants K_{al}. From the latter, the standard free energy
changes $\Delta G_i^\ominus$ for the three ternary reaction equations were obtained.
Table 4.5 gives the results of the thermodynamic treatment, while
the derived data are appended (Appendix VI).

4.4.3. Solution phase distorted coordinate diagrams

As described earlier, there is no 'best' way of plotting ternary
data in triangular coordinate diagrams. In the two methods used
here, the diagrams (figures 4.9 - 4.12) show only the numbers
and distribution of points that are required to represent ade-
quately the equilibrium characteristics of a ternary exchange
system. It is difficult to discern any selectivity trends, and
therefore a more useful representation of ternary equilibria
would be to superimpose the distorted coordinates of the solution
phase upon the coordinates of the crystal phase, so that any
point in the solution phase falls on top of its corresponding
equilibrium point for the crystal phase.

The computer procedure used to achieve this is based on defining

TABLE 4.4. Results from Binary Work

System	Γ	order of polynomial	K_a	$\Delta G^\ominus$ (kJ equiv⁻¹)
Li/Na-X(0.1)	0.967	3	0.099	+5.730
Li/K-X(0.1)	1.017	4	0.083	+6.165
K/Na-X(0.1)	1.031	4	0.752	+0.708
K/Na-X(0.1) (Two anions)	variable see Table 5.1	4	0.735	+0.762
K/Na-X(0.04)	1.013	4	0.799	+0.557
Ag/K-X(0.04)	1.004	3	194.430	-13.057
Ag/Na-X(0.04)	1.017	3	237.687	-13.555

is more complicated than in the binary case. Several criteria
were considered, and the two 'best' equations were chosen in-
dependently of one another; for example, a 4th order equation
was selected for $\ln K_{c3}/K_{c1}$ and a 1st order for $\ln K_{c3}/K_{c2}$ when
treating the ternary system of Na/K/Li (NO_3) at a concentration
of 0.04 equiv. dm^{-3}. This aspect is discussed at length in the
next chapter (section 5.3.2.).

After the equations were selected, the integration procedures
were carried out on the computer in the manner described in
sections 2.2.4 and 2.2.6 to obtain values of the crystal phase
activity corrections ϕ_A, ϕ_B and ϕ_C, and the thermodynamic equi-
librium constants K_{ai}. From the latter, the standard free energy
changes $\Delta G_i^\ominus$ for the three ternary reaction equations were obtained.
Table 4.5 gives the results of the thermodynamic treatment, while
the derived data are appended (Appendix VI).

4.4.3. Solution phase distorted coordinate diagrams

As described earlier, there is no 'best' way of plotting ternary
data on triangular coordinate diagrams. In the two methods used
here, the diagrams (figures 4.9 - 4.17) show only the numbers
and distribution of points that are required to represent ade-
quately the equilibrium characteristics of a ternary exchange
system. It is difficult to discern any selectivity trends, and
therefore a more useful representation of ternary equilibria
would be to superimpose the distorted coordinates of the solution
phase upon the coordinates of the crystal phase, so that any
point on the solution phase falls on top of its corresponding
equilibrium point for the crystal phase[111].

The computer procedure used to achieve this is based on defining

- 147 -

two parameters from experimental data these ... calculated ...

$$q_1 = A_s.B_c/A_c.B_s \quad \text{and} \quad q_2 = A_s.C_c/A_c.C_s$$

Here again, best fitting polynomials in A_s and B_s were found to express the dependence of q_1 and q_2 on A_s and B_s. The next step was to vary A_s in increments of 0.1 from 0 to 1, calculating q_1 and q_2 for small increments (usually 0.01) in B_s from $B_s = 1-A_s$ to $B_s = 0$ (thus defining C_s also) for each of the increments in A_s. Simultaneous solutions of these q_1 and q_2 values gave predicted values of A_c and B_c (and hence C_c). The procedure was repeated twice, first varying B_s in increments of 0.1, and then varying C_s in increments of 0.1 in order to obtain the (distorted) solid solution phase coordinates of all three cations. The computer then plotted the three sets of distorted coordinate diagrams (i.e. one for each cation), but it was found that the diagrams were useful only as an approximate indication because the curves linking the coordinates tended to 'flap' at the edges of the triangle. In order to improve upon this, the three coordinate diagrams were finally plotted separately using the appropriate distorted coordinate data produced by the computer, but also using the corresponding binary data in order to 'anchor' the points along the edges of the triangle. The three individual cation distorted coordinate diagrams were then re-plotted on a single triangular diagram to obtain an overall distorted coordinate diagram. The overall diagram and the three individual diagrams for the main Na/K/Li system are shown in figures 4.25 - 4.28 respectively. Accurate diagrams could not be obtained for the other ternary systems studied in this project because the ternary equilibrium data available was spread

TABLE 4.5. Results from Ternary Work

System	Γ_1	Γ_2	Γ_3	Γ_3/Γ_1	Γ_3/Γ_2
(1) Na/K/Li(0.1)	1.003	1.099	0.097	0.904	0.825
(2) Na/K/Li(0.04)	1.000	1.040	0.961	0.961	0.924
(3) Na/K/Li(0.04) (long term study)	1.000	1.040	0.961	0.961	0.924
(4) Na/K/Ag(0.04)	0.971	1.009	1.021	1.052	1.012

(where ΔG is given in kJ per 2 equivalents)

Orders of Polynomials	$K_c^{3/1}$	$K_c^{3/2}$	Φ_1 ΔG_1	K_{a1}	Φ_2 ΔG_2	K_{a2}	Φ_3 ΔG_3	K_{a3}
(1)	4	5	-5.898	10.809	-5.242	8.294	+11.139	0.012
(2)	4	1	-5.873	10.702	-5.246	8.311	+11.119	0.011
(3)	3	1	-5.949	11.038	-5.162	8.032	+11.112	0.011
(4)(a)	3	2	+15.002	2.3E-3	+12.111	7.5E-3	-27.114	56.5E3
(b)	4	4	+12.833	5.6E-3	+13.116	5.0E-3	-25.949	35.4E3

two parameters from experimental data so that

$$q_1 = A_s \cdot B_c / A_c \cdot B_s \quad \text{and} \quad q_2 = A_s \cdot C_c / A_c \cdot C_s$$

Here again, best fitting polynomials in A_s and B_s are found to express the dependence of q_1 and q_2 on A_s and B_s. The next step was to vary A_s in increments of 0.1 from 0 to 1, calculating q_1 and q_2 for small increments (usually 0.01) in B_s from $B_s = 1-A_s$ to $B_s = 0$ (thus defining C_s also) for each of the increments in A_s. Simultaneous solutions of these q_1 and q_2 values gave pre-dicted values of A_c and B_c (and hence C_c). The procedure was repeated twice, first varying B_s in increments of 0.1, and then varying C_s in increments of 0.1, in order to obtain the (distor-ted) solution phase coordinates of all three cations. The computer then plotted the three sets of distorted coordinate diagrams (i.e. one for each cation), but it was found that the diagrams were useful only as an approximate indication because the curves linking the coordinates tended to 'flap' at the edges of the triangle. In order to improve upon this, the three coordinate diagrams were finally plotted *manually*, using the appropriate distorted coordinate data printed out by the computer, but also using the corresponding binary data in order to "anchor" the points along the edges of the triangle. The three individ-ual cation distorted coordinate diagrams were then re-plotted on a single triangular diagram to obtain an overall distorted coordinate diagram. The overall diagram and the three individ-ual diagrams for the main Na/K/Li system are shown in figures 4.25 - 4.28 respectively. Accurate diagrams could not be ob-tained for the other ternary systems studied in this project because the ternary equilibrium data available was spread

- 149 -

insufficiently across the ternary surface to enable adequate definitions of the parameters q_1 and q_2.

4.5.   RESULTS FROM T.G.A., D.T.A. AND X-RAY ANALYSIS

T.G.A. and D.T.A. plots for the different zeolites are given in figures 4.29 and 4.30 respectively. For ease of comparison, the results of the three zeolites are plotted together in each case. Microdensitometer plots of the X-ray photographs are given in figures 4.31 - 4.36. (X-ray studies were also carried out on zeolites after subjecting them to thermal gravimetric analysis). The T.G.A. chart shows that the intracrystalline water losses from the three zeolites vary in magnitude according to the sequence Na-X<K-X<Li-X. The endotherms for the zeolites correspond to this pattern as shown in the D.T.A. charts. The D.T.A. chart also shows an exotherm for Na-X at approximately 300°C.

The major discontinuity for Li-X at approximately 750°C was probably due to sudden shrinkage of the sample which, on recrystallisation, left the thermocouple of the D.T.A. apparatus exposed. A breakdown of the zeolite structure at this temperature is suggested by these results, and the X-ray diffraction work confirms this (figure 4.30). On comparison of the microdensitometer charts (figures 4.31 - 4.36) of samples analysed before and after heat treatment, the following pattern is seen:

   Na-X and K-X   - samples rendered amorphous by heat
   Li-X   - the zeolite undergoes a metamorphosis.

4.6.   ERRORS

Errors usually arise from two sources. Firstly, there are experimental inaccuracies caused by the techniques or apparatus used and secondly approximations involved in the mathematical treat-

ment or computer processing of the data.

4.6.1. Experimental Errors

Errors occurring during analyses can be very significant. Flame photometry was the main technique used in cation analyses, but atomic absorption spectrometry and titrimetry were used also when analysing for silver. For the zeolite analyses (section 3.4), gravimetric methods were used to determine silica and aluminium. Due to the difficult nature of these methods, repeated analyses had to be carried out before reproducible results were obtained. The results were taken as reasonable when for silica the difference was less than 0.25 (%) and for aluminium was less than 0.05 (%).

The flame photometer gave excellent results for sodium, potassium and lithium provided the nebuliser was cleaned regularly. The reproducibility was almost perfect when the same samples were analysed on different occasions. The results of the interference studies carried out were in agreement with reported conclusions [107], *viz*, that the presence of sodium, potassium and lithium did not affect the analysis of one another and that aluminium and nitrate ions did not influence the results. At low levels of silver, sodium and potassium readings were not affected. Therefore, flame photometer readings can be taken as very reliable. Most of the silver analyses was carried out titrimetrically, and the accuracy of these determinations was governed by both the accuracy of the pipetting operations and the limit of calibration of the burette used. Since usually 0.4g of zeolite were used for exchange, the 250 cm^3 solutions of dissolved solid phase contained over 1.5 m equiv. of silver. Titrations were performed on 20 or 25 cm^3 aliquots of the solutions, using a 10 cm^3

'Grade A' burette graduated in units of 0.02 cm^3. Titrations
were performed by first doing a 'rough' analysis to determine an
approximate end point, and then repeating the procedure until
consistent results (within 0.03 cm^3) were obtained. The anal-
ytical method was very good, and usually three titrations suff-
iced to obtain consistency. A mean of these values was taken
as the final reading; the titre was standardised before use, and
a small calibration correction to the burette readings was made.

Some of the solution phase silver analyses had to be carried
out by atomic absorption techniques as the amount of silver present
was insufficient for accurate titrimetry. The most suspect source
of error lay here, as absorbance readings often fluctuated during
measurements. In order to minimise these errors, the calibration
of the instrument was checked regularly and standards were read
after every two measurements taken.

Apart from the instrumental errors, errors in making up the
original exchange solutions and dilution errors must be consid-
ered also. 'Grade A' quality glassware (burettes, pipettes,
volumetric flasks) were used where possible, and 'Grade B' items
were checked for accuracy using a weight-check or volume-check
method. The same collection of glassware were used for *all* the
non-radiochemical work done. When diluting samples (for flame
photometric analyses) the largest possible volumes were used (for
example, a 25 cm^3 pipette and a 500 cm^3 flask instead of a 5 cm^3
pipette and a 100 cm^3 flask); even for the solution phase, where
only 40-45 cm^3 solution was available, 10 cm^3, rather than 5 cm^3,
aliquots were used where possible.

After making up the exchange solutions, nearly all of the ones
containing silver, and several of the others, were checked for

compositional accuracy. It should be noted that, however, any
errors in preparing the original solution compositions would have
no affect on the equilibrium data used for the thermodynamic
treatment, and therefore, the final results.

4.6.2. Cation Balance Work

Both phases were always analysed for all cations, and therefore
a cation balance was carried out in all cases to check for con-
sistency and cation losses. This involved tabulating all comp-
ositions, and sub-totalling and totalling the results to obtain
totals of each cation for the whole system (i.e. solution and
solid phases) as well as totals for each phase (a sample section
of such a balance is shown in table 4.6). Then, the amount of
(say) potassium in the whole system could be checked against the
original composition, and the total cation content of each phase
could be checked against the corresponding original (theoretical
or measured) composition. The results showed that the overall
cation total for the whole system always was slightly lower (up
to about 2%) than the original total, suggesting that some loss
of material had occurred. An examination of the cation subtotals
for each phase showed that for most cases the value for the solid
phase was lower (up to 7.6%) than the measured exchange capacity
of the zeolite used while the solution phase total was higher
(up to 3.2%) than expected. Taking into account the individual
cation totals for the whole system, one could conclude that some
zeolite was lost or transferred at the centrifugal separation
stage. Since the method of separation involved (i) emptying
most of the solution phase (about 45 cm^3) from the separation
tube into a vial, and (ii) two subsequent washing operations
where the wash water is discarded, it would be acceptable to

TABLE 4.6. SAMPLE CATION BALANCE

No.	Zeolite Phase				Solution Phase				Total System				Solution/System			
	Na	K	Li	Σ	Na	K	Li	Σ	Na	K	Li	Σ	Na	K	Li	Σ
1(a)	1.809	0	0	1.809	2.500	1.250	1.250	5.000	4.309	1.250	1.250	6.809	-	-	-	-
(b)				95.96%				101.24%	101.02%	96.96%	98.64%	99.84%				
(c)	1.228	0.434	0.074	1.736	3.125	0.778	1.159	5.062	4.353	1.212	1.233	6.798	71.79%	64.19%	93.98%	74.46%
(d)	.707	.250	.043	1	.617	.154	.229	1	-	-	-	1	-	-	-	-
2(a)	1.809	0	0	1.809	1.200	0.400	0.400	2.000	3.009	0.400	0.400	3.809	-	-	-	-
(b)				95.36%				103.75%	100.63%	95.75%	97.25%	99.76%				
(c)	1.416	0.255	0.054	1.725	1.612	0.128	0.335	2.075	3.028	0.383	0.389	3.800	53.24%	33.42%	86.12%	54.61%
(d)	.821	.148	.031	1	.777	.062	.161	1	-	-	-	1	-	-	-	-

KEY:
(a) Original composition (measured exchange capacity for zeolite or solution composition) (m.equiv.)

(b) Experimental composition as a percentage of original

(c) Experimental composition (m.equiv.) or Percentage of cation in solution

(d) Experimental composition (fraction) used to plot isotherm

allow for about 2-3% of the zeolite (in the form of fines or 'unwetted' surface film) to be carried over each time. Such a transfer was indeed visually observable. This would explain a total loss of about 6-7% from the zeolite phase and a smaller gain in the solution phase, while resulting in a nett loss of about 3-4% from the whole system. Further evidence for this zeolite transfer comes from noting that at the two concentrations studied (i.e. 0.04 and 0.1 equiv. dm^{-3}), the surplus on the solution side was approximately the same in magnitude (about 0.050 - 0.065 m equiv.). (Since the cations nominally present in the solution phase were 2.0 and 5.0 m equiv. dm^{-3} respectively, this represented a different percentage gain for the two cases.)

It was interesting to note from the cation balance work that the amount of lithium entering a Na-X or K-X zeolite was usually a constant percentage of the total lithium in the overall system; i.e. the lithium in the zeolite was about 9%, at the higher solution concentration, and about 15%, at the lower concentration, of the total lithium in the system (see Solution/System column in table 4.6). The cation balance work also facilitated the accounting for of individual cations. The cation totals showed that silver and sodium could be measured to near a 100% of the theoretical composition, while the potassium total usually fell within the 94-97% level. Lithium levels were usually about 96-98% of the theroetical composition.

Often, the sodium levels were very slightly *higher* than 100%, i.e. about 100.5 - 101.0%; since a small loss of some zeolite, and hence some cation, was allowed for, these higher sodium measurements suggested either that the calculated exchange capacity of the zeolite was slightly inaccurate or that a small amount of

interference occurred during the flame photometric analyses (which was too small to be detected during the interference studies). The lower potassium totals also suggested some interference. These aspects were not investigated further. The percentages involved were always small, and their effect on subsequent thermodynamic treatment and final results is not significant because it is the *ratio* of cations for each phase that is used in the treatment.

4.6.3. Mathematical/Computer Errors

Considering the binary equilibria, the method used in this project to obtain isotherms was to plot the actual (experimental) values of A_c and A_s and draw the best curve through the points 'by eye'. No attempts were made to obtain a computer 'best fitted' isotherm[18]. The same 'real' A_c and A_s values were then used in the computer programs to obtain the derived data. Therefore, any experimental errors that were incorporated into the A_c and A_s values were carried through to the final results. As a check on these results, however, the computer procedures were also applied to the 'smoothed' A_c and A_s values which had been read off the isotherm. The results arising from these values were then compared with the corresponding 'real' results to study the effect of 'smoothing' the equilibrium. The difference in results was found to be small (eg: $\Delta G^\ominus = 0.71$ vs 0.73 and $\Delta G^\ominus = 0.56$ vs 0.54), thus justifying the usage of 'real' values.

Normalisation was not necessary for the treatment as the zeolites studied were capable of being exchanged to a 100% even though the K-X used in the work contained a sodium impurity of 1.63%. (The less fully exchanged Li-X was not used in binary exchange

- 156 -

studies). This impure K-X did produce ternary results instead
of binary ones, but since the amount of sodium in each phase was
very small, it was decided to ignore the sodium. The A_c and A_s
values were then calculated using potassium and either silver or
lithium compositions only. For the ternary studies, the sodium
impurities in Li-X and K-X zeolites did not matter because all
cations were measured after equilibrium.

All equilibrium points were initially calculated to the third
decimal place, to avoid an accumulation of "smoothing errors".
However, on rounding off the data of the Na/K/Li (0.1) ternary
system to two places, it was found on comparison with results
obtained from the three-decimal place data, that the K_m, K_c and
Γ values changed only slightly, and that for each order of
polynomial equation, the final results were quite similar. For
example, $\Delta G^{\ominus}$ values of - 6.33 vs - 6.36, - 3.49 vs -3.66 and
+9.82 vs +10.02 were found for the 5th order treatment. (N.B.
the $\Delta G^{\ominus}$ values arising from the three-decimal place data are
slightly higher for this order, but may be slightly lower than
the corresponding two-decimal place data for other orders). As
a result of this investigation, it is clear that rounding off
errors do not have a marked effect on the final results.

The other important point was to consider the minimum number of
equilibrium points necessary to obtain valid results. For the
main Na/K/Li system, there were 79 ternary points in all. These
were complemented by 56 binary points to cover the three conjugate
binary systems. The two Na/K/Li systems at the lower concentra-
tion of 0.04 equiv. dm^{-3} gave only 30 ternary points each, but
when used in conjunction with the binary data, final results were
obtained which were in excellent agreement with the results from

the main Na/K/Li system (i.e. at 0.1 equiv. dm^{-3} concentration).
For the Ag/Na/K system, there was a further problem; although
nearly 50 ternary points and 40 binary points were measured, the
extremely high selectivity of the zeolite for silver meant that
very little silver was left behind in the solution phase. In
several cases, this residual silver could not be measured accur-
ately. This point is clearly shown by the equilibrium diagrams
(figures 4.11 and 4.12) where most of the solution phase silver
compositions lie near the $Ag_s = 0$ base of the triangle. Only
solutions which correspond to crystal phase compositions of more
than 25% (points 6-11 on figure 4.11) contained sufficient silver
to be accurately analysed, and therefore, only 33 ternary points
could be effectively used in the treatment. However, after in-
cluding the appropriate binary data, very reasonable results were
obtained. These results are discussed further in the next
chapter.

A final source of error lies at the stage where the computer pro-
cedure uses polynomial equations to 'best-fit' the experiment-
ally calculated lnK_c data against measured crystal phase comp-
ositions. While the predicted curves defined by the equations
cannot pass through each data point precisely, a visual examina-
tion of the binary Kielland plots (figures 4.18 - 4.24) shows
that the computer predicted curves link the established data
points with great accuracy. Greater probability of error-of-fit
would be caused by 'gaps' in the spread of points where data is
not available, especially where the curves change direction, and
more significantly at the ends of the curves ($A_c \rightarrow 0$; $A_c \rightarrow 1$). This
aspect is discussed further in the next chapter (sections 5.2.2,
5.2.3, 5.3.2 and 5.3.3.).

Figure 4.1

Lithium ⇌ Sodium X   (0·1)   [one anion]
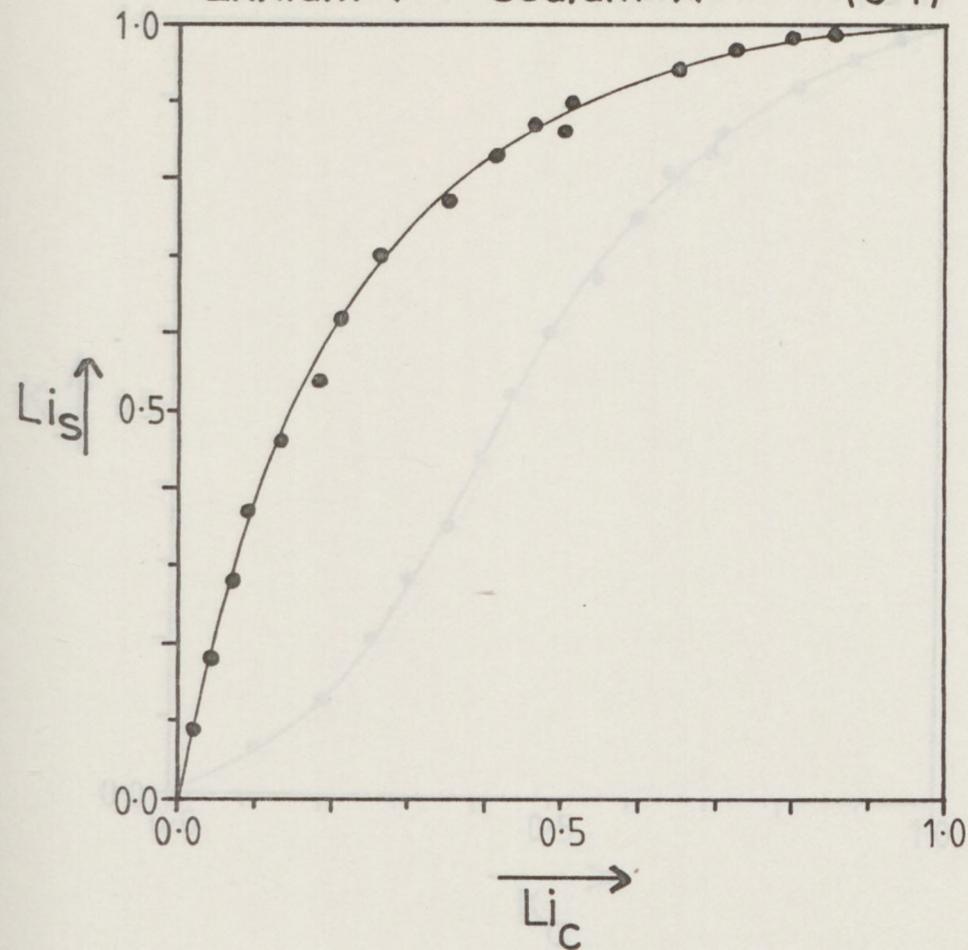
Figure 4.2

Lithium ⇌ Potassium X   (0·1)   [two anions]
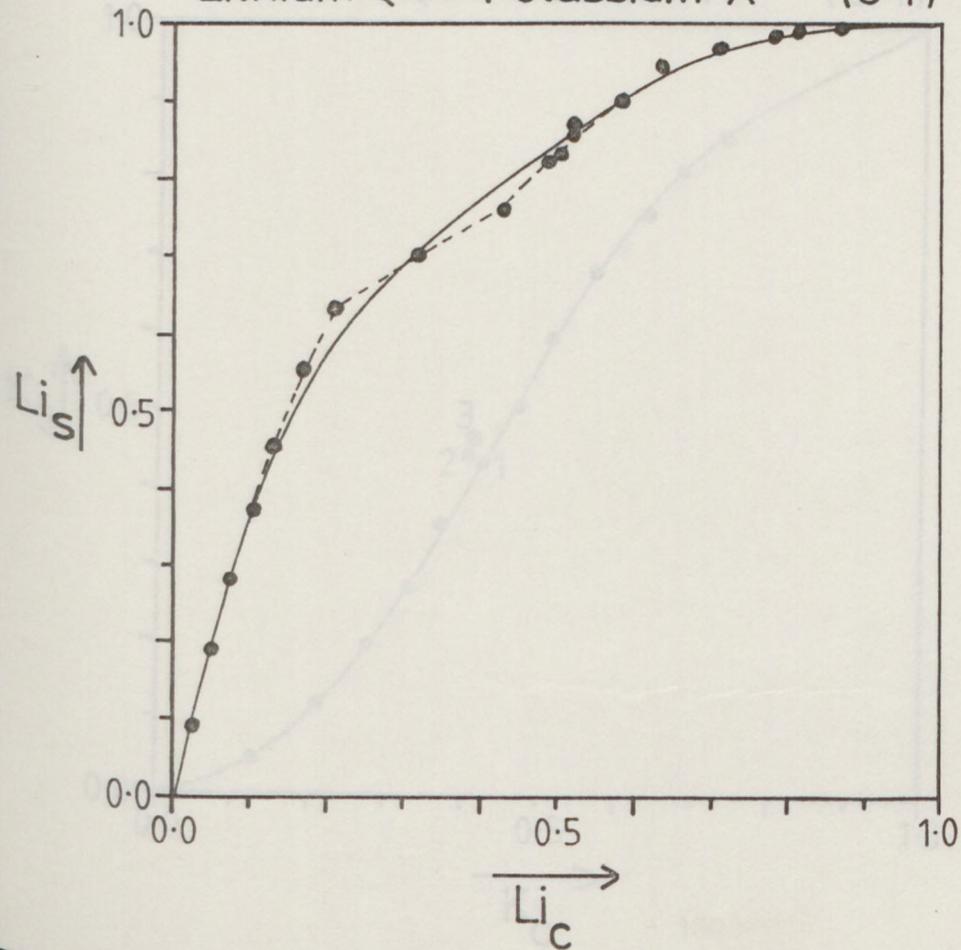
Potassium ⇌ Sodium X (0.1) [one anion]
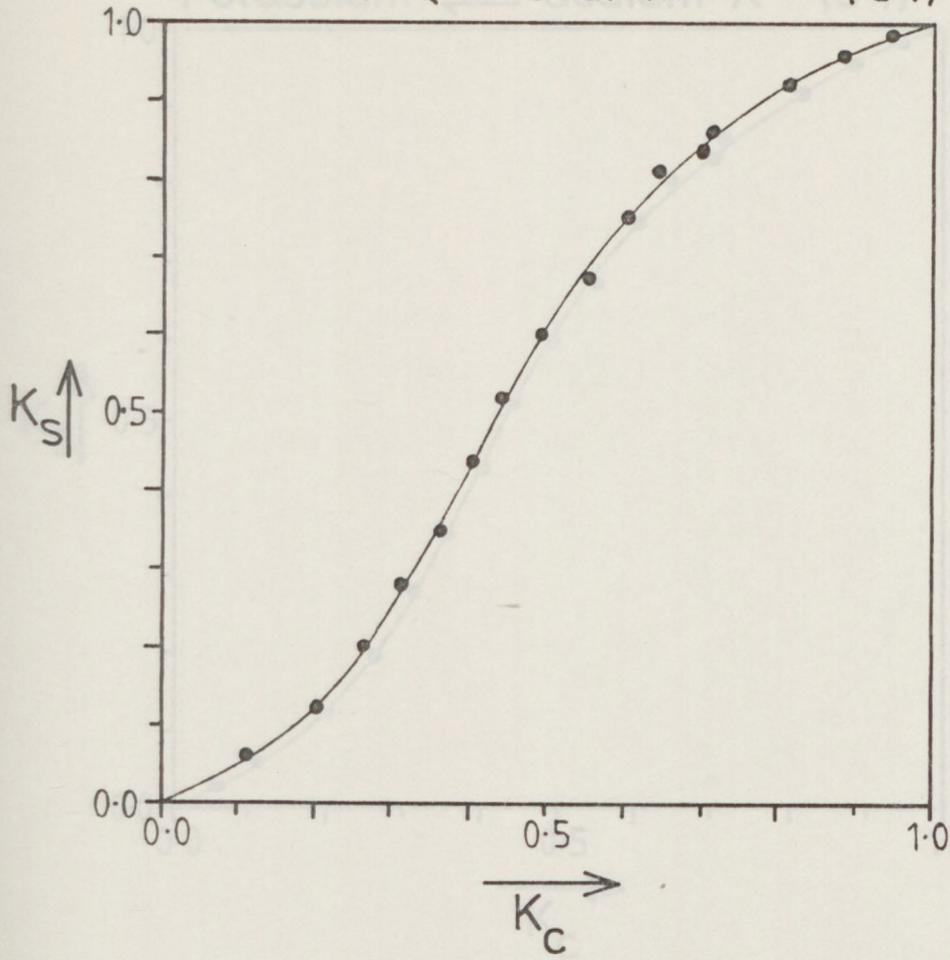
Figure 4.3

Potassium ⇌ Sodium X (0.1) [two anions]
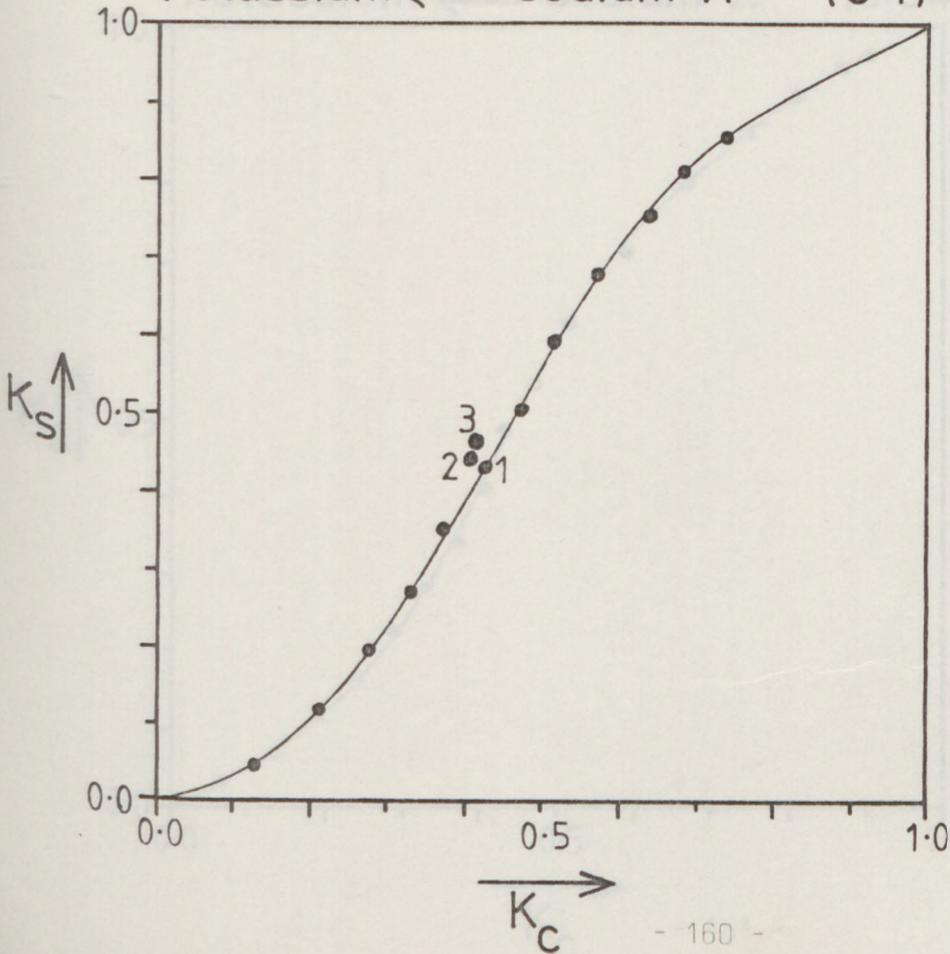
Figure 4.4

Potassium ⇌ Sodium X (0.1)
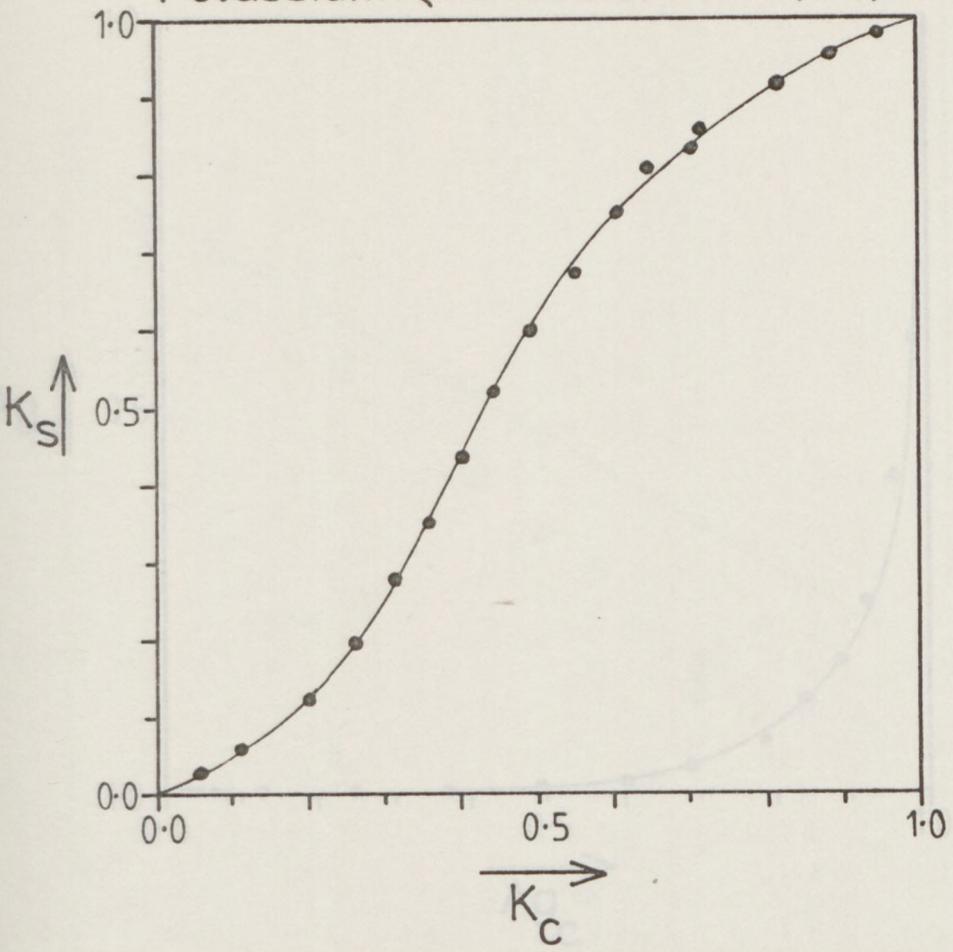
Figure 4.5

Potassium ⇌ Sodium X (0.04)
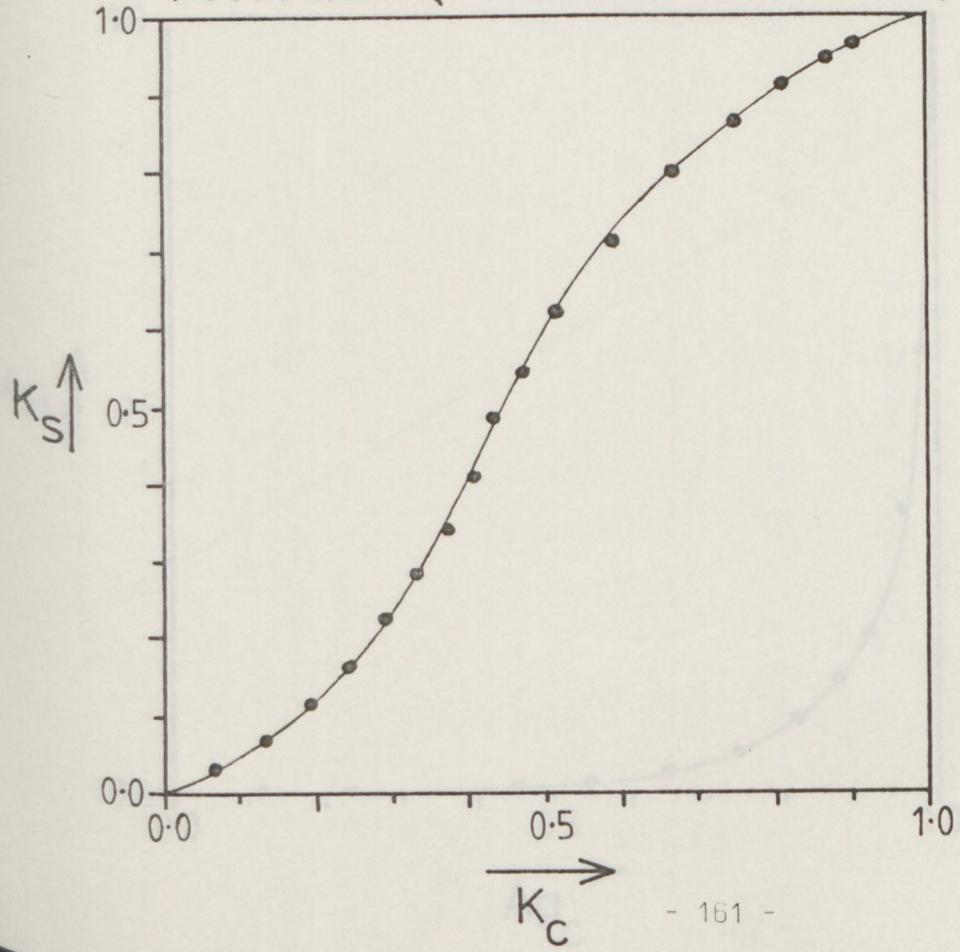
Figure 4.6

Silver (I) ⇌ Potassium X (0.04)
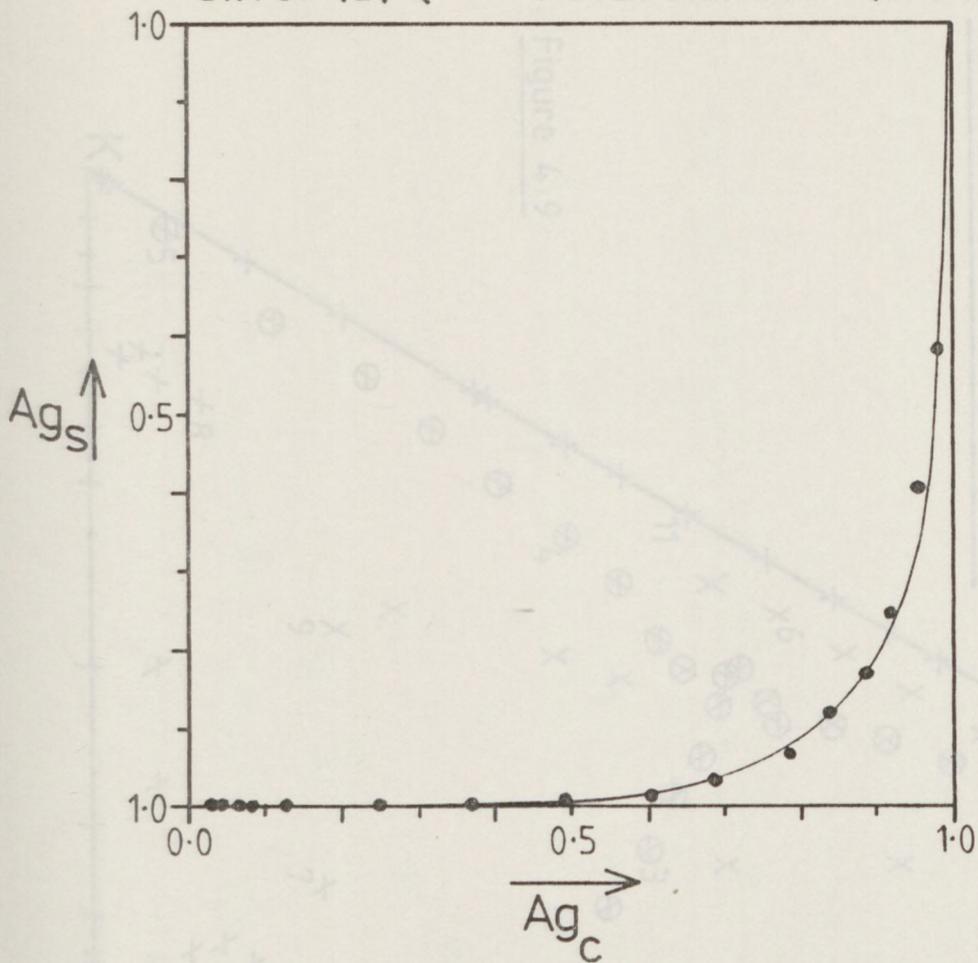
Figure 4.7

Silver (I) ⇌ Sodium X (0.04)
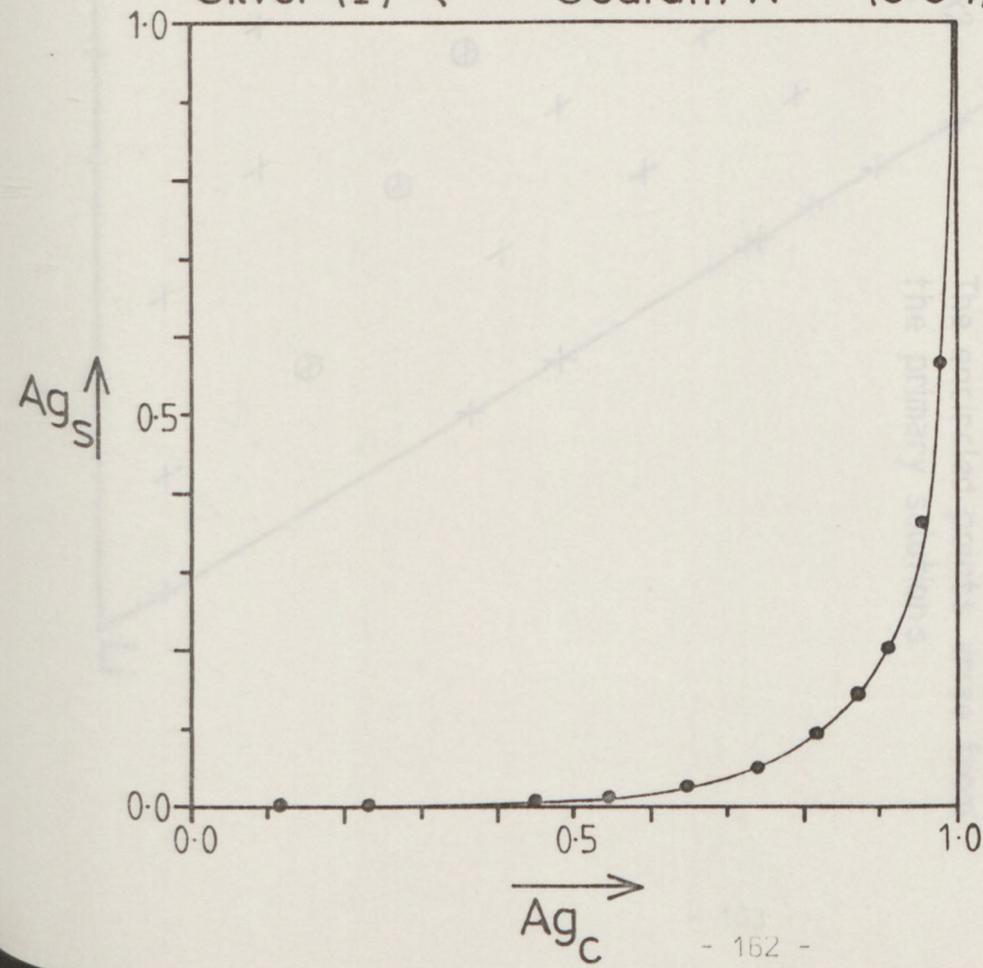
Figure 4.8

Na/K/Li(NO₃)-X system

0.1 equiv. dm⁻³

Solid phase composition

Figure 4.9

Ternary data

⊗ × from Na-X
⊕ ✕ from K-X
⊕ + from Li-X

+ Binary data
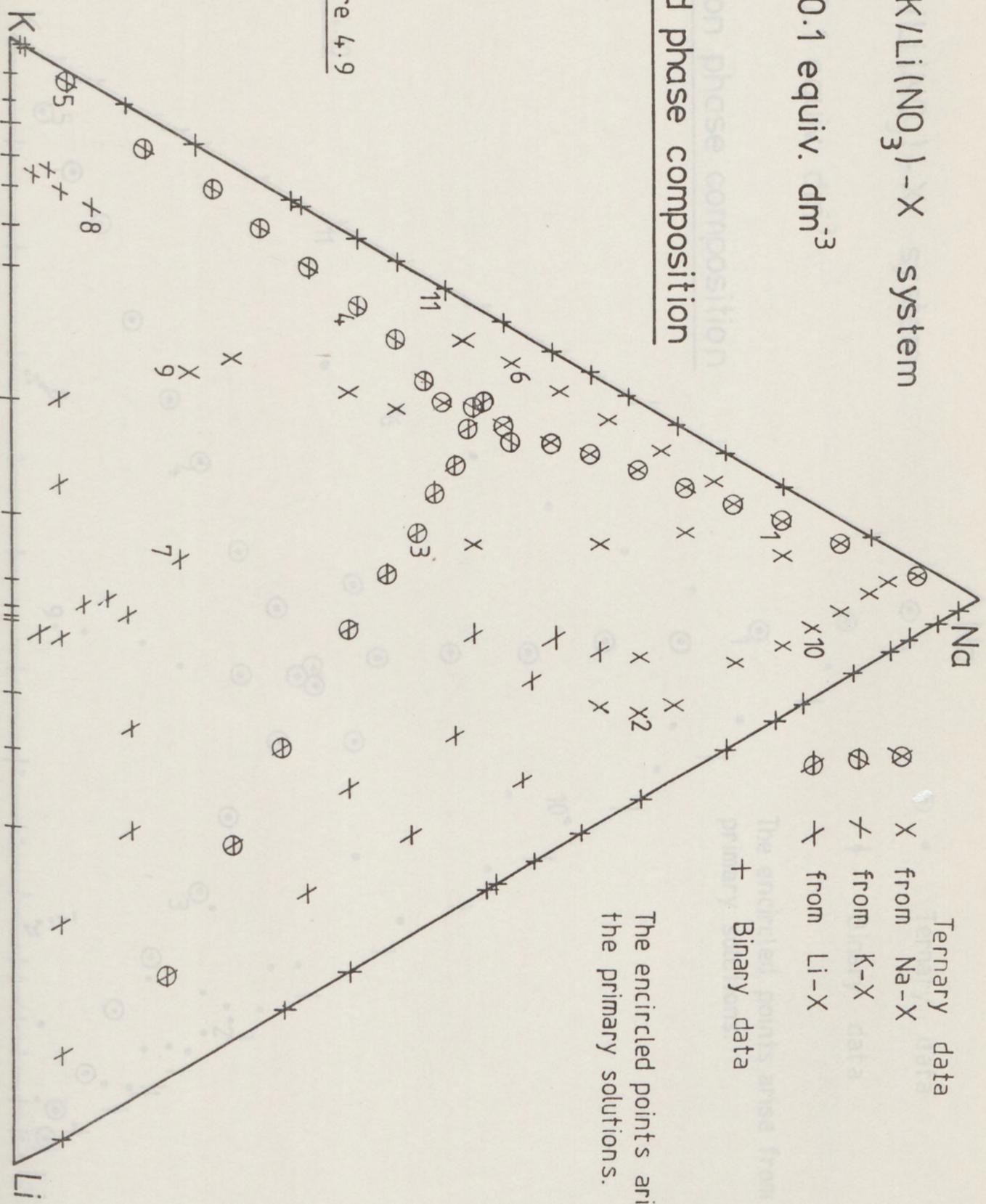
The encircled points arise from the primary solutions.

Na/K/Li(NO$_3$)-X system

0·1 equiv. dm^{-3}m

Solution phase composition

Figure 4.10

⊙ • from Ternary data

♦ Binary data

The encircled points arise from the primary solutions.

- 164 -

Na/K/Ag (NO_3) – X system

0.04 equiv. dm^{-3}

Solid phase composition

Figure 4.11

Ternary data
+ from Na–X
+ from K–X
* from Na–X/K–X mixture

+ Binary data
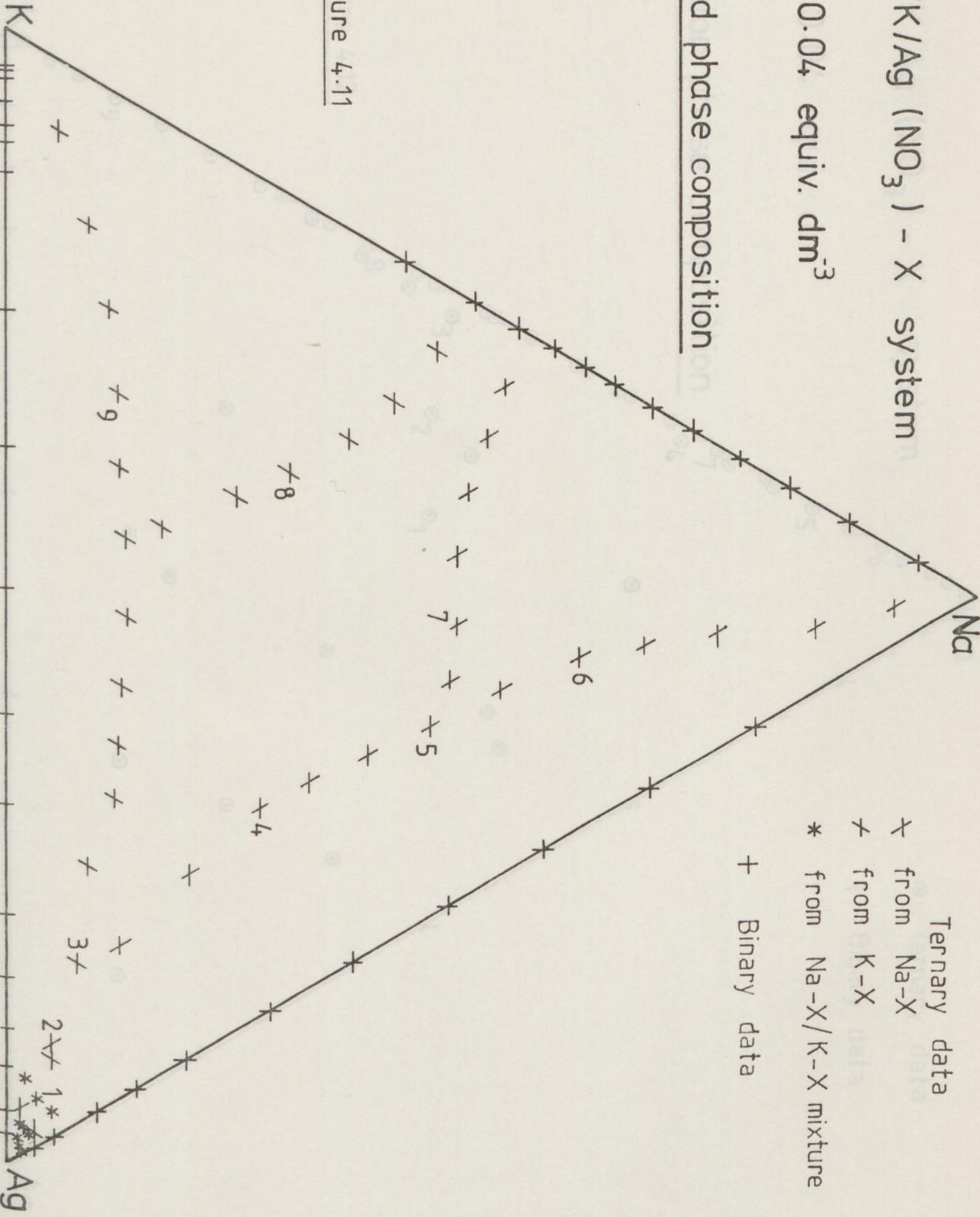
Na/K/Ag (NO$_3$) - X system

0.04 equiv. dm^{-3}

Solution phase composition

Figure 4.12

- ⊙ Ternary data
- ⊢ Binary data

*Na/K/Li (NO$_3$) - X system

0.1 equiv. dm^{-3}

Data from Radio-tracer studies

Solid & Solution phases

Solid phase data

$\rlap{\diagup}{\diagdown}$ from K-X
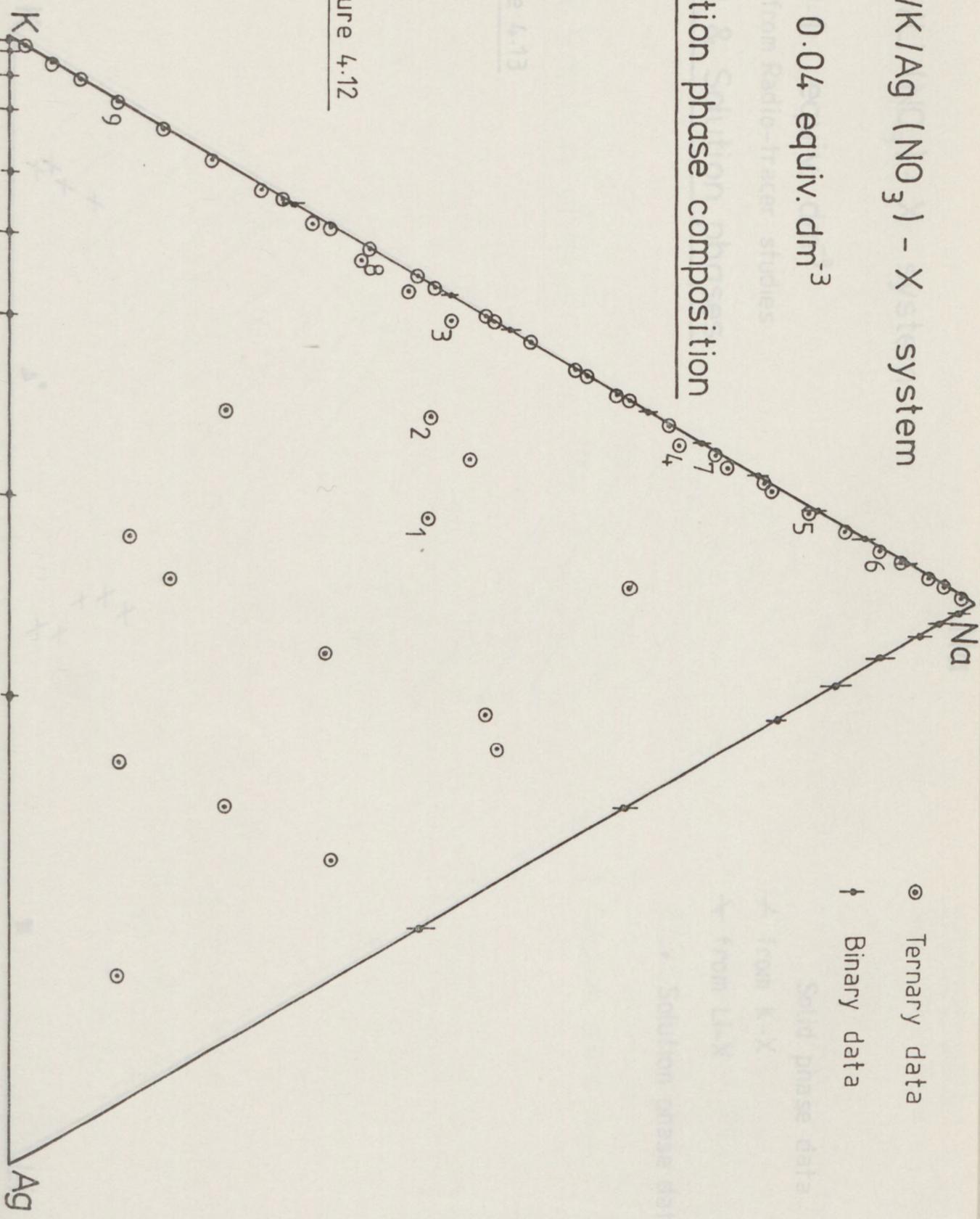
$\diagup$ from Li-X

• Solution phase data

Figure 4.13

Na/K/Li (NO$_3$) – X system

0.04 equiv. dm^{-3}

Figure 4.14

Solid & Solution phases

TERNARY DATA
Solid phase data

X   from Na–X
⅄   from K–X
⅂   from Li–X

•   Solution phase data

BINARY DATA

+   Solid phase data
•   Solution phase data

Na/K/Li (NO₃) – X system

0.04 equiv. dm⁻³
Long-term study

Solid & Solution phases

Solid phase data
× from Na-X
+ from K-X
⨯ from Li-X
• Solution phase data

Figure 4.15

Na/K/Li(NO$_3$)-X-system

Variable, T$_N$

(0.04-2.0) equiv. dm^{-3}

Solid & Solution phases
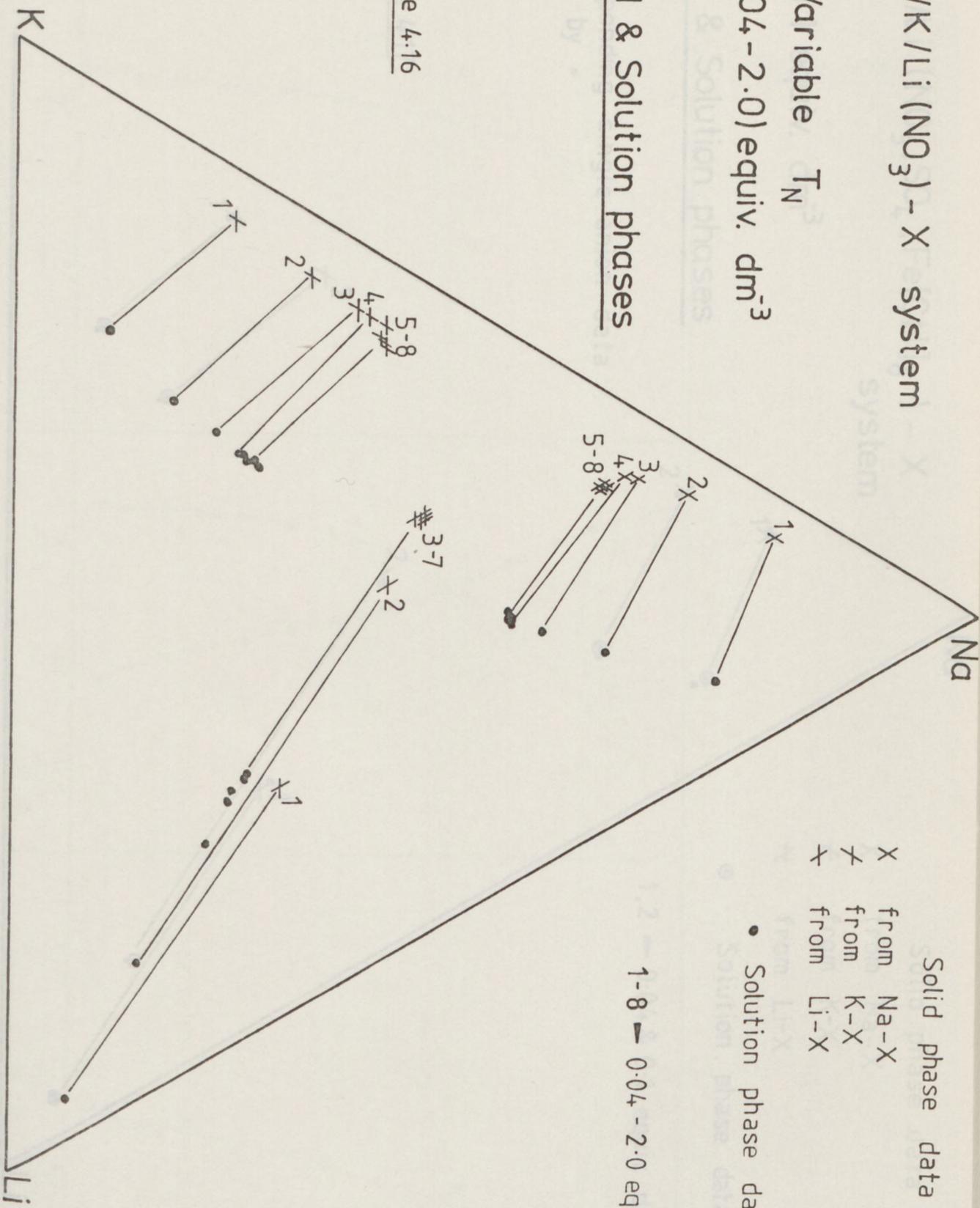
Figure 4.16

Solid phase data

X from Na-X
⅄ from K-X
⅋ from Li-X

• Solution phase data

1-8 ➤ 0.04-2.0 equiv. dm^{-3}

K

Na

Li

Na/K/Li (NO$_3$, SO$_4$, Fe[CN]$_6$) - X system

0.04 & 0.1 equiv. dm^{-3}

Solid & Solution phases

Solid phase data

X   from Na-X
⨯   from K-X
+   from Li-X

⊙   Solution phase data

1,2 = 0.04 & 0.1 equiv. dm^{-3}

Corresponding single-anion data
shown by ●
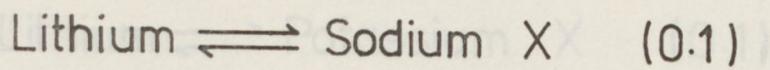
Figure 4.17

Figure 4.18
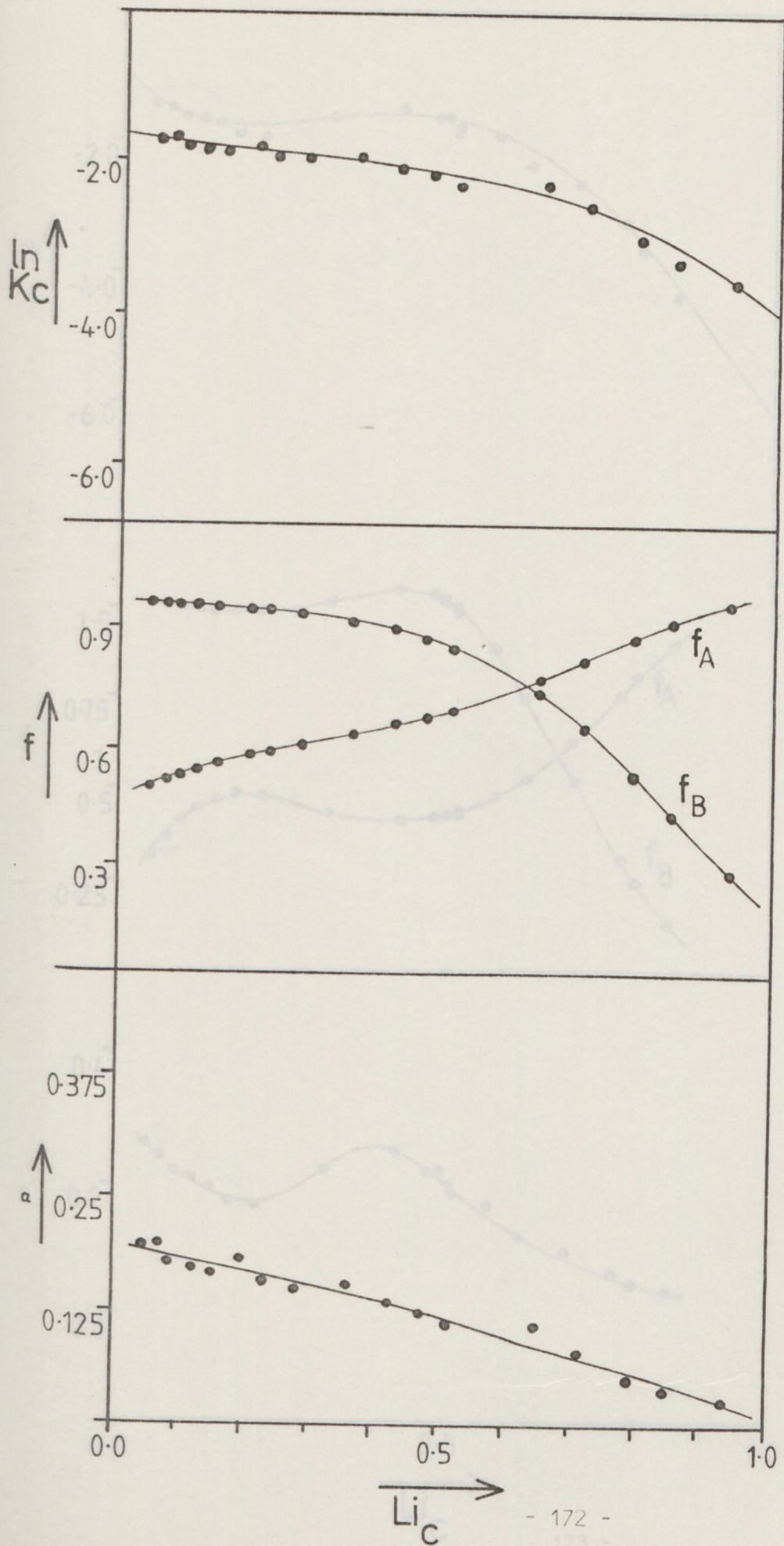
Lithium ⇌ Potassium X (0·1) [one anion]
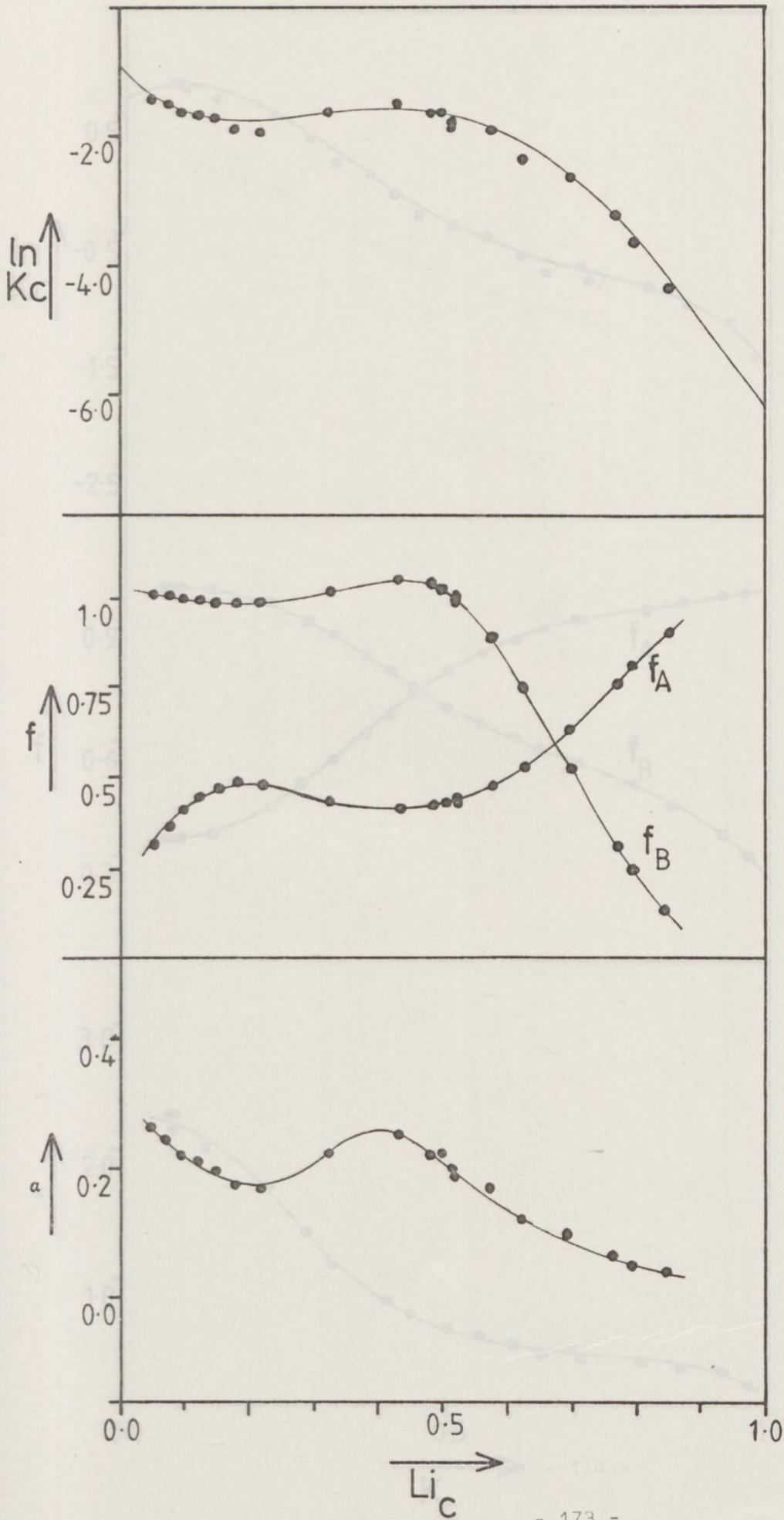
Figure 4.19

Potassium ⇌ Sodium X (0·1) [one anion]
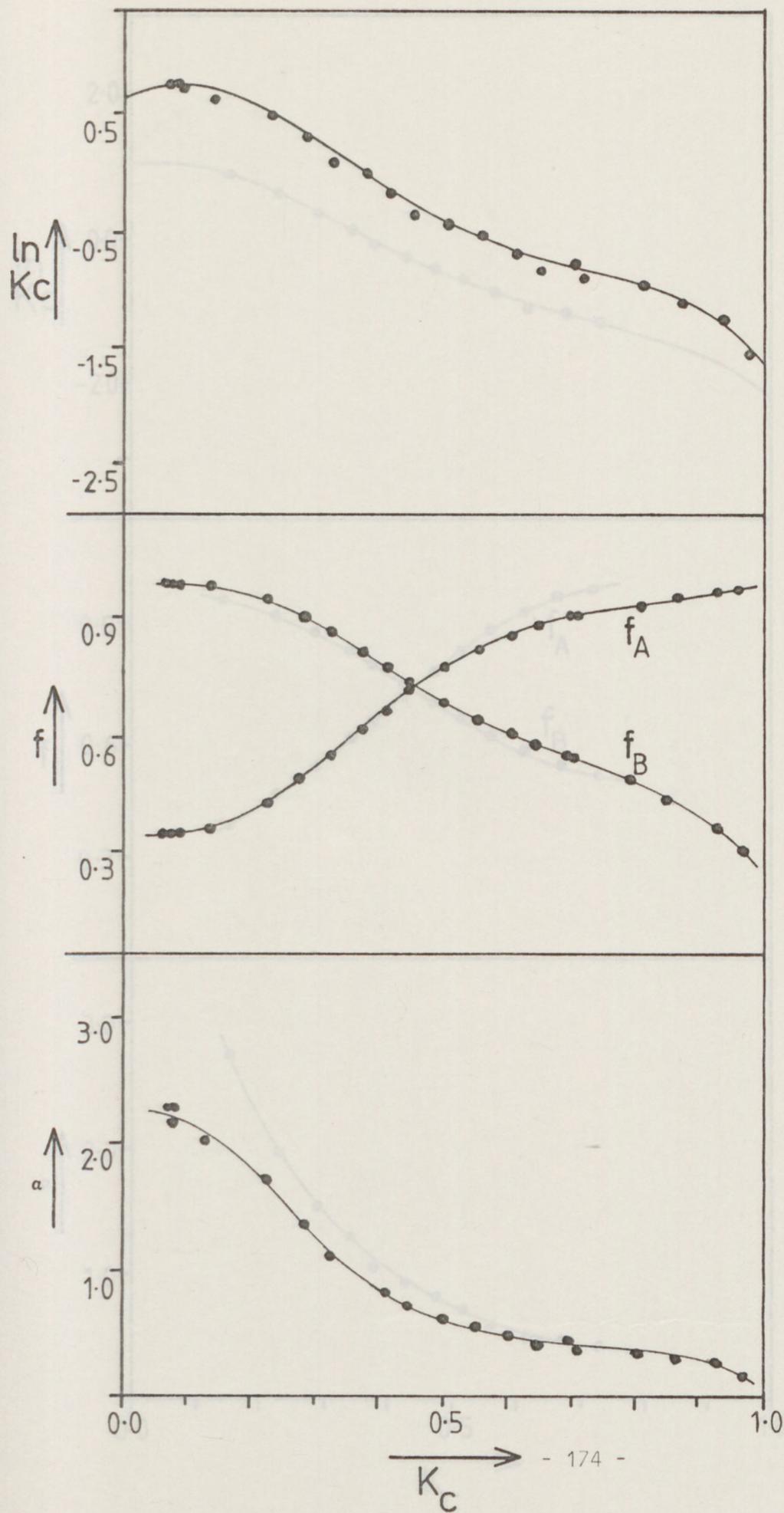
Figure 4·20

Potassium ⇌ Sodium X (0·1) [two anions]
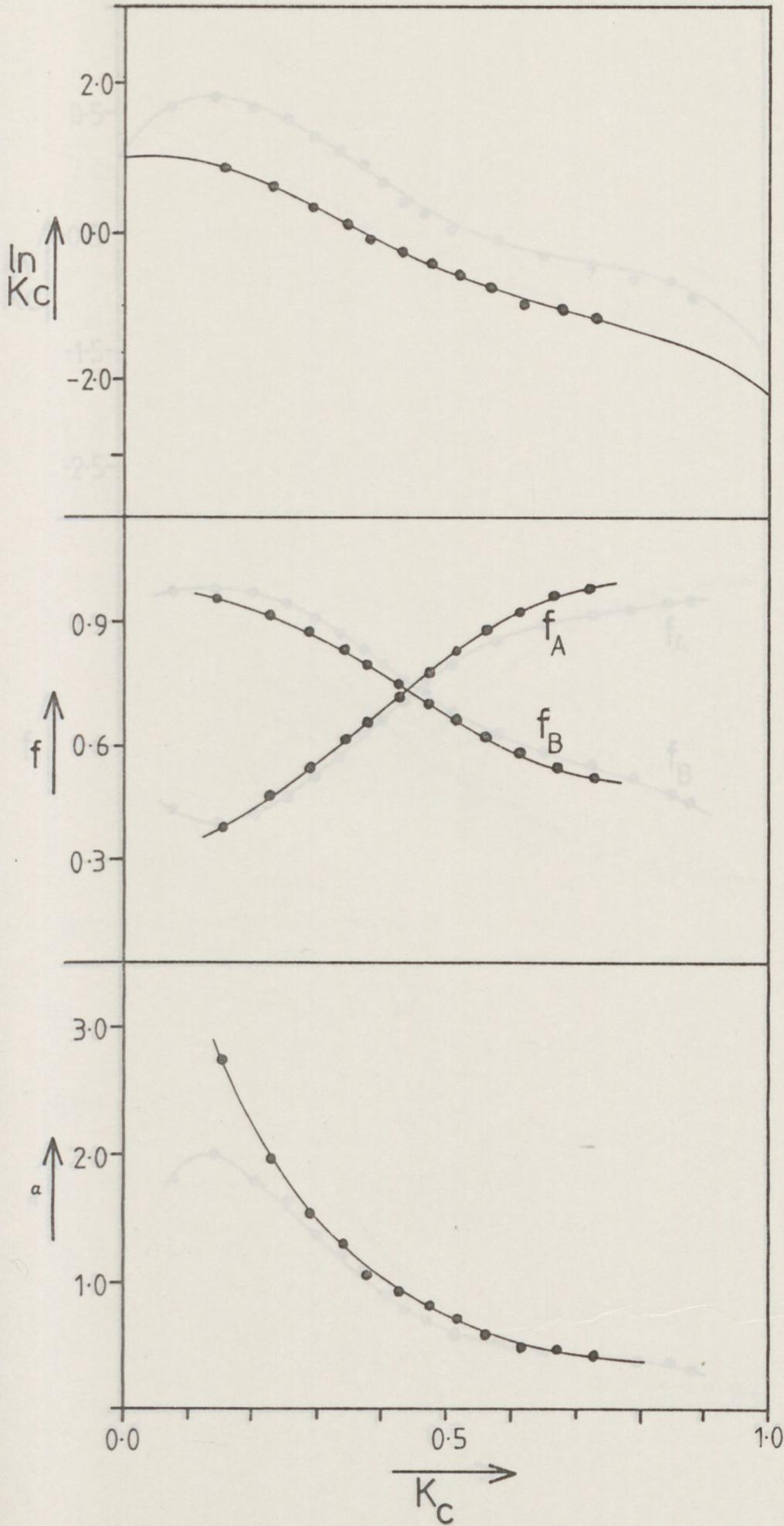
Figure 4·21
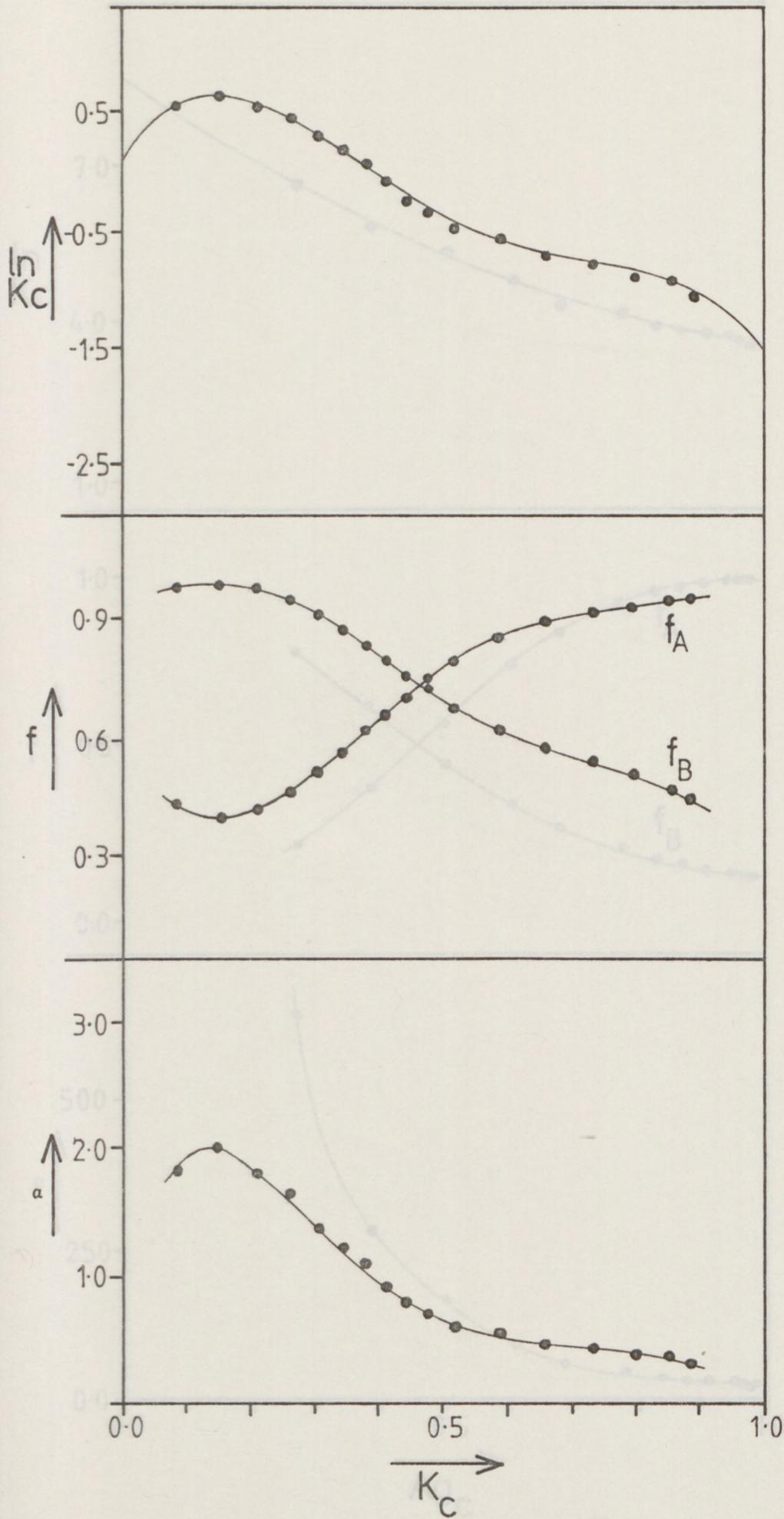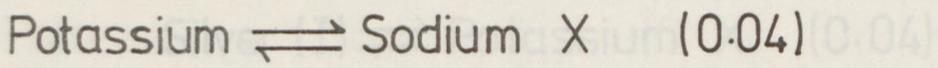
Potassium $\rightleftharpoons$ Sodium X (0.04)

Figure 4.22

Silver (I) ⇌ Potassium X (0.04)

Figure 4.23

Silver (I) ⇌ Sodium X   (0.04)
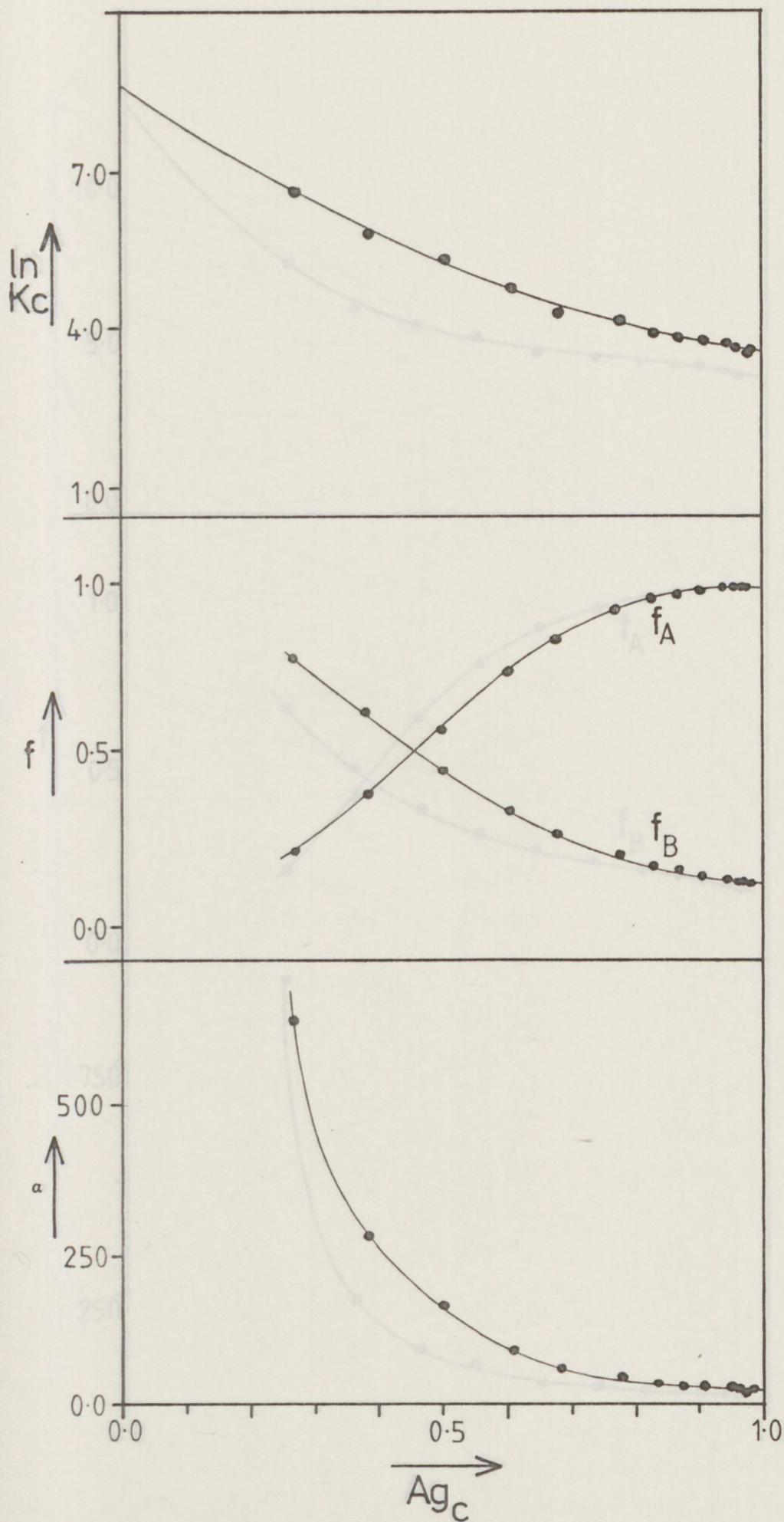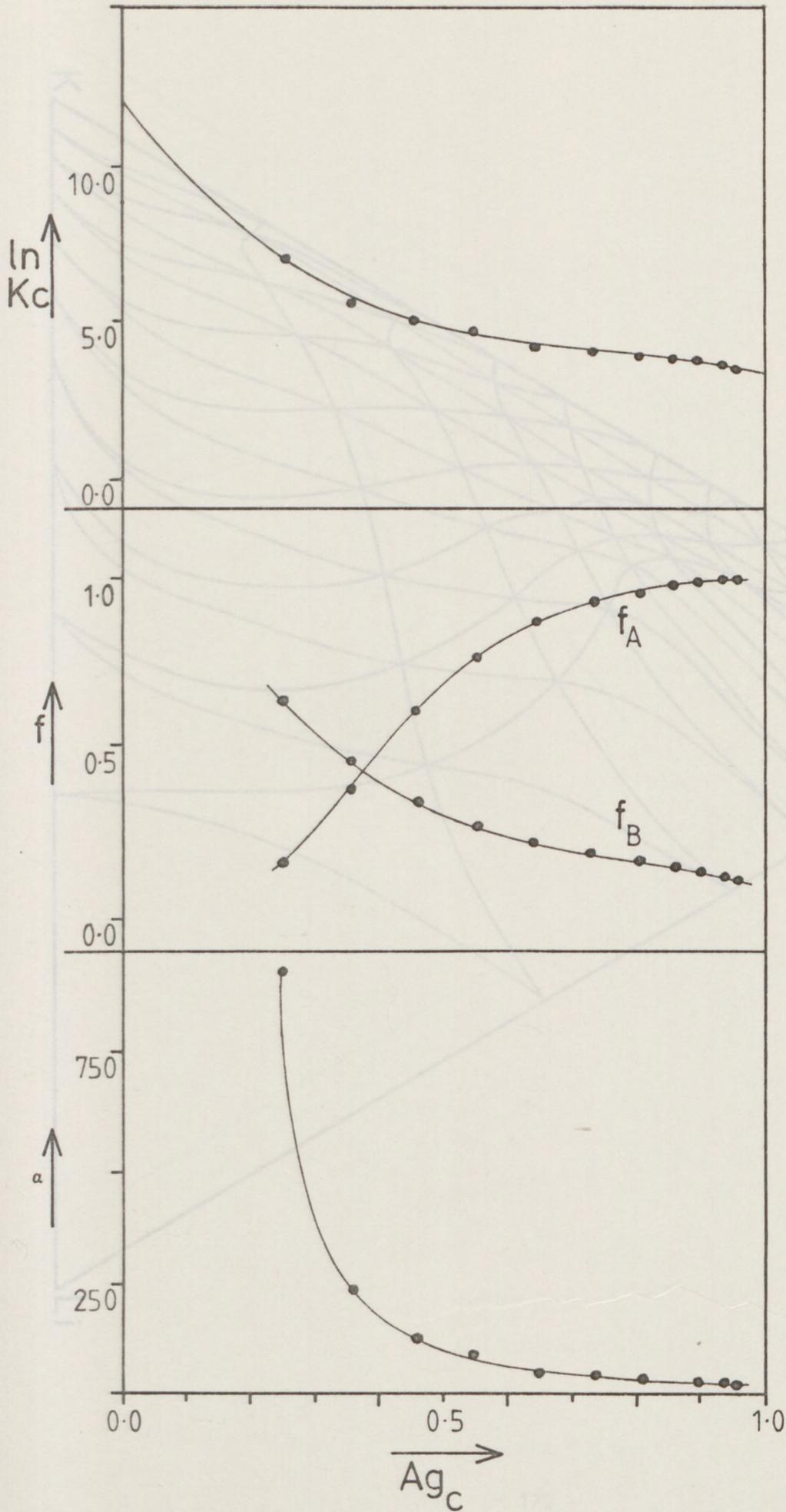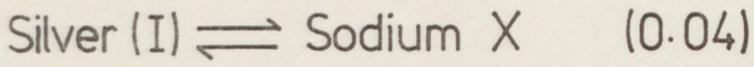
Figure 4.24

Figure 4.25

Overall Distorted Coordinate Diagram

Na/K/Li (0.1) system
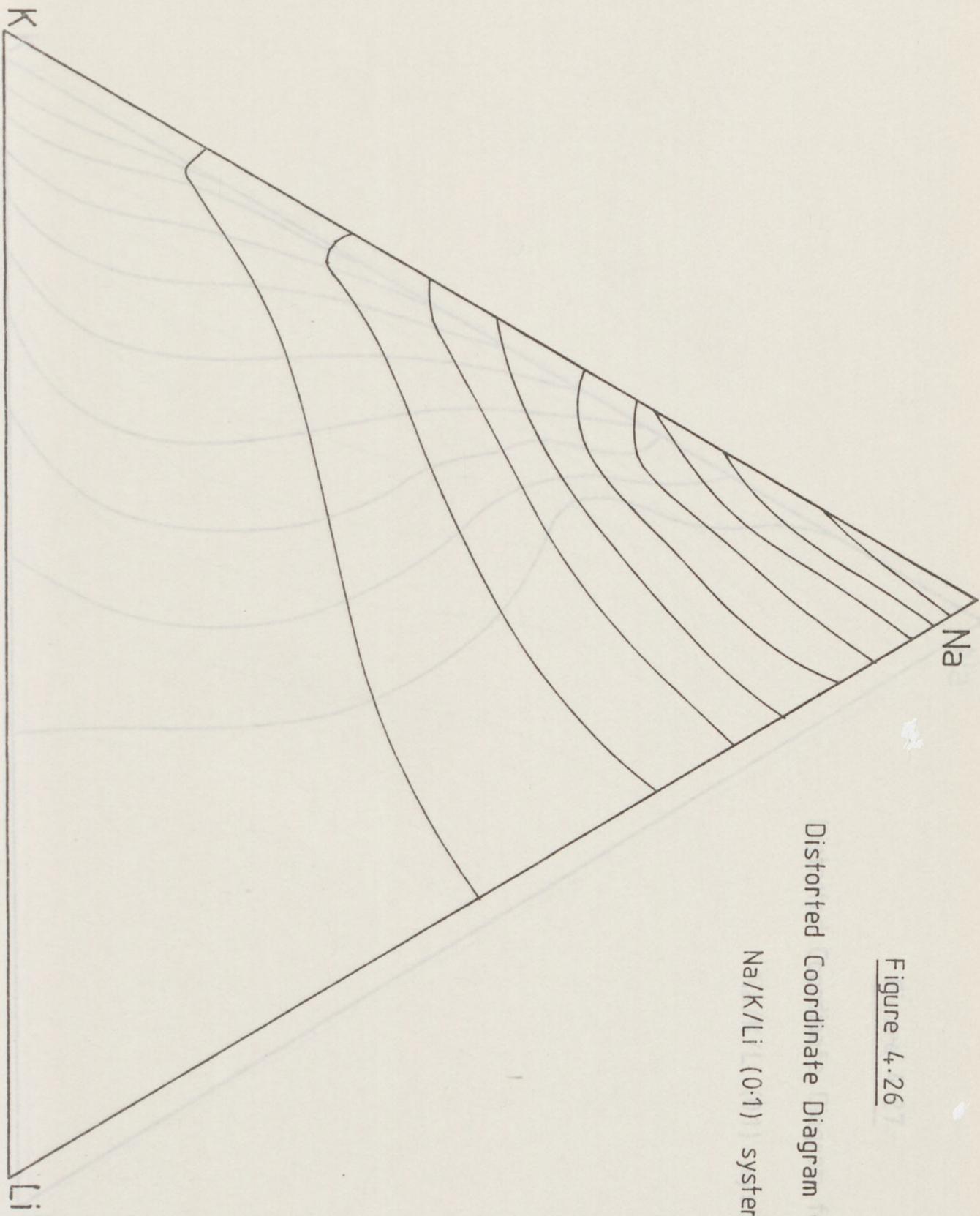
Figure 4·26

Distorted Coordinate Diagram for Sodium

Na/K/Li (0·1) system
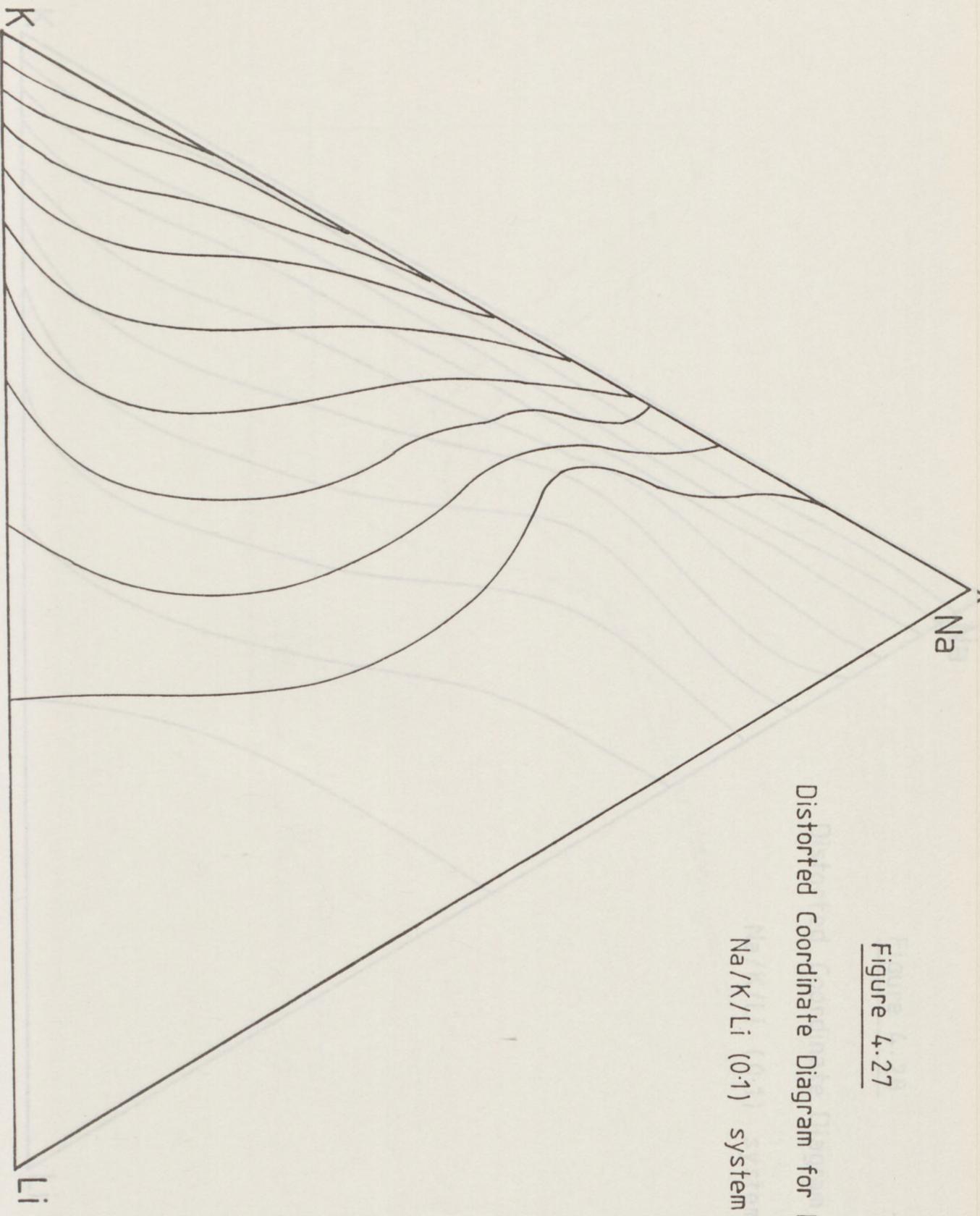
Figure 4.27

Distorted Coordinate Diagram for Potassium

Na/K/Li (0·1) system

Figure 4.28

Distorted Coordinate Diagram for Lithium

Na/K/Li (0·1) system
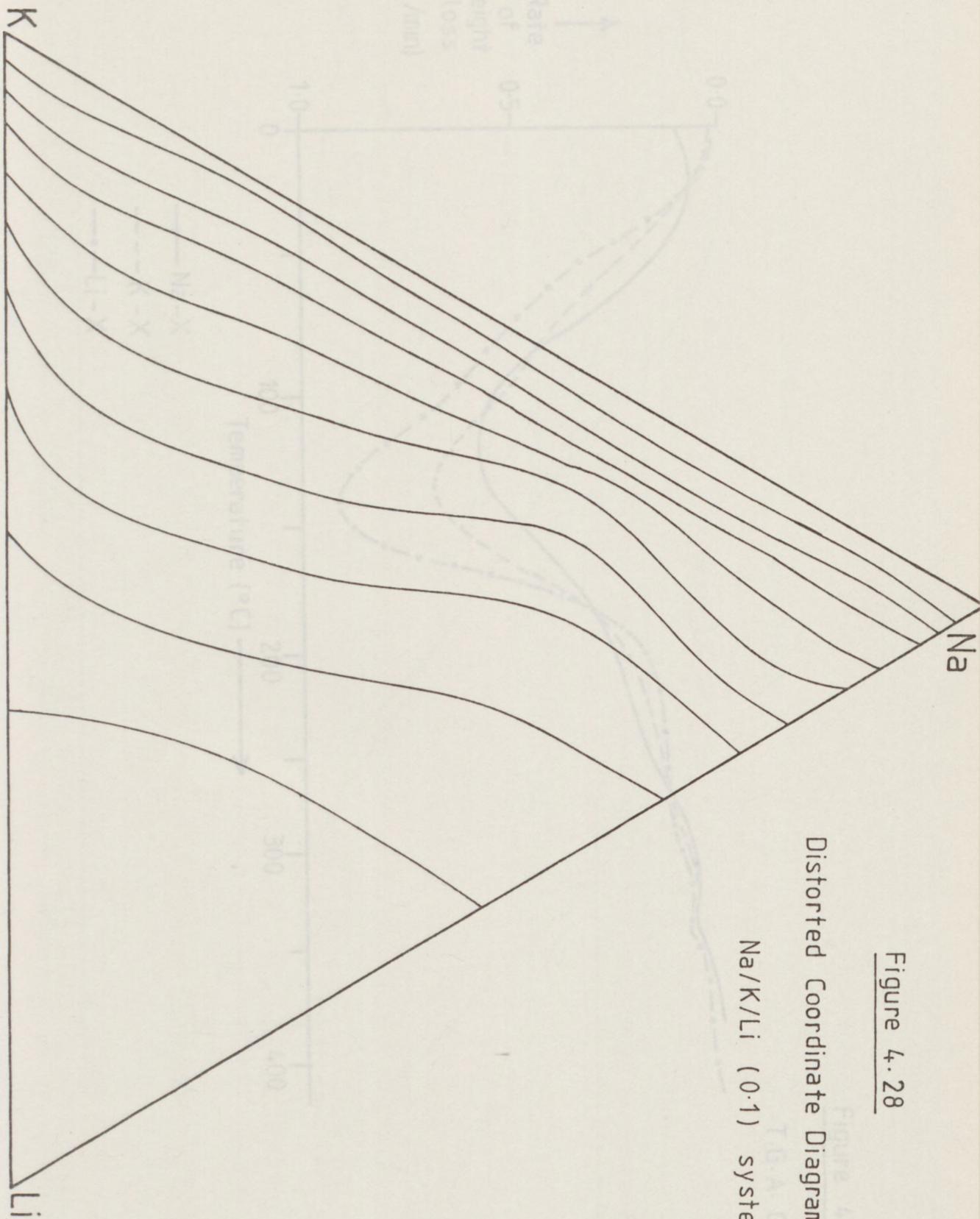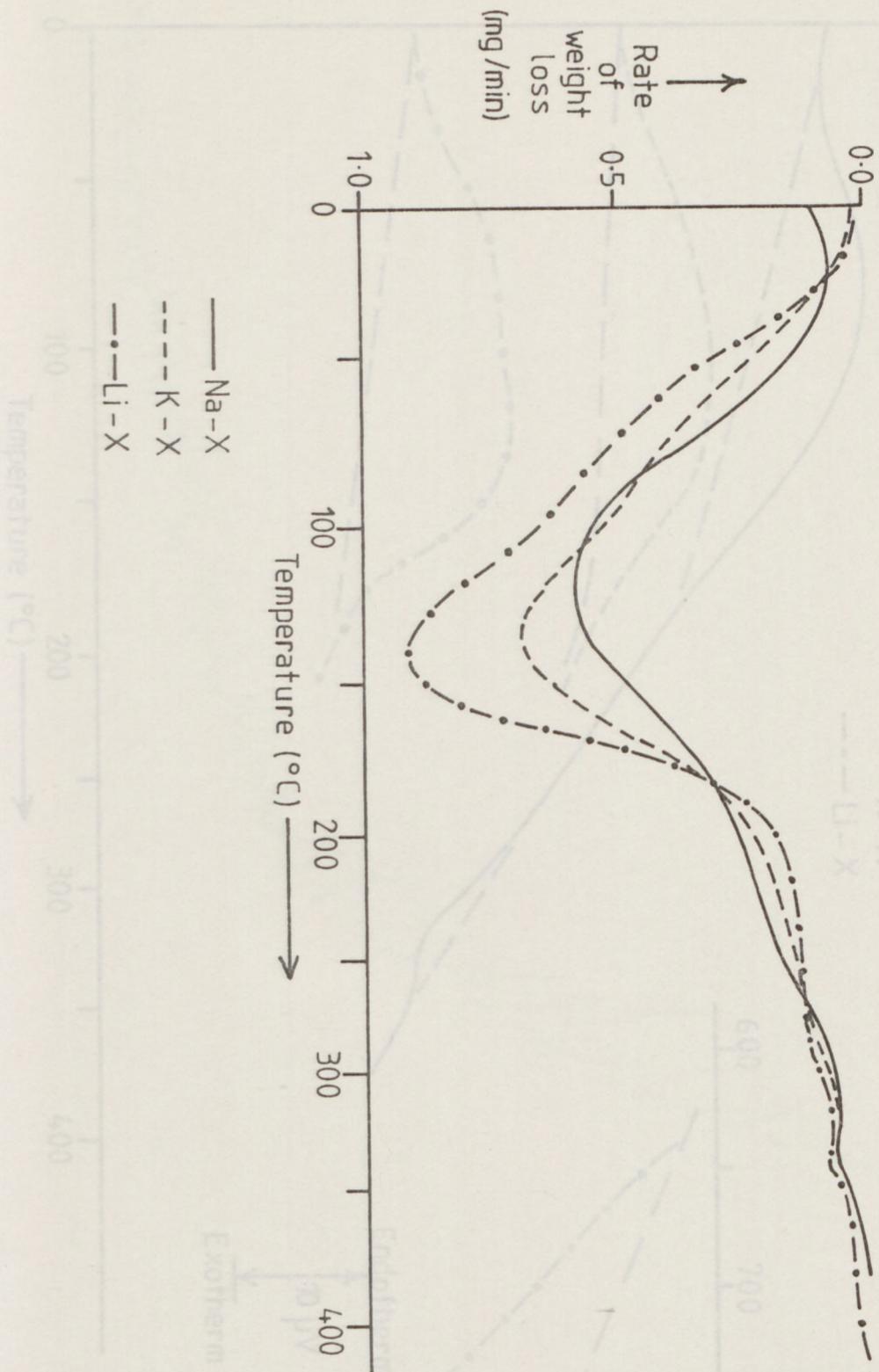
Figure 4.29

T.G.A. Chart
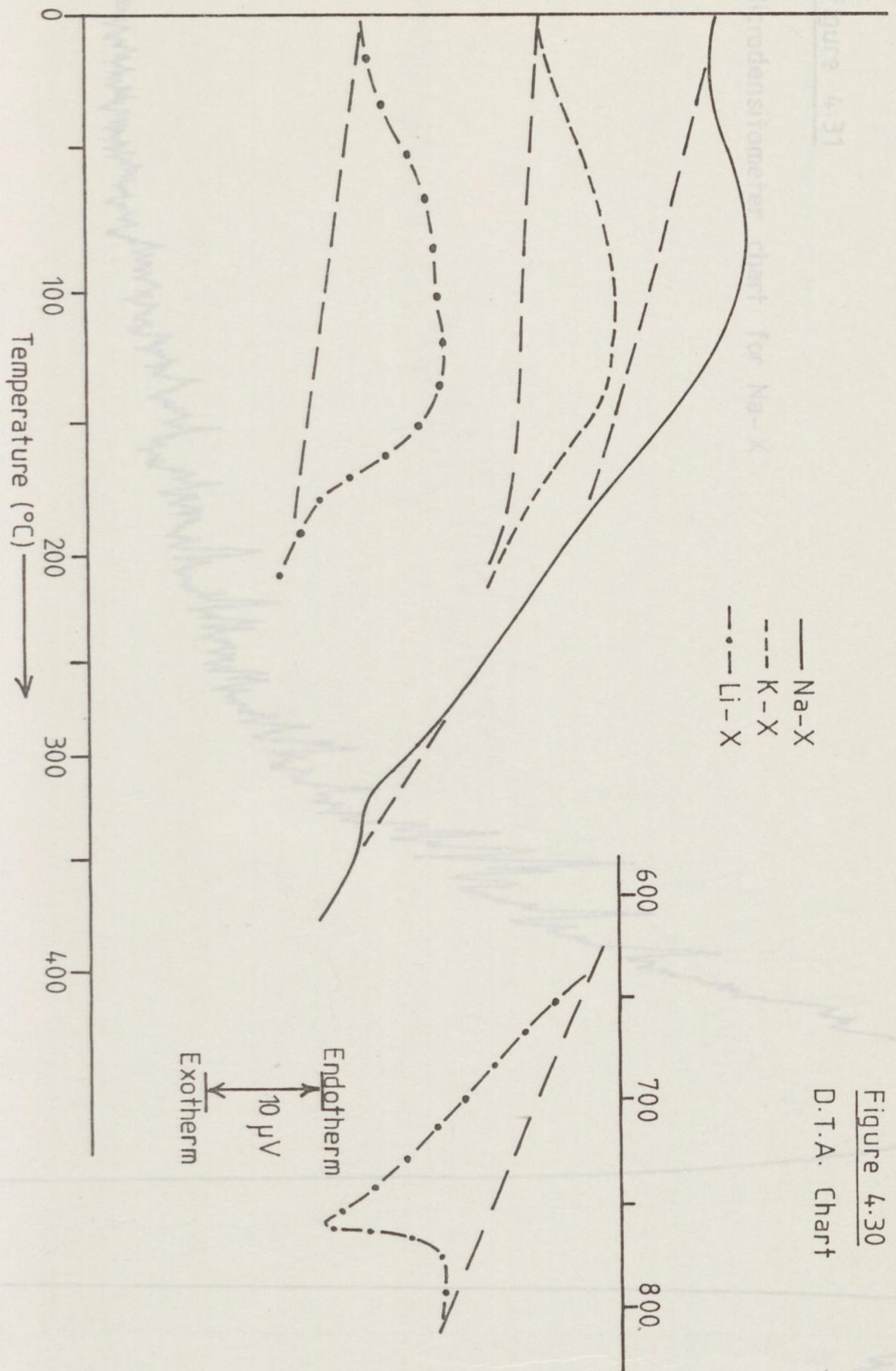
Figure 4.30

D.T.A. Chart

Figure 4.31

Microdensitometer chart for Na-X

Temperature (°C)

Na-X
K-X
Li-X

Exotherm ← | → Endotherm
10 μV

Figure 4.31

Microdensitometer chart for Na-X
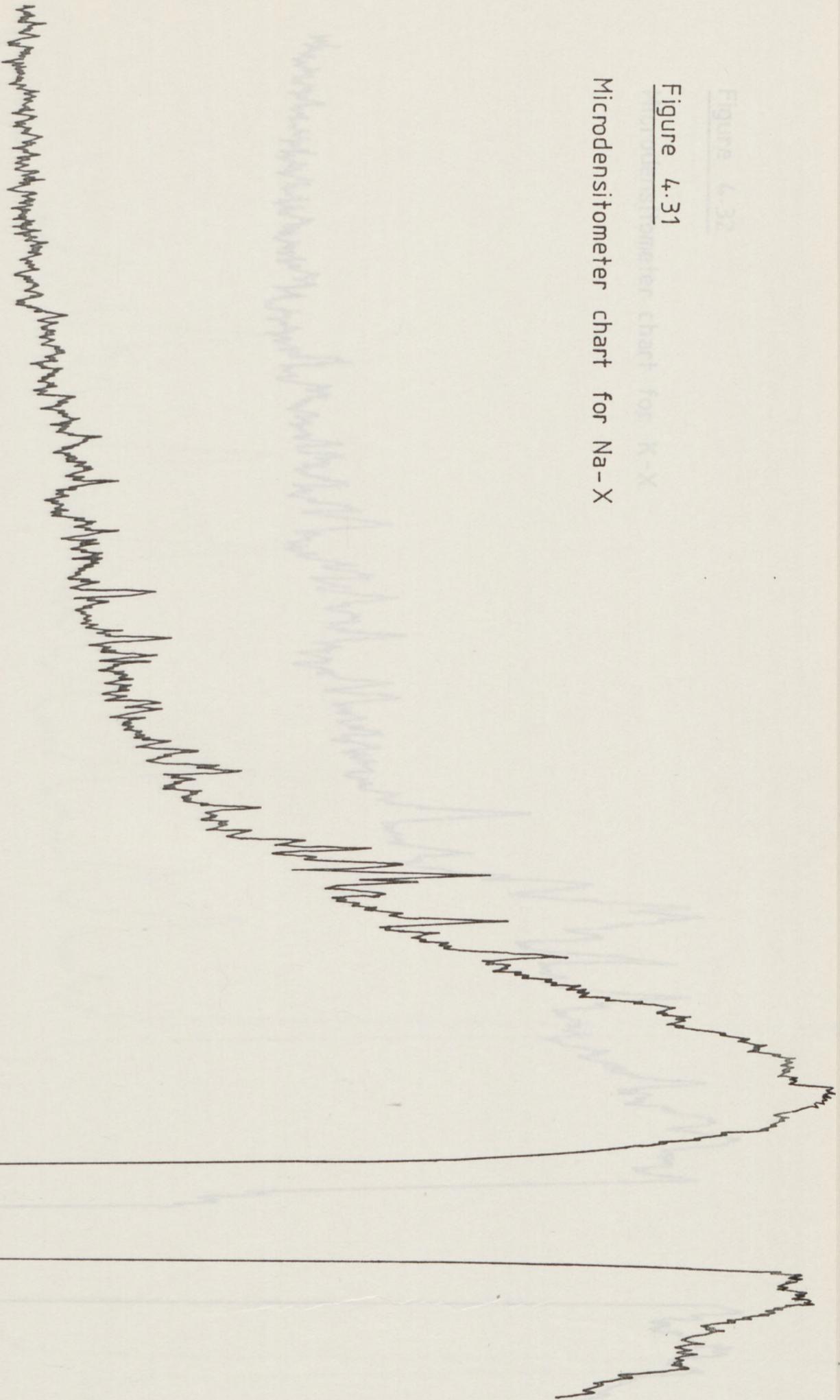
Figure 4.32

Microdensitometer chart for K-X
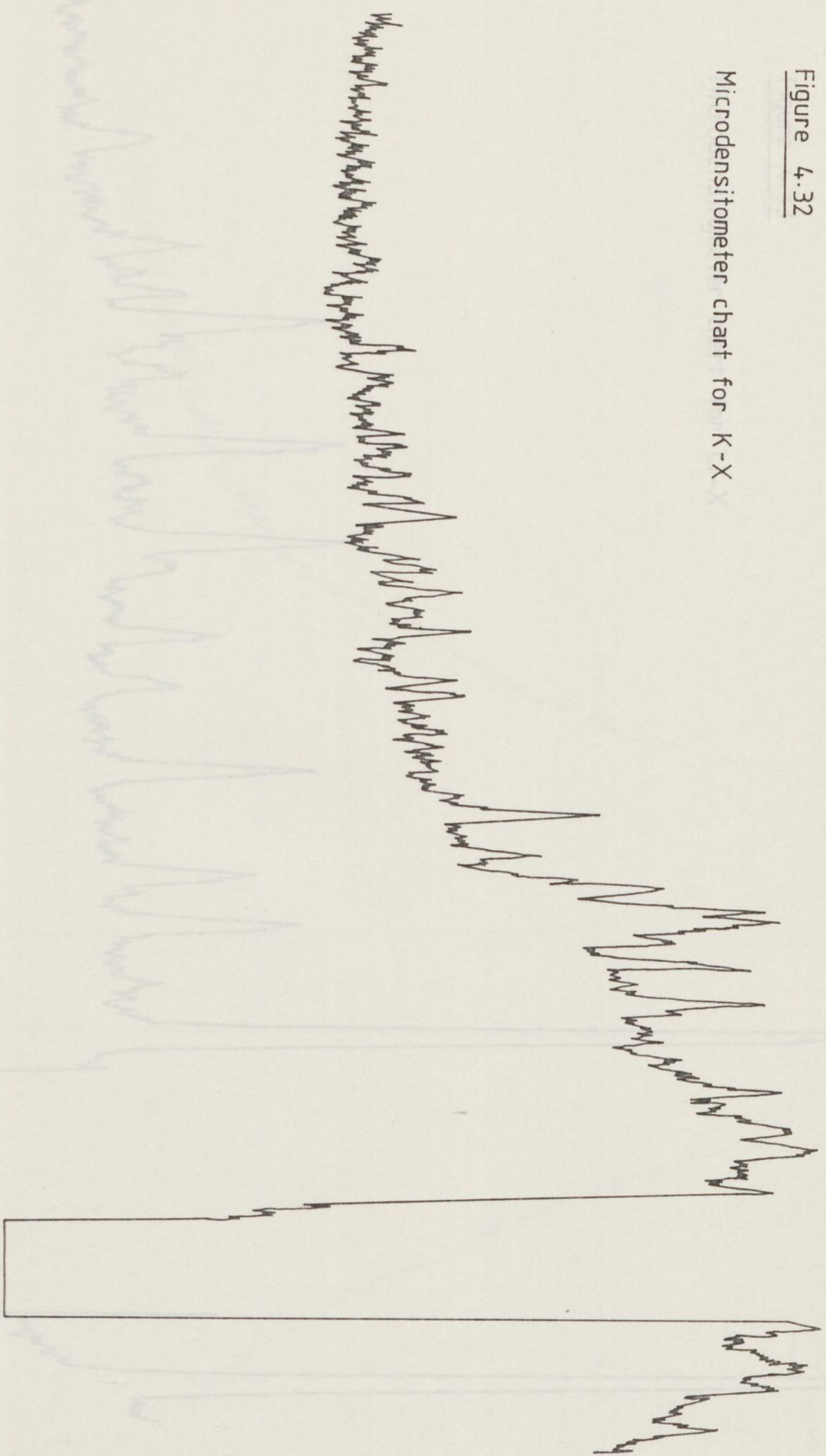
Figure 4.33

Microdensitometer chart for Li-X

(after heat treatment)
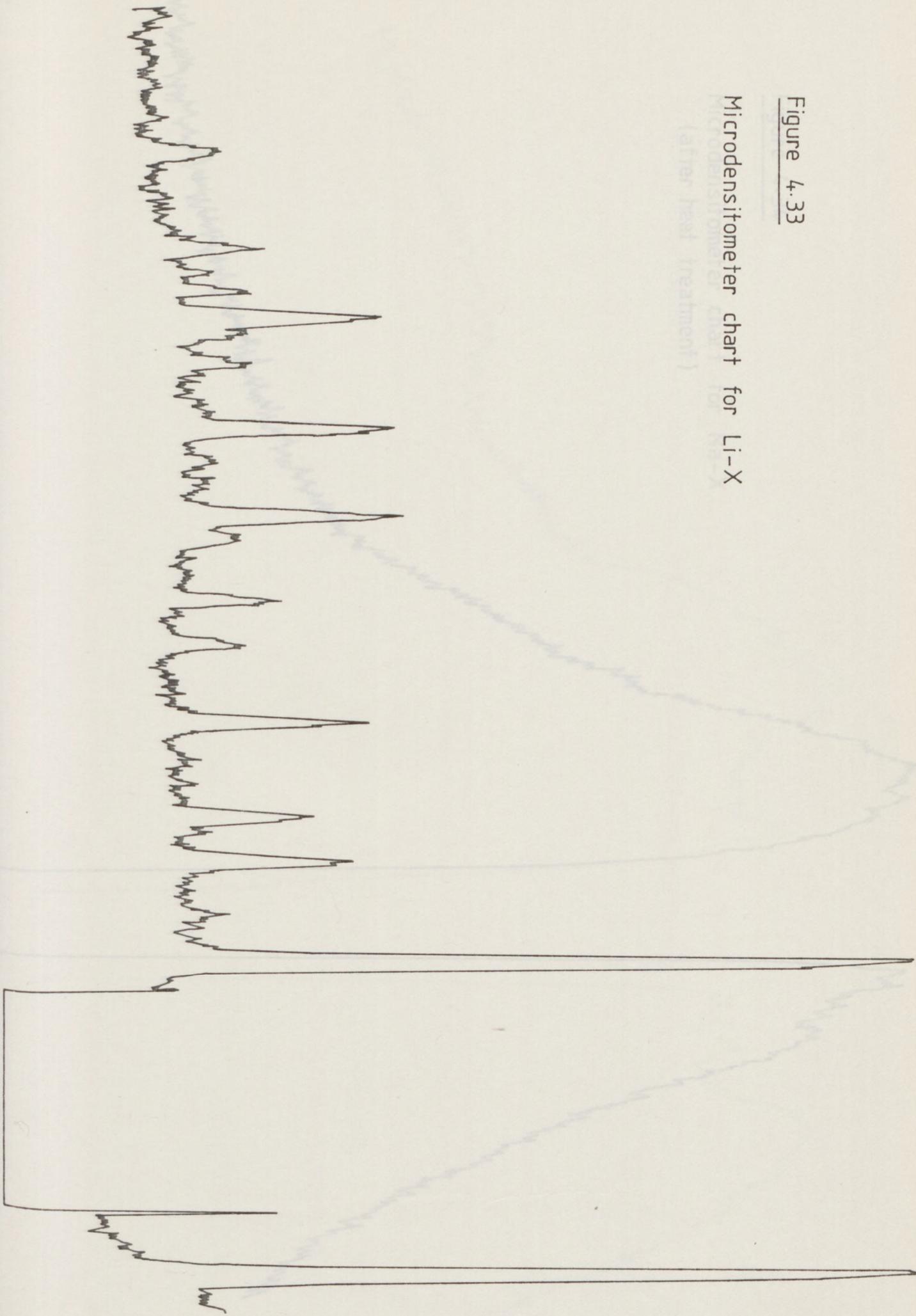
Figure 4.34

Microdensitometer chart for Na-X
(after heat treatment)
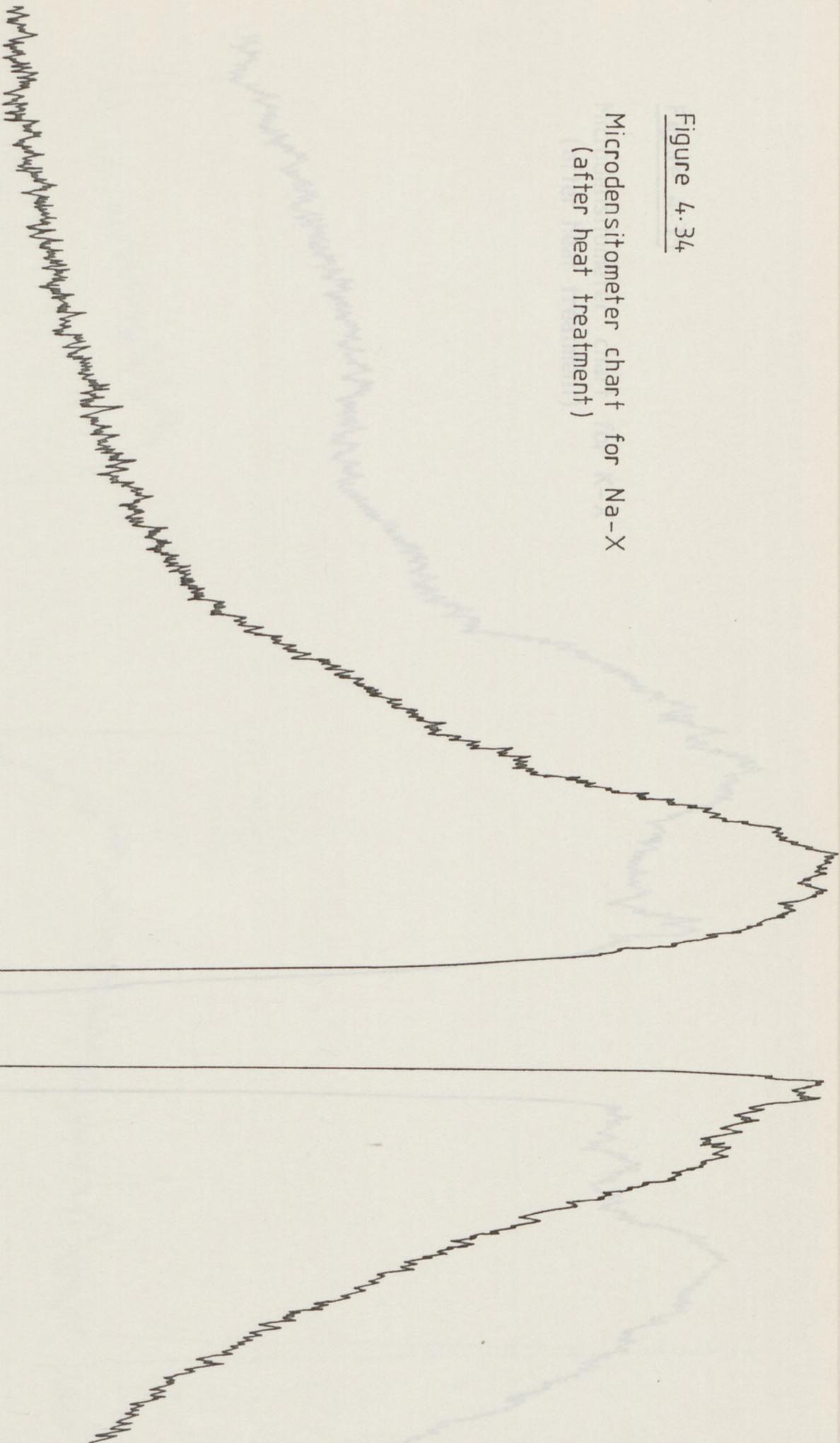
Figure 4.35

Microdensitometer chart for K-X
(after heat treatment)
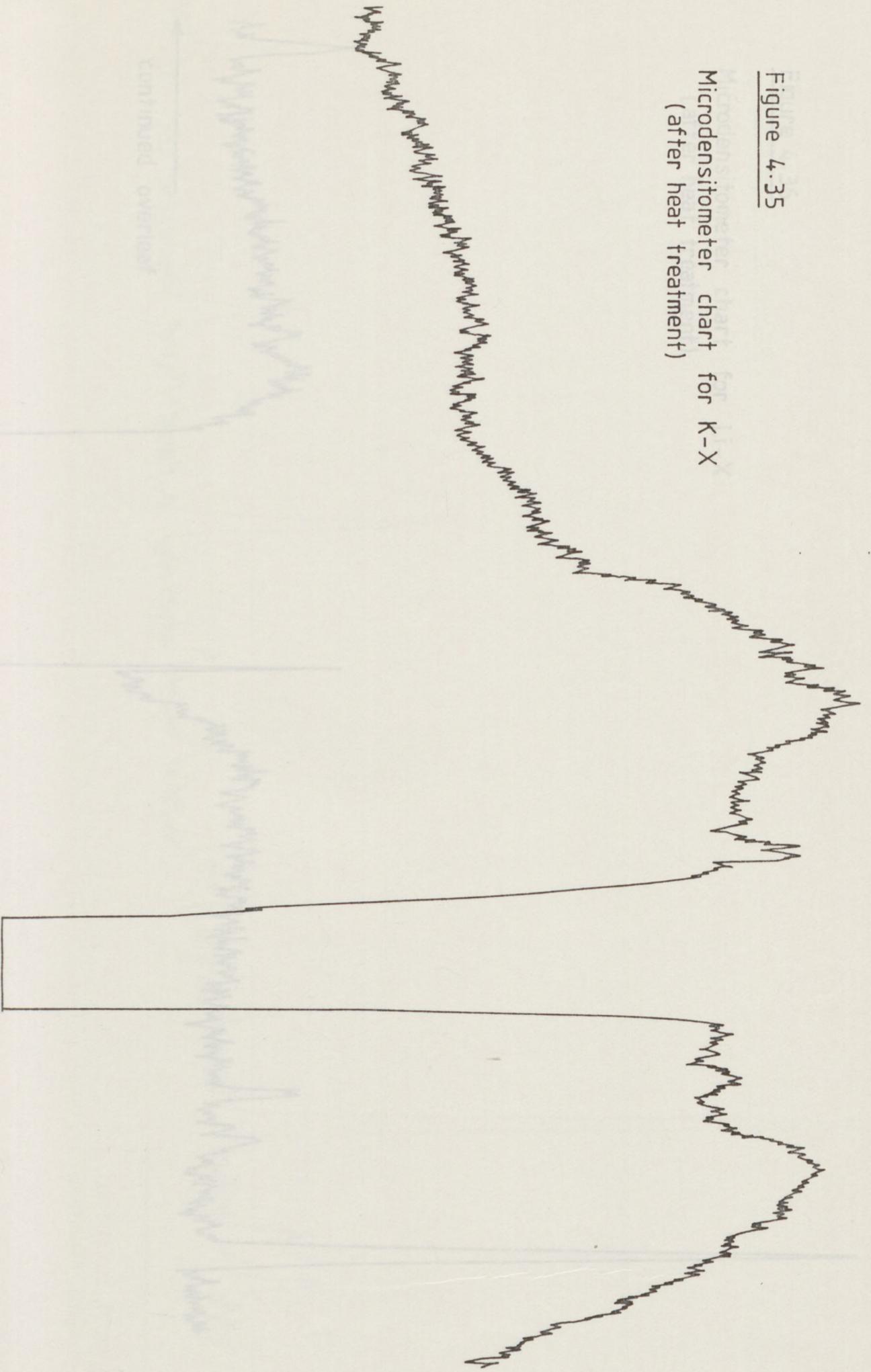
Figure 4.36

Microdensitometer chart for Li-X
(after heat treatment)

Figure 4.36 (continued)
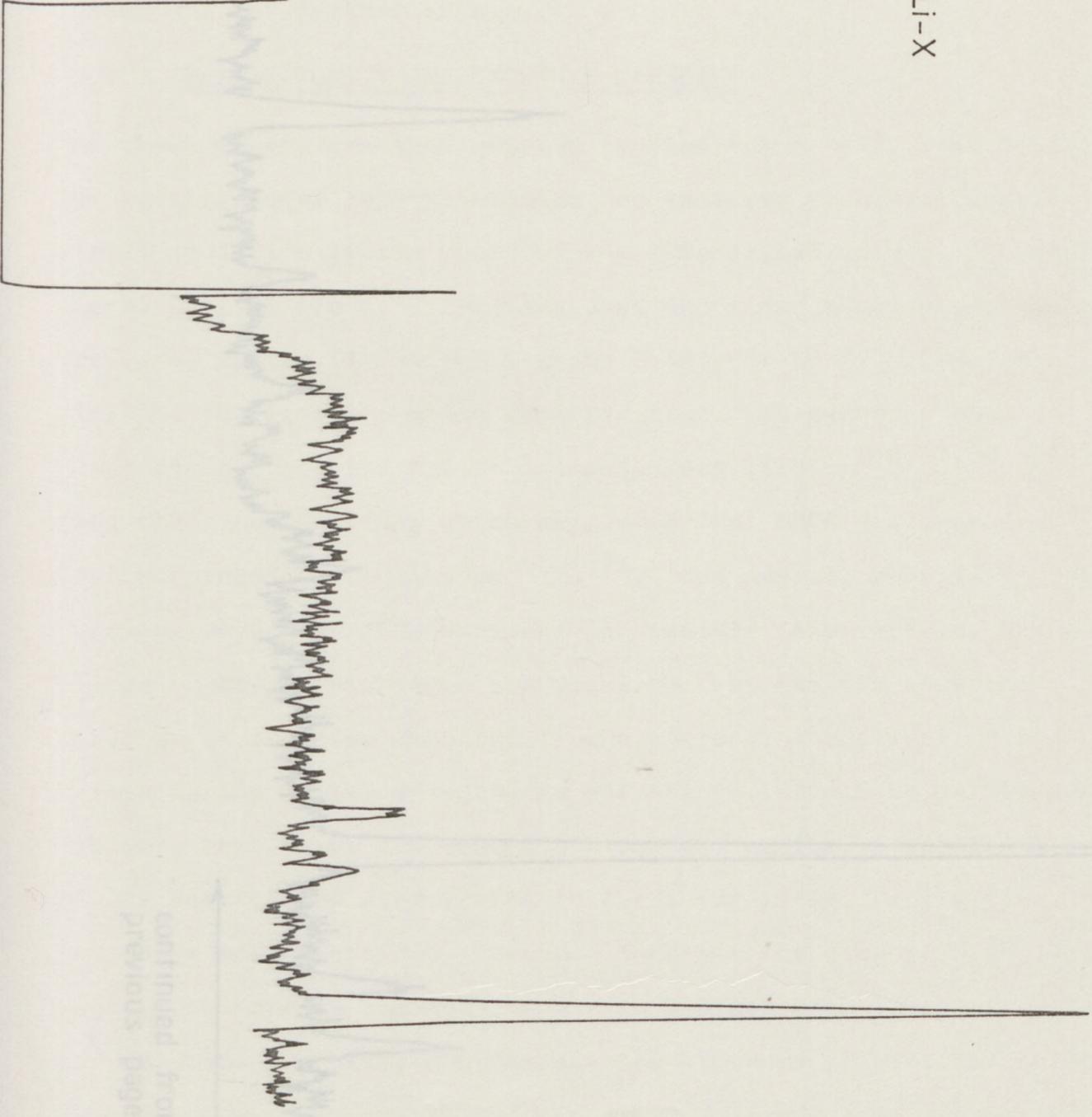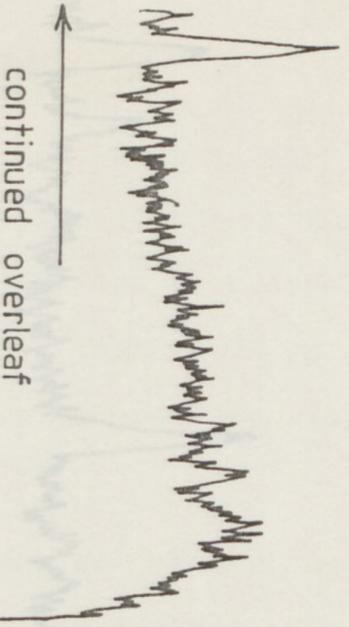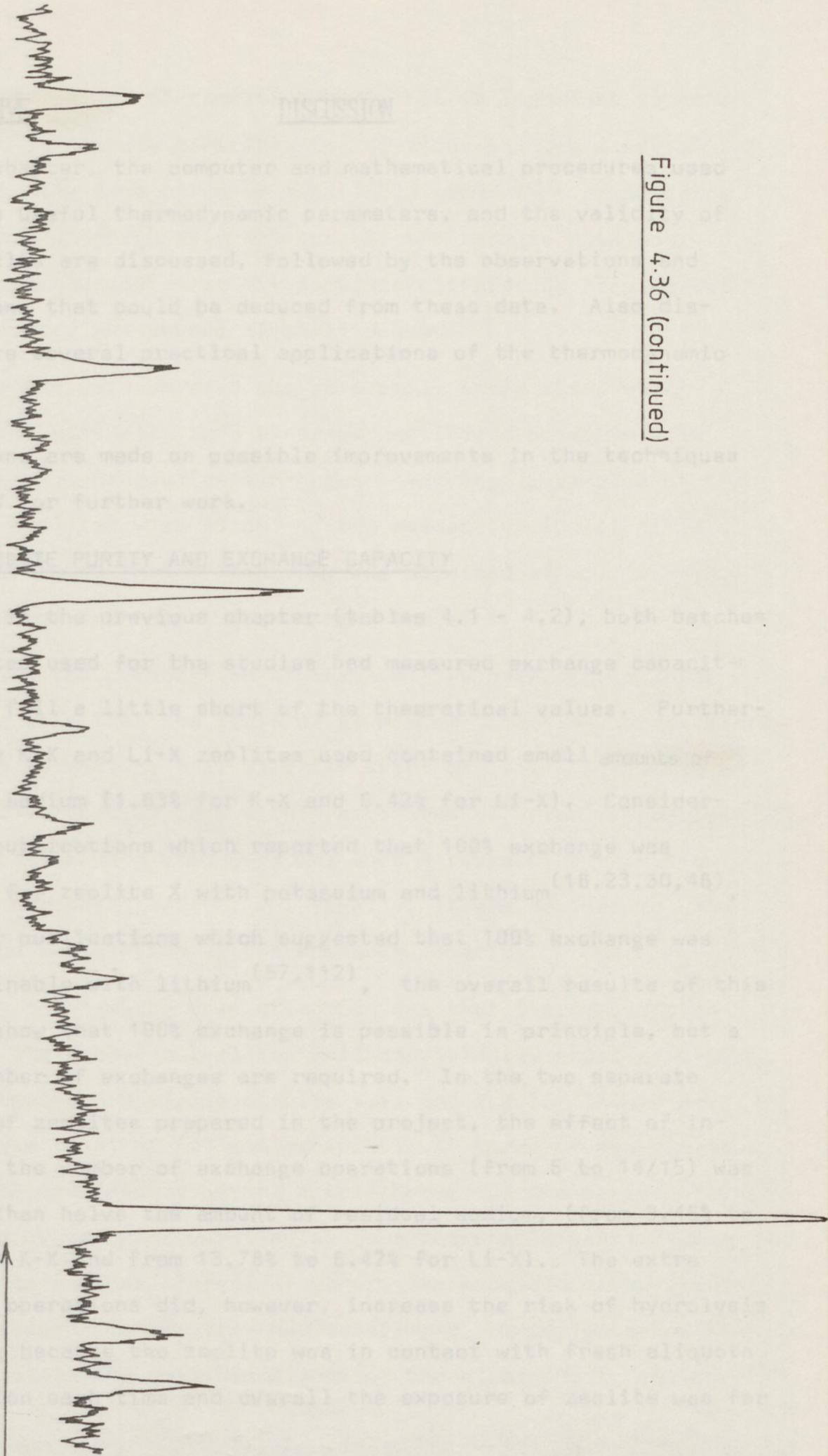
continued from
previous page

In this chapter, the computer and mathematical procedures used
to derive useful thermodynamic parameters, and the validity of
such results are discussed, followed by the observations and
conclusions that could be deduced from these data. Also dis-
cussed are several practical applications of the thermodynamic
data.

Suggestions are made on possible improvements in the techniques
used, and for further work.

5.1. ZEOLITE PURITY AND EXCHANGE CAPACITY

As shown in the previous chapter (tables 4.1 - 4.2), both batches
of zeolites used for the studies had measured exchange capacit-
ies that fell a little short of the theoretical values. Further-
more, the K-X and Li-X zeolites used contained small amounts of
residual sodium (1.63% for K-X and 6.42% for Li-X). Consider-
ing the publications which reported that 100% exchange was
possible for zeolite X with potassium and lithium[16,23,30,46],
and other publications which suggested that 100% exchange was
not attainable with lithium[57,112], the overall results of this
project show that 100% exchange is possible in principle, but a
large number of exchanges are required. In the two separate
batches of zeolites prepared in the project, the effect of in-
creasing the number of exchange operations (from 6 to 14/15) was
to more than halve the amount of residual sodium, (from 3.45% to
1.63% for K-X and from 13.78% to 6.42% for Li-X). The extra
exchange operations did, however, increase the risk of hydrolysis
occurring because the zeolite was in contact with fresh aliquots
of solution each time and overall the exposure of zeolite was for

a very long period of time (28 days). It is important to note

here that it appears desirable to carry out all the experimental

work using the same batch of zeolite in order that comparisons

may be made unambiguously between all the results obtained.

This approach would avoid any possible differences arising due

to the history and source of zeolite used.

Ion exchanges were carried out on a small scale also, which

proved that virtually 100% exchange was indeed possible with

K-X and Li-X. Exhaustive exchanges involving 1g samples of K-X

and Li-X zeolites with 50 cm^3 of the respective (pure) nitrate

solutions showed that 100% purity was obtained after five

exchanges for K-X or nine exchanges for Li-X.

Considering the composition of the zeolites used, it is inter-

esting to note that the ratio of aluminium to cation, particularly

aluminium to sodium, fell slightly short of 1:1. This small

defecit (less than 1%, and within experimental error) of cation

caused some concern when deciding upon a respective exchange

capacity for each zeolite, but finally, it was decided to use

the cation composition as the exchange capacity.

A further point which drew attention was that the composition

total of the analysed zeolites fell consistently short of a 100%

despite repeated analyses (tables 4.1. and 4.2.). Though an

approximate total of 99% was acceptable in terms of experimental

error, the consistency of the error throughout the period of the

project provoked some question as to a reasonable cause. In

addition to various sources of error, the possible occurrence of

some hydrolysis in solution was considered. Hydrolysis can

easily explain the small imbalance of the aluminium to cation

- 193 -

ratio, and the cation balance work carried out (section 4.6.2)
did suggest that some hydrolysis could have occurred, causing a
transfer of cations from the crystal phase to the solution.
Currently the concept of hydrolysis is under further investi-
gation, and preliminary results show that a degree of hydrolysis
does occur within a short period of the zeolite coming into
contact with pure water[113]. It appears however, that it is
successive washes with fresh water or solution which will cause
serious problems due to hydrolysis rather than the length of time
that the zeolite is suspended in just one solution[113]. Thus,
even 12½ weeks suspension had little effect when isotherm data
obtained after this period are compared with a 6 day suspension
(see section 5.3.1; figures 4.15 and 4.14). Preliminary work
has also shown that after the first contact with water, the amount
of further hydrolysis with successive washes is small[113].

In spite of the possibility of hydrolysis, the overall deficit
in the composition total cannot be explained by this factor.
The transfer of ions noticed during the cation balance work is
attributed to a transfer of zeolite at the centrifugation stage
(which involved some overall loss and some transfer to the solution
phase) as described in section 4.6.2.

5.2. BINARY ION EXCHANGE

5.2.1. Binary Isotherms

All the binary isotherms obtained (figures 4.1 - 4.8), show little
experimental scatter. The isotherm describing the K/Li equilib-
rium shows however some unusual features. Isotherm shapes are in
excellent agreement with published data where this is available
(18,23,30). Depicted preferences are therefore fully consistent

- 194 -

with published results of other workers[16,23,30,46]. The three K/Na isotherms (figures 4.3 - 4.6) have near-identical shapes, confirming that varying the solution concentration (0.04 vs 0.1 equiv. dm^{-3}), or varying the ionic strength while keeping the solution concentration constant by introducing a second (tri-valent) anion to the system, makes little difference to the exchange equilibrium. Combining these two factors, two further equilibrium points were obtained for the two-anion system (points 2 and 3 on figure 4.4 respectively) at higher concentrations of 0.25 and 0.5 equiv.dm^{-3}. These two points fall just off the isotherm, and are in the vicinity of their counterpart at 0.1 equiv.dm^{-3} (point 1 on figure 4.4), illustrating negligible change with solution strength. The slight displacement of the points are within experimental error. The K/Li isotherm warrants special mention. The unusual and non-random distribution of points in the middle part of the curve (figure 4.2) caused some concern, particularly because two non-coincident half-curves can be drawn through the two batches of points, with a semi-sigmoidal section to link them (figure 4.2). The scatter could not be attributed to experimental error because selected points were confirmed by repetition of experiments. Comparison with results of other workers was not possible as there have been no previous studies concerning lithium exchange in a *potassium* X zeolite. Taking into account the similarities between potassium and sodium in terms of zeolite X, and the similar non-preference for lithium exhibited by X, particularly when the ternary results are also considered, it is reasonable to expect an isotherm for the K/Li exchange that is fairly similar in shape to that for the Na/Li exchange. The anomaly in the isotherm points cannot,

however, be attributed to the presence of the sodium impurity (1.63%) in the K-X zeolite used on the basis that if potassium and sodium behave towards exchanging lithium in a similar manner, then the substitution of some potassium by sodium should not make any difference to the overall behaviour. No such anomalous behaviour was observed in the K/Ag isotherm (figure 4.7). Again, no comparison of this isotherm could be made with literature, but it could be convincingly argued that the enormous selectivity (compare the sharpness of curves in figures 4.7 and 4.8 with 4.1 and 4.2) for silver over potassium (and over sodium) could easily swamp any anomalous behaviour here. The similarity between the shapes of Na/Ag and K/Ag (figures 4.7 and 4.8) further emphasises the rationale for there being similar Na/Li and K/Li isotherms. This point is re-considered, after the results have been discussed, in section 5.2.3.

5.2.2. Thermodynamic Treatment

The methods used to treat the equilibrium data thermodynamically have been discussed earlier (sections 2.1 and 4.4). The procedure was straightforward as 100% exchange were possible with the zeolites used and normalisation was not therefore necessary.

As described in chapter 4, the 'best' order of the fitting poly-nomial equation was selected by a visual inspection of the Kielland plots, and by a comparison of the sum of residuals for each order. The lowest value of R was preferred, but the shape of the Kielland plot was usually important. In all the binary systems studied, the choice was between orders of 3 and 4; a comparison of the experimental Kielland plots (figures 4.18 - 4.24) shows that the distribution of the points required a 4th

order 'best fit' in many cases. The binary computer program also printed out a list of experimental lnK_c values against their computer predicted counterparts, so a visual inspection of the data was possible, allowing any obvious inconsistencies to be spotted.

The above mentioned computer procedure was used to treat all the binary systems studied in this project *except* the two-anion Na/K system. Since all the ions present in the previous exchange systems were univalent, the solution phase correction Γ remained constant throughout each system[84]. When the tri-valent ferri-cyanide ion was introduced into the system, the ionic strength, and hence Γ, started varying with the concentration of this second anion, even though the total solution concentration remained constant at 0.1 equiv. dm^{-3}. Furthermore, the solution phase treatment could not be fully carried out due to a lack of activity coefficient data.

Therefore, the binary treatment was modified for this case. The modification was made on the basis that the final outcome of the Na/K exchange should remain the same regardless of the presence of one or two anions. Therefore, for the two Na/K binary equil-ibria represented by figures 4.3 and 4.4, the small differences or shift of the isotherms must have been caused by the presence of the second anion, since the values of $\Delta G^{\ominus}$ and K_a should remain constant for the equilibria. If the differences between the single and two anion system isotherms can be defined in terms of the solution phase compositions A_{s1} and A_{s2} respectively in equilibrium with each crystal phase composition A_c, then

$$K_{a(1)} = K_{a(2)} \qquad \qquad \dots(5.1)$$

since

$$K_a = K_c \cdot f_A^{z_B}/f_B^{z_A} \qquad \qquad \dots(5.2)$$

and $f_A^{z_B}/f_B^{z_A}$ is invariant with ionic strength at low concentrations[60,114], it follows that

$$K_{c(1)} = K_{c(2)} = \text{constant} \qquad \qquad \dots(5.3)$$

i.e.

$$\left[\frac{m_B^{z_A} A_c^{z_B}}{m_A^{z_B} B_c^{z_A}}\right] \cdot \Gamma = \text{constant for both cases} \qquad \dots(5.4)$$

Therefore, for any particular crystal phase composition $A_c^{z_B} / B_c^{z_A}$,

$$\left(\frac{m_B^{z_A}}{m_A^{z_B}}\right)_{(1)} \cdot \Gamma_{(1)} = \text{constant} = \left(\frac{m_B^{z_A}}{m_A^{z_B}}\right)_{(2)} \cdot \Gamma_{(2)} \qquad \dots(5.5)$$

By rearranging,

$$\Gamma_{(2)} = \left(\frac{m_B^{z_A}}{m_A^{z_B}}\right)_{(1)} \cdot \left(\frac{m_A^{z_B}}{m_B^{z_A}}\right)_{(2)} \cdot \Gamma_{(1)} \qquad \dots(5.6)$$

Since generally $m_A = A_s \cdot T_N/z_A$ etc.

$$\Gamma_{(2)} = \left(\frac{A_{s2}}{A_{s1}}\right)^{z_B} \left(\frac{1-A_{s1}}{1-A_{s2}}\right)^{z_A} \left(\frac{T_{N1}}{T_{N2}}\right)^{(z_A-z_B)} \cdot \Gamma_{(1)} \qquad \dots(5.7)$$

Referring to figure 5.1 where both the Na/K binary isotherms are shown on the same diagram, it is apparent that when $\Gamma_{(1)}$ is known, $\Gamma_{(2)}$ can be found for a given composition (A_c, B_c) if the corresponding solution phase composition for the second system (A_{s2}, B_{s2}) is also known. In principle therefore, this provides a means of calculating hitherto unknown values of activity

coefficients of salts in a two cation/two anion mixture. (see
section 5.4.2).

The cations used in this project were all uni-valent, and the
above equation therefore simplifies further to

$$\Gamma_{(2)} = \left(\frac{A_{s2}}{A_{s1}}\right)\left(\frac{1-A_{s1}}{1-A_{s2}}\right) . \quad \Gamma_{(1)} \qquad \qquad ....(5.8)$$

thus eliminating the concentration dependence term.

Since all the necessary information related to system 1 was known
(i.e. the Na/K one anion system at 0.1 equiv.dm^{-3}) and the iso-
therm for the second system was available (i.e. the two anion
system at the same solution concentration), a simple computer
program could be written to carry out the calculations. The
difficulty arose from the need to read off the corresponding A_{s1}
and A_{s2} values for each A_c value from the joint isotherm (figure
5.1) because the two curves were very close together. (The
diagram is drawn on a large scale to accentuate the difference.)
The appropriate solution phase data were read off the *curves*
which were best fits 'by eye' drawn through the experimental
points. Thus, the calculation of Γ values for the two-anion system
involved using 'smoothed' data. This was done for two reasons:
Firstly, it was necessary to read off A_{s1} and A_{s2} values at the
same A_c value. This could not be done with the experimental
results because the respective A_c values for the two systems were
normally non-coincident. Secondly, it was necessary to put the
difference between corresponding A_s values into some orderly
fashion, and thereby avoid the small experimental scatter of
results.

Though the calculation of $\Gamma_{(2)}$ did not require any concentration
data (for this uni-valent case), the presence of the $\left[Fe(CN)_6\right]^{3-}$

- 199 -

ion did cause the Γ value to vary with ionic strength. To calculate ionic strength, it was also necessary to feed in the concentration (equivalents dm^{-3}) of *one* of the anions together with each corresponding pair of A_c and A_{s2} values; i.e. the value of A_c had to be 'related' to some known concentration (equivalents dm^{-3}) of anion. Since the anion composition remained constant during each equilibrium process, the data used for this computer program was obtained as follows.

For the two-anion system, the amount of potassium was varied in the exchange solutions by varying the (known) amount of potassium ferricyanide solution present. When the crystal phase was analysed after exchange, each measured A_c value could be 'related' to a corresponding concentration (equivalents dm^{-3}) of ferricyanide ions. Therefore, the same A_c values obtained experimentally for the two-anion system were used to read off the corresponding A_{s1} and A_{s2} values from the *smoothed* curves, and fed into the computer together with the appropriate ferricyanide ion concentrations (equivalents dm^{-3}). The computer then printed out the corresponding $\Gamma_{(2)}$ values and ionic strengths. All these data are shown in table 5.1. As a further comparison, however, the procedure was repeated using the 'smoothed' A_{s1} values with *experimental* A_{s2} values. Some of the $\Gamma_{(2)}$ values obtained in this way were slightly different to the corresponding previous $\Gamma_{(2)}$ values. The computer program used is shown in Appendix IV.

Once this was accomplished, the binary treatment was carried out. The computer program used for the treatment was similar to the one used to process the data from the single-anion binary system (see Appendix IV), but by-passed the solution phase treatment section. (If the Debye-Hückel or activity coefficient data

TABLE 5.1. Calculated Γ Values for Two-Anion System

A_c	A_{s1}	1st method		2nd method		I_2 (equiv.dm^{-3})
		A_{s2}	$\Gamma_{(2)}$	A_{s2}	$\Gamma_{(2)}$	
.130	.067	.051	0.772	.051	0.772	0.11
.211	.137	.119	0.885	.119	0.885	0.12
.276	.221	.194	0.875	.195	0.870	0.13
.331	.317	.279	0.860	.271	0.807	0.14
.371	.390	.349	0.865	.351	0.861	0.15
.421	.482	.437	0.860	.431	0.816	0.16
.469	.568	.520	0.850	.509	0.820	0.17
.516	.637	.600	0.881	.592	0.879	0.18
.564	.703	.678	0.917	.677	0.904	0.19
.619	.773	.748	0.899	.756	0.849	0.20
.682	.836	.810	0.862	.808	0.839	0.20
.737	.878	.857	0.858	.858	0.898	0.20

were available for *all* the salts of the two-anion system, the
calculation of $\Gamma_{(2)}$ by a separate method would have been un-
necessary, and only a small modification to the standard computer
program - to feed in the ferricyanide ion concentration so that
the ionic strength could be calculated - would have been required).
The remainder of the treatment was identical to that used for
the single-anion systems.

5.2.3.   Thermodynamic Data

The results for each binary system, in the form of changes in standard free energy, thermodynamic equilibrium constants and ratios of solution phase activity coefficients (constant for uni-valent cases) have been shown in table 4.4. Before discussing the actual values it is worth examining their validity in terms of the fitting equations chosen.

As mentioned in chapter 4, 'best-fit' curves, defined by a polynomial equation, were chosen on the basis of a visual examination of Kielland plots *and* from a comparison of sums of residuals defined in equation (4.4). An inspection of the Kielland plots (figures 4.18, 4.23 and 4.24) reveal that three of the systems, Na/Li, Na/Ag and K/Ag had simple distributions of points, requiring only a 3rd order 'fit', while the other four systems had points distributions which necessitated more complex 4th order fits (figures 4.19 - 4.22). Generally, the curves appear to 'fit' well, but some scatter of points is noticed, particularly for the K/Li exchange (figure 4.19), and the single-anion Na/K exchange at 0.1 equiv.dm^{-3} concentration (figure 4.20). Although the curves generally fit the experimental data well, they are susceptible to 'flapping' at the extrema, where insufficient data are available. Ideally, these areas need to be filled in with more data but the accuracy of such data is very strongly dependent on the analytical methods used.

In order to investigate the sensitivity of the curves and the final results, to the order of the polynomial, all systems were tested for *both* third and fourth orders. The results obtained from this are shown in table 5.2. The resultant Kielland plots

TABLE 5.2. Comparison of Binary Results for Different
Orders of Polynomial Equations

System	Order	Sum of residuals	$\Delta G^{\ominus}$ (kJ equiv.$^{-1}$)	K_a
Li/Na-X(0.1)	2	0.1074	+5.725	0.099
	3*	0.0863	+5.730	0.099
	4	0.0884	+5.726	0.099
Li/K-X(0.1)	3	0.1193	+6.324	0.078
	4*	0.0969	+6.165	0.083
K/Na-X(0.1)	3	0.0939	+0.740	0.742
	4*	0.0531	+0.708	0.752
K/Na-X(0.04)	3	0.0812	+0.472	0.827
	4*	0.0360	+0.557	0.799
Ag/K-X(0.04)	3*	0.0695	-13.057	194.430
	4	0.0735	-13.006	190.407
Ag/Na-X(0.04)	3*	0.1145	-13.555	237.687
	4	0.1202	-13.770	259.309
K/Na-X(0.1) two anions				
Method 1	3	0.0281	+0.507	0.815
	4	0.0164	+0.959	0.679
Method 2	3	0.0435	+0.459	0.831
	4	0.0463	+0.540	0.804
Method 3	3	0.0297	+0.527	0.808
	4*	0.0289	+0.762	0.735

N.B. The chosen orders are marked by an *.

for the alternate orders are shown for only three systems (figures 5.2.a - 5.2.c) but comparisons of these were made for all seven systems, in order to select a 'best-fit' and also to compare shapes and degrees of 'flapping'.

General observations on these results are that for most cases the effects of varying the order of the polynomial are very small but, as expected, the differences increase when the data deficiency increases (compare the three K/Na-X systems). An inspection of the corresponding Kielland plots reveals that the greater differences in results are caused by the changes in the shape of the Kielland plots between orders (figures 4.21 - 4.23 vs 5.2). Choosing the correct orders for the two single-anion Na/K systems is very straight-forward as the best fit by eye and the lowest value for the sum of residuals are unambiguously in agreement. At the higher concentration, the better fit is clearly obtained for order 4, and though the value of $\Delta G^{\ominus}$ changes little, the sum of residuals confirms that the fourth order should be selected. For the Na/K exchange at the lower concentration, changing from a fourth order to a third results in a 15.3% drop in $\Delta G^{\ominus}$ but the curve becomes an obvious worse 'fit' (figures 4.22 vs 5.2.b), and the sum of residuals increases quite markedly. These factors enable the fourth order to be selected as the 'correct' one. Furthermore, one would expect the outcome of any Na/K Kielland plot to be the same irrespective of the two different concentrations used, and hence the comparison of Kielland plots reveals that the fourth order shape (figure 4.22) is similar to the (already selected fourth-order) shape of its 0.1 equiv.dm^{-3} counterpart (figure 4.20). The two curves are very similar except for the sharp downturn in the $A_c \rightarrow 0$ region seen for the

Na/K(0.04) system. The greater shape-stability (i.e. lesser sen-
sitivity) of the Na/K(0.1) system seems to arise from the slight-
ly better end-definitions of the curve which reduces the amount
of 'flapping'.

The decision regarding the Na/K two-anion system was far more
complex (figure 4.21), firstly because three slightly different
sets of input data could be used in the computer program to
give reasonably different results, and secondly because a great-
er deficiency of curve-end data caused more 'flapping' and
changes of shape between orders. Considering the input data first
it was shown in section 5.2.2. that two separate methods could
be used to estimate the Γ data for the system. If the Γ values
obtained by using 'smoothed' A_{s1} *and* 'smoothed' A_{s2} values can
be called 'smoothed' Γ values, and conversely the Γ values ob-
tained by using 'smoothed' A_{s1} *but* experimental (or real) A_{s2}
values are called 'real' Γ values, then the subsequent binary
thermodynamic treatment can be applied to the two-anion system
by inputting (i) the 'smoothed' Γ and 'smoothed' A_{s2} values, or
(ii) the 'real' Γ and real A_{s2} values, or (iii) the 'smoothed'
Γ values with real A_{s2} values.

The so-called 'real' Γ values were obtained by using 'smoothed'
A_{s1} data from the Na/K(0.1) single-anion system. As mentioned
in section 4.6.3, these 'smoothed' data had also been treated
thermodynamically to obtain a $\Delta G^{\ominus}$ value which was compared with
the $\Delta G^{\ominus}$ value obtained from experimental data. The difference
was very small ($\Delta G^{\ominus}$ = 0.726 vs 0.708 kJ equiv.$^{-1}$), and therefore,
the substitution of 'smoothed' A_{s1} data for experimental A_{s1}
data should not affect the outcome of the Γ calculations. For
the two-anion system, however, such an interchangability between

experimental and 'smoothed' A_{s2} data cannot be taken for granted.

Even though the experimental and 'smoothed' A_{s2} data are quite

similar in magnitude (see table 5.1), discernible anomalies

exist in the resultant Γ values (table 5.1). Neither set of Γ

values seem to show a distinct relationship with A_{s2} values, or

more importantly, with the ionic strength. This meant that it

was not possible to choose between the two sets of Γ values, and

it was decided to continue with both sets, considering them to be

equally valid. The overall validity of these Γ data, and the

possible reasons for the discrepancies, are discussed later in

section 5.4.

The thermodynamic treatment was applied to pairs of 'real' Γ and

real A_{s2} values so that experimental individuality was retained,

and to pairs of 'smoothed' Γ and A_{s2} values so that the experi-

mental data becomes more orderly. The 'smoothed' Γ data were

used with real A_{s2} values so that some intermediate results could

be observed. As shown at the bottom of table 5.2, the results

from the different methods vary, more so for the 4th order than

the 3rd order because of the greater degree of 'flapping' arising

from poor edge definition. The six Kielland plots indicated

the following points. All the third and fourth order curves

fitted the available data equally well. The fourth order curve

from method 2 (i.e. 'real' Γ, real A_{s2} data) and all three

third order curves (figure 5.2.c) were opposite in shape to the

curves selected for the two Na/K single-anion systems. The

other two 4th order curves (methods 1 and 3) were similar in shape

to one another and to the curves from the Na/K single-anion

systems. Furthermore, the values of the sums of residuals for

methods 1 and 3 suggested that the 4th order was better. Since similar shaped Kielland plots are expected for all three Na/K systems (because K_c is invariant with the ionic strength; see section 5.2.2.), this enabled four plots to be discounted. The next step was to closely compare the two contending two-anion system curves against each of the two curves obtained for the Na/K single-anion exchanges. It was then found that the curve from method 3 ('smoothed' Γ, real results) was very much more similar in shape to the established curves, and therefore, this particular curve, and the resultant $\Delta G^{\ominus}$ value, were selected as being the most 'correct'. However, it is important to remember that the final results are quite sensitive to the values of Γ used (compare methods 2 and 3 where only the Γ data differ; table 5.2), and therefore, that the correctness of this choice is subject to the validity of Γ data. This example illustrates the need for adequate experimental results to fully define the curve at the edges so that the tendency to 'flap' is minimised.

The deficiency of experimental data in the $0 < A_c < 0.25$ region of the two silver systems is not so serious, because the orderly distributed points could be fitted extremely well with third order polynomials which are less susceptible to flapping. Fourth order polynomials gave no better fit with the curve shape un-changed (see figures 4.23 and 5.2.a), and the results remained essentially the same (table 5.2); therefore third order was sel-ected for each case on the basis of the values of the sums of residuals.

The validity of the methods used, and hence the final results, thus established, the crystal phase activity coefficients were examined in terms of the effect of polynomial order on the values.

The derived crystal phase coefficients are shown with all the other derived data in Appendix V for each system. These co-efficients were found to be fairly insensitive to the orders of polynomials. The differences in f_A and f_B values between differ-ent orders reflected the concurrent differences between $\Delta G^{\ominus}$ values.

An examination of the A_c vs f_A and f_B plots (figures 4.18-4.24) reveals the following points: the plots for the three Na/K systems are essentially identical (figures 4.20-4.22), thus also confirm-ing the method of treatment used for the two-anion system. The two silver systems show similar curves (figures 4.23 and 4.24) though the coefficients differ in magnitude. The two lithium systems show dissimilar curves (figures 4.18 and 4.19) but at $Li_c < 0.3$, the f_B values (for sodium and potassium, respectively) are nearly identical.

Considering $\Delta G^{\ominus}$ values next, it is seen that the values for the three Na/K equilibria differ by as much as 0.2 kJ equiv.$^{-1}$ (see table 4.4). However, knowing the sensitivity of the integral defined by the curve on small variations in the shape of the curve, these can be considered to be in good agreement. The differences between values are big only relative to the magni-tude of the values. As an example, if the Kielland plots for the two single-anion systems (figures 4.20 and 4.22) are exam-ined, the only significant difference between the curves is found at low K_c values where the curve for the system at the lower concentration falls off sharply. The difference in $\Delta G^{\ominus}$ values is primarily due to this. Since the end of the curve is defined better by the Na/K(0.1) system, it would seem that the

higher $\Delta G^{\ominus}$ value is more credible.

Comparing the final results (table 4.4) with published $\Delta G^{\ominus}$
values, for Na/K exchange Sherry gives 0.586±0.042[30], Rees et
al give -0.795[23] and Fletcher and Townsend give +0.397[114].
(All $\Delta G^{\ominus}$ values in kJ equiv^{-1}). These results illustrate the
variability of values associated with a system where the pref-
erence for one cation over another is very small.

The $\Delta G^{\ominus}$ value for the Na/Li system, 5.73, was very close to that
given by Rees et al, 5.648[23], and very near the lower limit of
Sherry's value of 6.694 ± 0.837[30]. The value for the Na/Ag
system, -13.555, compares reasonably well with those of Fletcher,
-11.27[18], and Sherry, -10.544 ± 0 .084[30].

The value for the K/Ag system, -13.057, is quite similar to that
for the Na/Ag system and reflects the similarity in behaviour of
the zeolite towards silver in the presence of sodium or potassium.
The K/Li exchange gave rise to an unusual shape in the isotherm
(figure 4.2) and the other plots (figure 4.19) in the 0.2 < Li$_c$<
0.5 region. The α-plot implies that the affinity for lithium
goes through a low and a high before finally dropping off at
high lithium loadings. Such a change in selectivity is also ob-
served in the Kielland plot (figure 4.19).

5.2.4. The Binary 'Triangle-rule'

The 'triangle-rule' has been used by several workers[61,66,116-118] to predict thermodynamic affinities for binary exchange
systems involving various pairs of exchanging ions. The basis of
the rule is to determine experimentally the standard free energy
of exchange for two related binary exchanges and then to predict
$\Delta G^{\ominus}$ for the third and conjugate binary system by arithmetical

manipulation of the standard free energy changes. For example if the binary equilibria given by (using univalent cations for simplicity)

$$A^+_{(s)} + B^+_{(c)} \rightleftharpoons A^+_{(c)} + B^+_{(s)} \qquad \ldots\ldots(5.9)$$

and

$$C^+_{(s)} + A^+_{(c)} \rightleftharpoons C^+_{(c)} + A^+_{(s)} \qquad \ldots\ldots(5.10)$$
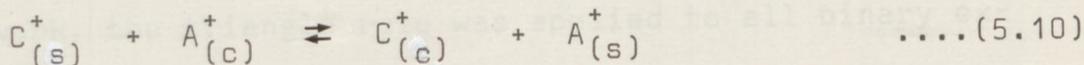
are known, and the respective standard free energy changes are $\Delta G^{\ominus}_1$, and $\Delta G^{\ominus}_2$, then the standard free energy change for the third equilibrium (obtained by adding the two equations above)

$$C^+_{(s)} + B^+_{(c)} \rightleftharpoons C^+_{(c)} + B^+_{(s)} \qquad \ldots\ldots(5.11)$$
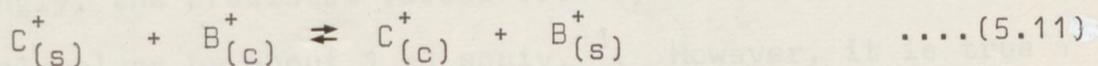
is

$$\Delta G^{\ominus}_3 = \Delta G^{\ominus}_1 + \Delta G^{\ominus}_2 \qquad \ldots\ldots(5.12)$$

The application of the rule is illustrated well by Barrer and Klinowski[66] who experimentally determined the thermodynamic parameters for the binary exchanges of the ions Cs^+, K^+, Li^+, NH^+_4, Ba^{2+}, Sr^{2+} and Ca^{2+} into the sodium and ammonium forms of synthetic mordenite, and then used pairs of equilibria to predict in each case the equilibrium constants and standard free energy changes for the related third exchange.

None of the predicted values, however, were verified experimentally. The thermodynamic affinities for the transition metals Mn^{2+}, Co^{2+}, Ni^{2+}, Cu^{2+} and Zn^{2+} in synthetic mordenite were predicted by Townsend[61] but experimental verification was not carried out.

There are however, several cases where the predicted $\Delta G^{\ominus}$ values have been compared with experimental values, and good agreement found. The work of Barrer and Munday[118] on the K/Li system in

zeolite KF and the work of Golden and Jenkins[116] on the Na/Li and Na/Co systems in synthetic mordenite are examples. Golden and Jenkins' studies confirmed the predicted values of $\Delta G^{\ominus}$ given by Townsend[61] for the Na/Co-MOR system and by Barrer and Klinowski for the Na/Li-MOR system[66].

In this work, the triangle rule was applied to all binary exchanges, and in all possible cases, the predicted values were compared to the experimental counterparts. The results are given in table 5.3.

Surprisingly, the predicted values usually differ from the experimental values by about 1 kJ equiv.$^{-1}$. However, it is true that since the predicted values are derived from experimental data, an error in any of these could significantly affect the predictions. If, for example, Fltecher's value of $\Delta G^{\ominus} = -11.27$ for Ag/Na exchange[18] was used, the predictions for Ag/K and K/Na exchanges would be -11.827 and +1.787 kJ equiv.$^{-1}$ respectively, a difference of 2.3 kJ. Errors in prediction will be maximised when the system examined shows little affinity for one of the ions over the other, especially if the data used for predictions are from systems displaying a high selectivity. Thus the K/Na-X system (table 5.3) shows a very marked difference between measured and predicted values. This discrepancy should be compared with predicted and measured values for the Li/Na-X or Li/K-X systems, both of which displayed a marked selectivity for one ion. The discrepancies here (in percentage terms) are smaller.

When two systems displaying high selectivity for one ion over another are used to predict a third which shows even higher selectivity for one component, agreement can be very good.

Thus compare predictions for the Ag/Li-X exchange obtained
using the Ag/Na and Li/Na pairs with the prediction for the same
exchange using the Ag/K and Li/K pairs. Agreement is excellent
(table 5.3).

In conclusion, it appears that the triangle rule should only be
used with very great caution, and the agreement between Golden
and Jenkins' experimental data[118] and the predictions of either
Townsend[?] or Barrer and Klinowski[86] could be coincidental.
Since in addition the triangle rule can only yield an estimate
of overall affinities[114] rather than selectivity as a function
of composition the rule is of little utility beyond that of
establishing the validity of a thermodynamic model[114].

5.3. TERNARY EXCHANGE

5.3.1. Ternary Isotherms

All the ternary isotherms are shown in figures 4.9 - 4.17. While
the isotherms depicted in this form can show the number and
spread of the experimental points one cannot determine easily
... information regarding selectivity trends from isotherms
depicted in this manner. It is interesting to note the marked
contrast between the Na/K/Li system and the Na/K/Ag isotherm.
Considering first the Na/K/Li isotherms (figures 4.9,4.10,4.14
and 4.17) if a line were to be drawn through all the crystal phase
compositions arising from each set of ternary solutions used (see
section 3.7), the points resulting from K-X and Na-X show that
the selectivity of the zeolite for sodium or potassium over lith-
ium is ... such a five-fold or lower concentration, reducing to
... times at the higher concentrations. The points result-
ing from the use of Li-X as the starting material show in add-
ition, that there is a very slight preference for sodium over
potassium.

TABLE 5.3. Experimental and Predicted Values of Binary K_a and $\Delta G^\ominus$ (kJ equiv^{-1})

Binary System	Experimental K_a	Experimental $\Delta G^\ominus$ (kJ equiv.$^{-1}$)	Triangle rule K_a	Triangle rule $\Delta G^\ominus$ (kJ equiv.$^{-1}$)
Li/Na-X(0.1)	0.099	+5.730	0.062	+6.873
Li/K-X(0.1)	0.083	+6.165	0.132	+5.022
K/Na-X(0.1)	0.752	+0.708	1.192	-0.435
K/Na-X(0.04) two-anions	0.735	+0.762	0.818	-0.498
K/Na-X(0.04)	0.799	+0.557		
Ag/K-X(0.04)	194.430	-13.057	297.644	-14.112
Ag/Na-X(0.04)	237.687	-13.555	155.285	-12.500
(i)Ag/Li-X(from Na)	-	-	2401.46	-19.285
(ii)Ag/Li-X(from K)	-	-	2341.16	-19.222

Thus compare predictions for the Ag/Li-X exchange obtained using the Ag/Na and Li/Na pairs with the prediction for the same exchange using the Ag/K and Li/K pairs. Agreement is excellent (table 5.3).

In conclusion, it appears that the triangle rule should only be used with very great caution, and the agreement between Golden and Jenkins' experimental data[116] and the predictions of either Townsend[61] or Barrer and Klinowski[66] could be coincidental. Since in addition the triangle rule can only yield an estimate of overall affinities[114] rather than selectivity as a function of composition, the rule is of little utility beyond that of establishing the validity of a thermodynamic model[114].

5.3. TERNARY EXCHANGE

5.3.1. Ternary Isotherms

All the ternary isotherms are shown in figures 4.9 - 4.17. While the isotherms depicted in this form can show the number and spread of the experimental points, one cannot determine easily much information regarding selectivity trends from isotherms depicted in this manner. It is interesting to note the marked contrast between the Na/K/Li system and the Na/K/Ag isotherm. Considering first the Na/K/Li isotherms (figures 4.9,4.10,4.14 and 4.15) if a line were to be drawn through all the crystal phase compositions arising from each set of primary solutions used (see section 3.7), the points resulting from K-X and Na-X show that the selectivity of the zeolite for sodium or potassium over lith-ium is as much as five-fold at lower concentrations, reducing to about 3½ times at the higher concentrations. The points result-ing from the use of Li-X as the starting material, show in add-ition, that there is a very slight preference for sodium over potassium.

The similarity between the long-term and 6-day isotherms (i.e. at 0.04 equiv.dm^{-3} concentration - see figures 4.15 and 4.14), is highly significant in that it shows that the prolonged contact with an aqueous solution did not (surprisingly) cause noticeable breakdown of the zeolite structure. This consistency in results (Appendix VI) is confirmed also by the cation balance work. Close examination of the two isotherms reveals that the only important difference between them is caused by a small shift of points arising from Li-X towards the sodium side of the triangle. These two isotherms show, therefore, that (in this system at least), hydrolysis is not a time-related phenomenon. Recent parallel studies by co-workers[113] have shown that there is more reason to accept that hydrolysis is a rapid process, resulting in the release of a small quantity of alkali metal in solution and a small degree of hydronium exchange. Further hydrolysis requires fresh solution, which disturbs the equilibrium.

Figure 4.17 shows the results obtained for the Na/K/Li system when three anions also were present (i.e. results for the Na/K/Li system with nitrate, sulphate and ferricyanide ions). These studies were carried out at total solution concentrations of 0.04 and 0.1 equiv. dm^{-3}. The equilibrium compositions of the corresponding single-anion system are also shown, and from the proximity of these points it is immediately apparent that the presence of the extra anions (i.e. sulphate and ferricyanide ions) has little effect on the equilibria considered. This matter is discussed further later in terms of current developments in understanding of the solution phase activity corrections[86,87] - see section 5.4.3.

Considering the isotherm for the very different Na/K/Ag ternary exchange (figures 4.11 and 4.12), the contrast from the Na/K/Li system is immediately seen. Comparison of corresponding solid phase (figure 4.11) and solution phase (figure 4.12) points shows the enormous affinity exhibited by the zeolite for silver over sodium and potassium. Usually very little silver remained in the solution phase after exchange equilibrium had taken place. The points where the solution silver composition exceeded 10% were only obtained by using exchange solutions containing amounts of silver greater than the exchange capacity of the amount of zeolite used.

The higher selectivity for silver resulted in several analytical difficulties. For equilibria where the crystal phase silver composition was relatively low (less than 25%), the corresponding solution phase silver composition was too low to be detected by atomic absorption spectroscopy. (This meant that the data that could be used in the computer treatment was limited). Even where the crystal phase silver composition increased up to as much as 80%, the corrsponding solution phase contained less than 4% silver, and for the cases where the solution phase silver composition was greater than 20%, the corresponding crystal phase contained >92% silver, imposing some problems in the determination of potassium and sodium (see Appendix VI for complete compositional data). A 'pseudo-binary' isotherm was drawn where the potassium and sodium ions were treated jointly as the outgoing ion. The curve obtained resembled the K/Ag and Na/Ag binary isotherms (figures 4.23 and 4.24) very closely, showing that the high selectivity the zeolite displayed for silver dominated all other effects in the ternary system.

5.3.2. Fitting of Ternary Data using Polynomials

As emphasised earlier, the thermodynamic treatment of ternary equilibria and particularly the fitting procedures are more complex than the binary treatment. The initial stage involves the feeding in of equilibrium data (A_c, B_c, A_s, B_s), the appropriate valences and the Debye-Hückel parameters a and b for the respective salts in solution. From these, the three mass action quotients related to the three ternary equilibria (described by equation (2.60) et al), are calculated, followed by the calculation of Γ values for the solution. (The solution phase treatment is discussed later in section 5.4). The appropriate mass action quotients and solution phase correction ratios then yield the required ratios of corrected selectivity quotients K_{c3}/K_{c1} and K_{c3}/K_{c2}, which are evaluated for each equilibrium point.

The complex least-squares method fitting routine commences at this stage. Two polynomial equations were used to represent the relationship between the crystal phase composition (A_c, B_c) and the values of $\ln(K_{c3}/K_{c1})$ and $\ln(K_{c3}/K_{c2})$ in the manner described in section 4.4.2, and for each order of polynomial used, a value for the sum of residuals, R was obtained.

The next stage involved the integration procedures described in sections 2.2.4 and 2.2.6 to evaluate the crystal phase activity coefficients and the thermodynamic equilibrium constants. Finally, the appropriate standard free energies for each ternary exchange reaction were calculated.

The means of choosing the 'best' order of polynomial equation which describes each relationship can be more subtle than in a

- 216 -

binary case and the dangers of a "subjective" choice are therefore greater. The computer program printed out a sum of residuals for each order together with a list of $\ln(K_c$ ratio) values calculated from experimental data against $\ln(K_c$ ratio) values predicted from the corresponding polynomial equation. A visual inspection of this list of $\ln(K_c$ ratio) values allows any obvious inconsistencies to be spotted, and the corresponding order to be disregarded. The next step in the treatment was to construct contours (figures 5.3 - 5.31) which describe the variance of predicted $\ln(K_c$ ratio) values with the crystal phase composition. This was first done for one order of polynomial equation for each of the two K_{c3}/K_{c1} and K_{c3}/K_{c2} ratios, by feeding in the appropriate coefficients of the polynomial equation into the computer. The equations were then solved to obtain predicted K_{c3}/K_{c1} and K_{c3}/K_{c2} values for different values of A_c by varying A_c in increments of 0.02 from 0.02 to 0.98 (thus avoiding the computer-incompatible zero values), and for each of these increments, varying B_c in increments of 0.02 from 0 to $(1-A_c)$, thus defining C_c also. Thus the appropriate $\ln(K_c$ ratio) value was calculated for each composition as defined by A_c, B_c. The program next entailed taking the highest and lowest values of these predicted $\ln(K_c$ ratio) values, and by dividing by ten (for convenience) the difference between the highest and lowest values, establishing the range of $\ln(K_c$ ratio) values in terms of eleven equi-distant contour values or steps. The particular order of polynomial used to establish these steps was usually three. Thus for example, if the highest and lowest values were 20 and 9 respectively, then the eleven steps established would vary by 1.1.

Once the steps were known, the whole program was repeated, this time for each of the respective sets of polynomial orders, listing *only* the $\ln(K_c$ ratio)values that fell within ±0.03 of the aforementioned contour values, together with the corresponding A_c, B_c values.

In this way, a list of predicted $\ln(K_c$ ratio) values against crystal phase composition A_c, B_c, divided into sub-sections defined by the steps, was obtained. These crystal phase data within each sub-section (i.e. corresponding to one of the contour values) were used to construct the respective contour (for the value of that step) on a triangular diagram (see figures 5.3 - 5.12). Theoretically, eleven contours should appear on the triangle each time, but on many occasions the number obtained was less. This was because the high and low values selected for order three were quite dissimilar to those from other orders, causing some contours to fall outside the scope of the triangle, and thus emphasising the need to find the right criteria to apply in making the ultimate choice as to which was the 'best-fit' polynomial. It must be remembered that the contours are a visual representation of mathematical equations which sometimes fall partially or wholly within the area defined by the triangle. Since the variance of the $\ln(K_c$ ratio) values were shown in terms of eleven arbitrary contours, the absence of some contours from the triangle in some cases has no significance except to note that the $\ln(K_c$ ratio) values for that polynomial order differ much in magnitude from those for order three at the high and/or low end of the values.

The contour diagrams are representations of ratios of corrected

selectivity quotients, and information regarding the variation of the (corrected) selectivity for one cation over another (say 3 over 2 or 3 over 1) against the crystal phase composition can be obtained from them. Essentially, the contour diagram (but *not* individual contours) is the ternary analogue to the binary Kielland diagram. Obviously, the complexity of the contours in-creases with increasing order of polynomial equation (compare figures 5.3 - 5.7 and 5.8 - 5.12). This is merely due to the increased flexibility of the equations and naturally has not any necessary physical significance.

The next task was to attempt to plot contour diagrams 'by eye' also. The first step was to allocate the original $\ln(K_c \text{ ratio})$ values (calculated from experimental results, prior to the poly-nomial fitting procedures) into twelve bands. This was done manually by designating a different symbol to the $\ln(K_c \text{ ratio})$ values that fell *between* the steps defined earlier; i.e. the bands were defined by the values in-between the steps, with two extra bands lying above the highest value and below the lowest value. Appropriate distinguishing symbols were then used to plot the corresponding experimental crystal phase compositions A_c, B_c on a triangular diagram. Since the points depicted by different symbols were situated *between* the appropriate contour lines, these contour lines were drawn in 'by eye', banding to-gether all the points with the same symbol. In this way, all the experimental (crystal phase) points are allocated into a contour diagram, based on the corresponding experimental $\ln(K_c \text{ ratio})$ values. This operation was carried out for both $\ln(K_c \text{ ratio})$ sets considered, i.e. K_{c3}/K_{c1} and K_{c3}/K_{c2}, and therefore two such 'by eye' contour diagrams were obtained for each ternary system.

(figures 5.13 and 5.14).

All crystal points were plotted with the appropriate symbols, but
a few such points (15 out of 158 for the main Na/K/Li system)
fell into a band which was inconsistent with its immediate
neighbours. This kind of displacement mostly required changing
of the band symbol to that of an adjacent band as it was reason-
able to expect that the discrepancy was caused by experimental
error. There were only three points (out of the 158) which fell
widely off the appropriate bands. It is obvious that in order to
define the shapes of the contour lines adequately, a large number
of (experimental) points are necessary on the triangular diagrams.
For the main Na/K/Li system the 79 experimental points for each
phase were sufficient for two unambiguous contour diagrams, but
for the other three ternary studies, the 30 or so points fell far
short of the required minimum number of points.

The resulting 'by eye' contour plots could then be compared with
best-fit contour diagrams obtained by computer. Any similarity
between the 'by eye' diagram and a particular computer plot was
important in deciding which order of polynomial equation was most
appropriate. Usually however, the differences between the computer
diagrams for adjacent orders, particularly between 3,4 and 5 were
very small. Some of the contour diagrams have been colour coded
(figures 5.13 - 5.20) in order to facilitate the comparisons.

In order to decrease the obvious marked subjectivity of the
procedures adopted so far, it was decided next to introduce some
binary data. The rationale for this was the need to constrain
the polynomials by using anchor points. As described earlier in
section 5.2.3, when polynomial curve fitting procedures were

applied to a binary system, a certain amount of 'flapping' occurred as the polynomial order was increased where insufficient data was available to fully define the Kielland plot at each end (i.e. $A_c \to 0$ or $A_c \to 1$). The amount of 'flapping', particularly for higher order polynomials increases enormously for a ternary system because of the extra dimension associated with surface fitting. The problem is now serious along each edge of the triangular diagram, and particularly at the apices (which correspond to the ends of binary polynomials used to fit binary exchange data). 'Flapping' can be minimised first by having data points well spread over the surface of the triangle, but also in order to reduce the 'flapping' at the edges of the triangle, it is obviously sensible to include corresponding binary results where possible. As outlined earlier in section 2.2.2, there is some similarity between the definitions of the binary and ternary thermodynamic parameters. Considering the definitions of the corrected selectivity quotients, for a ternary system the useful ratios are (see equations (2.95)-(2.97)).

$$K_{c3}/K_{c1} = (a_A . C_c / a_C . A_c)^3 \qquad \ldots \ldots (5.13)$$

and

$$K_{c3}/K_{c2} = (a_B . C_c / a_C . B_c)^3 \qquad \ldots \ldots (5.14)$$

For the three conjugate binary systems,

$$K_{c3,1} = a_A . C_c / a_C . A_c \qquad \ldots \ldots (5.15)$$

$$K_{c3,2} = a_B . C_c / a_C . B_c \qquad \ldots \ldots (5.16)$$

and

$$K_{c2,1} = a_A . B_c / a_B . A_c \qquad \ldots \ldots (5.17)$$

It is apparent that when equations (5.15) and (5.16) are raised
to the power of three, they become formally compatible with the
ternary equations (5.13) and (5.14) respectively. (Note that
this compatibility is *only* formal in nature. At first glance
it would appear that (for example) eqns.(5.13)and (5.15)lead to
the relationship $K_{c3}/K_{c1} = (K_{c3,1})^3$. This is *not* correct for two
reasons. Firstly, in eqn.(5.13) $A_c = 1-B_c-C_c$, whereas in (5.15)
$A_c = 1-C_c$. Secondly, the values of a_A in each of the two equations
can be different, since although $a_A = m_A \cdot \gamma_A$ in both cases, the
value of γ_A is a function of interactions involving only *two*
cations in eqn.(5.15) but *three* cations in eqn.(5.13)).

Thus when the fitting procedure was carried out on either of the
two K_c ratios (say $\ln(K_{c3}/K_{c1})$), then *one* of the three sides of
the triangle could be fixed by using corresponding binary data.
This therefore enables additional constraint to be placed on the
polynomial at that edge of the triangle, resulting in less over-
all 'flapping'.

The binary data was obtained in the required (cubed) form very
easily by modifying the appropriate computer program. Adding
these data to the mainstream ternary data too was accomplished
quite easily just before the fitting procedure. The fitting pro-
cedure remained unchanged otherwise because the computer treated
the cubed binary data as ternary data.

The outcome of this improvement was of significance. For the
contour diagrams, visually observable differences resulted for
higher orders (see figures 5.5 - 5.7 vs 5.15-5.17 and 5.10 - 5.12
vs 5.18-5.20), but the main differences lay particularly with
the ternary systems which had an insufficient amount of experi-

- 222 -

mental data to carry out the treatment in its original form.

These aspects are fully discussed in the next section. The
ternary compatible form of binary data were also used to define
one of the edges of each 'by eye' diagram (figures 5.13 and 5.14),
thereby improving them slightly.

Contour diagrams plotted by the computer were obtained for all
four ternary systems studied but the 'by eye' contours could not
be unambiguously drawn for the three smaller systems because the
limited number of ternary experimental points (30-33 each) could
not define the contours adequately. Therefore, for these three
systems, a visual confirmation of the 'correct' contour diagrams
was not carried out. Selection of the 'correct' order was made
on a quantitative basis as discussed in the next section. Only
the computer predicted contour diagrams for the *chosen* orders are
shown (figures 5.21 - 5.28). Two attempted 'by eye' diagrams for
the Na/K/Ag system (figures 5.30 and 5.31) are also given.

There were two ternary studies to which the thermodynamic treat-
ment could not be applied because the experimental data was not
sufficient. These two, the variable solution concentration study
and the three-anion study, were carried out primarily to establish
the applicability and limitations of the Fletcher-Townsend thermo-
dynamic model. The results from the three-anion study were found
to be similar to those from the corresponding single anion work
(figure 4.17 and section 5.3.1) and had there been sufficient
equilibrium data, the thermodynamic model could have been applied.
The complexities which arise from the very involved solution
phase corrections are further discussed in section 5.4.3.

- 223 -

5.3.3. Thermodynamic Data

The results for each ternary system *viz* the changes in standard free energy, thermodynamic equilibrium constants and ratios of solution phase activity coefficients (constant for univalent cases) were shown previously in table 4.5. The validity of these results needs to be discussed at this stage, before any comparisons and/or conclusions are drawn.

As discussed previously, the computer techniques used can influence the results at the polynomial 'fitting' stage for both binary (section 5.2.3) and ternary systems (section 5.3.2).

It was established in the previous section that polynomial 'flapping' can be reduced by having a large number of experimental points spread over the whole of the triangle, and that a more significant reduction can be achieved for each polynomial by fixing *one* of the edges of the triangle by the use of binary data. Since the degree of 'flapping' increases with the order of the polynomial, it is useful to compare the results and sums of residuals for each order by treating all four ternary systems with and without the binary data. These results are given in tables 5.4 - 5.7, and at the bottom of each table, the final combination of orders which were preferred, are shown, together with the corresponding final results.

Considering first the effect of using ternary data only (table 5.4(i)),the values of $\Delta G^{\ominus}$ appear to vary up and down between different orders. The variation is quite pronounced for $\Delta G_1^{\ominus}$ (relating to the $2Na_s \rightarrow 2Na_c$ equilibrium) and $\Delta G_2^{\ominus}$ ($2K_s \rightarrow 2K_c$ equilibrium). Thus, $\Delta G_1^{\ominus}$ moves from -6.2 down to -8.2 and then up to -6.4 between orders 1 to 5; $\Delta G_2^{\ominus}$ moves up initially and then moves

TABLE 5.4. <u>Ternary Treatment for Na/K/Li(0.1) System</u>

(i) 'Ternary only' data.

Order used	Sum of residuals K_{c3}/K_{c1}	K_{c3}/K_{c2}	$\Delta G_1^{\ominus}$	$\Delta G_2^{\ominus}$ (kJ per 2 equiv.)	$\Delta G_3^{\ominus}$
1	.62682	.65988	-6.237	-3.228	+9.465
2	.60861	.49258	-6.449	-2.868	+9.316
3	.52930	.49300	-8.166	-1.942	+10.107
4	.52807	.45907	-7.244	-2.637	+9.880
5	.53338	.44825	-6.360	-3.657	+10.016

(ii) 'Ternary + binary' data

Order used	Sum of residuals K_{c3}/K_{c1}	K_{c3}/K_{c2}	$\Delta G_1^{\ominus}$	$\Delta G_2^{\ominus}$ (kJ per 2 equiv)	$\Delta G_3^{\ominus}$
1	.64479	.77037	-6.064	-4.292	+10.356
2	.62831	.68854	-6.052	-4.535	+10.588
3	.55233	.67180	-6.306	-4.642	+10.948
4	.54427	.60578	-5.998	-5.041	+11.039
5	.54912	.54954	-5.875	-5.253	+11.128
4,5*	.54427	.54954	-5.898	-5.242	+11.139

TABLE 5.5. Ternary Treatment for Na/K/Li(0.04) System

(i) 'Ternary only' data

Order used	Sum of residuals K_{c3}/K_{c1}	K_{c3}/K_{c2}	$\Delta G_1^{\ominus}$	$\Delta G_2^{\ominus}$ (kJ per 2 equiv.)	$\Delta G_3^{\ominus}$
1	.36777	.41926	-4.990	-5.238	+10.227
2	.35984	.40930	-4.723	-1.939	+6.662
3	.21050	.29477	+11.281	-29.240	+17.959
4	.20040	.27099	+1.207	-38.961	+37.754
5	.12890	.28130	+20.317	-65.232	+44.914

(ii) 'Ternary + binary' data

Order used	Sum of residuals K_{c3}/K_{c1}	K_{c3}/K_{c2}	$\Delta G_1^{\ominus}$	$\Delta G_2^{\ominus}$ (kJ per 2 equiv.)	$\Delta G_3^{\ominus}$
1	.48293	.50134	-5.559	-5.404	+10.962
2	.52703	.71509	-5.611	-5.363	+10.974
3	.29996	.68352	-5.678	-5.512	+11.275
4	.28897	.71683	-5.633	-5.725	+11.359
5	.29332	.74080	-5.632	-5.753	+11.385
4,1*	.28897	.50134	-5.873	-5.246	+11.119

TABLE 5.6. Ternary Treatment for Na/K/Li (long term) System

(i) 'Ternary only' data

Order used	Sum of residuals K_{c3}/K_{c1}	K_{c3}/K_{c2}	$\Delta G_1^{\ominus}$	$\Delta G_2^{\ominus}$ (kJ per 2 equiv.)	$\Delta G_3^{\ominus}$
1	.37598	.35227	-5.609	-4.456	+10.065
2	.33091	.28151	-8.102	+4.021	+4.081
3	.27765	.28608	-16.162	+15.827	+0.335
4	.20742	.23074	-31.730	+33.660	-1.930
5	.20505	.22129	-53.786	+74.620	-20.839

(ii) 'Ternary + binary' data

Order used	Sum of residuals K_{c3}/K_{c1}	K_{c3}/K_{c2}	$\Delta G_1^{\ominus}$	$\Delta G_2^{\ominus}$ (kJ per 2 equiv.)	$\Delta G_3^{\ominus}$
1	.46226	.47580	-5.777	-5.248	+11.025
2	.51907	.68405	-5.543	-5.493	+11.037
3	.30003	.63818	-5.728	-5.605	+11.333
4	.31360	.61012	-5.716	-5.617	+11.332
5	.32741	.64397	-5.682	-5.684	+11.366
3,1*	.30003	.47580	-5.949	-5.162	+11.112

TABLE 5.7. <u>Ternary Treatment for Na/K/Ag System</u>

(i) 'Ternary only' data

Order used	Sum of residuals K_{c3}/K_{c1}	K_{c3}/K_{c2}	$\Delta G_1^{\ominus}$	$\Delta G_2^{\ominus}$ (kJ per 2 equiv.)	$\Delta G_3^{\ominus}$
1	1.3600	1.1304	+16.024	+10.128	−26.152
2	1.3508	1.1058	+15.608	+11.801	−27.409
3	1.2715	1.0868	+19.832	+14.923	−34.754
4	1.1553	1.1085	−19.412	+32.395	−12.983
5	1.0114	1.0185	+234.67	−149.56	−85.113

(ii) 'Ternary + binary' data

Order used	Sum of residuals K_{c3}/K_{c1}	K_{c3}/K_{c2}	$\Delta G_1^{\ominus}$	$\Delta G_2^{\ominus}$ (kJ per 2 equiv.)	$\Delta G_3^{\ominus}$
1	1.4106	1.1517	+14.305	+11.486	−25.791
2	1.3641	1.1302	+14.126	+12.550	−26.676
3	1.3080	1.1432	+14.611	+12.895	−27.506
4*	1.2967	1.1206	+12.833	+13.116	−24.949
5	1.1820	1.1064	+24.376	+5.615	−29.991
3,2*	1.3080	1.1302	+15.002	+12.111	−27.114

down while $\Delta G_3^{\ominus}$ shows a very small overall increase. Orders 1,2 and 5 seem to give similar results but orders 3 and 4 show significant differences. This sort of variation of results should be expected because changing orders allows the polynomials to change direction. This in turn would cause the area defined by each polynomial curve to vary in magnitude. Since the values of K_a are dependent on the *difference* between two such areas, the relationship between the orders of polynomials and the resultant $\Delta G^{\ominus}$ values are quite complicated.

When the results obtained from the 'ternary + binary' data are considered (table 5.4.(ii)), these fluctuations in $\Delta G^{\ominus}$ values reduced markedly, and the results between orders appear to be much more close together in magnitude.

Comparisons of the sums of residuals show that the lowest values are seen for orders 4 and 5 for the ratios $\ln K_{c3}/K_{c1}$ and $\ln K_{c3}/K_{c2}$ respectively, and this remains true whether the binary data are added or not. The magnitudes of the sums of residuals seem to indicate that a lower value is usually obtained when only the ternary data are used (0.53 vs 0.55 for order 3, K_{c3}/K_{c1} and 0.46 vs 0.61 for order 4, K_{c3}/K_{c2}). If an overall low value was selected, then (surprisingly) the 'best fits' would seem to stem from the 'ternary only' data. This point is raised again after the results of the other three ternary systems have also been discussed.

Considering the two Na/K/Li(0.04) systems next (tables 5.5 and 5.6), the results emphatically indicate that the addition

of binary data has a great restraining effect on the $\Delta G^{\ominus}$
values. Bearing in mind that only 30 experimental points were
available for each of these two systems, and that these points
were not spread over all of the triangle (see figures 4.14
and 4.15), a large amount of 'flapping' was to be expected.
This was proved to be the case when only the ternary data
were utilised, particularly at the higher orders where, for
example, $\Delta G^{\ominus}$ values of -65.2, +37.8 and +74.62 kJ equiv.$^{-1}$
are seen! However, when the binary data were included in the
treatment, the $\Delta G^{\ominus}$ values reverted to the more reasonable
values shown. In an ideal case, where polynomial 'flapping'
has been reduced to near zero, the variation in $\Delta G^{\ominus}$ values
between orders should also be extremely small. Therefore, the
attainment of reasonably consistent $\Delta G^{\ominus}$ values for different
orders is conclusive evidence that the inclusion of appropriate
binary data can control the 'flapping' sufficiently to allow
an accurate integration to be carried out, *if* it can be proved
that the final results obtained in this manner were correct.

For the two systems discussed here, sufficient experimental
data were not available to obtain 'by eye' contour diagrams.
Therefore, visual confirmation of orders could not be carried
out, and the 'correct' orders were chosen on the basis of the
lowest sums of residuals. The contour diagrams associated
with the selected orders, 4 and 1 for the 6-day study, and 3
and 1 for the long-term study, are shown in figures 5.21-5.24,
respectively. Comparison of these with their Na/K/Li (0.1)
counterparts, figures 5.8, 5.15 and 5.16 show that the simi-
larities are very good, and this would be expected for a

ternary system made up of the same cations. More definitive

confirmation of the treatment comes when the final results of

all three Na/K/Li systems are compared. These results are

fully discussed later.

While the appropriate 'correct' orders were selected on the

basis of the lowest sums of residuals arising from the 'ternary

and binary' data, the results on tables 5.5 and 5.6 indicate

that the corresponding 'ternary only' sums of residuals remain

lower still. When this phenomenon was noticed earlier for the

Na/K/Li (0.1) case, there was some doubt as to whether the

better 'fits' were obtained with or without the appropriate

binary data. The two Na/K/Li (0.04) systems, however, show

conclusively that the inclusion of binary data indeed stabil-

ises each surface fitting operation by curbing the random

'flapping' behaviour; therefore an overall better fit must be

obtained by using the 'ternary + binary' data. This emphasises

the importance of not relying too heavily on the absolute

magnitudes of sums of residuals. It is well-known and obvious

that curve fitting data where y is only a function of x can

only be meaningful if a substantial number of experimental

points in excess of the chosen polynomial order are available;

for the fitting of a surface, where $y = f(x,z)$, a very large

set of experimental points are essential.

Finally, considering the Na/K/Ag (0.04) system (table 5.7), the

'ternary + binary' data give consistent results for orders 1 to

4, but for order 5, a very large step change is seen for $\Delta G^{\ominus}_1$

(from about +14 to +24.4)and $\Delta G^{\ominus}_2$ (from about +12.5 to +5.6).

For the 'ternary only' case, the 5th order brings about very

large jumps for all three $\Delta G^{\ominus}$ values, yet this again gives

the lowest values for the sums of residuals, again underlining

the danger of relying too heavily on these functions. In

contrast, close inspection of table 5.7 reveals that the values

of the sums of residuals for orders 2,3 and 4 are quite close

to one another. For K_{c3}/K_{c1}, the values for orders 3 and 4

were 1.31 and 1.30 respectively, and for K_{c3}/K_{c2}, the values

for orders 2,3 and 4 were 1.13, 1.14 and 1.12 respectively.

Because of the very close proximity of these values, it was

decided to consider an orders 3,2 treatment also. The results

from the latter treatment are seen to be fairly similar to

the 4,4 case but the suspect results from the 5,5 treatment

are quite different.

Unfortunately, the 'by eye' contour diagrams could not help

much towards choosing the 'correct' order in this case. The

diagram for $\ln(K_{c3}/K_{c1})$, seen in figures 5.30, is similar to

the diagrams for both 3rd and 4th order (figures 5.25 and 5.26),

very slightly nearer order 4, but a reasonable 'by eye' diagram

for $\ln(K_{c3}/K_{c2})$ could not be obtained at all due to the lack

of sufficient equilibrium data points. The available points

and the demarcation lines are shown in figure 5.31 but an in-

spection of the computer diagrams (figures 5.28 and 5.29)

shows that the 'by eye' diagram can be drawn to look like

either computer diagram. Therefore, any meaningful comparison

of these diagrams was not possible.

The unreliable nature of an order 5 fit is seen clearly from

figure 5.27 (for K_{c3}/K_{c1}) where the contours differ *markedly*

from the order 4 counterpart (figure 5.26). Similar major

differences were observed for K_{c3}/K_{c2} between orders 4 and 5.

"Chemical" considerations are not helpful either in finally
deciding which is the best order to choose in this case.
Thus a combined 3,2 treatment gave a slightly higher $\Delta G_1^\ominus$
value which was incompatible with the binary results (which
imply that sodium and potassium behave similarly in the presence
of silver), but the actual ternary equilibrium data, in con-
trast, do indicate that potassium is very slightly preferred
over sodium by the Ag-X zeolite. This is apparent from
figure 4.11 (showing the crystal phase composition) where the
sodium uptake into K-X is seen to be smaller than the potassium
uptake into Na-X. This should therefore give a slightly
higher $\Delta G_1^\ominus$ value, as observed for orders 3,2. In the end it
was therefore decided to show both sets of results, as the
actual final results probably lie in-between the values of
the 4,4 and 3,2 polynomial fits.

The contour diagrams have so far been used to establish the
best fit for a particular (ternary) $\ln(K_c$ ratio) in a manner
similar to the use of the binary Kielland plot. The physical
significance of the binary Kielland plot is that it indicates
how the corrected selectivity for a particular cation varies
with the composition of the same cation in the zeolite. It is
therefore worth looking at the ternary contour diagram to see
if similar information can be discerned.

To be precise, the $\ln K_{c3}/K_{c1}$ and $\ln K_{c3}/K_{c2}$ contour diagrams
allow trends in the corrected selectivity for one cation over
just *one* other cation (i.e. ignoring the presence of the

third cation) against crystal phase composition to be dis-
cerned. Thus, the K_c ratios are 'pseudo-binary' coefficients.
Contours which are close together show that this 'selectivity'
changes rapidly and contours which are far apart show the
opposite. In order to quantify these observations, the two
ratios used in the treatment have to be examined. Thus
$\ln K_{c3}/K_{c1}$ indicates the corrected selectivity for lithium or
silver over sodium. For lithium, the K_{c3}/K_{c1} ratio would
have values of less than 1, and for silver, the values would
be greater than one. A similar rationale applies to the
K_{c3}/K_{c2} ratio. The usage of natural logarithms decreases the
magnitude of this difference in 'selectivity' but the signs of
the $\ln(K_c \text{ratio})$ values, plus the relative magnitudes (see
Appendix VI), corroborate the observed selectivity trends for
silver and lithium.

In section 5.4.3 it is shown that the solution phase correct-
ions necessary for the ternary systems studied in this project
are significant. Therefore, it is dangerous to draw conclusions
from the contour diagrams in terms of the selectivity depicted
by them. The contour diagrams have therefore been used essen-
tially as a guide to choosing the order of polynomial for a
particular ratio of K_c terms.

5.4. SOLUTION PHASE ACTIVITY COEFFICIENTS

Solution phase corrections were carried out in the manner
described in sections 2.1.2, 2.1.3 and 2.1.5. The activity
coefficients correct for the deviation of the concentrations
from ideality, which usually result from the ion-ion inter-

actions in real solutions.

For the ion exchange process, the standard states for the
solution phase are taken as the hypothetical ideal molal
(concentration mol kg^{-1}) solutions[77,78] (section 2.1.2).
In an ideal solution therefore, the activity coefficients would
be all equal to unity (i.e. $\gamma_A = \gamma_B = \gamma_C = 1$) and the approp-
riate binary or ternary Γ ratios, defined in equations (2.18),
(2.61), (2.130) and (2.131), would also be equal to unity.
Therefore, deviations of Γ values from unity reflect the
degree of non-ideality that occurs in the solution phase.
Multiplying the mass action quotient by the correct Γ value
gives the quotient K_c:

$$K_c = K_m \cdot \Gamma \qquad \qquad \dots(5.18)$$

All values for Γ functions obtained from the thermodynamic
treatment are shown in tables 4.4 , 4.5, 5.1 and 5.9. For
binary and ternary systems where *all* ions were uni-valent
(i.e. both cations *and* anions), these Γ values were constant.
This is because the ionic strength is invariant as the rela-
tive concentrations of the different ions in solution are
varied at a *constant* total solution concentration (mostly
0.04 or 0.1 equiv. dm^{-3}).

5.4.1. Binary Systems

Considering first the binary results where all ions are uni-
valent (table 4.4) it is obvious that the solution phase
corrections are very small for the systems studied. Even the
higher concentration systems containing sodium show a

correction only slightly greater than 3% while the K/Li system is less (1.7%). For the lower concentrations, the Γ values are lower as expected with a maximum of 1.7% for the Na/Ag system and a minimum of 0.4% for the K/Ag system. For the two-anion system (table 5.1), the correction is very much larger than the single-anion cases, with Γ values varying from 0.772 to 0.917. Neglecting the solution phase correction for this system would therefore lead to much larger errors in the treatment.

For the single-anion systems, especially at the lower concentrations or when sodium is absent, the smallness of the solution phase corrections means the corrected selectivity quotient K_c is approximately equal to the mass action quotient K_m. Since K_m is identical to the separation factor α when all the cations are univalent, it follows that $K_c \simeq \alpha$. Thus, the Kielland plot would be very similar to a $\ln(\alpha)$ vs A_c plot (see figure 4.19 and Appendix V).

For the binary systems studied in this project, Γ is defined as the ratio of solution phase corrections, γ_B/γ_A (see section 2.1.2). The ratio γ_B/γ_A is evaluated from the corresponding mean molal stoichiometric activity coefficients $\gamma_{\pm AX}$, $\gamma_{\pm BX}$ after allowing for the presence of other ions in a mixed solution (section 2.1.3). For a mixed solution, containing two cations A,B *and* two anions X,Y, the means of calculating each mean molal activity coefficient is somewhat more complicated, and is best achieved by using the general equation (2.159) described in section 2.2.5. Thus for salt AX, this expression is

$$\log \gamma_{\pm AX}^{(B,Y)} = \frac{1}{4I}\left[4I + z_B m_B(z_A - 2z_B - z_X) + z_Y m_Y(z_X - 2z_Y - z_A)\right]\log\gamma_{\pm AX}$$

$$+ \frac{1}{4I(z_A + z_X)}\left[z_A m_B(z_B + z_X)^2 \log\gamma_{\pm BX} + z_X m_Y(z_Y + z_A)^2 \log\gamma_{\pm AY}\right.$$

$$+ A(1 + I^{-\frac{1}{2}})^{-1}\left\{z_A z_B z_X m_B(z_A - z_B)^2 + z_A z_X z_Y m_Y(z_X - z_Y)^2\right\}\Big] \quad ....(5.19)$$

Note that the terms involving Q (which allow for the differences between molal and rational functions; see section 2.2.5) have been dropped.

Similar expressions exist to define $\log \gamma_{\pm BX}^{(A,Y)}$, $\log\gamma_{\pm AY}^{(B,X)}$ and $\log \gamma_{\pm BY}^{(A,X)}$.

For a two-anion binary system it is possible to obtain parallel expressions for Γ in terms of the different anions. Thus Γ can be defined either as

$$\Gamma = \left[\frac{\left[\gamma_{\pm BX}^{(A,X,Y)}\right]^{z_A(z_B + z_X)}}{\left[\gamma_{\pm AX}^{(B,X,Y)}\right]^{z_B(z_A + z_X)}}\right]^{1/z_X} \quad ....(5.20)$$

or as

$$\Gamma = \left[\frac{\left[\gamma_{\pm BY}^{(A,X,Y)}\right]^{z_A(z_B + z_Y)}}{\left[\gamma_{\pm AY}^{(B,X,Y)}\right]^{z_B(z_A + z_Y)}}\right]^{1/z_Y} \quad ....(5.21)$$

If all the information relevant to equation (5.19) *et sequens* are known, then Γ can be obtained from equation (5.20) or (5.21), and since the derivations leading to the alternate formulations are purely arithmetic, then the two resultant Γ values should be *identical*, providing the experimental data on which their calculation is based are accurate. With the two-anion system studied here, the mean molal stoichiometric

activity coefficient for sodium ferricyanide was unknown.
Since data for the other three salts were available, it should
therefore be possible to calculate values of $\gamma_\pm$ for sodium
ferricyanide as a function of ionic strength using isotherm data.
This could lead to a new method of determining activity co-
efficients which, once the necessary mathematical and computing
formulations were worked out, may be easier than other compar-
ative methods such as the isopiestic method[89].

5.4.2. Prediction of Activity Coefficients

Rearranging equation (5.20), we obtain

$$z_X \log \Gamma_2 = z_A(z_B+z_X) \log\gamma_{\pm BX}^{(A,X,Y)} - z_B(z_A+z_X)\log\gamma_{\pm AX}^{(B,X,Y)}$$

$$....(5.22)$$

Multiplying equation (5.19) by $z_B(z_A+z_X)$ gives

$$z_B(z_A+z_X)\log\gamma_{\pm AX}^{(B,X,Y)} = \frac{z_B(z_A+z_X)}{4I}\left[4I+z_B m_B(z_A-2z_B-z_X)+z_Y m_Y \right.$$

$$(z_X-2z_Y-z_A) \left.\right]\log\gamma_{\pm AX} + \frac{z_B}{4I}\left[z_A m_B(z_B+z_X)^2\log\gamma_{\pm BX}+z_X m_Y(z_Y+z_A)^2 \right.$$

$$\log\gamma_{\pm AY}+ A(1+I^{-\frac{1}{2}})^{-1}(z_A z_X)\left\{ z_B m_B(z_A-z_B)^2+z_Y m_Y(z_X-z_Y)^2\right\}\left.\right]$$

$$....(5.23)$$

Multiplying by $z_A(z_B+z_X)$, the equation defining $\log\gamma_{\pm BX}^{(A,X,Y)}$, which is analogous to equation (5.19), gives

$$z_A(z_B+z_X)\log\gamma_{\pm BX}^{(A,X,Y)} = \frac{z_A(z_B+z_X)}{4I}\left[4I+z_A m_A(z_B-2z_A-z_X)+z_Y m_Y \right.$$

$$(z_X-2z_Y-z_B)\left.\right]\log\gamma_{\pm BX} + \frac{z_A}{4I}\left[z_B m_A(z_A+z_X)^2\log\gamma_{\pm AX}+z_X m_Y(z_Y+z_B)^2 \right.$$

$$\log\gamma_{\pm BY} + A(1+I^{-\frac{1}{2}})^{-1}(z_B z_X)\left\{ z_A m_A(z_B-z_A)^2 + z_Y m_Y(z_X-z_Y)^2\right\}\left.\right]$$

$$....(5.24)$$

Subtraction of equation (5.23) from (5.24), and subsequent simplification gives

$$z_X\log\Gamma_2 = \frac{z_A}{4I}(z_B+z_X)\left[4I+(z_B-z_X)(z_A m_A-z_Y m_Y)-2(z_A^2 m_A+z_Y^2 m_Y)\right.$$

$$\left.-z_B^2 m_B-z_B z_X m_B\right]\log\gamma_{\pm BX} -\frac{z_B}{4I}(z_A+z_X)\left[4I+(z_A-z_X)(z_B m_B-z_Y m_Y)-2\right.$$

$$(z_B^2 m_B+z_Y^2 m_Y)-z_A^2 m_A-z_A z_X m_A\left.\right]\log\gamma_{\pm AX} +\frac{A(1+I^{-\frac{1}{2}})^{-1}}{4I}(z_A z_B z_X)\left[(z_B-z_A)^2\right.$$

$$(z_A m_A-z_B m_B)\left.\right]-\frac{z_B z_X m_Y}{4I}(z_Y+z_A)^2\log\gamma_{\pm AY}+\frac{z_A z_X m_Y}{4I}(z_Y+z_B)^2\log\gamma_{\pm BY}$$

$$....(5.25)$$

In this equation the unknown term is seen at the end of the right hand side. The equation is then rearranged to get an expression in terms of $\log\gamma_{\pm BY}$, at the same time, further simplification is achieved by the appropriate substitutions of the following two equations which define the ionic strength and solution normality (concentration in equiv.dm^{-3}) respectively:

$$I = \tfrac{1}{2}(z_A^{\,2}m_A + z_B^{\,2}m_B + z_X^{\,2}m_X + z_Y^{\,2}m_Y) \qquad \ldots\ldots(5.26)$$

$$T_N = z_A m_A + z_B m_B = z_X m_X + z_Y m_Y \qquad \ldots\ldots(5.27)$$

Then, because $z_A = z_B$ here

$$z_A z_X m_Y (z_Y + z_B)^2 \log\gamma_{\pm BY} = 4I z_X \log\Gamma_2 - z_A z_X m_X (z_B + z_X)^2 \log\gamma_{\pm BX}$$

$$+ z_B z_X m_X (z_A + z_X)^2 \log\gamma_{\pm AX} + z_B z_X m_Y (z_Y + z_A)^2 \log\gamma_{\pm AY} \qquad \ldots\ldots(5.28)$$

Therefore,

$$\log\gamma_{\pm BY} = \frac{1}{z_A m_Y (z_Y + z_B)^2} \Big[4I\log\Gamma_2 + z_B m_X (z_A + z_X)^2 \log\gamma_{\pm AX} + z_B m_Y$$

$$(z_A + z_Y)^2 \log\gamma_{\pm AY} - z_A m_X (z_B + z_X)^2 \log\gamma_{\pm BX} \Big] \qquad \ldots\ldots(5.29)$$

Thus, the value of $\gamma_{\pm BY}$ can be predicted from the known values of $\gamma_{\pm AY}$, $\gamma_{\pm AX}$ and $\gamma_{\pm BX}$ if the value of Γ_2 is also known.

For the particular two-anion system studied, where one anion is nitrate and the other ferricyanide, $z_Y = 3$ and $z_A = z_B = z_X = 1$. Equation (5.29) then simplifies to

$$\log\gamma_{\pm BY} = \frac{1}{16m_Y} \Big[4I\log\Gamma_2 + 4m_X\log\gamma_{\pm AX} + 16m_Y\log\gamma_{\pm AY} - 4m_X\log\gamma_{\pm BX} \Big]$$

$$\ldots\ldots(5.30)$$

Therefore,

$$\gamma_{\pm BY} = \left[\left(\gamma_{\pm AX} \Big/ \gamma_{\pm BX} \right)^{m_X} \left(\gamma_{\pm AY} \right)^{4m_Y} (\Gamma_2)^I \right]^{1/4\,m_Y} \qquad \ldots\ldots(5.31)$$

The value of $\gamma_{\pm BY}$ is obtained by simply substituting the
appropriate values of the other parameters. The computer
program written to evaluate $\gamma_{\pm BY}$ is shown in Appendix IV. The
particular usefulness of this method is that the activity
coefficient of one *pure* salt at a given ionic strength is
derived in terms of the activity coefficients of all the other
three pure salts. Data are available in the literature for a
large number of pure salts, so the method is in principle
of wide applicability.

Once the pure salt coefficients are known, these values can be
used in an equation derived from the general equation (2.159)
to evaluate the appropriate mixed salt coefficients. For the
two-cation/two-anion case considered here, the required
equation is obtained by further simplifying equation (5.19)
after suitable substitutions with equations (5.26) and (5.27).
This gives,

$$\log\gamma_{\pm AX}^{(B,Y)} = \frac{1}{4I(z_A+z_X)} \left[(z_A+z_X)^2(z_A m_A+z_X m_X)\log\gamma_{\pm AX} + z_A m_B \right.$$

$$(z_B+z_X)^2\log\gamma_{\pm BX} + z_X m_Y(z_A+z_Y)^2\log\gamma_{\pm AY} + A(1+I^{-\frac{1}{2}})^{-1}(z_A z_X)$$

$$\left. \left\{ z_B m_B(z_A-z_B)^2 + z_Y m_Y(z_X-z_Y)^2 \right\} \right] \qquad \ldots\ldots(5.32)$$

Analogous equations can be derived to define the other three
mixed salt coefficients.

After the derivation of the pure salt coefficient prediction
model was complete, it was tested for the Na/K two-anion system
using the Γ_2 values determined earlier. The results obtained

TABLE 5.8. <u>Computer Predicted $\gamma_{\pm}$ Values for Sodium Ferricyanide</u>

Ionic strength (equiv.dm^{-3})	$Fe(CN)_6^{3-}$ concentration (equiv.dm^{-3})	$\gamma_{\pm}$ values for ferricyanide salts	
		potassium (calculated)	sodium (predicted)
.13	.03	.431	.260
.14	.04	.422	.270
.15	.05	.413	.294
.16	.06	.406	.293
.17	.07	.399	.292
.18	.08	.392	.314
.19	.09	.386	.335
.20	.10	.380	.324
.20	.10	.380	.304
.20	.10	.380	.302

are shown in Table 5.8., above.

The $\gamma_{\pm}$ values for potassium and sodium ferricyanide were plotted against the ionic strength (figure 5.32). The most important things apparent from the table and the plot are that while the predicted values vary non-uniformly with the ionic strength, (a result which must inevitably arise when using data taken from experimental isotherms) the trend of variation is in the opposite direction to values for potassium ferricyanides. The probably erroneous nature of the predicted $\gamma_{\pm}$ values is also noticeable for I = 0.2 where non-constant values are obtained. The data are also inconsistent with the Debye-Hückel equations since

attempts to determine the Debye-Hückel a and b values by the
method described in section 4.4.1 proved unsuccessful, with
widely different or even negative values for a being obtained.
The reason for the errors in the $\gamma_\pm$ values is therefore attrib-
uted to the inconsistent Γ values used in the evaluation. This
method of predicting $\gamma_\pm$ values remains unproven, and therefore,
it is recommended that the method be tested for more suitable
systems in the future.

5.4.3. Ternary Systems

5.4.3.1. Ternary systems with one co-anion only.

The ternary thermodynamic treatment[85-88] described earlier
(section 2.2) is carried out using *ratios* of Γ values, i.e.
Γ_3/Γ_1 and Γ_3/Γ_2. Since the individual Γ values, defined by
equation (2.61) et sequens, are not required by the treatment,
mathematical expressions are used to derive the two required
ratios directly (see section 2.2.5). For consideration of the
solution phase it is more useful to obtain the individual Γ
values in order to note the individual effects of the ions
present on the magnitude of the correction. Availability of
individual Γ values also permits direct comparisons with the
magnitudes of binary solution phase corrections. Therefore, the
mathematical expressions were modified to enable these Γ values
to be calculated. For example, addition of equation (2.126)
and (2.127) gives

$$z_B z_C (z_A + z_X) \ln\gamma_{\pm AX} + z_A z_C (z_B + z_X) \ln\gamma_{\pm BX} - 2 z_A z_B (z_C + z_X) \ln\gamma_{\pm CX}$$

$$= z_X (z_B z_C \ln\gamma_A + z_A z_C \ln\gamma_B - 2 z_A z_B \ln\gamma_C) \quad ....(5.33)$$

Thus,

$$\Gamma_3 = \gamma_A^{z_B z_C} \cdot \gamma_B^{z_A z_C} / \gamma_C^{2z_A z_B} = \left[\frac{\gamma_{\pm AX}^{z_B z_C (z_A + z_X)} \cdot \gamma_{\pm BX}^{z_A z_C (z_B + z_X)}}{\gamma_{\pm CX}^{2z_A z_B (z_C + z_X)}} \right]^{1/z_X}$$

....(5.34)

Similar expressions were obtained to define Γ_1 and Γ_2. By using values of $\gamma_{\pm AX}$ etc. for the *mixed* salt solutions, the mixed salt Γ ratios that apply to the experimental solutions were obtained. These Γ values are shown in table 4.5 together with the two ratios used in the thermodynamic treatment.

From the Γ values it is clear that large corrections exist only at the higher concentration where the values vary from unity by as much as 10% (see Γ_2 and Γ_3 for the Na/K/Li(0.1) system). In contrast, Γ_1 is only 0.3% higher than unity. This trend is seen for the Na/K/Li (0.04) system also, where Γ_1 is extremely small while Γ_2 and Γ_3 show a 4% variance from unity. The corrections for the silver system seem to be generally smaller, with the deviation from unity varying only between 1 and 3%. Except at the higher concentration the corrections are quite similar to those for the binary solutions.

The ternary Na/K/Li(NO_3) system was also studied at higher concentrations, three equilibrium points being measured at each concentration covered (i.e. 0.25 to 2.0 equiv.dm^{-3}). The Γ values calculated for these concentrations are shown in Table 5.9 below together with the corresponding values from the more comprehensive 0.04 and 0.1 equiv. dm^{-3} concentration studies.

As expected, the solution phase corrections became larger in magnitude as the solution concentration increased. The biggest

- 244 -

TABLE 5.9. <u>Variance of Γ with Solution Concentration</u>

<u>Na/K/Li System</u>

Solution concentration (equiv.dm^{-3})	Γ_1	Γ_2	Γ_3
0.04	1.0004	1.0400	0.9611
0.1	1.0029	1.0995	0.9069
0.25	1.0122	1.2569	0.7860
0.5	1.0317	1.5613	0.6208
0.75	1.0535	1.9330	0.4911
1.0	1.0767	2.3893	0.3887
1.5	1.1267	3.6405	0.2438
2.0	1.1803	5.5351	0.1531

corrections are associated with the $2K_s \rightarrow 2K_c$ reaction where the Γ_2 value changes from 1.04 to 5.54. The Γ_2 correction is already highly significant at a total normality of 0.25 equiv. dm^{-3}, where the Γ_2 correction is already >25%.

5.4.3.2. <u>Ternary systems with several accompanying co-anions</u>

In this section some simplifications to the original treatment of Fletcher and Townsend[87] are discussed. The basic thermo-dynamic approach used to determine the appropriate Γ ratios in terms of the mixed salt mean molal stoichiometric activity coefficients was fully described earlier, in section 2.2.5. The required mixed salt coefficents are determined from the general equation (2.159), the nature of which is such that each mixed

salt coefficient is derived in terms of the pure salt co-
efficient of the same salt and the pure salt coefficients of
the related salts (which are in the mixed solution). For the
three-cation three-anion system considered here there are *nine*
such mixed salt coefficients in the form of

$$\gamma_{\pm AX}^{(B,C,X,Y,Z)} = f(\gamma_{\pm AX}, \gamma_{\pm BX}, \gamma_{\pm CX}, \gamma_{\pm AY}, \gamma_{\pm AZ}) \quad \ldots\ldots(5.35)$$

$$\gamma_{\pm BX}^{(A,C,X,Y,Z)} = f(\gamma_{\pm AX}, \gamma_{\pm BX}, \gamma_{\pm CX}, \gamma_{\pm BY}, \gamma_{\pm BZ}) \quad \ldots\ldots(5.36)$$

and
$$\gamma_{\pm CX}^{(A,B,X,Y,Z)} = f(\gamma_{\pm AX}, \gamma_{\pm BX}, \gamma_{\pm CX}, \gamma_{\pm CY}, \gamma_{\pm CZ}) \quad \ldots\ldots(5.37)$$

Therefore, the derivation of each mixed salt coefficient requires
five pure salt coefficients. In the experimental work carried
out on a three-cation, three-anion system, the salts potassium
ferricyanide, sodium sulphate and lithium nitrate were used,
data for all three salts were available in literature. However,
equations (5.35) - (5.37) show that data for all nine possible
combinations of salts is required. Both $\gamma_{\pm AY}$ and $\gamma_{\pm CY}$ are how-
ever unknown (where A = Na^+ and C = Li^+ and Y = $Fe(CN)_6^{3-}$), and
therefore, only $\gamma_{\pm BX}$ and $\gamma_{\pm BZ}$ *mixed* salt coefficients can be
evaluated. This shows the great importance of having all the
relevant information available.

The thermodynamic treatment is however carried out in terms of
only two Γ ratios, Γ_3/Γ_1 and Γ_3/Γ_2, and it is therefore worth
considering how these may be derived from the information
available. In section 2.2.5.2 it was shown that the ratios are
derived in terms of the following relationships (see equations
2.143 and 2.144).

$$\Gamma_3/\Gamma_1 = f(\gamma_{\pm AX}, \gamma_{\pm CX}, \gamma_{\pm AY}, \gamma_{\pm BY}, \gamma_{\pm BZ}, \gamma_{\pm CZ}) \quad \ldots\ldots(5.38)$$

and

$$\Gamma_3/\Gamma_2 = f(\gamma_{\pm BX}, \gamma_{\pm CX}, \gamma_{\pm AY}, \gamma_{\pm CY}, \gamma_{\pm BZ}, \gamma_{\pm AZ}) \quad ....(5.39)$$

Since the two Γ ratios are expressed in terms of all *nine* co-efficients and since all the $\gamma_{\pm}$ values used are *mixed* salt co-efficients, it is also obvious that the derivation of the re-quired Γ ratios *cannot* be accomplished by the equations described in section 2.2.5 *unless* all the necessary activity coefficients are available. It was therefore decided to investigate ways of reducing the dependency of Γ ratios on the total number of salts present in the solution; i.e. to see if it is possible to express Γ ratios in terms of only a few mixed salt activity co-efficients.

It was shown in the two-anion binary work (sections 5.2.2. and 5.4.1) that the appropriate Γ term can be derived in terms of *either anion*, and that in this case two identical Γ values can be obtained from the two anions used. The redundancy of equations for Γ should be greater for a ternary case. Therefore, similar manipulations of mathematical expressions were carried out to define the two ternary Γ ratios in terms of (if possible) just one anion only. The starting points for this derivation were equations (2.22)(2.23) and (2.125) shown in section 2.2.5.1, which were changed from their logarithm form and raised to the powers of $z_B z_C$, $z_A z_C$ and $z_A z_B$ respectively to obtain

$$\gamma_{\pm AX}^{z_B z_C (z_A + z_X)} = \gamma_A^{z_X z_B z_C} \cdot \gamma_X^{z_A z_B z_C} \quad ....(5.40)$$

$$\gamma_{\pm BX}^{z_A z_C (z_B + z_X)} = \gamma_B^{z_X z_A z_C} \cdot \gamma_X^{z_A z_B z_C} \quad ....(5.41)$$

and

$$\gamma_{\pm CX}^{z_A z_B (z_C + z_X)} = \gamma_C^{z_X z_A z_B} \cdot \gamma_X^{z_A z_B z_C} \quad ....(5.42)$$

Therefore,

$$\Gamma_1 = \frac{\gamma_B^{z_A z_C} \gamma_C^{z_A z_B}}{\gamma_A^{2z_B z_C}} = \left[\frac{\gamma_{\pm BX}^{z_A z_C (z_B + z_X)} \gamma_{\pm CX}^{z_A z_B (z_C + z_X)}}{\gamma_{\pm AX}^{2z_B z_C (z_A + z_X)}} \right]^{1/z_X}_{(Y,Z)}$$

....(5.43)

The suffix (Y,Z) indicates that these two anions are also present in the system. Similar expressions can be derived for Γ_2 and Γ_3 solely in terms of one anion. Therefore, the required ratios are,

$$\Gamma_3 / \Gamma_1 = \left[\frac{\gamma_{\pm AX}^{z_C (z_A + z_X)}}{\gamma_{\pm CX}^{z_A (z_C + z_X)}} \right]^{3z_B / z_X}_{(Y,Z)}$$

....(5.44)

and

$$\Gamma_3 / \Gamma_2 = \left[\frac{\gamma_{\pm BX}^{z_C (z_B + z_X)}}{\gamma_{\pm CX}^{z_B (z_C + z_X)}} \right]^{3z_A / z_X}_{(Y,Z)}$$

....(5.45)

It must be, however, remembered that all the $\gamma_\pm$ terms used refer to *mixed* salt solutions. In terms of mixed salt coefficients therefore,

$$\Gamma_3 / \Gamma_1 = f(\gamma_{\pm AX}, \gamma_{\pm CX})$$ ....(5.46)

and

$$\Gamma_3 / \Gamma_2 = f(\gamma_{\pm BX}, \gamma_{\pm CX})$$ ....(5.47)

Comparison with the corresponding equations (5.38) and (5.39), it is immediately obvious that the complexity of the expressions has been reduced significantly, particularly when equations (5.33) *et sequens* which describe the dependency of each mixed salt coefficient on five appropriate pure salt coefficients is taken into perspective. The two required Γ ratios can now

be expressed in terms of the *pure* salt coefficients,

$$\Gamma_3/\Gamma_1 = f(\gamma_{\pm AX}, \gamma_{\pm BX}, \gamma_{\pm CX}, \gamma_{\pm AY}, \gamma_{\pm AZ}, \gamma_{\pm CZ}, \gamma_{\pm CY}) \quad ....(5.48)$$

and

$$\Gamma_3/\Gamma_2 = f(\gamma_{\pm AX}, \gamma_{\pm BX}, \gamma_{\pm CX}, \gamma_{\pm BY}, \gamma_{\pm BZ}, \gamma_{\pm CZ}, \gamma_{\pm CY}) \quad ....(5.49)$$

Both these equations involve the unknown $\gamma_{\pm CY}$ and the former equation also involves $\gamma_{\pm AY}$.

The two Γ ratios derived above were based on anion X (nominally the nitrate ion). Two identical derivations can be made using anion Z (the sulphate ion), and two more using anion Y (the ferricyanide ion). When the appropriate *pure* salt coefficients are taken into account, further equations of the form of

$$\Gamma_3/\Gamma_1 = f(\gamma_{\pm AZ}, \gamma_{\pm BZ}, \gamma_{\pm CZ}, \gamma_{\pm AX}, \gamma_{\pm AY}, \gamma_{\pm CX}, \gamma_{\pm CY}) \quad ....(5.50)$$

$$\Gamma_3/\Gamma_2 = f(\gamma_{\pm AZ}, \gamma_{\pm BZ}, \gamma_{\pm CZ}, \gamma_{\pm BX}, \gamma_{\pm BY}, \gamma_{\pm CX}, \gamma_{\pm CY}) \quad ....(5.51)$$

$$\Gamma_3/\Gamma_1 = f(\gamma_{\pm AY}, \gamma_{\pm BY}, \gamma_{\pm CY}, \gamma_{\pm AX}, \gamma_{\pm AZ}, \gamma_{\pm CX}, \gamma_{\pm CZ}) \quad ....(5.52)$$

and

$$\Gamma_3/\Gamma_2 = f(\gamma_{\pm AY}, \gamma_{\pm BY}, \gamma_{\pm CY}, \gamma_{\pm BX}, \gamma_{\pm BZ}, \gamma_{\pm CX}, \gamma_{\pm CZ}) \quad ....(5.53)$$

are obtained.

Whatever methods were used to evaluate the Γ ratios, because the correction applies to the *same* solution system, identical values must be obtained for each Γ ratio. In the equations shown above, Γ_3/Γ_2 is defined in terms of only one unknown, *viz*: $\gamma_{\pm CY}$. If Γ_3/Γ_2 can be evaluated directly from any pair of equations defining it, say equations (5.49) and (5.51), using a process that would eliminate the $\gamma_{\pm CY}$ term then the value of Γ_3/Γ_2 can be re-substituted in either equation to obtain a value for $\gamma_{\pm CY}$. Once both these terms are known, subsecutive substitutions in

equations (5.53) and (5.52) respectively can lead to the eval-
uation of $\gamma_{\pm AY}$ and Γ_3/Γ_1. If this method was successful, the
required Γ ratios, Γ_3/Γ_1 and Γ_3/Γ_2, and the unknown pure salt
coefficients, $\gamma_{\pm AY}$ and $\gamma_{\pm CY}$, would be derived solely from math-
ematical expressions.

The necessary expressions are derived from equation (2.159) in
a method analogous to the binary derivation described in
section 5.4.1. Thence,

$$\log\gamma_{\pm AX}^{(B,C,X,Y,Z)} = \frac{1}{4I(z_A+z_X)}\left[(z_A+z_X)^2(z_A m_A+z_X m_X)\log\gamma_{\pm AX}+z_A m_B\right.$$

$$(z_B+z_X)^2\log\gamma_{\pm BX}+z_A m_C(z_C+z_X)^2\log\gamma_{\pm CX}+z_X m_Y(z_A+z_Y)^2\log\gamma_{\pm AY}+z_X m_Z$$

$$(z_A+z_Z)^2\log\gamma_{\pm AZ}+z_A z_X A(1+I^{-\frac{1}{2}})^{-1}\left\{z_B m_B(z_A-z_B)^2+z_C m_C(z_A-z_C)^2\right.$$

$$\left.\left.+z_Y m_Y(z_X-z_Y)^2+z_Z m_Z(z_X-z_Z)^2\right\}\right] \qquad \ldots\ldots(5.54)$$

Similar equations can be derived to define the other mixed salt
coefficients. Comparison of equation (5.54) with its binary
analogue, equation (5.32), shows that they are similar except
that the ternary equation includes extra terms to allow for the
additional ions in solution.

From equation (5.44),

$$\log\Gamma_3/\Gamma_1 = 3z_B/z_X\left[z_C(z_A+z_X)\log\gamma_{\pm AX}-z_A(z_C+z_X)\log\gamma_{\pm CX}\right] \quad\ldots\ldots(5.55)$$

where the $\gamma_\pm$ values refer to the *mixed* solution. Therefore, by
multiplying equation (5.54) above by $3z_B z_C(z_A+z_X)/z_X$ and sub-
tracting from it the product of the analogous equation defining
$\log\gamma_{\pm CX}^{(A,B,X,Y,Z)}$ and $3z_A z_B(z_C+z_X)/z_X$, we obtain

$$\log(\Gamma_3/\Gamma_1)_X = \frac{3z_B}{4I}\left[z_C m_X (z_A+z_X)^2 \log\gamma_{\pm AX} - z_A m_X (z_C+z_X)^2 \log\gamma_{\pm CX} + z_C m_Y\right.$$

$$(z_Y+z_A)^2 \log\gamma_{\pm AY} + z_C m_Z (z_Z+z_A)^2 \log\gamma_{\pm AZ} - z_A m_Y (z_Y+z_C)^2 \log\gamma_{\pm CY} - z_A m_Z$$

$$(z_Z+z_C)^2 \log\gamma_{\pm CZ} + z_A z_C (z_A-z_C) A (1+I^{-\frac{1}{2}})^{-1} \left\{z_B m_B (z_A+z_C-2z_B)+\right.$$

$$\left.\left.(z_C m_C - z_A m_A)(z_A-z_C)\right\}\right] \qquad \ldots\ldots(5.56)$$

It is apparent that the term including A becomes zero when $z_A = z_C$. The suffix X denotes that the derivation had been carried out in terms of anion X.

Two analogous equations can be derived similarly in terms of the other two anions Y and Z. It was however then found that all three equations defining Γ_3/Γ_1 were identical (see equation below), and as such, could not be used to solve for the unknown quantities.

$$\log(\Gamma_3/\Gamma_1)_Y = \frac{3z_B}{4I}\left[z_C m_Y (z_A+z_Y)^2 \log\gamma_{\pm AY} - z_A m_Y (z_C+z_Y)^2 \log\gamma_{\pm CY}\right.$$

$$+z_C m_X (z_X+z_A)^2 \log\gamma_{\pm AX} + z_C m_Z (z_Z+z_A)^2 \log\gamma_{\pm AZ} - z_A m_X (z_X+z_C)^2 \log\gamma_{\pm CX}$$

$$-z_A m_Z (z_Z+z_C)^2 \log\gamma_{\pm CZ} + z_A z_C (z_A-z_C) A (1+I^{-\frac{1}{2}})^{-1} \left\{z_B m_B (z_A+z_C-2z_B)\right.$$

$$\left.\left.+(z_C m_C - z_A m_A)(z_A-z_C)\right\}\right] \qquad \ldots\ldots(5.57)$$

These equations do, however, show that the relationships (5.48) - (5.53) governing the dependencies of Γ ratios on the appropriate *pure* salt coefficients can be corrected because the salts of ion B have no effect on Γ_3/Γ_1 and salts of ion A have no effect on Γ_3/Γ_2. These corrected relationships are

$$\Gamma_3/\Gamma_1 = f(\gamma_{\pm AX}, \gamma_{\pm CX}, \gamma_{\pm AY}, \gamma_{\pm CY}, \gamma_{\pm AZ}, \gamma_{\pm CZ}) \qquad \dots(5.58)$$

and

$$\Gamma_3/\Gamma_2 = f(\gamma_{\pm BX}, \gamma_{\pm CX}, \gamma_{\pm BY}, \gamma_{\pm CY}, \gamma_{\pm BZ}, \gamma_{\pm CZ}) \qquad \dots(5.59)$$

It is now obvious that only these two equations exist to define the two ratios concerned, regardless of the anion the equations arise from. At the same time, these equations show conclusively that it is equally valid to derive the required Γ ratios in terms of any one of the three anions present. This in turn simplifies the mathematics involved in the multi-anion solution phase treatment as opposed to the more complex equations presented by Fletcher and Townsend[87] (see section 2.2.5.2).

As for the solution phase treatment, the required Γ ratios could not be solved by mathematical expressions only. It was not possible to carry out a derivation based on an empirical relationship as was done for the binary case (see section 5.2.2) because the ternary case is far more complex. It would not have been possible to read off values from ternary isotherms in order to calculate the three-anion Γ ratios from the corresponding one-anion Γ ratios, even if a large number of three-anion ternary equilibrium data were known.

For these reasons, a full solution phase treatment could not be carried out for the three-anion ternary system studied. From the above-derived mathematical expressions it is apparent that such a treatment would require information on *all* the (combinations of) salts present in the solution. If that information were available, the Γ ratios would have been evaluated by substituting in equation (5.56) and an analogous equation

defining Γ_3/Γ_2.

5.5. <u>PREDICTION OF TERNARY EQUILIBRIA FROM BINARY DATA</u>

There have been several models put forward by various authors
which enable the prediction of some aspect of ternary ion ex-
change behaviour from known binary data, applicable to differ-
ent types of ion-exchangers[29,101,102,119-122]. These range
from the simple ternary 'triangle rule' (discussed below in
section 5.5.1) which allows changes in free energy for ternary
systems to be predicted, to more complex models which enable
ternary equilibrium compositions or activity corrections to be
predicted. The details of these different predictive models
have been discussed in depth with particular reference to their
applicability to zeolites recently by Townsend and Fletcher[111],
who broadly categorise the approaches into two groups; those
that use combinations of corrected selectivity quotients in order
to predict the ternary quotients[29,119,120], and those that
use solid solution models in order to predict ternary activity
coefficient data[102,121,122].

The first method involves defining pseudo-binary coefficients,
which are formally analogous to the corresponding binary corr-
ected selectivity quotients, by treating the three cation system
as a binary one and ignoring the presence of the third cation
in turn. Basically, this third cation is assumed to be non-
influential, thus implying ideal behaviour[111], but more use-
ful, modified versions exist. In the model developed for resins
by Soldatov and Bychkova[101], one of the cations is assumed
to affect the other two near-identically. This 'similar
behaviour' concept is also used by Barri and Rees in their

treatment of zeolite A involving a Na/Ca/Mg ternary system[29].
In their discussion, Fletcher and Townsend[111] attribute the
weaknesses of the above approaches to the need to obtain
sufficient binary *and* ternary experimental data, so that the
two 'near-identical' ions may be chosen, before prediction is
attempted.

The second method, which allows ternary activity corrections to
be predicted by using solid solution models, has been essenti-
ally developed for clays[102,121,122]. The best-known of these,
the Elprince-Babcock model[102], has already been described in
section 2.2.8, and data from this project have been used to
test the applicability of the model to the zeolite/solution
systems used here. The outcome of the Elprince-Babcock model
study is discussed later in section 5.5.2, but it is worth
briefly reviewing two other approaches here, which are found
in the literature.

Both these approaches are based on the 'sub-regular' solution
model of Hardy[123], and utilise a convergent power series (i.e.
the Margules equation) to represent the behaviour of activity
coefficients in a multicomponent solid solution. The earlier
(1980) model of Elprince, Vanslow and Sposito[121] assumes
that the activity coefficient of a particular ion in a ternary
system is derived from the Margules equation truncated after
the cubic terms and solely from binary experimental data. Using
this model, good agreement was obtained between experimental
and predicted ternary data for the system NH_4/Ba/La-montmorill-
onite[121]. Chu and Sposito's 1981 modification[122] introduces
a new, additional parameter into the model which requires some

experimental data on the *ternary* equilibrium in order to
evaluate the appropriate activity coefficients, an additional
requirement which is similar to that of Barri and Rees'
approach[29]. For the NH_4/Ba/La-montmorillonite system tested
by Elprince, Vanslow and Sposito[121], this parameter was
found to approximate zero, thus explaining the good agreement
seen previously. Since the 'sub-regular' model has been success-
fully applied to clays, Fletcher and Townsend have attempted
to apply the model to a NH_4/Na/K-mordenite system by using
appropriate binary data and comparing the resultant predicted
data with experimental measured ternary data[111]. The out-
come of this study was that the predicted values disagreed very
much with the experimentally derived values, and Fletcher and
Townsend explain the failure in terms of the strong site heter-
ogeneity in the zeolite compared to a more simple clay[111].

5.5.1. Ternary 'Triangle Rule'

This 'triangle-rule' permits the change in free energy for a
particular ternary equilibrium to be predicted from the known
values of $\Delta G^{\ominus}$ for the two conjugate binary equilibria. Consider
the two binary and single ternary equilibria described by the
equations given below. (Univalent ions are used for convenience)

$$A^+_{(s)} + B^+_{(c)} \rightleftharpoons A^+_{(c)} + B^+_{(s)} \qquad ....(5.57)$$

$$A^+_{(s)} + C^+_{(c)} \rightleftharpoons A^+_{(c)} + C^+_{(s)} \qquad ....(5.58)$$

and

$$2A^+_{(s)} + B^+_{(c)} + C^+_{(c)} \rightleftharpoons 2A^+_{(c)} + B^+_{(s)} + C^+_{(s)}$$
$$....(5.59)$$
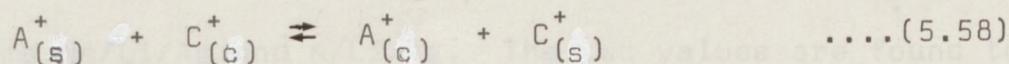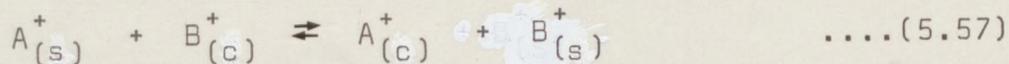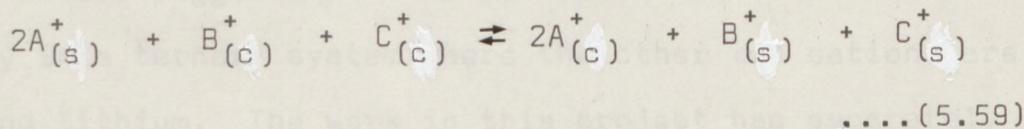
It is immediately apparent that equation (5.59) represents the

sum of equations (5.57) and (5.58), and that equation (5.59)
is similar to equations (2.56), (2.57) and (2.58) which
define the three ion exchange equilibria required to describe
the ternary ion exchange situation fully. It therefore follows
that the value of any ternary $\Delta G^{\ominus}$ term can be predicted by add-
ing the two corresponding binary $\Delta G^{\ominus}$ terms.

If the new thermodynamic model for ternary systems of Fletcher
and Townsend[85-88] is fully compatible with Gaines and Thomas'
approach for binary systems, then such predictions of ternary
$\Delta G^{\ominus}$ values from binary data should agree. Predicted results are
shown alongside the experimentally determined $\Delta G^{\ominus}$ values in
table 5.10.

The agreement between predicted and experimental values is good.
In section 5.3.3. the fitting problems observed in the Na/K/Ag-X
system were discussed, and it was not found possible to choose
between a 3,2 or 4,4 polynomial fit. The additional evidence
supplied by application of the triangle rule suggests that the
4,4 fit is better. In general, the closeness of the predicted
and experimental values for all systems studied can be taken as
a confirmation of the correctness firstly of the thermodynamic
treatment, and secondly of the fitting procedures used in this
project.

Also shown in table 5.10 are the predicted values of $\Delta G^{\ominus}_1$ for
the systems Na/Li/Ag and K/Li/Ag. The two values are found to
be quite close, suggesting that potassium and sodium behave
similarly in a ternary system where the other two cations are
silver and lithium. The work in this project has separately

TABLE 5.10 Ternary $\Delta G^{\ominus}$ Values Predicted from 'Triangle rule'

Ternary System	Predicted $\Delta G^{\ominus}$ (kJ equiv.$^{-1}$)	Experimental $\Delta G^{\ominus}$ (kJ equiv.$^{-1}$)
Na/K/Li (1) $Na_s \rightarrow Na_c$	-3.219	-2.949
(2) $K_s \rightarrow K_c$	-2.729	-2.621
(3) $Li_s \rightarrow Li_c$	+5.948	+5.570
Na/K/Ag (1) $Na_s \rightarrow Na_c$	+6.499	+7.501(3,2) +6.416(4,4)
(2) $K_s \rightarrow K_c$	+6.807	+6.056(3,2) +6.558(4,4)
(3) $Ag_s \rightarrow Ag_c$	-13.306	-13.557(3,2) -12.975(4,4)
Na/Li/Ag:- $Na_s \rightarrow Na_c$	+3.913	
K/Li/Ag:- $K_s \rightarrow K_c$	+3.449	-

shown that the behaviour of sodium and potassium towards lithium
and silver were similar and therefore the former two cations
would be expected to behave in a similar manner when a ternary
system made up of lithium and silver and sodium or potassium
is considered.

5.5.2. The Elprince-Babcock Model

The theoretical background to this model has been described
earlier in section 2.2.8, and therefore, only the treatment

and results are discussed here. The treatment involved using the binary zeolite phase activity coefficients f_A and f_B to evaluate the interaction energy terms Λ_{AB} and Λ_{BA} defined by equation (2.172). This was carried out by use of a computer which iteratively solved equations (2.184) and (2.185) and produced the required Λ values. The computer program used for this procedure is shown in Appendix IV, together with the corresponding flow diagram. Essentially, the computer program involves feeding in the zeolite phase composition, corresponding activity coefficients and an initial (estimated) Λ_{AB} value. The computer calculates a corresponding Λ_{BA} value, and from that calculates a new Λ_{AB} value which is compared with the starting Λ_{AB} value. According to the sign of the difference in values, a step change in the starting Λ_{AB} is made, and the operation is repeated continually until a unique solution to Λ_{AB} (and thus Λ_{BA}) is found. The program also calculates g^E (excess Gibbs free energy) by (i) equation (2.177) (i.e. from input data) and (ii) equation (2.183) (i.e. from derived Λ values) so that mathematical validity of the procedures can be perceived by suitable comparisons. Finally, the program also evaluates the binary equilibrium constant using equation (2.190).

At this stage a small modification was made to the Elprince-Babcock model in order to increase the validity of the model towards zeolites. The model assumed originally that the ratio of solution phase activity coefficients γ_B/γ_A is always unity; a modification was therefore made to equation (2.190) to incorporate Γ values into the equilibrium constant. A second

- 258 -

modification was made subsequently. The equilibrium constants calculated for each set of A_c, A_s values usually differed from one another slightly because the f_A and f_B values used in the calculation are based on a (chosen) polynomial equation representing $\ln K_c$ values. Since K_a should really be a *constant* for a given system at a particular temperature and concentration, it was decided to use the equilibrium constants calculated in the computer binary treatment (section 4.4, table 4.4), rather than the values calculated by equation (2.190). These K_a values automatically contained the solution phase correction appropriate to each binary system studied.

The program was then run for all seven binary systems studied in this project, using the crystal phase activity coefficients calculated by the curve fitting procedure. The results obtained are shown in tables 5.11-5.17 and are also shown graphically as a function of the crystal phase composition in figures 5.33- 5.36.

Elprince and Babcock's studies implied that Λ values would be *constant* for a given system at a particular temperature and concentration[102]. However, the results obtained in this project show that all the Λ values obtained vary with crystal phase composition (tables 5.11-5.17, figures 5.33-5.36). More seriously, there were discontinuities in the Λ values for the Na/Li and K/Li systems at certain crystal phase compositions. Also, solutions for Λ terms could not be found for the Na/K(0.1) and (0.04) systems at the extrema of available data. While Λ terms could be found for all the crystal phase compositions of the Na/Ag, K/Ag and Na/K (two-anion) systems, these three

TABLE 5.11   <u>BINARY ION EXCHANGE DATA AND CORRESPONDING</u>

<u>ELPRINCE AND BABCOCK Λ VALUES</u>

(i)   Na/Li   (0.1) System   (see figure 5.33(a))

	Li_c	Li_s	Λ Li-Na	Λ Na-Li
1	.020	.092	1.423	1.341
2	.044	.185	1.518	1.275
3	.065	.276	1.609	1.215
4	.094	.372	1.744	1.131
5	.126	.460	1.909	1.035
6	.181	.542	2.233	0.866
7	.208	.620	2.413	0.782
8	.263	.700	2.834	0.608
9	.345	.769	-	-
10	.412	.834	-	-
11	.462	.871	-	-
12	.505	.900	-	-
13	.647	.941	-	-
14	.717	.967	-	-
15	.798	.986	3.430	0.436
16	.858	.993	3.225	0.518
17	.952	.9984	2.993	0.638

TABLE 5.12 BINARY ION EXCHANGE DATA AND CORRESPONDING

ELPRINCE AND BABCOCK Λ VALUES

(ii) K/Li (0.1) System (see figure 5.33(b))

	Li_c	Li_s	Λ Li-K	Λ K-Li
1	.024	.093	1.225	1.935
2	.049	.187	1.465	1.749
3	.073	.282	1.756	1.557
4	.103	.375	2.230	1.297
5	.129	.442	2.787	1.053
6	.160	.498	3.775	0.721
7	.198	.563	-	-
8	.321	.695	-	-
9	.424	.792	-	-
10	.483	.840	-	-
11	.499	.853	-	-
12	.515	.865	-	-
13	.516	.865	-	-
14	.578	.913	-	-
15	.631	.946	-	-
16	.706	.971	-	-
17	.781	.989	6.357	0.484
18	.808	.994	5.977	0.601
19	.864	.998	5.389	0.857

TABLE 5.13   BINARY ION EXCHANGE DATA AND CORRESPONDING

ELPRINCE AND BABCOCK Λ VALUES

(iii) Na/K (0.04) System (see figure 5.34(a))

	Na_c	Na_s	Λ_{Na-K}	Λ_{K-Na}
1	.099	.037	0.757	2.442
2	.130	.057	0.958	2.176
3	.189	.088	1.424	1.710
4	.258	.138	2.044	1.270
5	.335	.201	2.601	0.971
6	.411	.292	2.735	0.908
7	.484	.375	2.494	1.034
8	.529	.455	2.254	1.186
9	.564	.517	2.044	1.344
10	.597	.587	1.831	1.536
11	.629	.660	1.611	1.777
12	.666	.714	1.328	2.172
13	.707	.774	0.945	2.929
14	.754	.838	-	-
15	.808	.886	-	-
16	.868	.930	-	-
17	.9387	.9662	-	-

TABLE 5.14 <u>BINARY ION EXCHANGE DATA AND CORRESPONDING</u>

<u>ELPRINCE AND BABCOCK Λ VALUES</u>

(iv) Na/K (0.1) Single-anion System
(see figure 5.34(b))

	Na_c	Na_s	$Λ_{Na-K}$	$Λ_{K-Na}$
1	.0124	.0025	0.529	2.950
2	.058	.017	0.675	2.695
3	.122	.043	0.976	2.286
4	.187	.080	1.389	1.866
5	.289	.140	2.136	1.323
6	.299	.164	2.204	1.282
7	.356	.192	2.530	1.102
8	.397	.248	2.671	1.030
9	.452	.330	2.721	1.005
10	.506	.399	2.637	1.050
11	.562	.479	2.459	1.160
12	.602	.565	2.298	1.275
13	.641	.652	2.124	1.420
14	.694	.721	1.864	1.688
15	.740	.800	1.611	2.024
16	.800	.875	1.213	2.777
17	.892	.944	-	-
18	.943	.973	-	-
19	.948	.977	-	-
20	.955	.980	-	-

(v) Na/K (0.1) Two-anion System (see figure 5.34(c))

	Na_c	Na_s	Λ_{Na-K}	Λ_{K-Na}
1	.263	.142	2.050	1.494
2	.318	.192	2.286	1.350
3	.381	.244	2.452	1.253
4	.436	.323	2.494	1.229
5	.484	.408	2.459	1.250
6	.531	.491	2.376	1.307
7	.579	.569	2.253	1.400
8	.629	.649	2.096	1.537
9	.669	.729	1.954	1.682
10	.724	.805	1.736	1.955
11	.789	.881	1.432	2.464
12	.870	.949	0.884	3.956

TABLE 5.16 <u>BINARY ION EXCHANGE DATA AND CORRESPONDING</u>

<u>ELPRINCE AND BABCOCK Λ VALUES</u>

(vi) K/Ag (0.04) System (see figure 5.35)

	K_c	K_s	Λ_{K-Ag}	Λ_{Ag-K}
1	.0044	.111	-	-
2	.0116	.241	7.774	0.872
3	.023	.415	7.554	0.901
4	0.043	.593	7.208	0.949
5	.083	.753	6.635	1.037
6	:119	.826	6.216	1.108
7	.162	.880	5.799	1.189
8	.218	.934	5.353	1.288
9	.317	.965	4.738	1.459
10	.397	.984	4.346	1.601
11	.508	.994	3.904	1.817
12	.631	.9980	3.507	2.100
13	.751	.9995	3.189	2.446

TABLE 5.17 <u>BINARY ION EXCHANGE DATA AND CORRESPONDING</u>
<u>ELPRINCE AND BABCOCK Λ VALUES</u>

(vii) Na/Ag (0.04) System (see figure 5.36)

	Na_c	Na_s	Λ Na-Ag	Λ Ag-Na
1	.0271	.429	3.996	1.787
2	.049	.636	4.310	1.706
3	.091	.797	4.987	1.545
4	.132	.857	5.740	1.383
5	.183	.903	6.766	1.185
6	.270	.945	9.088	0.815
7	.355	.969	9.750	0.722
8	.455	.988	9.934	0.698
9	.551	.994	9.169	0.828
10	.660	.9979	7.987	1.121
11	.769	.9997	6.846	1.634

- 266 -

TABLE 5.17 <u>BINARY ION EXCHANGE DATA AND CORRESPONDING</u>
<u>ELPRINCE AND BABCOCK Λ VALUES</u>

(vii) Na/Ag (0.04) System (see figure 5.36)

	Na_c	Na_s	Λ Na-Ag	Λ Ag-Na
1	.0271	.429	3.996	1.787
2	.049	.636	4.310	1.706
3	.091	.797	4.987	1.545
4	.132	.857	5.740	1.383
5	.183	.903	6.766	1.185
6	.270	.945	9.088	0.815
7	.355	.969	9.750	0.722
8	.455	.988	9.934	0.698
9	.551	.994	9.169	0.828
10	.660	.9979	7.987	1.121
11	.769	.9997	6.846	1.634

systems suffered from inadequate data in the $A_c > 0.75$ regions
(where $A = Na, K, K$ respectively).

Comparisons can be made between corresponding Λ values for some
systems. As would be expected, the three Na/K systems show
similar trends in Λ_{12} and Λ_{21} values (see figure 5.34), and
the values are also similar. For the Na/K (0.04) system, Λ
values could not be determined when $Na_c > 0.71$, while for the
Na/K (0.1) system, Λ terms could be solved to slightly higher
sodium loadings. For the Na/K (two-anion) system, even
$Na_c = 0.87$ (the highest sodium loading measured) remained with-
in the solvable range.

There were similarities between the Na/Li and K/Li systems too.
The regions $0.16 < Li_c < 0.78$ (for K/Li) and $0.27 < Li_c < 0.79$
(for Na/Li) remained unsolvable, most probably because the Λ_{21}
value slipped below zero (figure 5.33). Generally, the Λ_{21}
and Λ_{12} values for the Na/Li system were lower than the corr-
esponding values for the K/Li system (except at very low
lithium loadings).

The Na/Ag and K/Ag systems showed very dissimilar trends. The
variation in Λ values with crystal phase composition is oppo-
site in trend to one another (see figures 5.35 and 5.36).
Generally, the Λ_{12} values were greater in magnitude for the
Na/Ag system while the Λ_{21} values were smaller. The Na/Ag
system also showed a change in the direction of Λ values around
the $Na_c = 0.4-0.5$ region. No such reversal was seen for the
K/Ag system for the range of data available.

Despite the non-constancy of the Λ values for the binary

systems studied here, it was decided to investigate the Elprince-Babcock model further. The next stage of the model involved deriving ternary crystal phase coefficients from the Λ values, using equations (2.187), (2.188) and (2.189). For the ternary work the ions were taken as Na=1, K=2 and Li or Ag =3. The procedure was to select a known ternary crystal phase composition A_c, B_c (C_c then being defined) from the available data, obtain the corresponding Λ values from the graphs (figures 5.33-5.36), and then determine the ternary f values from the appropriate equation (2.187 - 2.189). These f values were then compared with the corresponding f values derived by the ternary thermodynamic treatment. Further, these f values were then used in conjunction with the appropriate binary equilibrium constants and ternary crystal phase compositions to predict the corresponding ternary solution phase compositions using equations (2.195) and (2.196). The latter two stages (i.e. calculations of f values and solution phase compositions,) were carried out by means of another computer program which is also shown in Appendix IV.

The validity of the final results depends especially on the Elprince and Babcock assumption that a particular Λ value associated with a given A_c value is the same whether the crystal phase composition is binary (A_c,B_c) or ternary (A_c,B_c,C_c). Furthermore, the model could not be tested for all available ternary data because of the gaps in the Λ data at certain crystal phase compositions which prevented many Λ values being read off the Λ vs. A_c plots. Unfortunately, these gaps meant that only 9 points (out of 33) for the Na/K/Ag system and only

5 points (out of 79) for the Na/K/Li (0.1) system could be tested.

The non-constancy of the Λ terms gave rise to a problem when the Λ values for the system under test were obtained (tables 5.18-5.19). Each crystal phase composition (A_c, B_c, C_c) involves *four* Λ terms for *each* cation fraction involved in a given composition (see table 5.18). Thus 12 Λ terms can be obtained for each crystal phase composition. If the Λ terms were invariant with the composition though, 6 out of these 12 would be duplicates of the others, and only 6 Λ values would exist. It is obvious from Elprince and Babcock equations (2.187) - (2.189) that only *six* Λ values can be used in the determination of crystal phase activity coefficients. The Λ values in tables 5.18 - 5.19 show clearly that each pair of 'duplicate' values (say, Λ_{Na-K} obtained from Na_c and K_c values respectively) are different to one another. Sometimes the differences are marked (eg. Λ_{Na-Ag} at low Na_c values) but generally however, a particular pair of Λ values are reasonably close to each other.

In order to obtain just the six required Λ values, an arithmetic mean of each pair of Λ values was taken, and these mean values (shown in table 5.20) were used in the computer program to obtain the crystal phase activity coefficients, and thence, the predicted solution phase compositions.

The results obtained are shown in tables 5.21 and 5.22. It is quite apparent that the experimental and predicted f values (table 5.21) differ significantly. These differences are reflected in the differences between observed and predicted

TABLE 5.18 Elprince-Babcock Λ Values for Na/K/Ag(0.04) System

(a)	Na_c	Λ_{Na-K}	Λ_{K-Na}	Λ_{Na-Ag}	Λ_{Ag-Na}
1	.115	0.89	2.29	5.46	1.46
2	.117	0.91	2.27	5.50	1.45
3	.119	0.92	2.26	5.53	1.44
4	.119	0.92	2.26	5.53	1.44
5	.121	0.94	2.25	5.55	1.43
6	.124	0.97	2.23	5.60	1.42
7	.160	1.21	1.92	6.30	1.27
8	.238	1.88	1.37	8.22	0.98
9	.291	2.34	1.14	9.10	0.83

(b)	K_c	Λ_{K-Na}	Λ_{Na-K}	Λ_{K-Ag}	Λ_{Ag-K}
1	.313	2.50	1.12	4.75	1.47
2	.622	0.89	2.76	3.53	2.10
3	.557	0.93	2.66	3.73	1.94
4	.362	1.87	1.52	4.50	1.56
5	.492	1.09	2.36	3.95	1.80
6	.423	1.40	1.97	4.23	1.67
7	.481	1.14	2.30	4.00	1.77
8	.472	1.18	2.25	4.03	1.76
9	.466	1.20	2.20	4.06	1.73

(c)	Ag_c	Λ_{Ag-Na}	Λ_{Na-Ag}	Λ_{Ag-K}	Λ_{K-Ag}
1	.572	0.69	10.05	1.67	4.20
2	.261	1.45	7.15	2.42	3.23
3	.324	1.17	7.60	2.23	3.38
4	.519	0.73	9.82	1.78	4.00
5	.387	0.97	8.03	2.07	3.55
6	.453	0.82	9.26	1.92	3.77
7	.359	1.04	8.19	2.15	3.48
8	.290	1.30	7.44	2.33	3.30
9	.243	1.55	6.99	2.48	3.17

TABLE 5.19 <u>Elprince-Babcock Λ Values for Na/K/Li(0.1) System</u>

(a)	Na_c	Λ_{Na-K}	Λ_{K-Na}	Λ_{Na-Li}	Λ_{Li-Na}
1	.032	0.61	2.62	0.63	2.95
2	.047	0.66	2.74	0.64	2.98
3	.063	0.72	2.64	0.62	3.02
4	.142	1.12	2.12	0.54	3.22
5	.749	1.55	2.38	0.69	2.69

(b)	K_c	Λ_{K-Na}	Λ_{Na-K}	Λ_{K-Li}	Λ_{Li-K}
1	.874	2.22	1.03	1.10	2.76
2	.848	2.05	1.18	0.78	3.53
3	.924	2.56	0.77	1.55	1.78
4	.835	1.95	1.26	0.55	3.96
5	.215	2.60	1.30	0.51	6.29

(c)	Li_c	Λ_{Li-Na}	Λ_{Na-Li}	Λ_{Li-K}	Λ_{K-Li}
1	.094	1.75	1.13	2.06	1.44
2	.105	1.80	1.10	2.29	1.32
3	.013	1.38	1.38	1.10	2.02
4	.023	1.42	1.35	1.17	1.95
5	.036	1.48	1.32	1.31	1.88

TABLE 5.20 Mean Λ Values Used in the Elprince-Babcock Model Coefficients

(a) Na/K/Ag (0.04) System

	Λ_{Na-K}	Λ_{K-Na}	Λ_{K-Ag}	Λ_{Ag-K}	Λ_{Ag-Na}	Λ_{Na-Ag}
1	1.01	2.40	4.48	1.57	1.08	7.76
2	1.84	1.58	3.38	2.26	1.45	6.33
3	1.79	1.60	3.56	2.09	1.31	6.57
4	1.22	2.07	4.25	1.67	1.09	7.68
5	1.65	1.67	3.75	1.94	1.20	6.79
6	1.47	1.82	4.00	1.80	1.12	7.43
7	1.76	1.53	3.74	1.96	1.16	7.25
8	2.07	1.28	3.67	2.05	1.14	7.83
9	2.27	1.17	3.62	2.11	1.19	8.05

(b) Na/K/Li (0.1) system

	Λ_{Na-K}	Λ_{K-Na}	Λ_{K-Li}	Λ_{Li-K}	Λ_{Li-Na}	Λ_{Na-Li}
1	0.82	2.42	1.27	2.41	2.35	0.88
2	0.92	2.40	2.10	2.91	2.39	0.87
3	0.75	2.60	1.79	1.44	2.20	1.00
4	1.19	2.04	1.25	2.57	2.32	0.95
5	1.43	2.49	1.20	3.80	2.09	1.01

TABLE 5.21 Experimental and Predicted Crystal Phase Activity Coefficients

Na_c	Experimental			Predicted		
	f_A	f_B	f_C	f_A	f_B	f_C
(a) Na/K/Ag (0.04) system						
1	.115	.4722	.3809	.8495	.2553	.3580	.7544
2	.117	.4715	.7904	.4368	.4078	.7501	.9238
3	.119	.3946	.6905	.5333	.3905	.6617	.3760
4	.119	.4438	.4334	.7978	.2842	.4120	.8381
5	.121	.3818	.5972	.6287	.3682	.5748	.4735
6	.124	.4086	.5089	.7228	.3224	.4871	.5775
7	.160	.4124	.6331	.6368	.3815	.6002	.4363
8	.238	.4704	.7518	.6293	.4226	.6724	.3363
9	.291	.5128	.8586	.6189	.3224	.4436	.5883
(b) Na/K/Li (0.1) system						
1	.032	.5741	1.3288	.6364	.3961	.9844	.3930
2	.047	.5569	1.4582	.6629	.4573	.9557	.2062
3	.063	.7714	1.6132	.5497	.3676	.9890	.3780
4	.142	.7038	1.7216	.6546	.4644	.9643	.3882
5	.749	1.2855	.6490	.7053	.9442	.4103	.4908

TABLE 5.22   Experimental and Predicted Solution Phase Compositions

Nac	Experimental			Predicted		
	A_s	B_s	C_s	A_s	B_s	C_s
(a) Na/K/Ag (0.04) System						
1 .115	.365	.620	.0150	.171	.814	.0152
2 .117	.115	.884	.00098	.075	.924	.00074
3 .119	.160	.839	.00147	.091	.907	.00149
4 .119	.316	.676	.00776	.152	.838	.00964
5 .121	.210	.787	.00296	.112	.886	.00284
6 .124	.261	.734	.00490	.134	.861	.00536
7 .160	.284	.714	.00245	.144	.853	.00262
8 .238	.332	.662	.00696	.202	.797	.00117
9 .291	.373	.626	.00097	.408	.585	.00654
(b) Na/K/Li (0.1) System						
1 .032	.009	.694	.297	.0083	.650	.342
2 .047	.013	.694	.293	.016	.742	.242
3 .063	.034	.920	.046	.018	.922	.061
4 .142	.062	.845	.093	.054	.835	.112
5 .749	.694	.118	.188	.705	.105	.190

solution phase compositions also (table 5.22). Generally, these results show that the Elprince-Babcock model is inapplicable to zeolites.

Reasons for what now appears to be a general failure of the Elprince-Babcock model when applied to zeolites have been discussed elsewhere[85,111,117], and are only considered briefly here. Elprince and Babcock applied the model to clays[102], which have layer structures with exchanging cations residing between layers, so the excess free energy term $(\lambda_{AB} - \lambda_{AA})$ in equation (2.172) might well be considered to be very nearly independent of the exchanger phase composition since the ions are, in effect, in aqueous solution. Guggenheim essentially made the same assumption in his early model for solution phase non-ideality[91]. For zeolites, the situation is different because of the existence of microheterogeneous phases, *viz.* distinct site sets in relatively narrow channels, often containing very limited quantities of water molecules. The binary activity coefficients used in this project are phenomenological ones obtained by use of the Gibbs-Duhem equation (see section 2.1.4), and are a complicated function (at a given composition) of both the population of ions and their departure from ideality *within each site set*[85]. For n sets of sites, the thermodynamic equilibrium constant is

$$ K_a = \prod_{i=1}^{n} \left[K_i \right]^{X_i} \qquad \ldots (5.60) $$

where

$$ X_i = \frac{z_A m_{A,i} + z_B m_{B,i}}{\displaystyle\sum_{i=1}^{n} (z_A m_{A,i} + z_B m_{B,i})} \qquad \ldots (5.61) $$

and $m_{A,i}$ and $m_{B,i}$ are the concentrations of (mol kg^{-1}) of ions A and B respectively in the *ith* set; K_i also refers to the *ith* set. Equation (5.60) can be expanded[84] and combined with equations (2.14) and (2.18) to give

$$K_a = \left[\frac{m_B^{z_A}}{m_A^{z_B}} \right] \cdot \Gamma \cdot \prod_{i=1}^{n} \left[\frac{A_{c,i}^{z_B} f_{A,i}^{z_B}}{B_{c,i}^{z_A} f_{B,i}^{z_A}} \right]^{X_i} \quad \ldots\ldots(5.62)$$

where the terms $f_{A,i}$ and $f_{B,i}$ describe the departure from ideality of ions A$^{z_A^\pm}$ and B$^{z_B^\pm}$ in the *ith* sub-lattice, and are related to the phenomenologically determined coefficients f_A and f_B by

$$\frac{f_A^{z_B}}{f_B^{z_A}} = \prod_{i=1}^{n} \left[\frac{f_{A,i}^{z_B}}{f_{B,i}^{z_A}} \right]^{X_i} \quad \ldots\ldots(5.63)$$

Because of the site heterogeneity of zeolites, this means that each site set can have its own excess energy term $(\lambda_{AB} - \lambda_{AA})_i$, resulting in a $\Lambda_{AB,i}$ value characteristic for each set. Furthermore, the total population of ions in any one set of sites, defined by equation (5.61) above, can change with zeolite composition[125]. Thus the contribution made by a particular $\Lambda_{AB,i}$ term towards the overall Λ_{AB} value will vary with composition. The ambiguities noticed when applying the Elprince-Babcock model to the zeolite systems studied in this project are therefore a result of an intrinsic property of the zeolite. This cannot be described as a failure of the Elprince-Babcock model, which worked quite well for clays, but rather a limitation on its application to zeolites because of the nature of these materials.

In earlier attempts to use the Elprince-Babcock model[111,117], it was not possible to get Λ values for all three of the conjugate binary systems used. This prevented the prediction stage of the model from being tested. In this project, two sets of binary systems were used to test the model, and the testing was carried out right through to the prediction stage because Λ values could be found for a fairly wide range of crystal phase compositions, although some discontinuities existed. Therefore, it can now be said conclusively for the first time that the Elprince-Babcock model cannot effectively predict ternary equilibria from binary data for zeolite systems.

5.6. GENERAL CONCLUSION

The main task of this project was to test the phenomenological model developed by Fletcher and Townsend[85-88] for ternary ion exchange in zeolites. The many stages of the model have been proven to be valid. The model worked successfully for a ternary uni-valent system where the third ion was highly preferred by the zeolite (silver) or minimally preferred (lithium). The solution phase predictions regarding the constancy of Γ was successfully tested using two different solution concentrations (0.04 and 0.1 equiv.dm^{-3}), and there are indications that the model can be applied to systems where the solution concentration was as high as 2.0 equiv.dm^{-3}, if sufficient data are available. The solution phase treatment stage of the model was shown to be valid at the high concentrations and also where three multi-valent anions were present. The original formulations of Γ_3/Γ_1 and Γ_3/Γ_2 of Fletcher and Townsend[87] have

been simplified.

The validity of the surface fitting stage of the model was shown to be correct by testing different systems and further-more, it was shown how the model could be successfully applied to systems where only a few ternary data points are available if some corresponding binary data were also incorporated into the fitting procedure.

Binary studies showed that zeolite X was capable of exchang-ing up to 100% when the cations sodium, potassium, lithium or silver were used, though a high ratio of cation concentration to zeolite was necessary if the cation was least preferred by the zeolite. The binary work showed the following select-ivity trend:

$$Li < Na < K < Ag$$
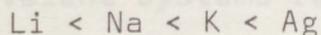
where the selectivity for potassium over sodium becomes rever-sed when the potassium loading in the zeolite exceeds 40%.

The binary thermodynamic treatment was also applied to a two-anion system where one anion had a valency greater than one. Valid results were obtained for this system even though a straight forward solution phase treatment could not be carried out due to lack of data. Furthermore, the semi-empirical solution phase treatment adopted for this system was developed mathematically to obtain expressions which allowed an unknown mean molal stoichiometric activity coefficient of a given salt to be predicted from zeolite equilibrium data. This prediction model could not be conclusively tested due to the uni-valent nature of the systems used.

Such a prediction model was shown to be inapplicable to a
ternary system. The ternary solution phase treatment was
developed to a point where it was shown that even using a
slightly simpler approach than used by Fletcher and Townsend[87],
the full solution phase treatment could not be carried out
unless the $\gamma_\pm$ values for *all* the salts in the system were
known.

Though the use of three uni-valent cations simplified the
mathematics of the model enormously, the very nature of uni-
valency removed the ability to test some aspects of the model
fully. For both binary and ternary systems it was not possible
to predict compositions at different solution concentrations
by applying suitable expressions. This is because the exchange
isotherms for uni-valent systems remain almost unchanged with
varying concentration (at the low concentrations used). The
binary and ternary isotherms obtained for the same cations at
different concentrations were also shown mainly to be similar
in this project.

Also carried out were predictions using the 'triangle rule'
where ternary equilibrium constants were predicted by use of
corresponding binary equilibrium constants. These predicted
values were compared with the experimental values, and were
found to be in very good agreement. Attempts were also made to
predict binary equilibrium constants using equilibrium constant
data from the conjugate binary systems, but here good agreement
was not found.

The zeolite phase activity coefficients obtained from the

(rigorous) thermodynamic treatment of binary exchange equilibria were used to predict the corresponding ternary activity coefficients using the Elprince-Babcock model which was originally developed for (and applied successfully to) clays. It was shown that the model cannot be applied to zeolites, due to the site heterogeneity associated with zeolites.

As a result of a long-term ion exchange study, it was shown that prolonged contact (12½ weeks) with water did not cause the zeolite to break down structurally. Furthermore, the similarity of results from the long-term study and an analogous short-term (6 days) study showed that any hydrolysis that occurs is primarily a function of successive contacts with *fresh* batches of solution, rather than long-term immersings in one solution[113].

For further work it is suggested that the following areas be investigated.

1) Multi-anion systems:

A suitable system where all the necessary solution phase information is available can be used to obtain an adequate quantity of data in order to test the Fletcher-Townsend model more fully.

2) High concentration systems:

Detailed studies at high concentrations are yet required in order to examine salt imbibition in multicomponent exchange systems.

3) Cations of different valences:

Ternary and quaternary systems involving multivalent exchange ions must be studied (preferably using cations capable of 100%

exchange). The presence of such cations would allow compositions at different concentrations to be predicted.

4) Partial exchange aspects:

The utility and applicability of normalization procedures for multicomponent exchange should be investigated in a further study.

5) Prediction of $\gamma_{\pm}$ values:

By using suitable binary exchange systems, further studies should be undertaken on the means by which activity coefficient values could be predicted using zeolites.
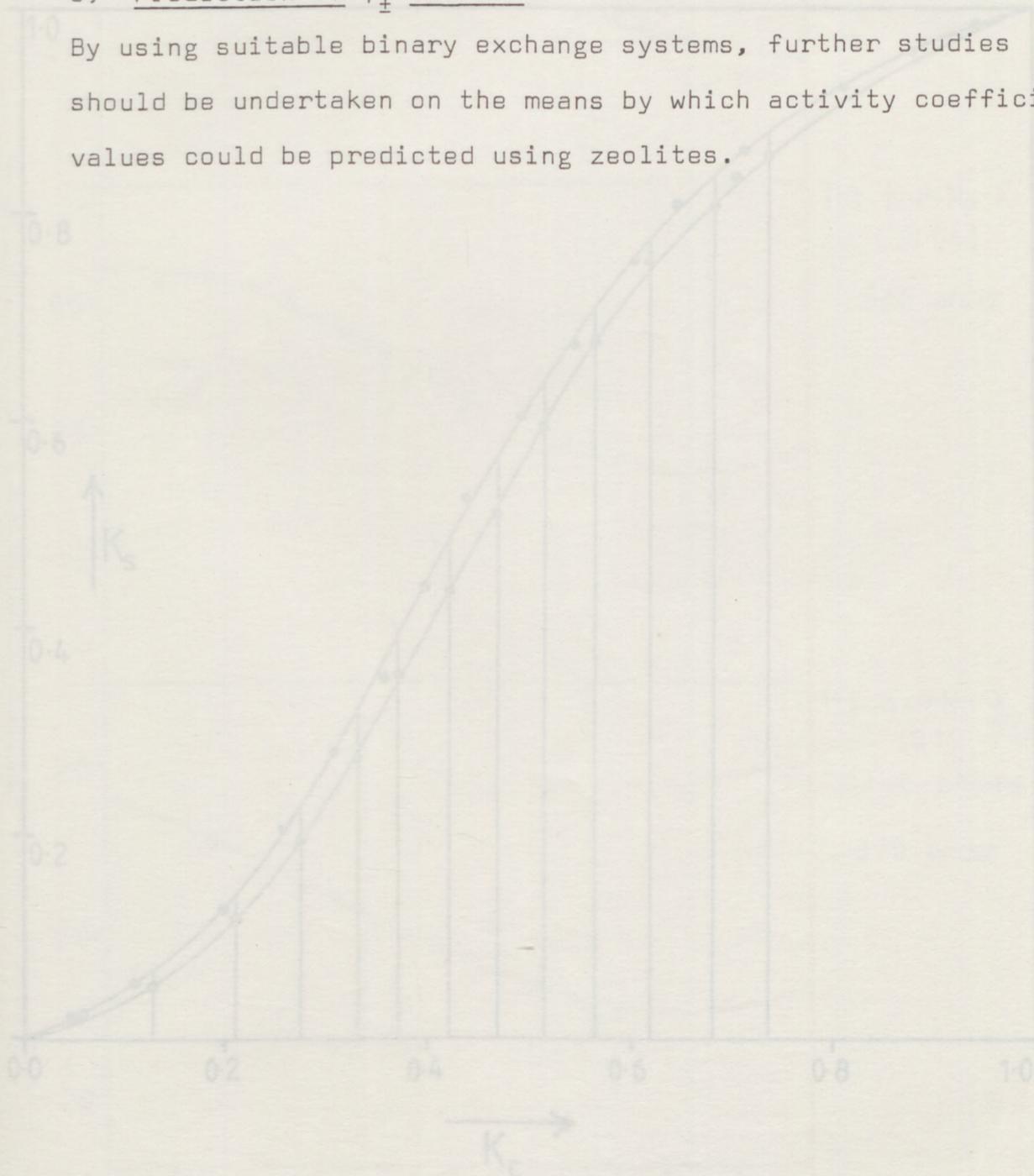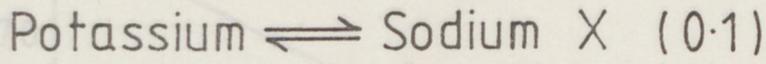
Potassium $\rightleftharpoons$ Sodium X (0·1)
One-anion system (above)
Two-anion system (below)

Figure 5.1

Figure 5.2

(a) Ag $\rightleftharpoons$ K-X
(0.04)
4th order
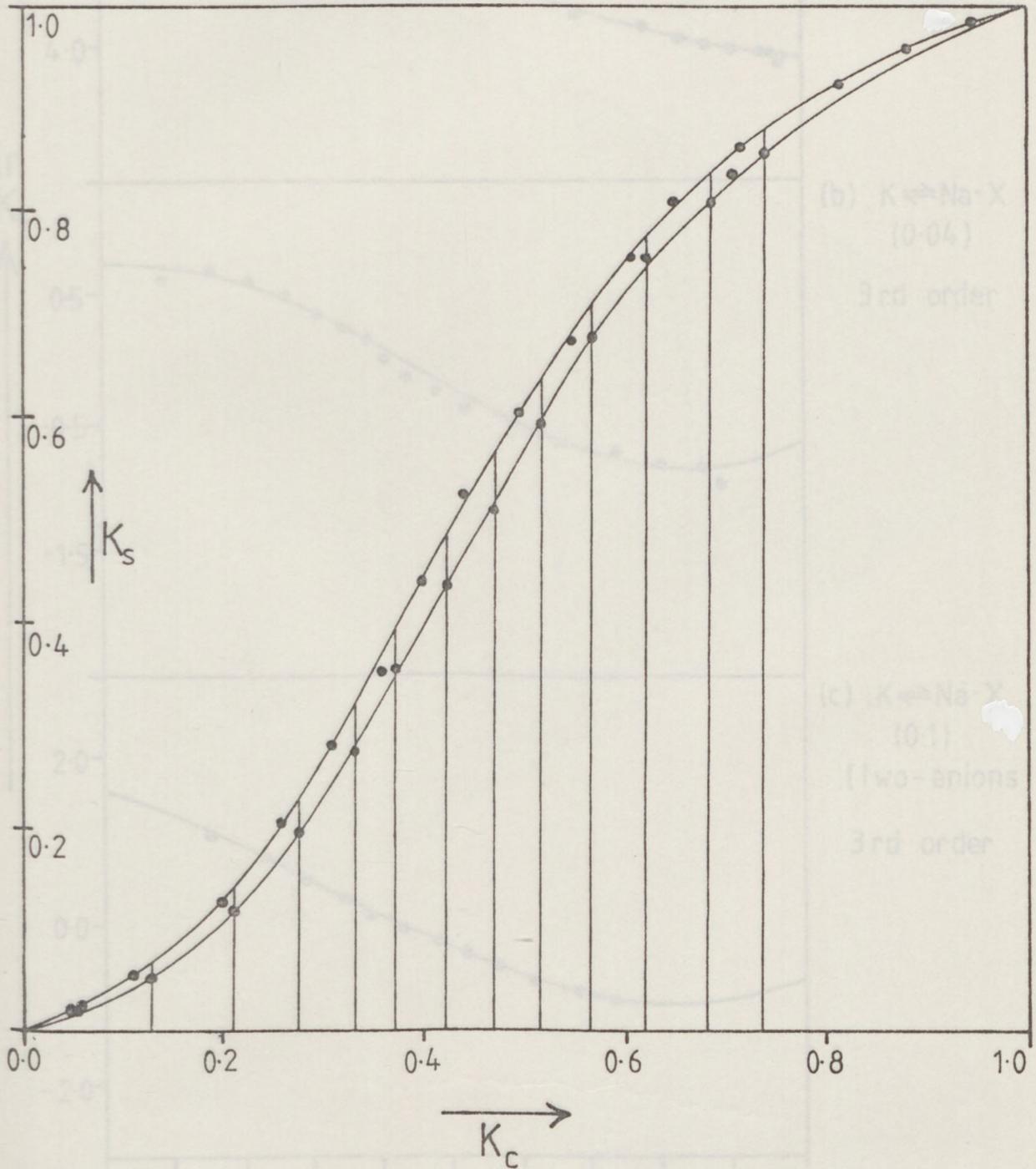
(b) K $\rightleftharpoons$ Na-X
(0.04)
3rd order

(c) K $\rightleftharpoons$ Na-X
(0.1)
[two-anions]
3rd order

ln K_c

A_c
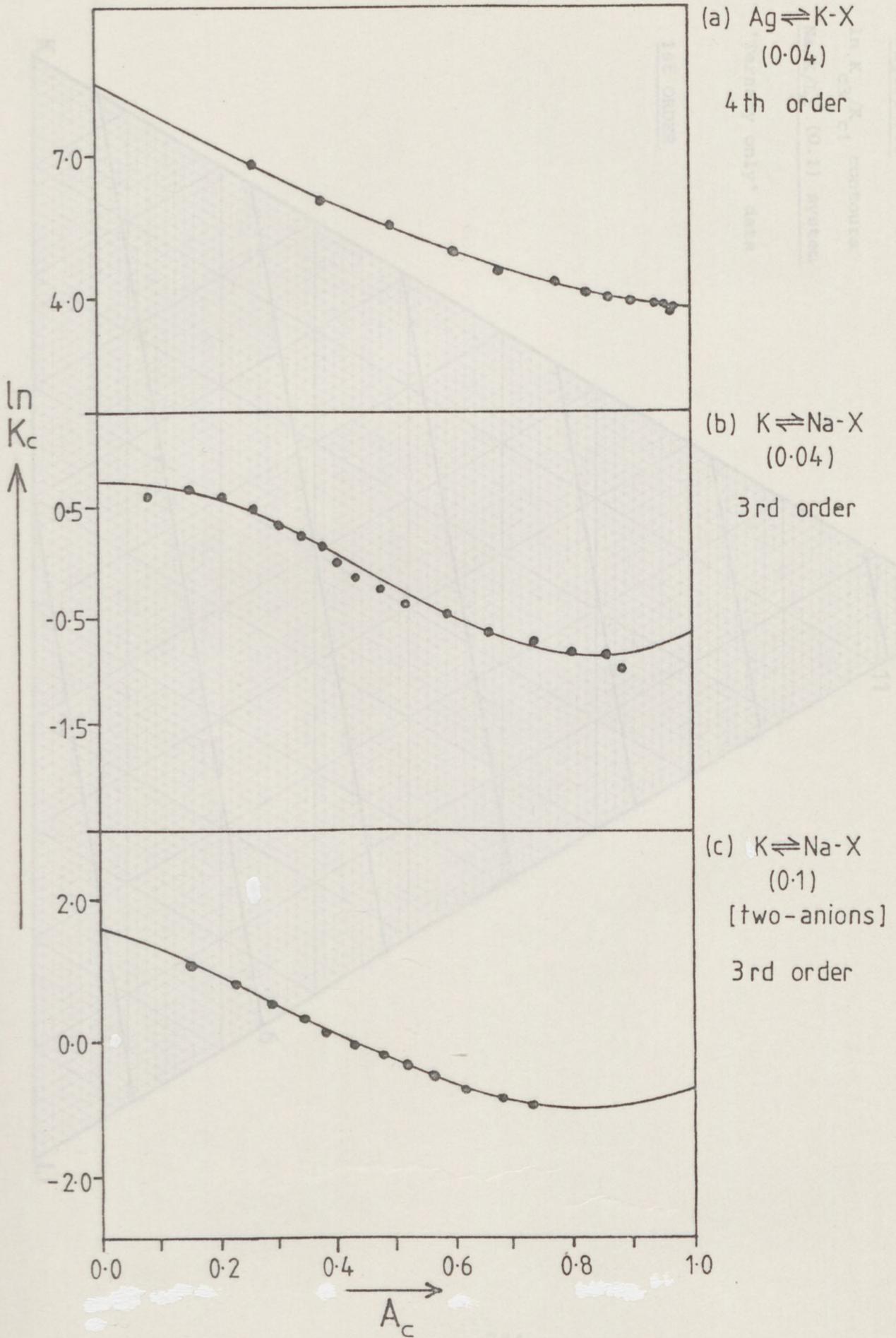
Figure 5.3

$\ln K_{c3}/K_{c1}$ contours

Na/K/Li (0.1) system

'Ternary only' data

1st ORDER
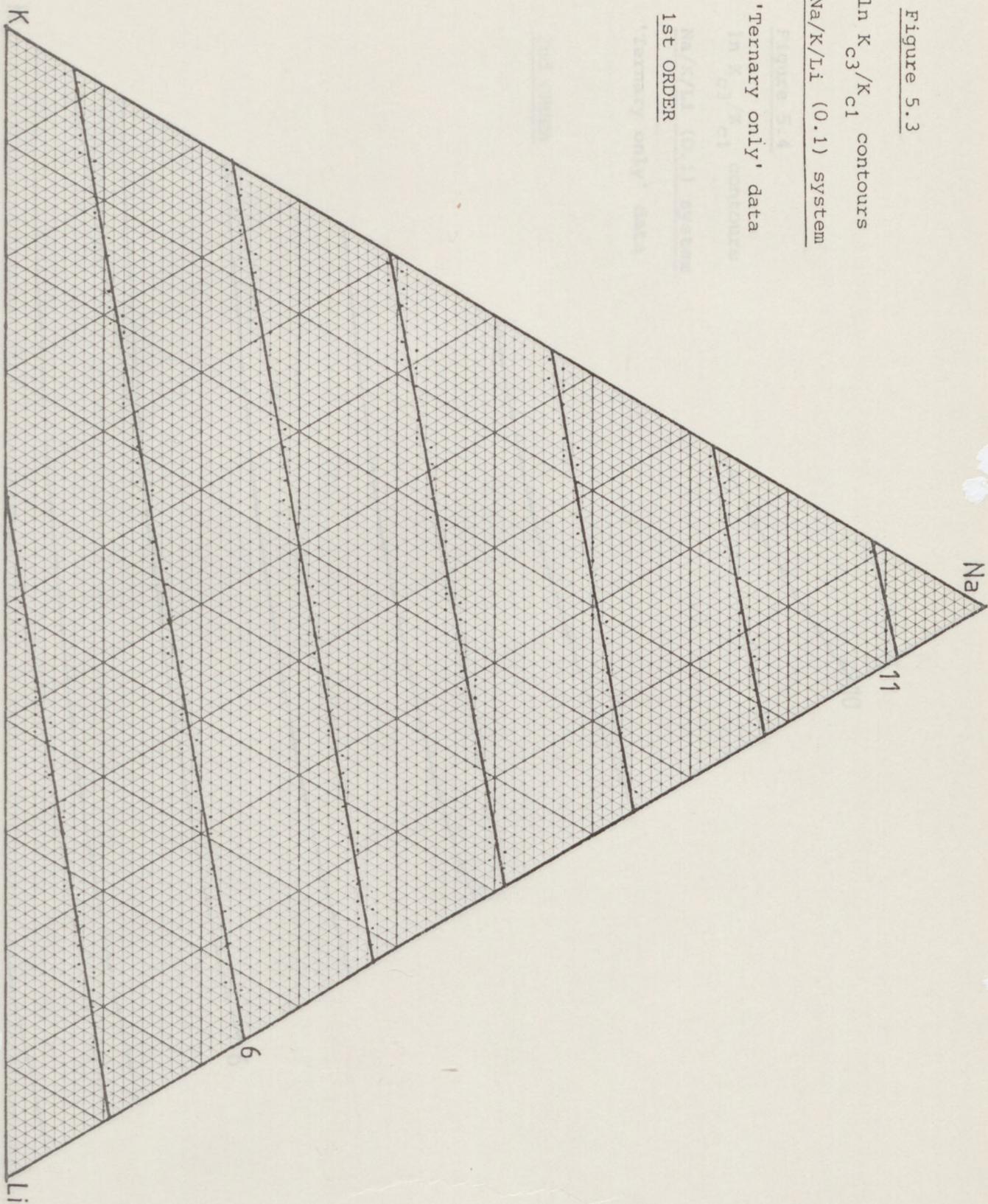
Figure 5.4

ln K_{c3}/K_{c1} contours

Na/K/Li (0.1) system

'Ternary only' data
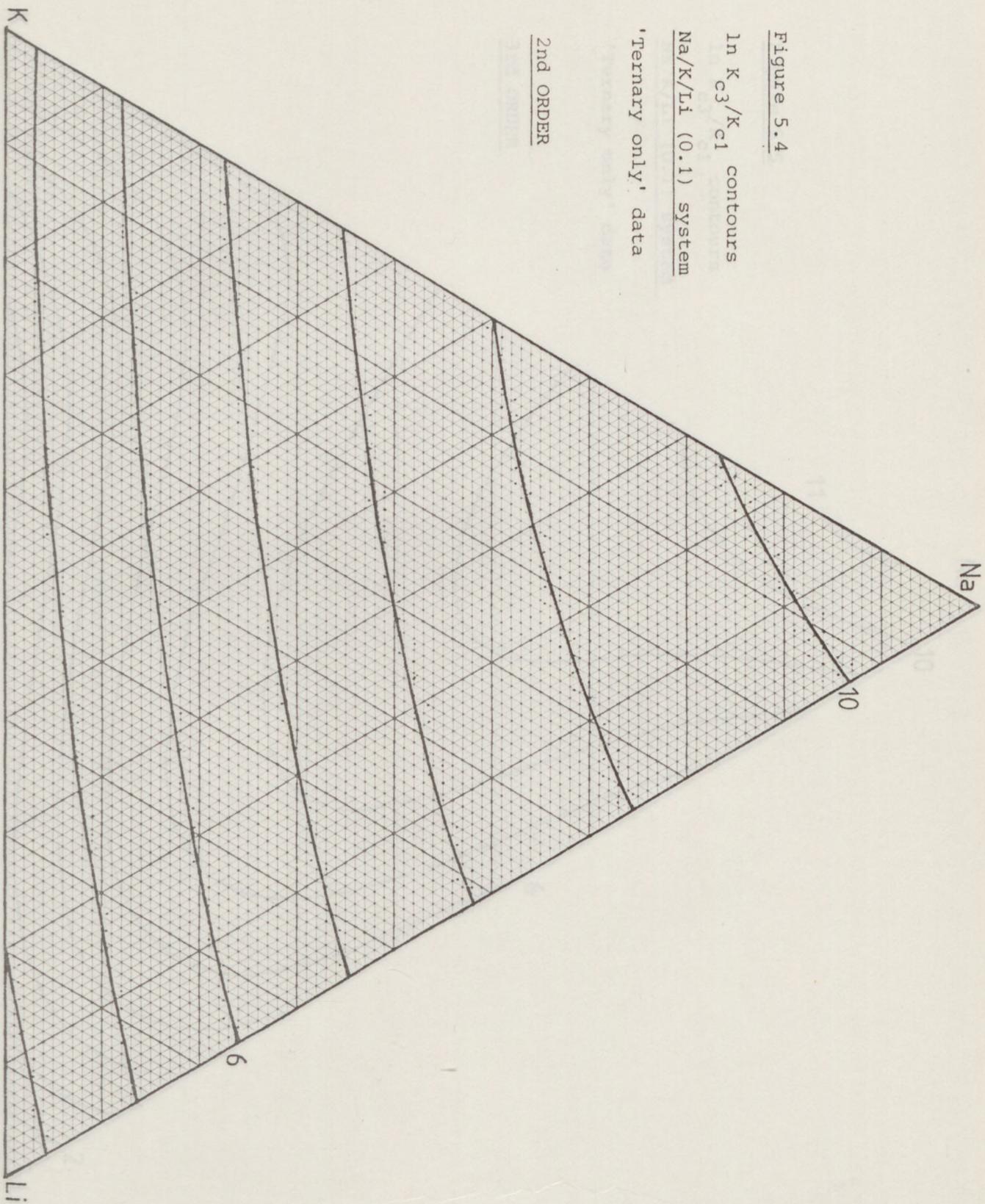
2nd ORDER

Figure 5.5

$\ln K_{c3}/K_{c1}$ contours

Na/K/Li (0.1) system

'Ternary only' data

3rd ORDER
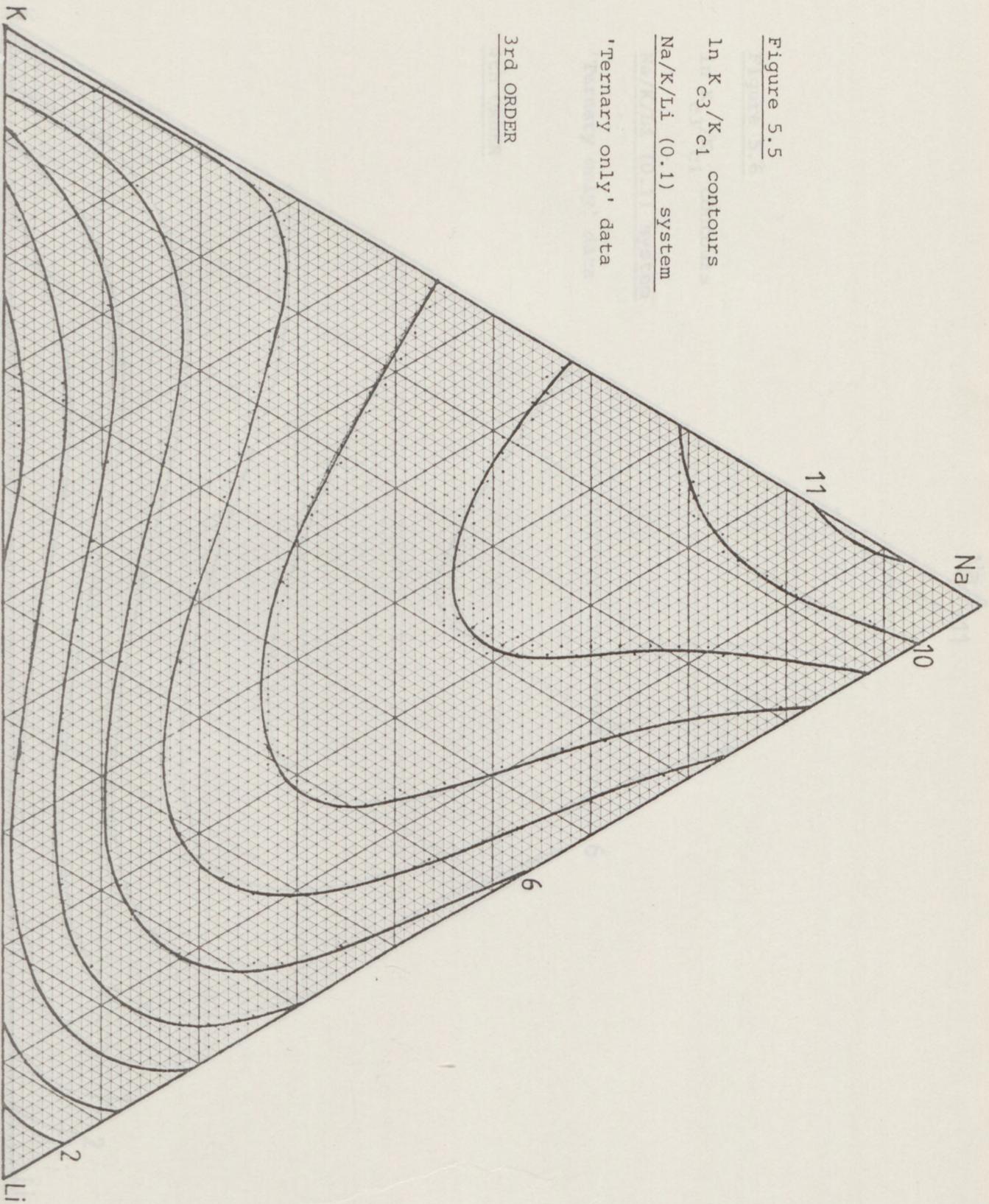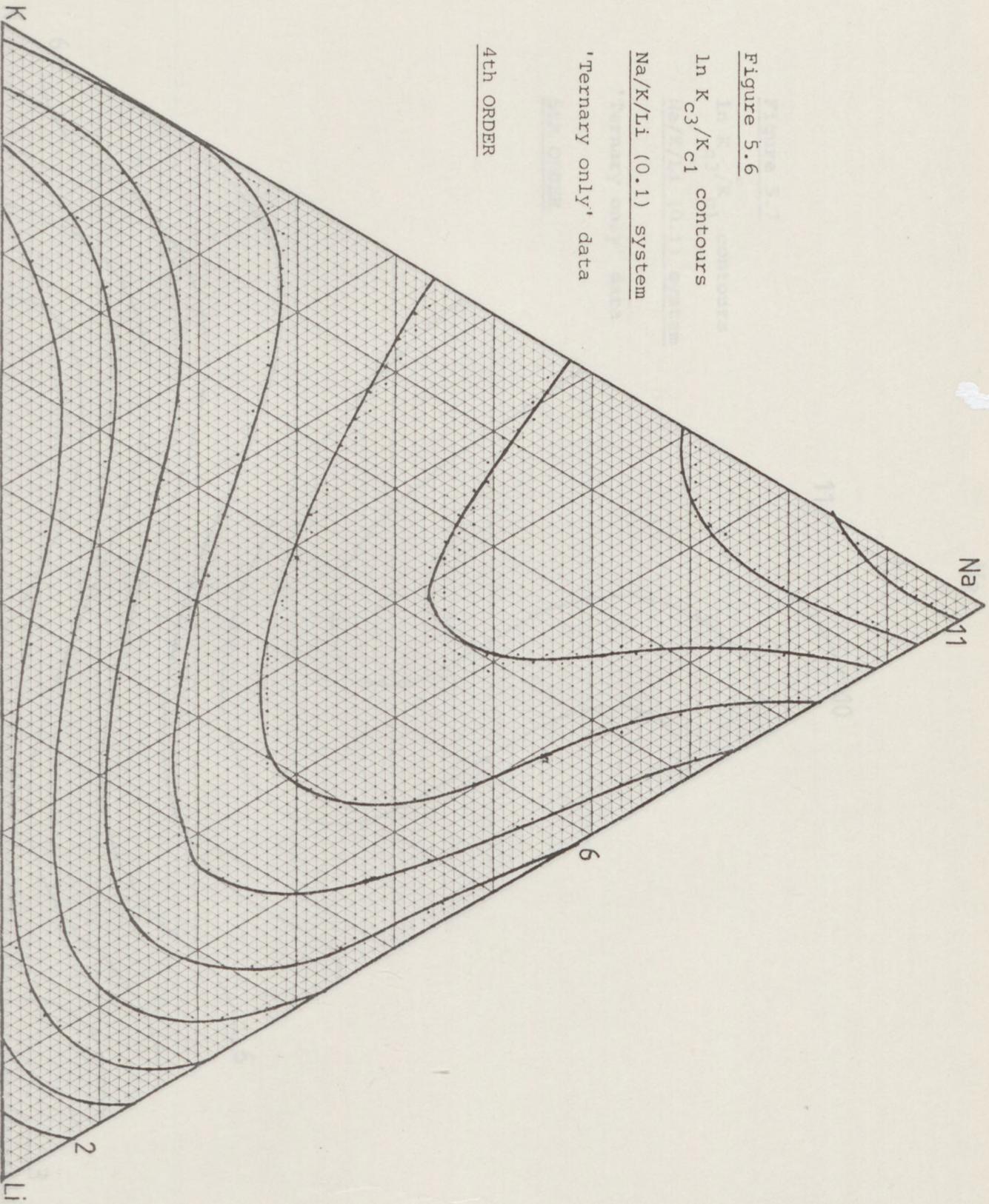
Figure 5.6

$\ln K_{c3}/K_{c1}$ contours

Na/K/Li (0.1) system

'Ternary only' data

4th ORDER

Figure 5.7

ln K_{c3}/K_{c1} contours

Na/K/Li (0.1) system

'Ternary only' data

5th ORDER
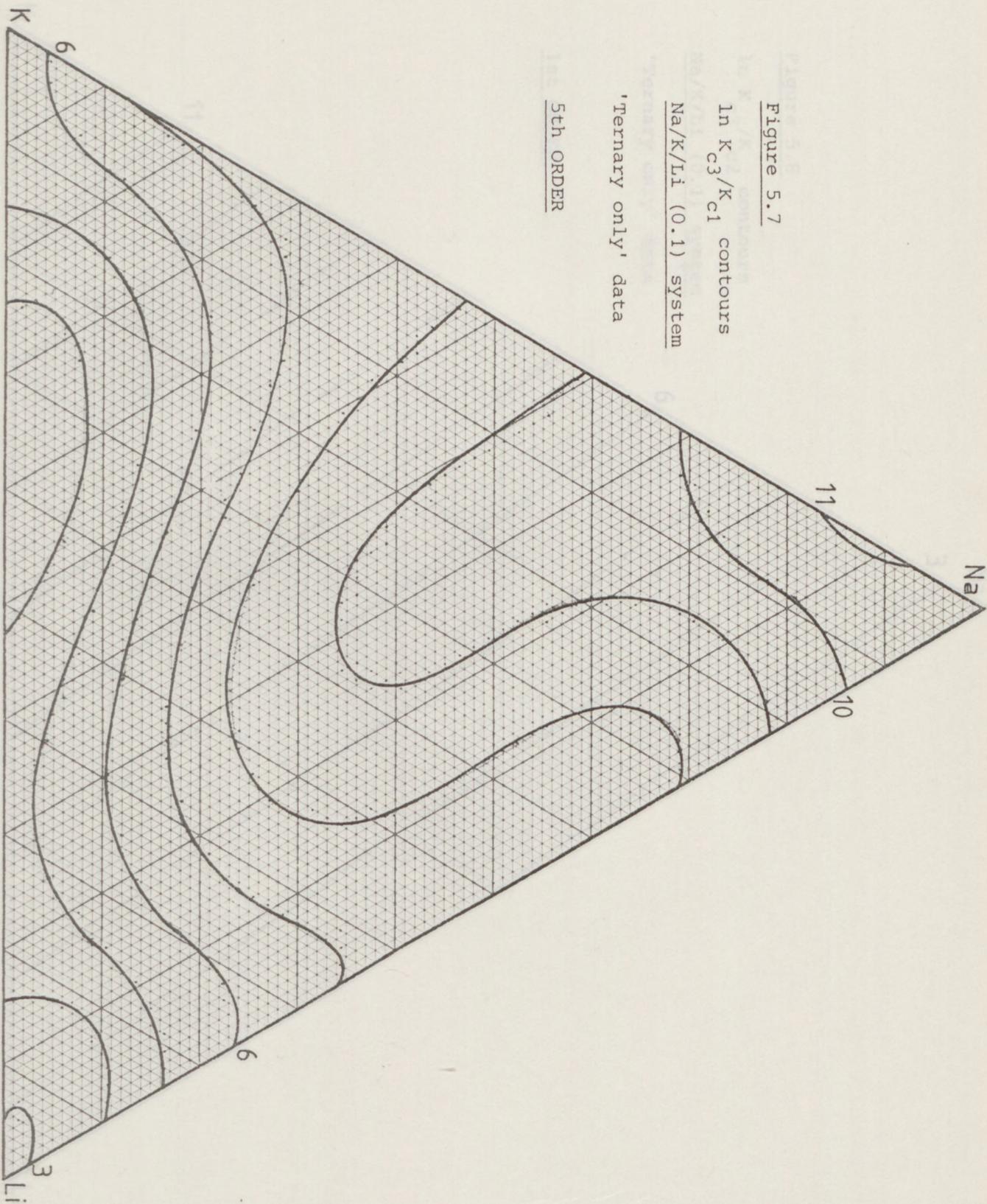
Figure 5.8
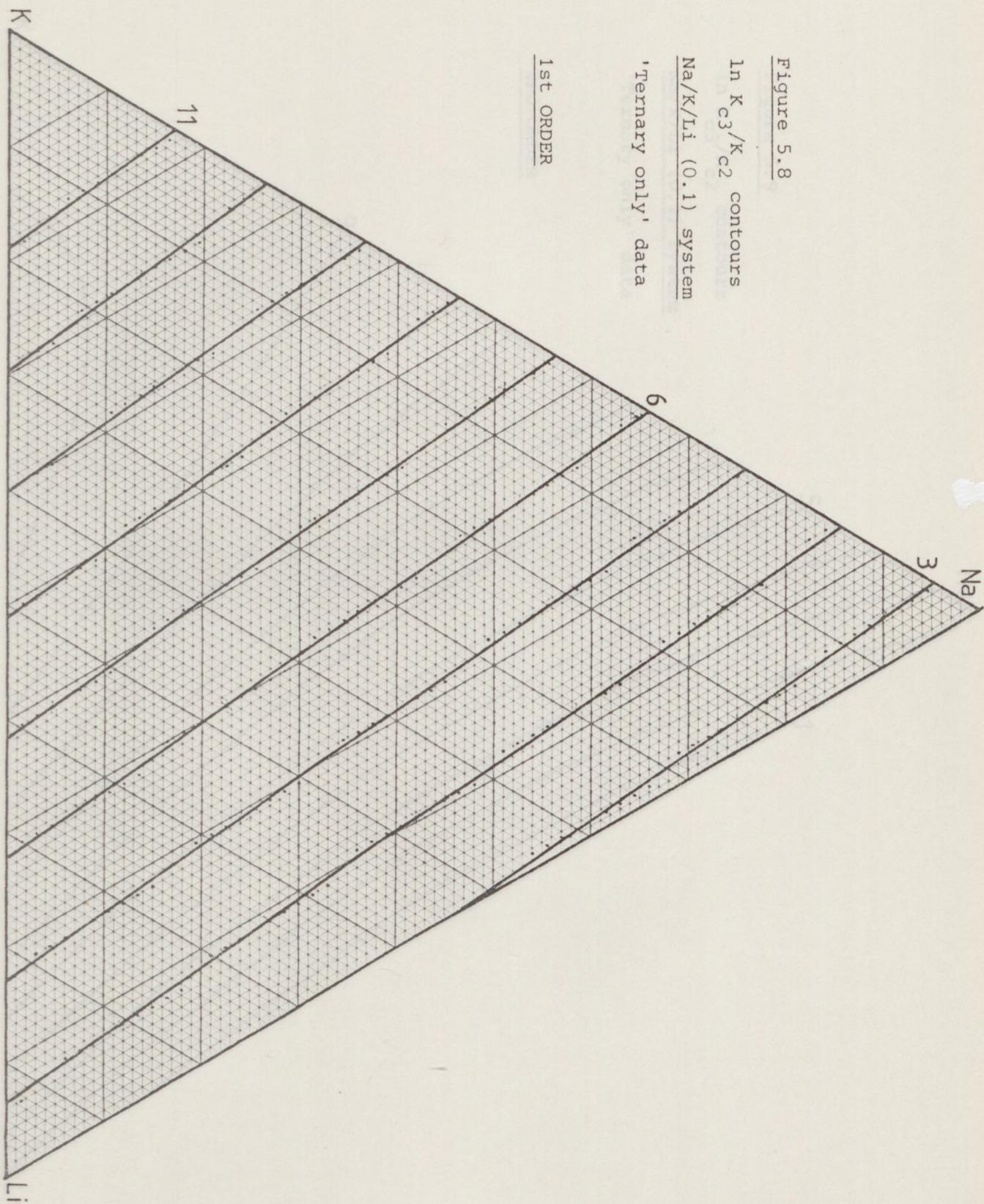
ln K_{c3}/K_{c2} contours

Na/K/Li (0.1) system

'Ternary only' data

1st ORDER

Figure 5.9
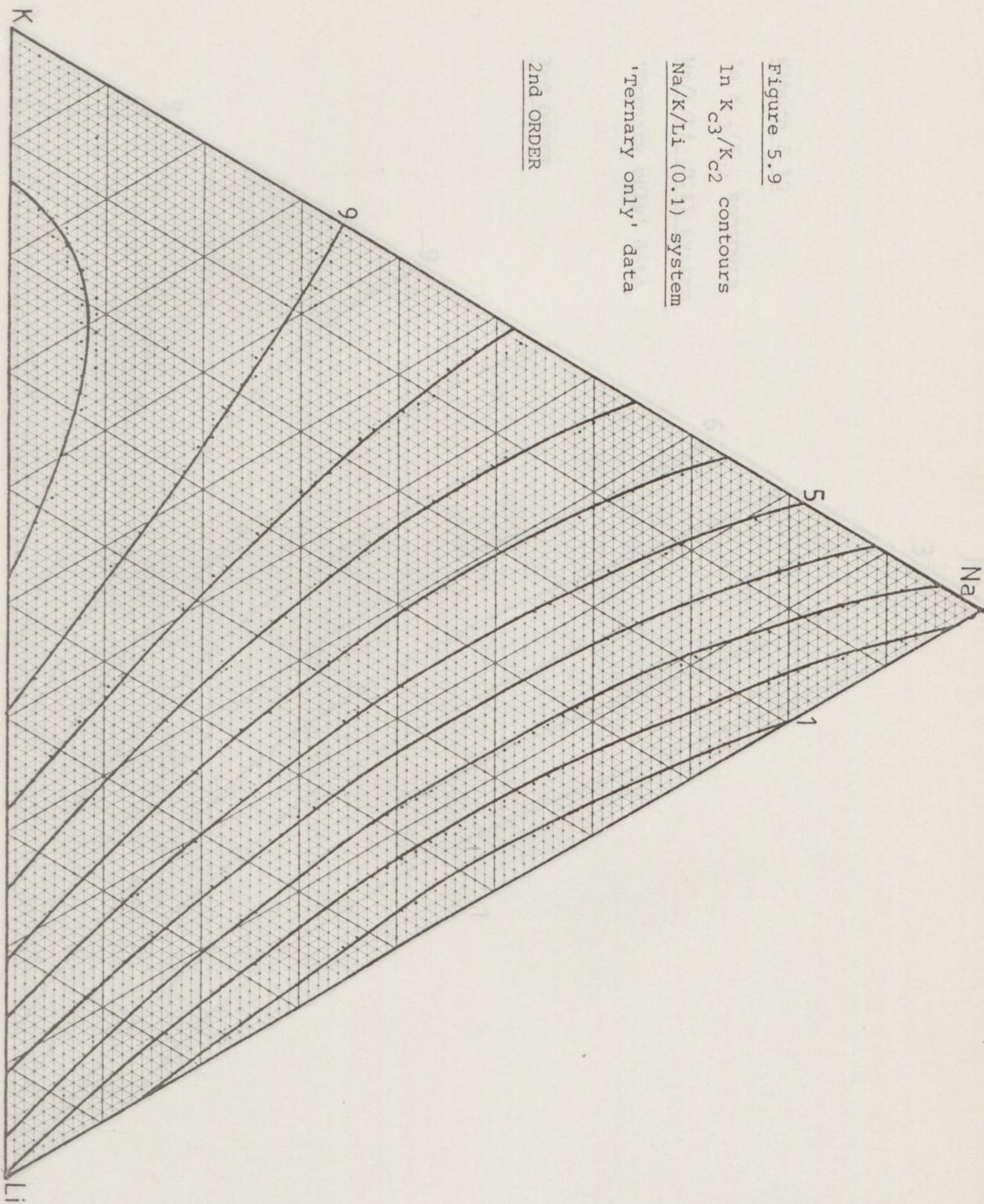
ln K_{c3}/K_{c2} contours

Na/K/Li (0.1) system

'Ternary only' data

2nd ORDER

Figure 5.10
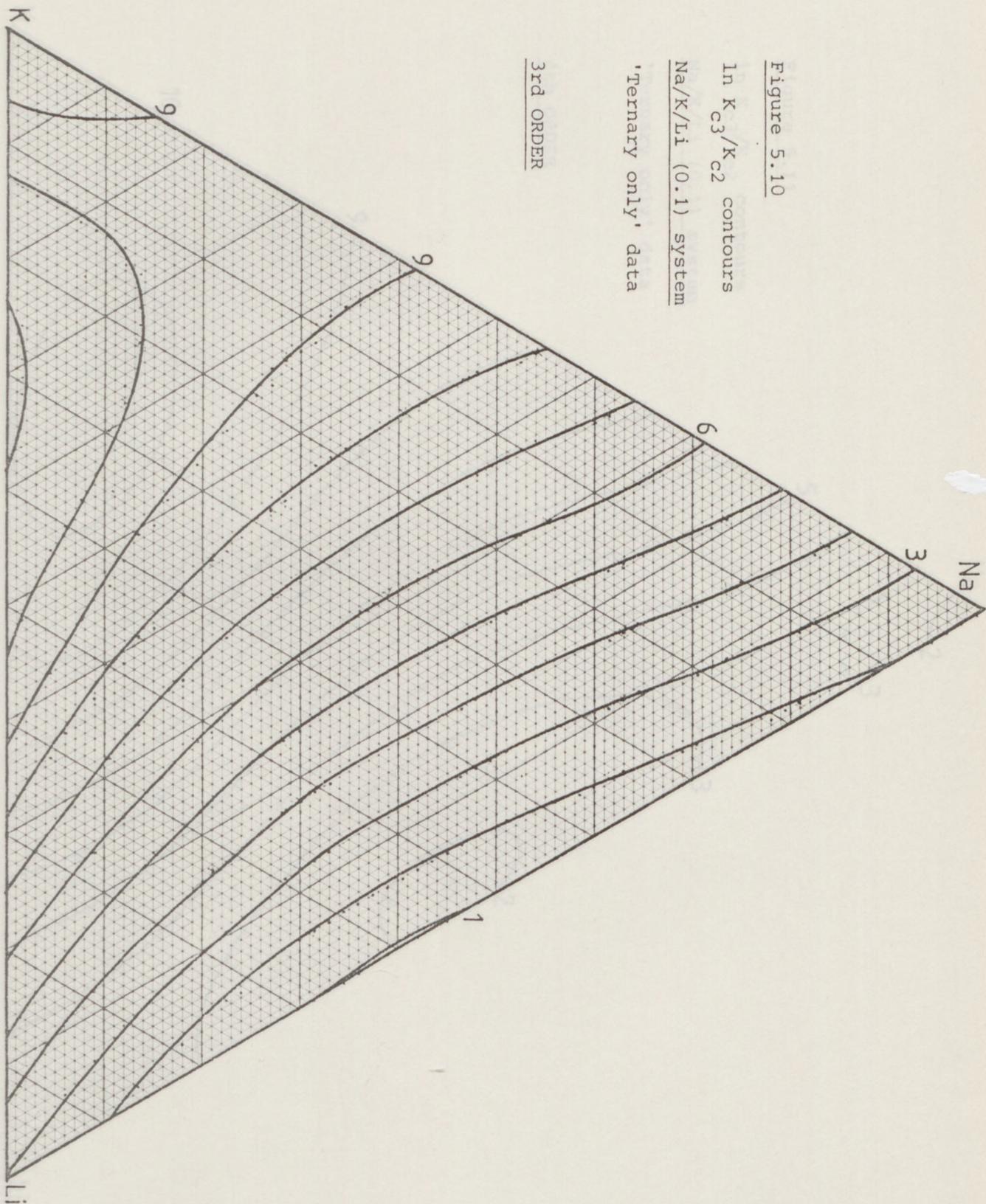
ln K_{c3}/K_{c2} contours

Na/K/Li (0.1) system

'Ternary only' data

3rd ORDER

Figure 5.11
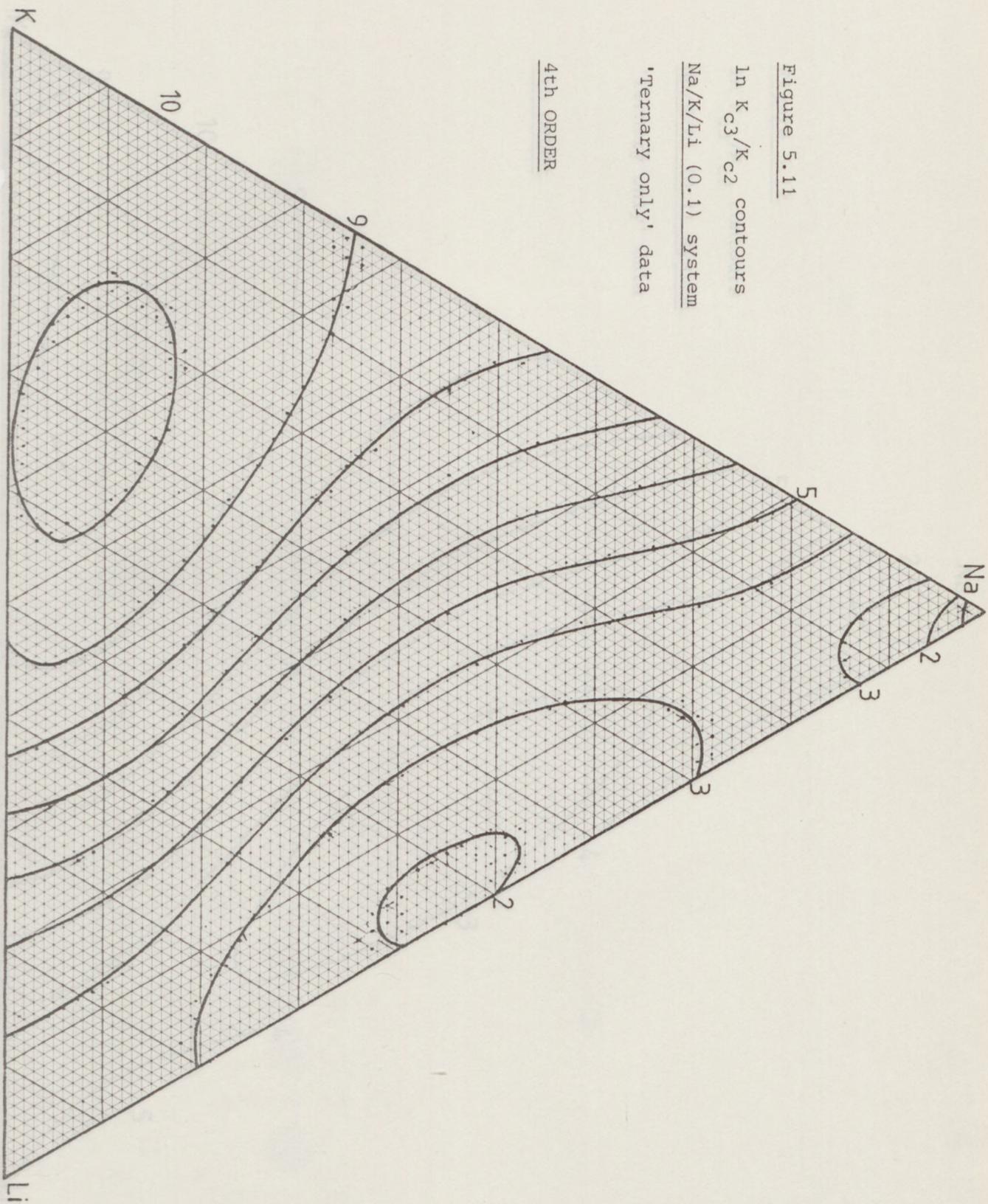
ln K_{c3}/K_{c2} contours

Na/K/Li (0.1) system

'Ternary only' data

4th ORDER

Figure 5.12

ln K_{c3}/K_{c2} contours

Na/K/Li (0.1) system

'Ternary only' data

5th ORDER
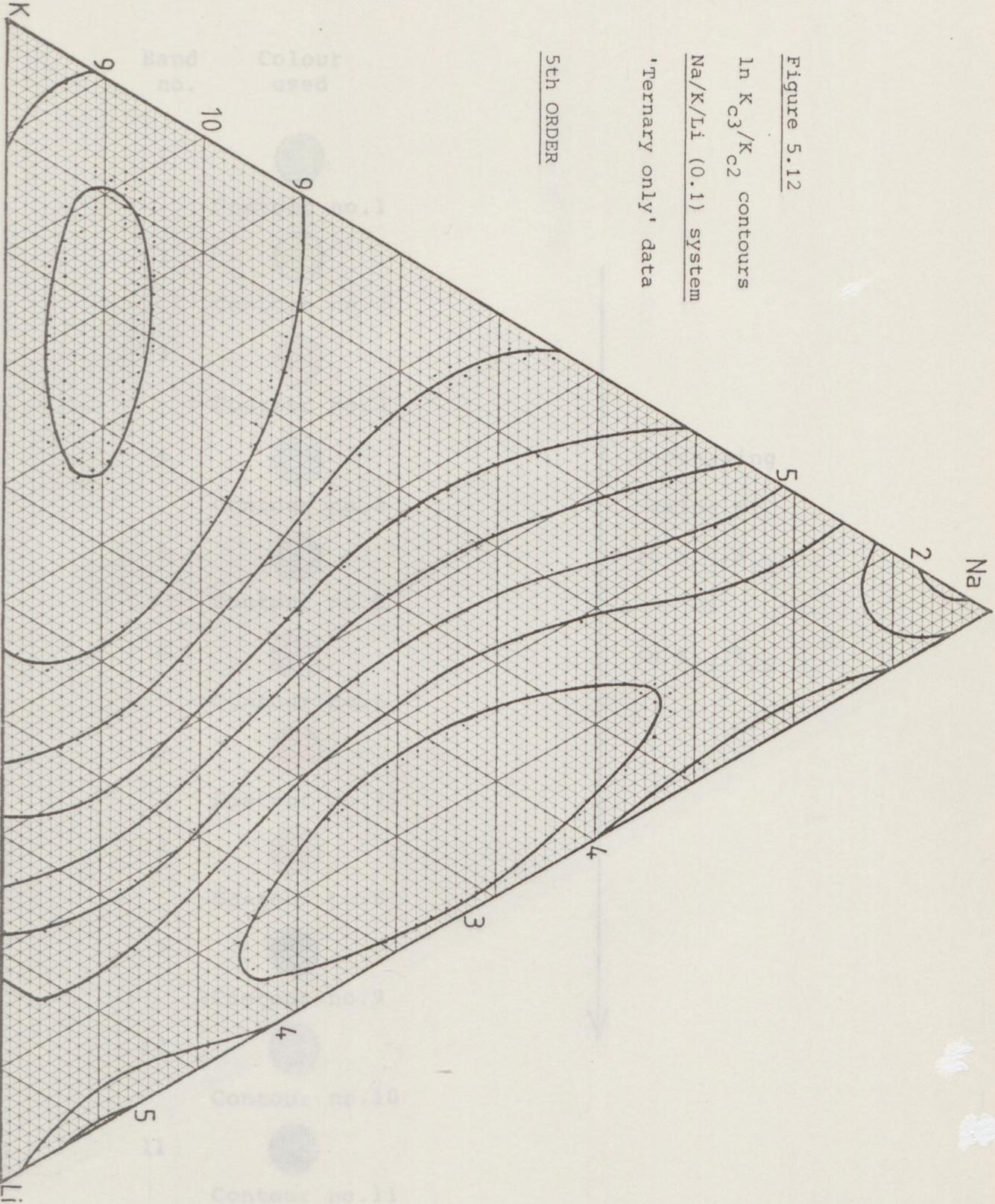
Band no.	Colour used
1	
	Contour no.1
2	
	Contour no.2
3	
	Contour no.3
4	
	Contour no.4
5	
	Contour no.5
6	
	Contour no.6
7	
	Contour no.7
8	
	Contour no.8
9	
	Contour no.9
10	
	Contour no.10
11	
	Contour no.11
12	

Increasing

value of

$\ln K_{c3}/K_{c1}$

or

$\ln K_{c3}/K_{c2}$

Figure 5.13

ln K_{c3}/K_{c1} contours

Na/K/Li (0.1) system

'Ternary + binary' data
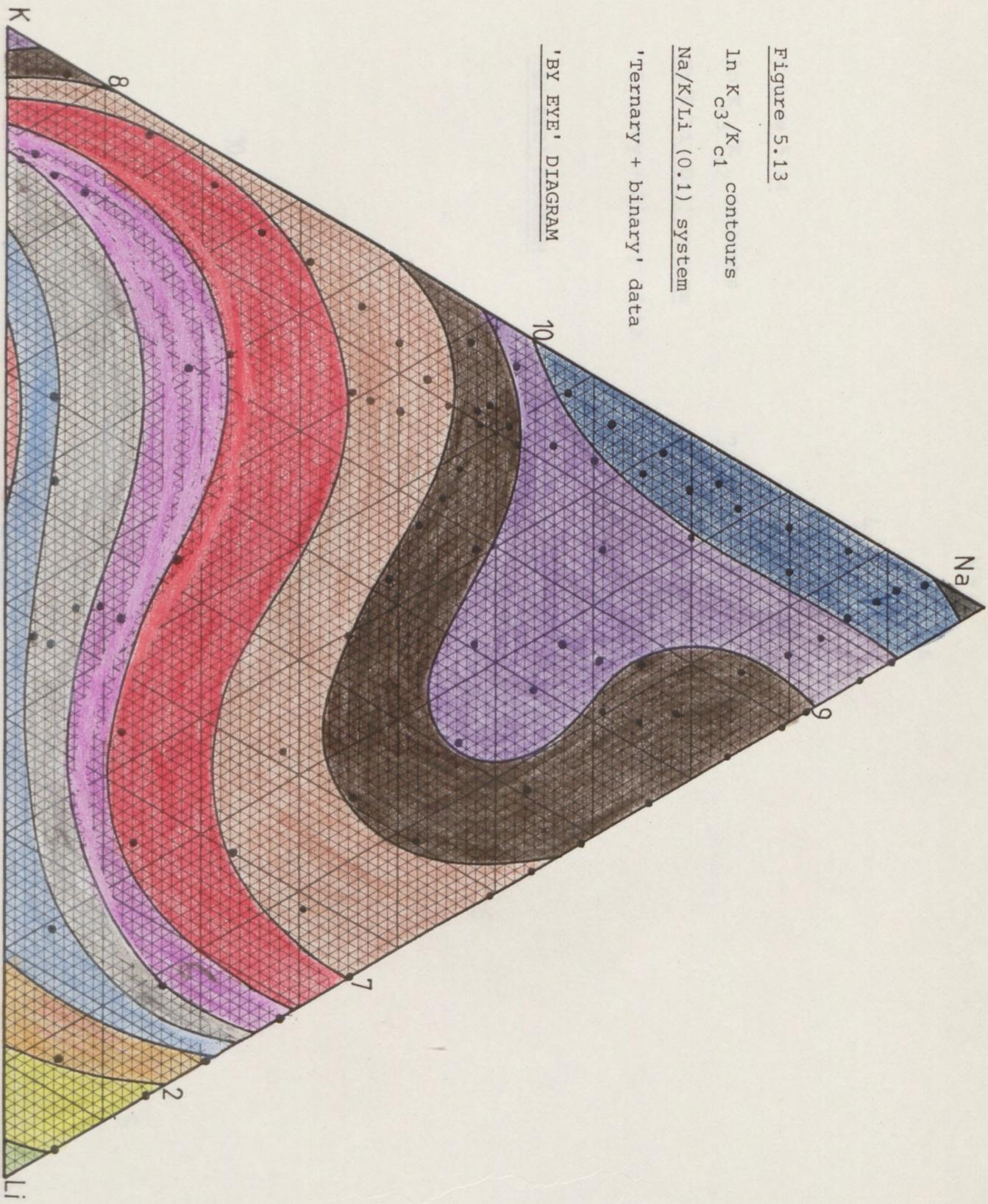
'BY EYE' DIAGRAM

Figure 5.14

ln K_{c3}/K_{c2} contours

Na/K/Li (0.1) system

'Ternary + binary' data

'BY EYE' DIAGRAM
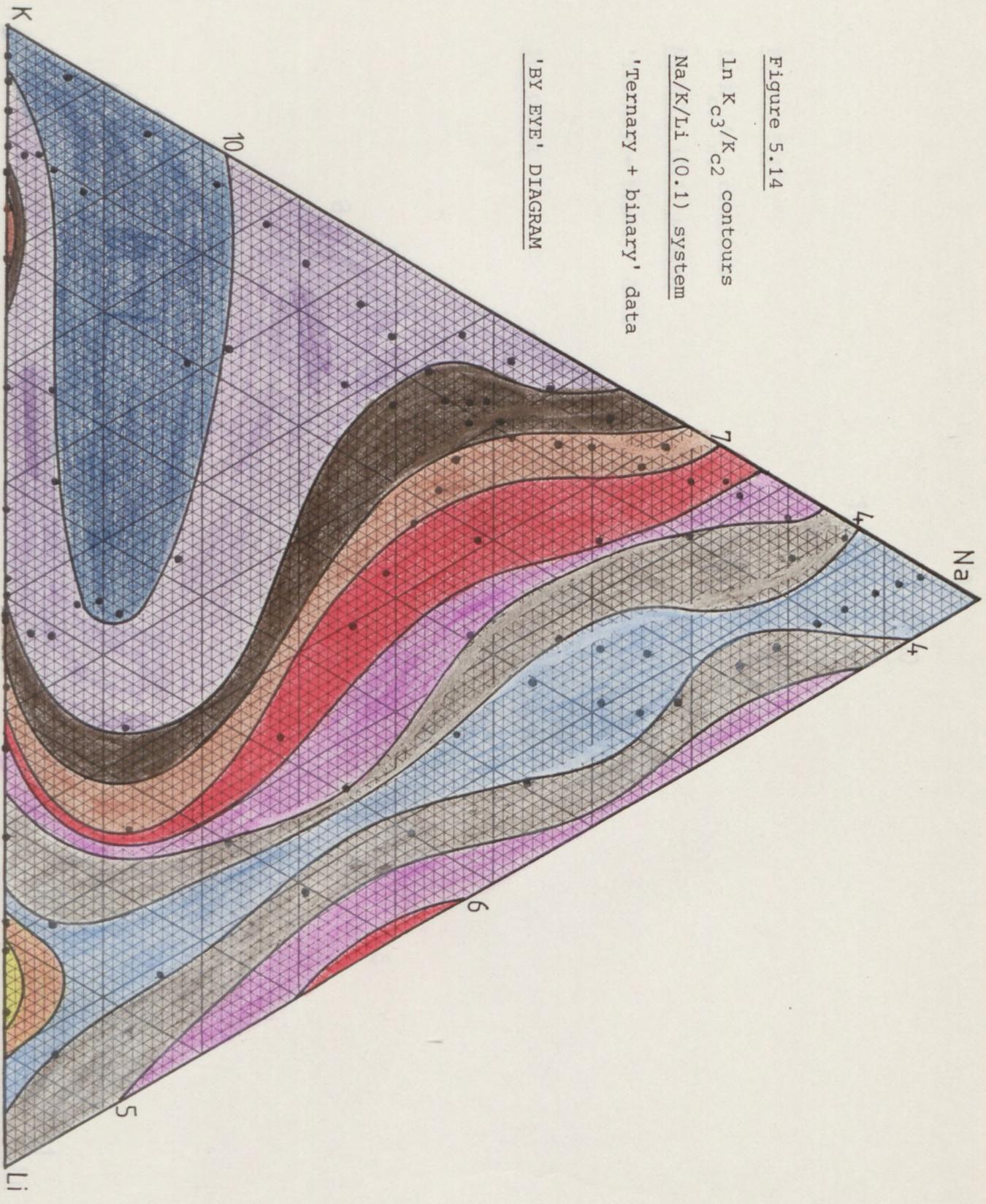
Figure 5.15

ln K_{c3}/K_{c1} contours

Na/K/Li (0.1) system

'Ternary + binary' data
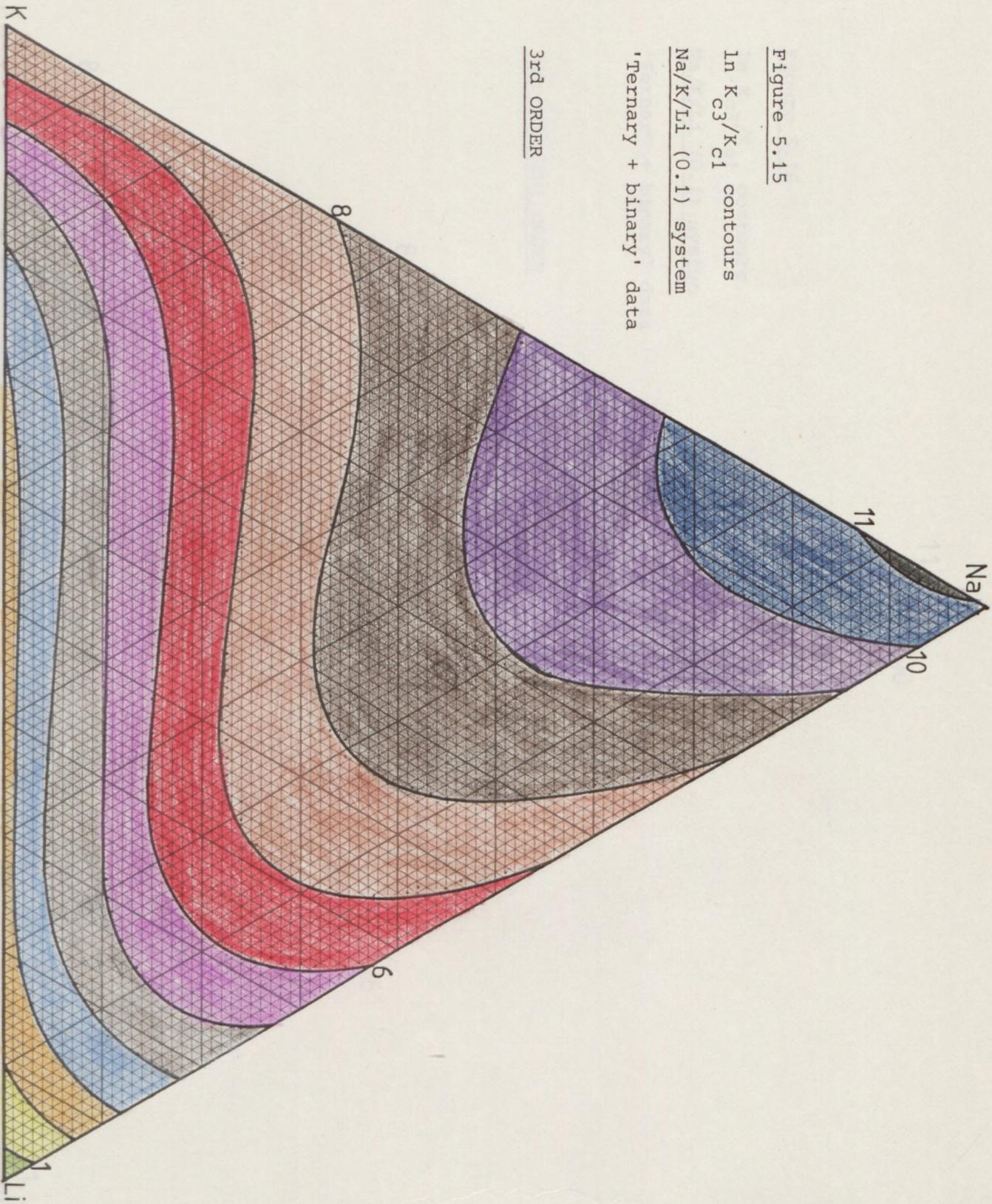
3rd ORDER

Figure 5.16

$\ln K_{c3}/K_{c1}$ contours

Na/K/Li (0.1) system

'Ternary + binary' data

4th (CHOSEN) ORDER
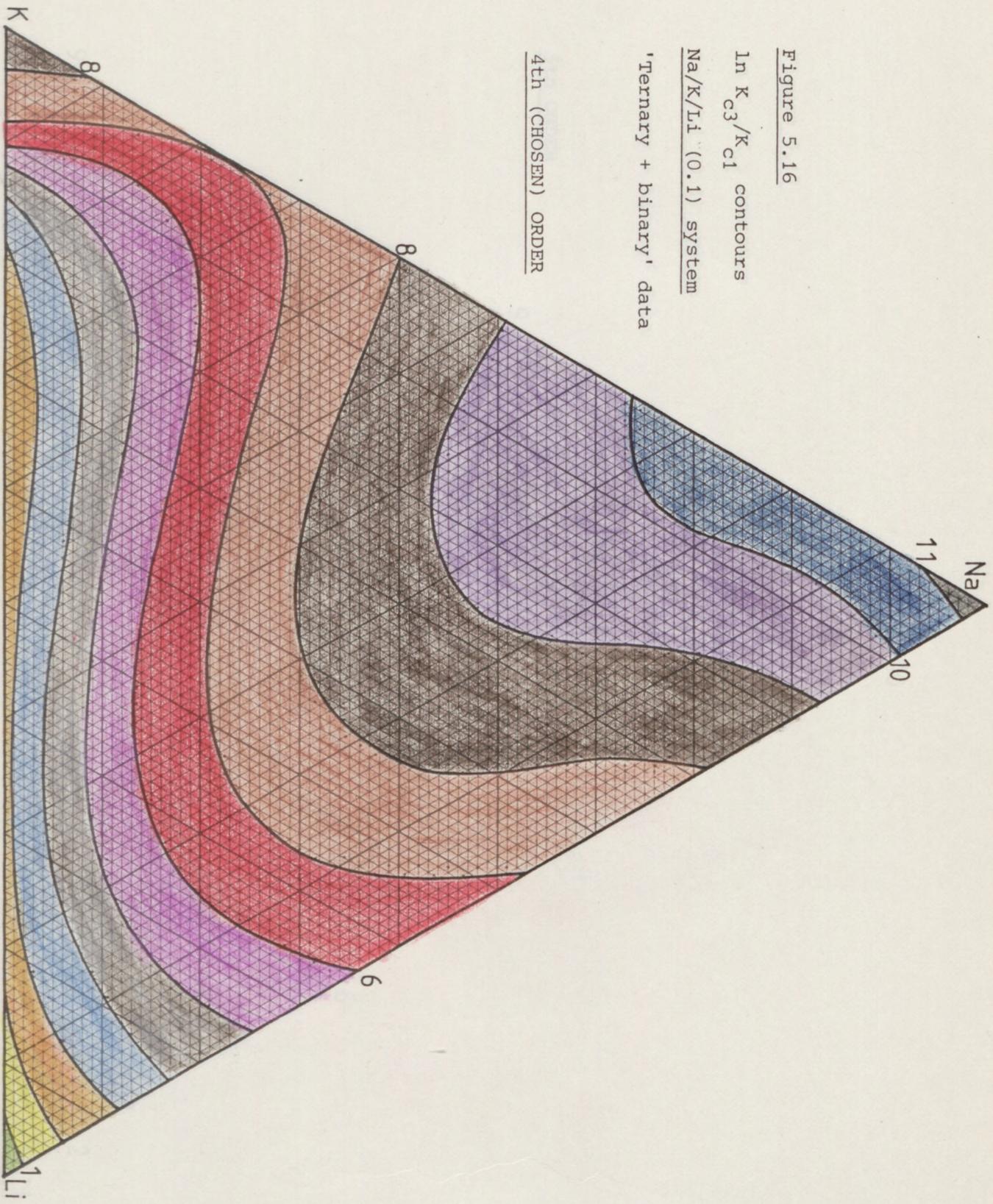
Figure 5.17

ln K_{c3}/K_{c1} contours

Na/K/Li (0.1) system

'Ternary + binary' data
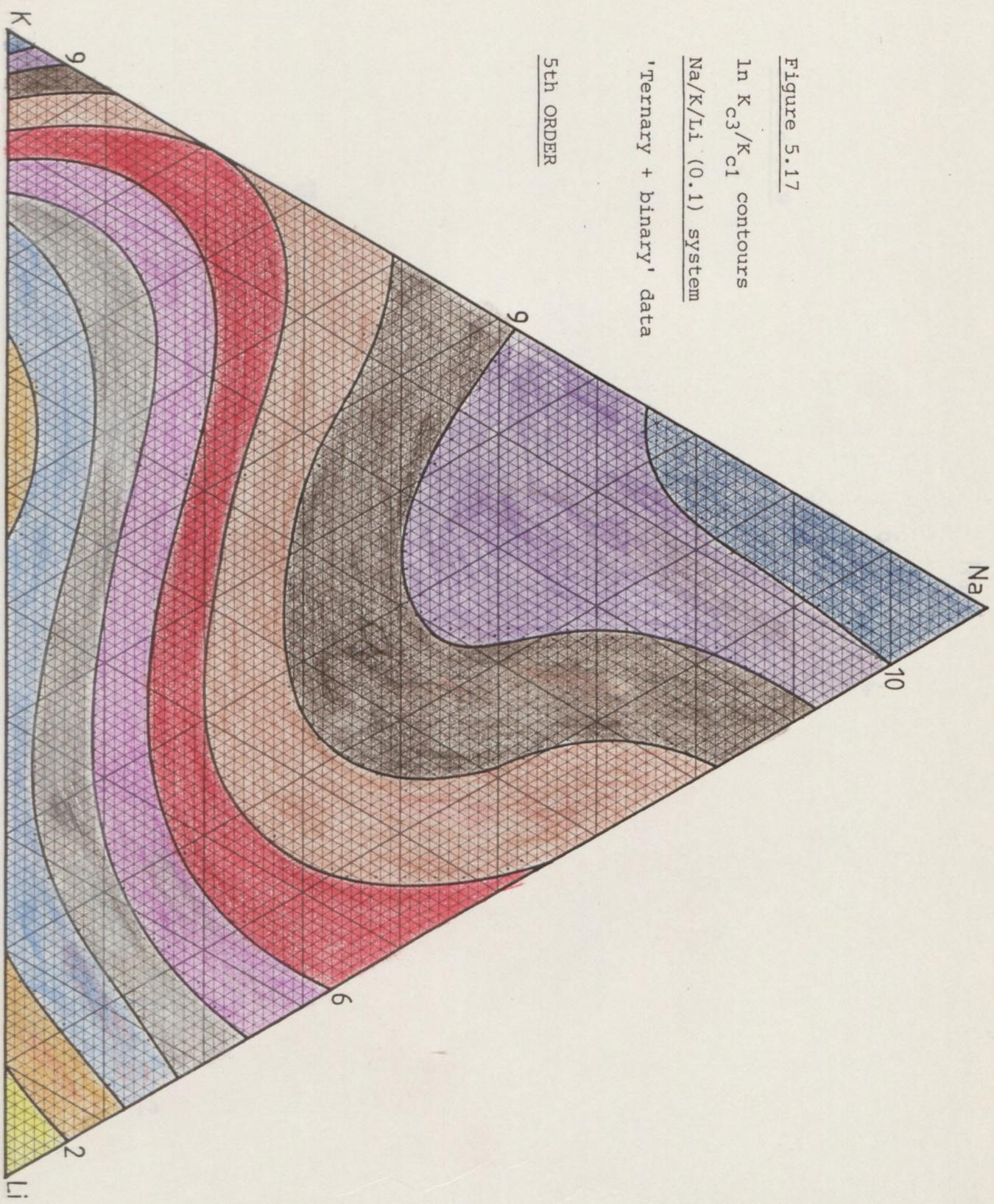
5th ORDER

Figure 5.18

ln K_{c3}/K_{c2} contours

Na/K/Li (0.1) system

'Ternary + binary' data

3rd ORDER
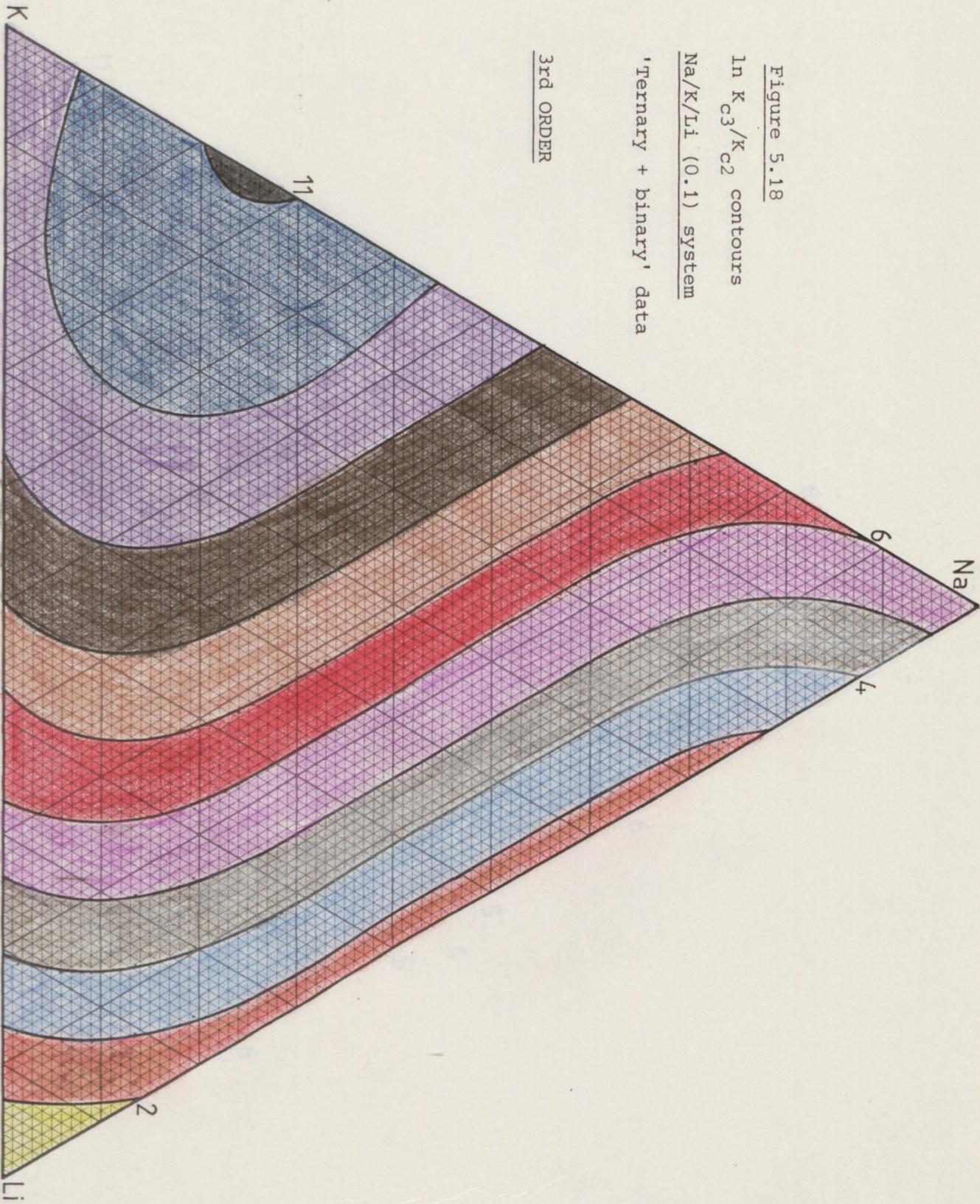
Figure 5.19

ln K_{c3}/K_{c2} contours

Na/K/Li (0.1) system

'Ternary + binary' data

4th ORDER
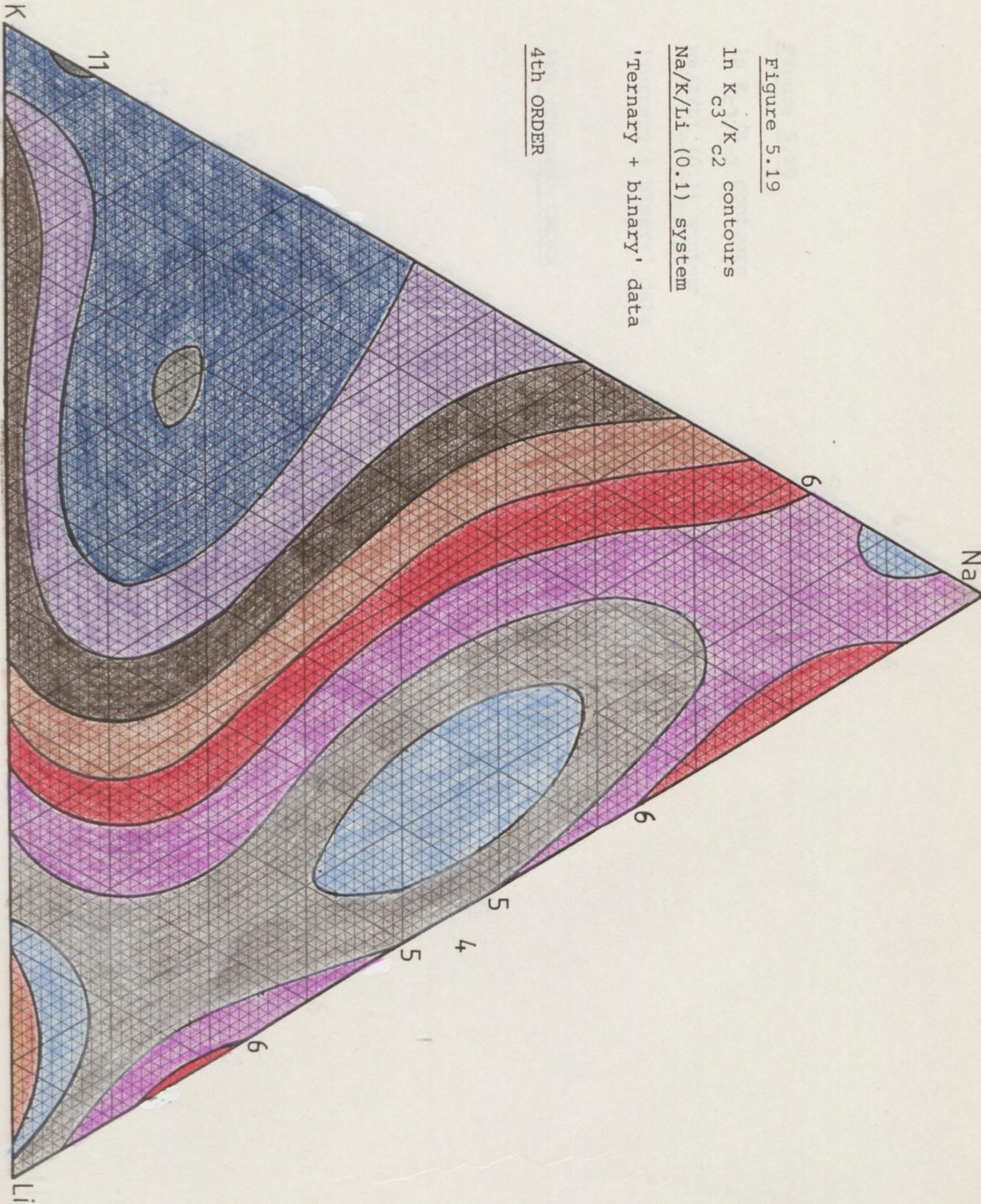
Figure 5.20

ln K_{c3}/K_{c2} contours

Na/K/Li (0.1) system

'Ternary + binary' data

5th (CHOSEN) ORDER
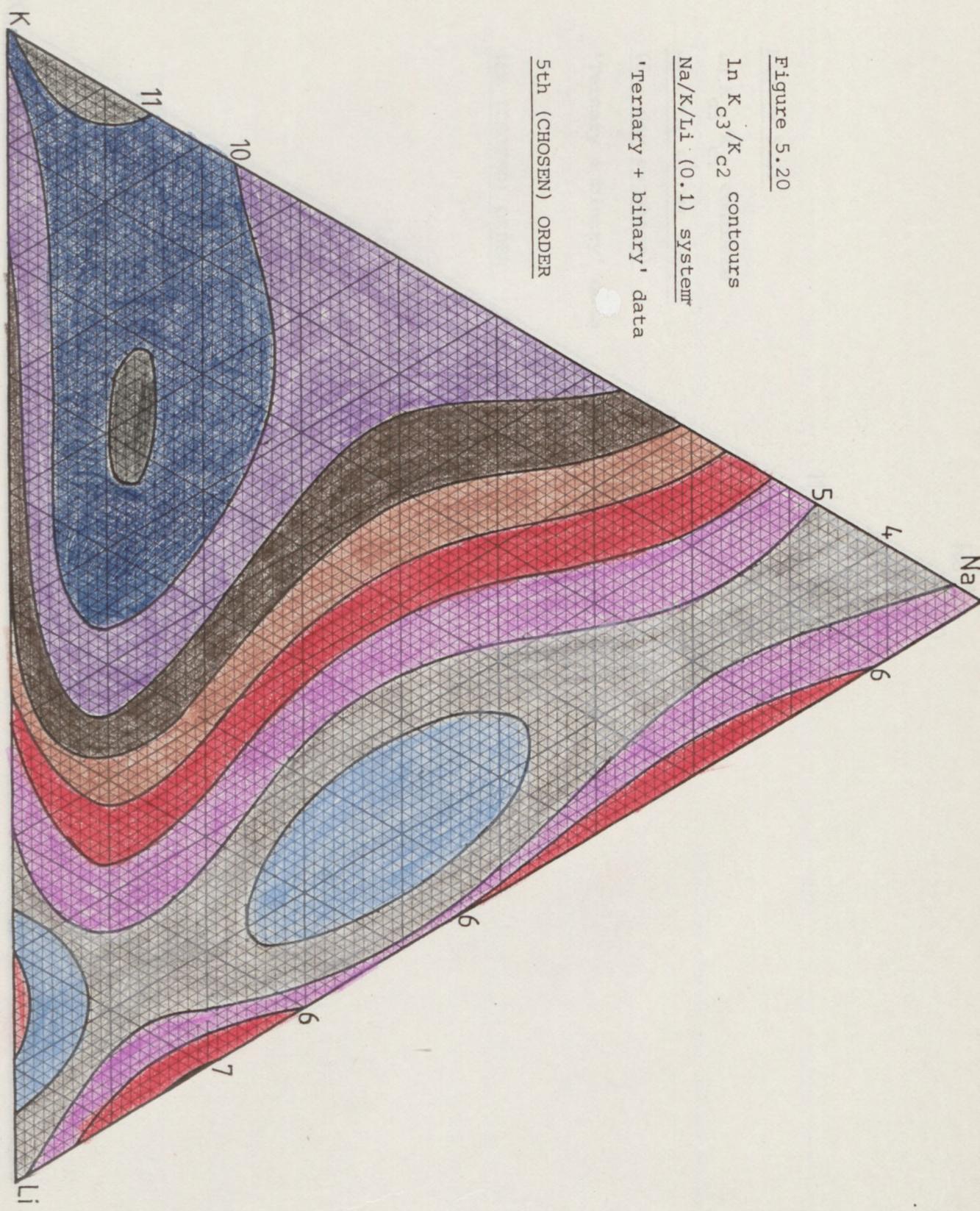
Figure 5.21

ln K_{c3}/K_{c1} contours

Na/K/Li (0.04) system

(6 – day exchange)

'Ternary + binary' data

4th (CHOSEN) ORDER

Figure 5.22

ln K_{c3}/K_{c2} contours
Na/K/Li (0.04) system
(6 – day exchange)
'Ternary + binary' data

1st (CHOSEN) ORDER

K

10

5

Na

1

Li
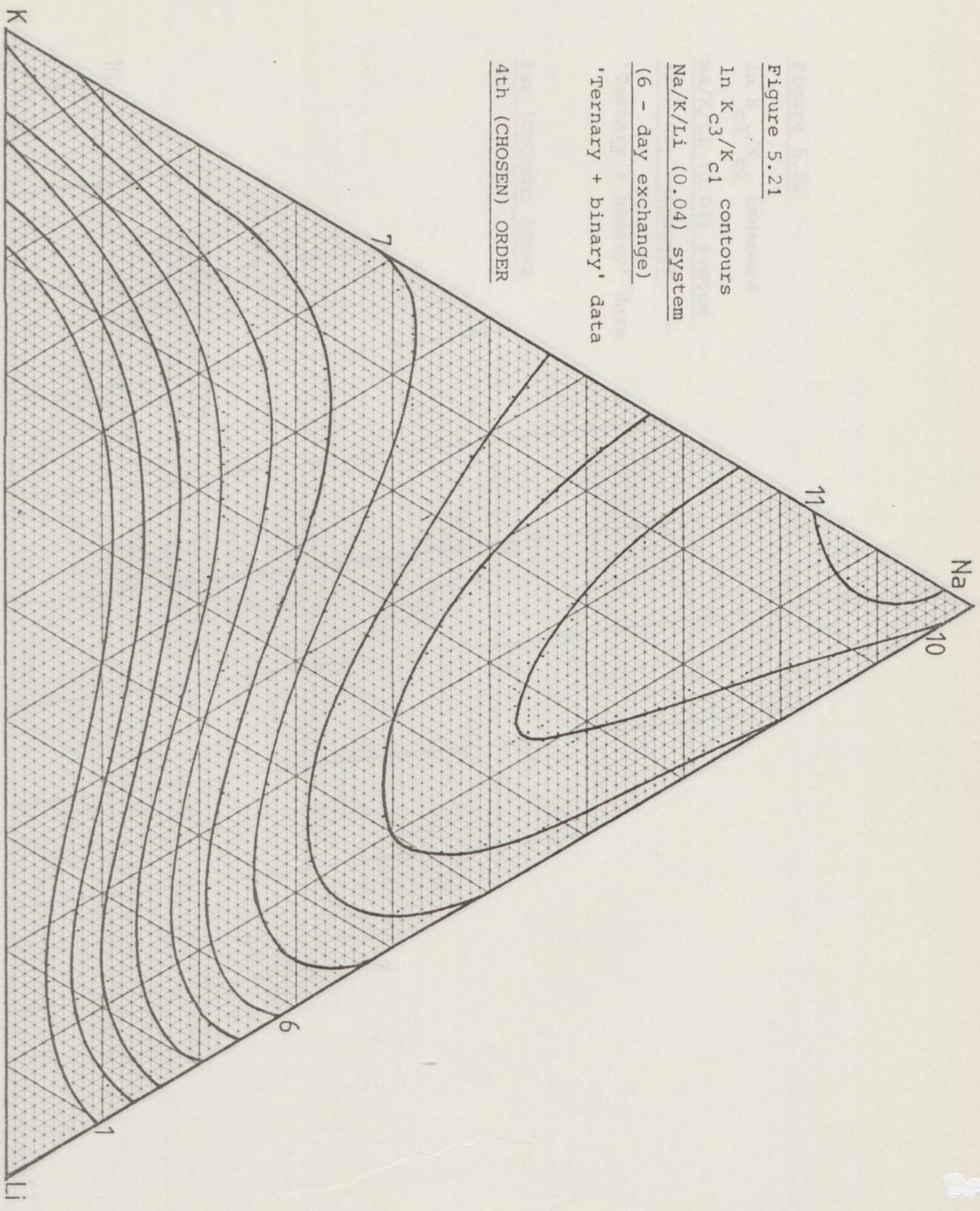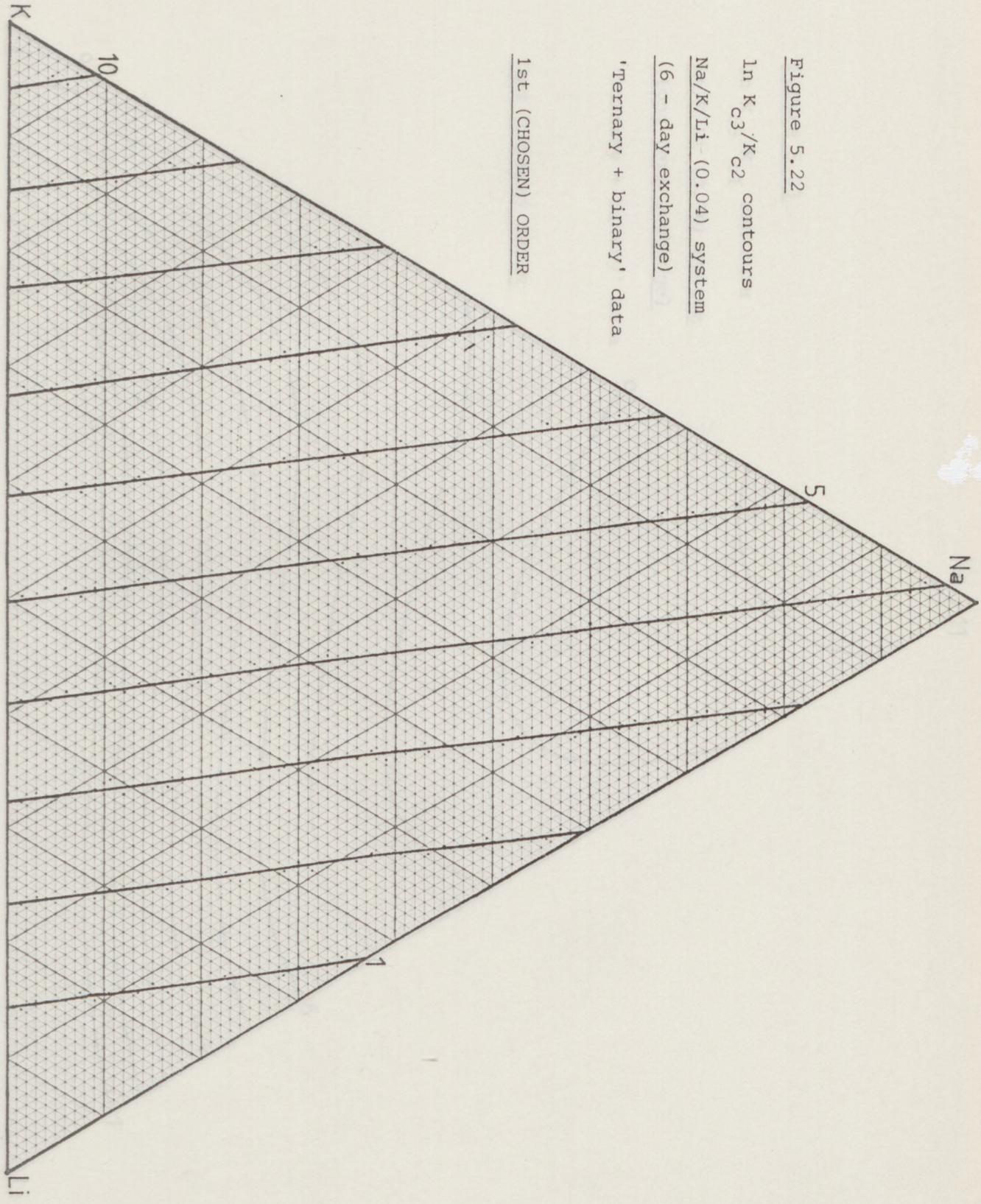
Figure 5.23

ln K_{c3}/K_{c1} contours

Na/K/Li (0.04) system

(long-term exchange)

'Ternary + binary' data

3rd (CHOSEN) ORDER
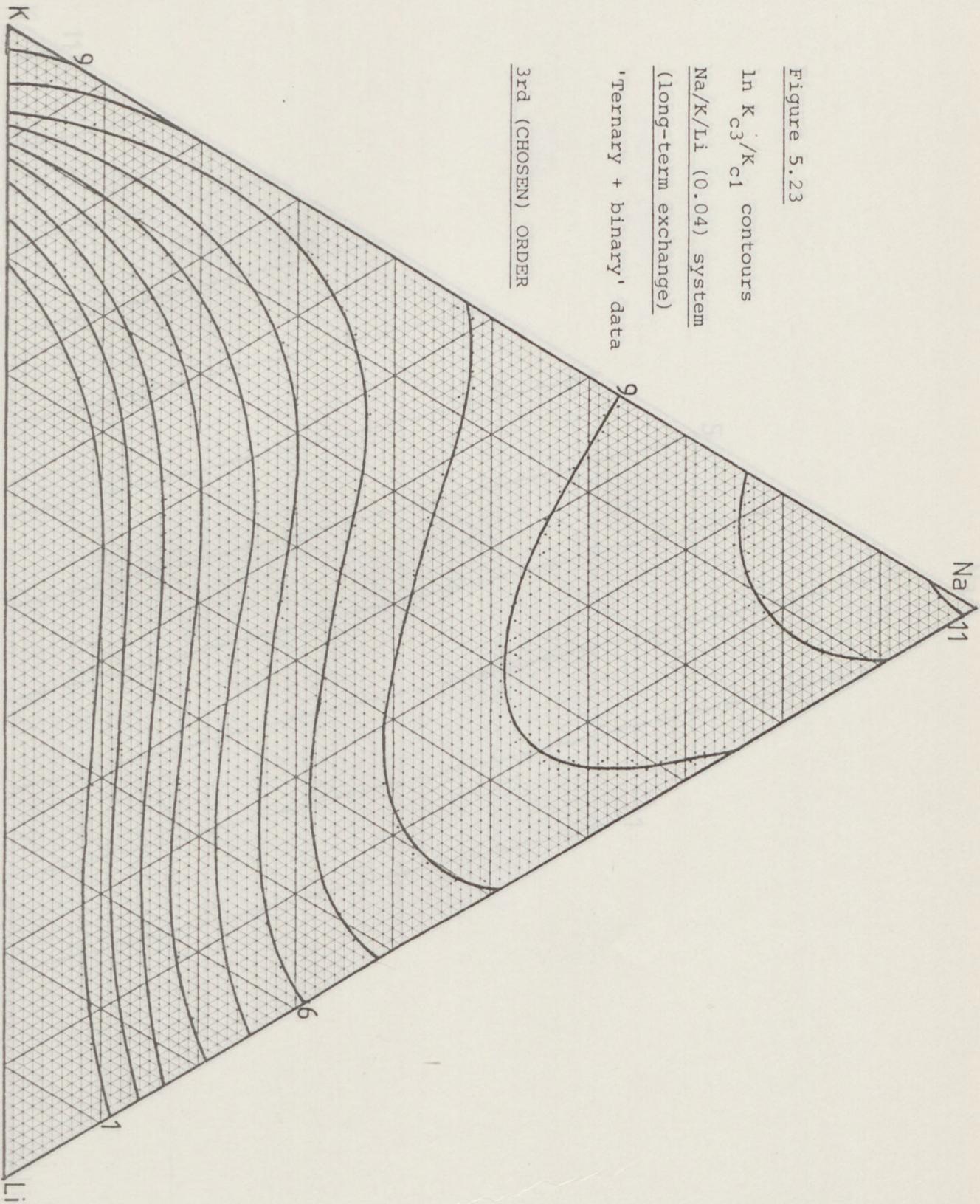
Figure 5.24

ln K_{c3}/K_{c2} contours

Na/K/Li (0.04) system

(long-term exchange)

'Ternary + binary' data

1st (CHOSEN) ORDER
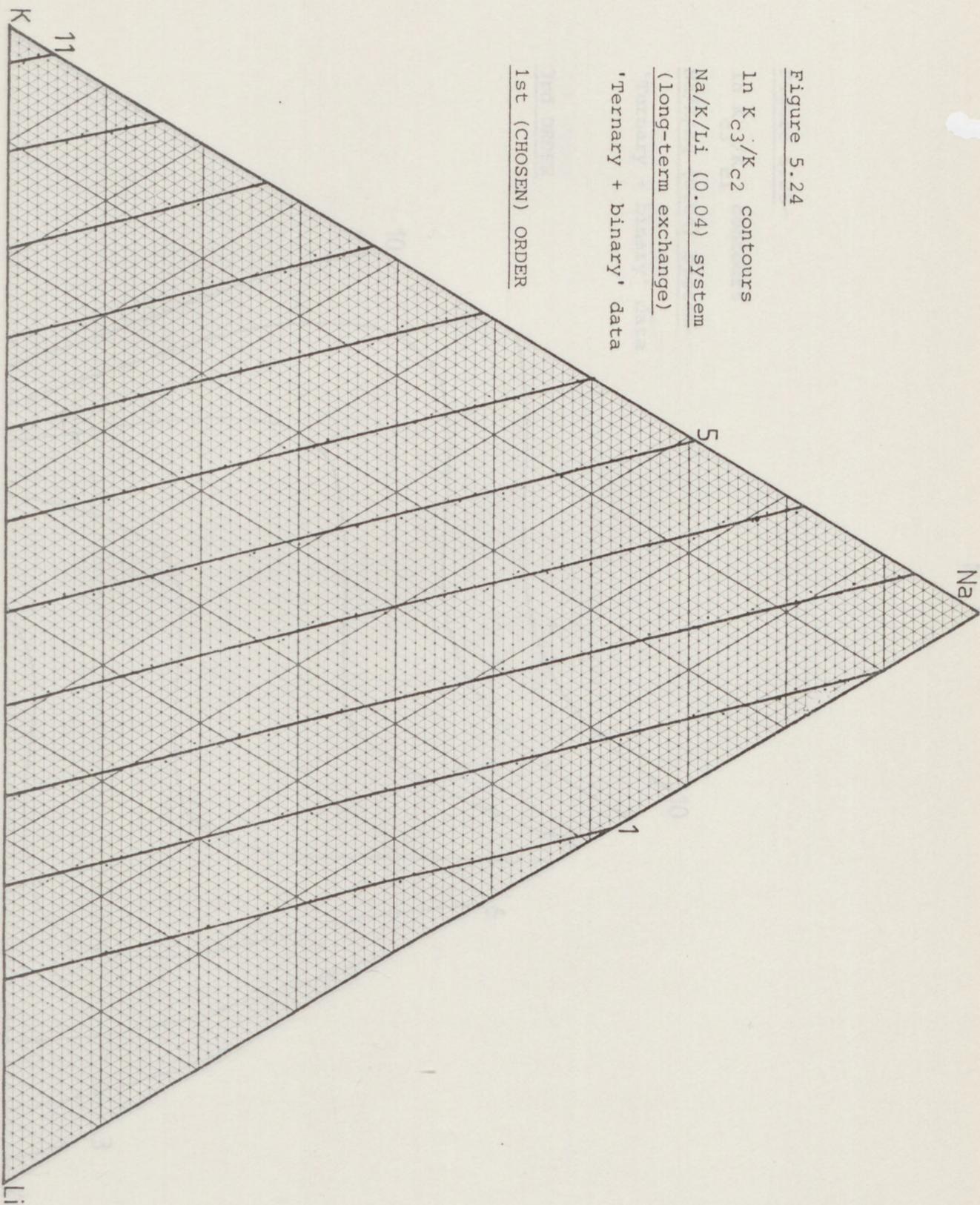
Figure 5.25

ln K$_{c3}$/K$_{c1}$ contours

Na/K/Ag (0.04) system

'Ternary + binary' data
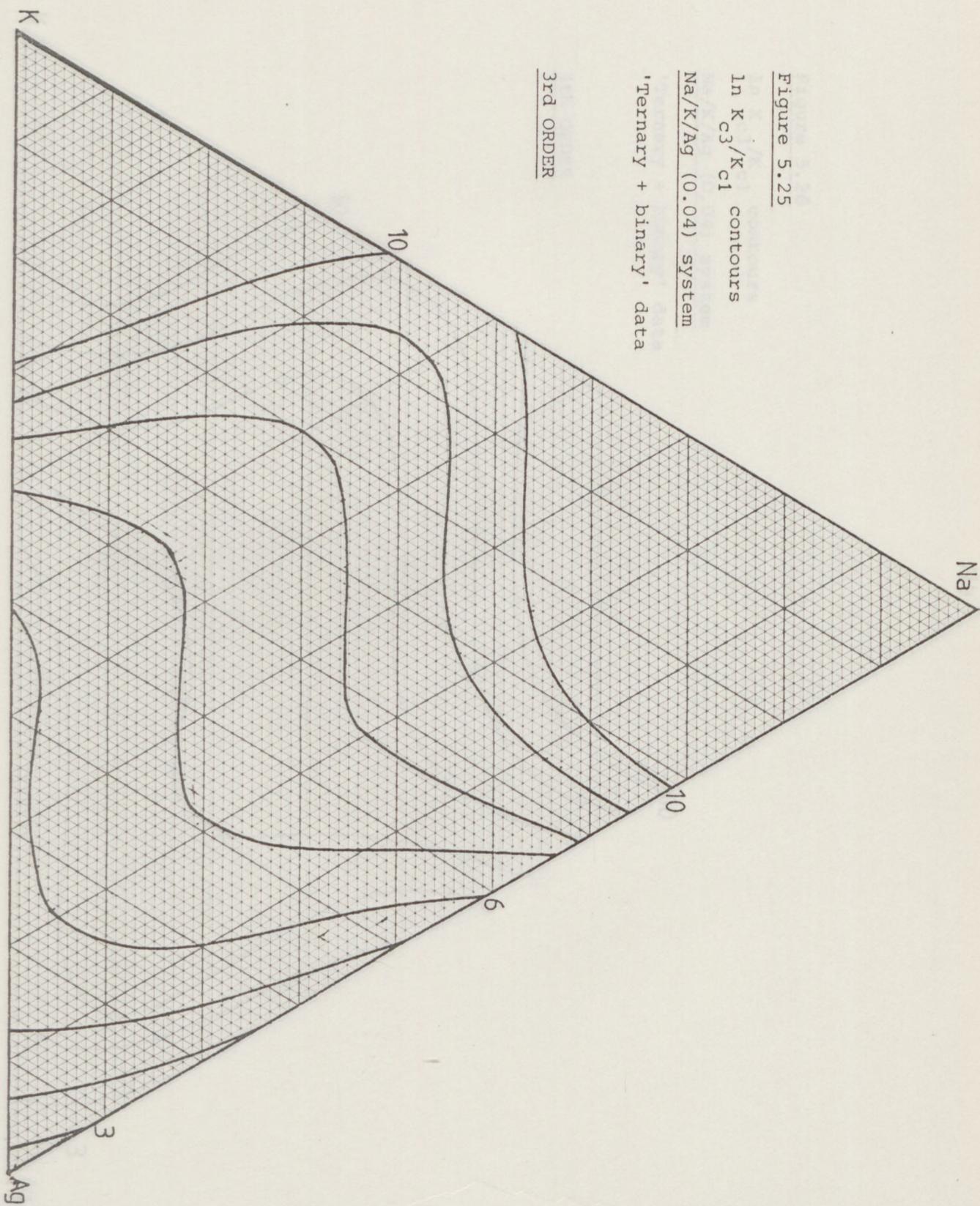
3rd ORDER

Figure 5.26

ln K_{c3}/K_{c1} contours

Na/K/Ag (0.04) system

'Ternary + binary' data
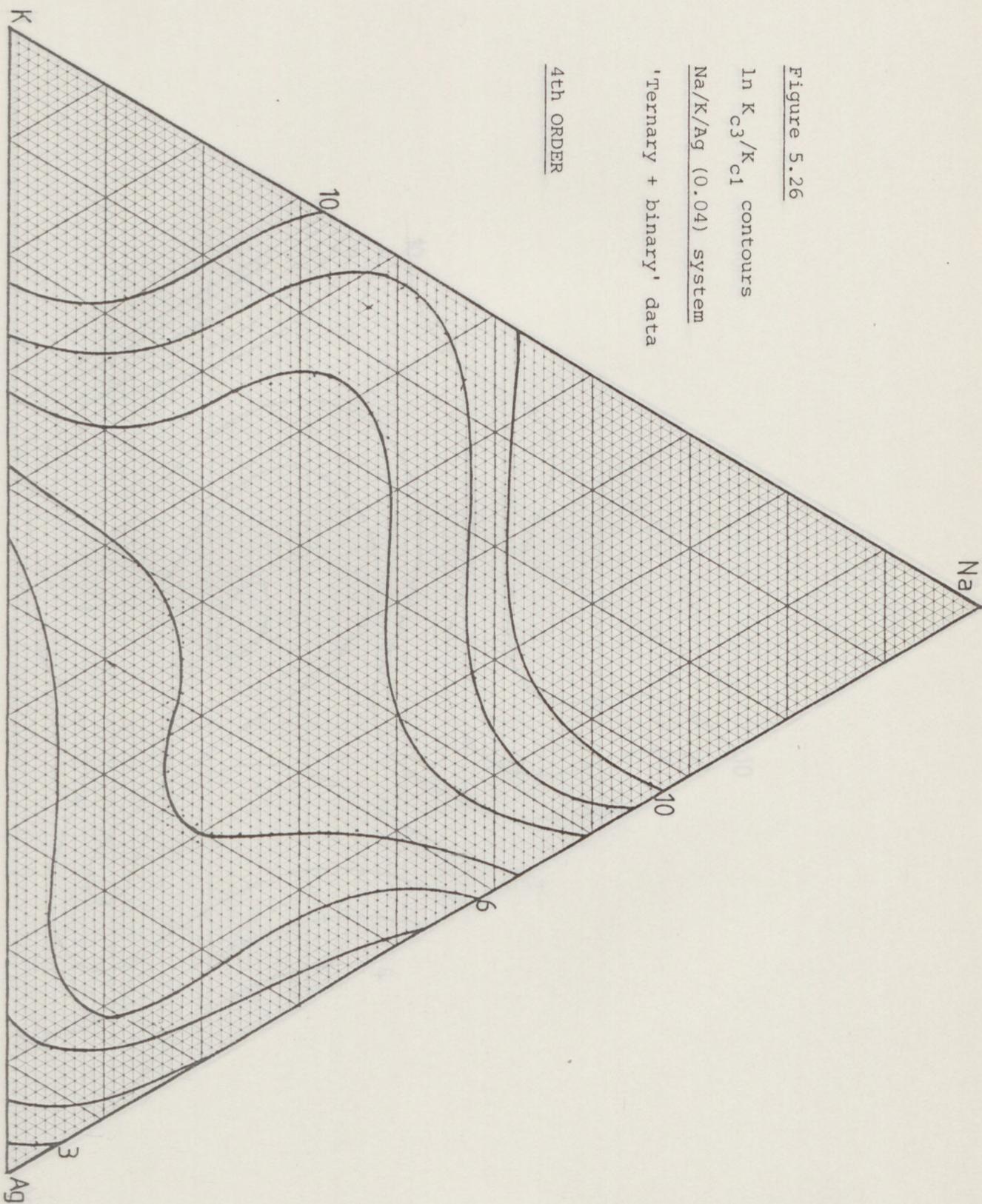
4th ORDER

Figure 5.27

ln K_{c3}/K_{c1} contours

Na/K/Ag (0.04) system

'Ternary + binary' data
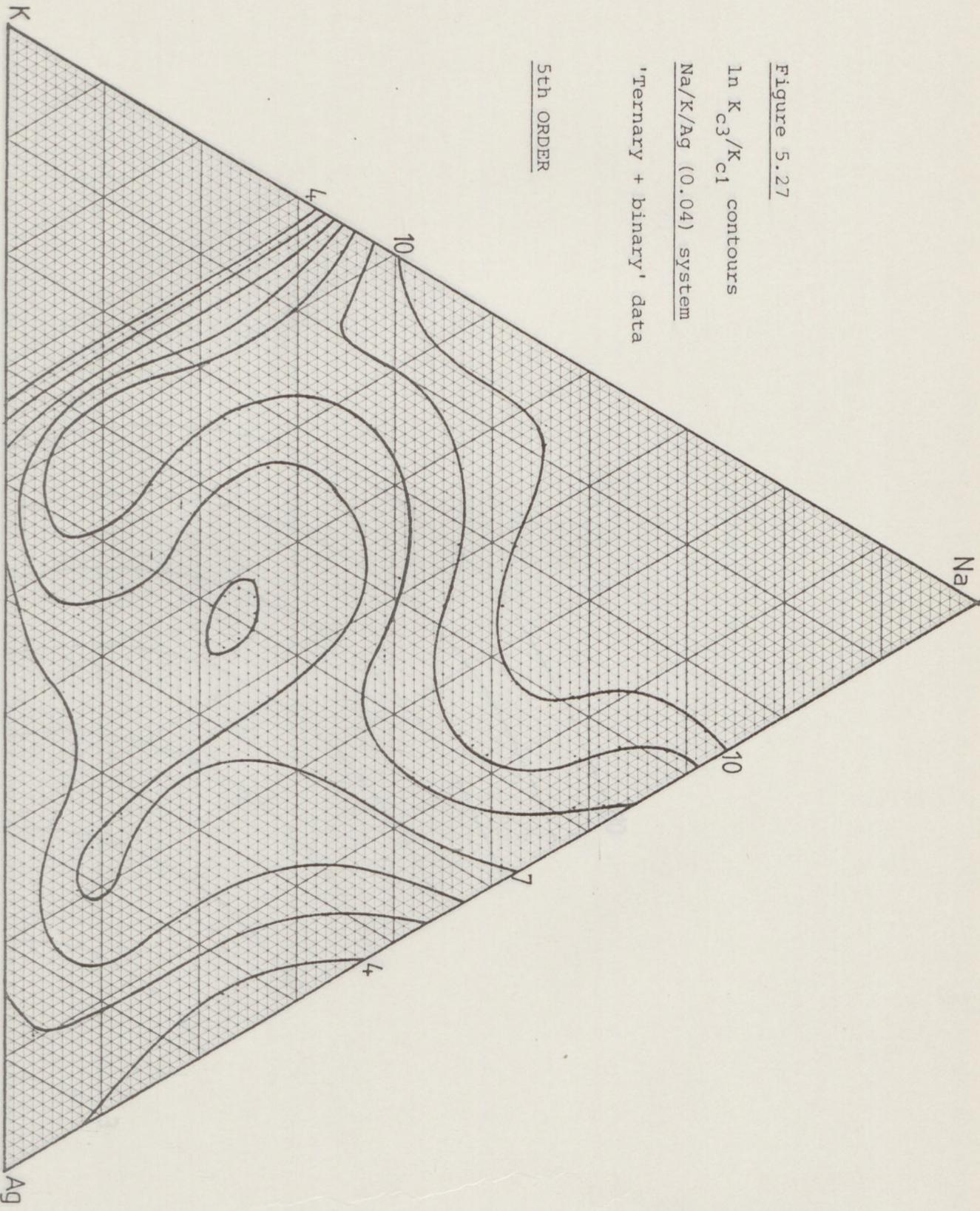
5th ORDER

Figure 5.28

ln K_{c3}/K_{c2} contours

Na/K/Ag (0.04) system

'Ternary + binary' data

2nd ORDER
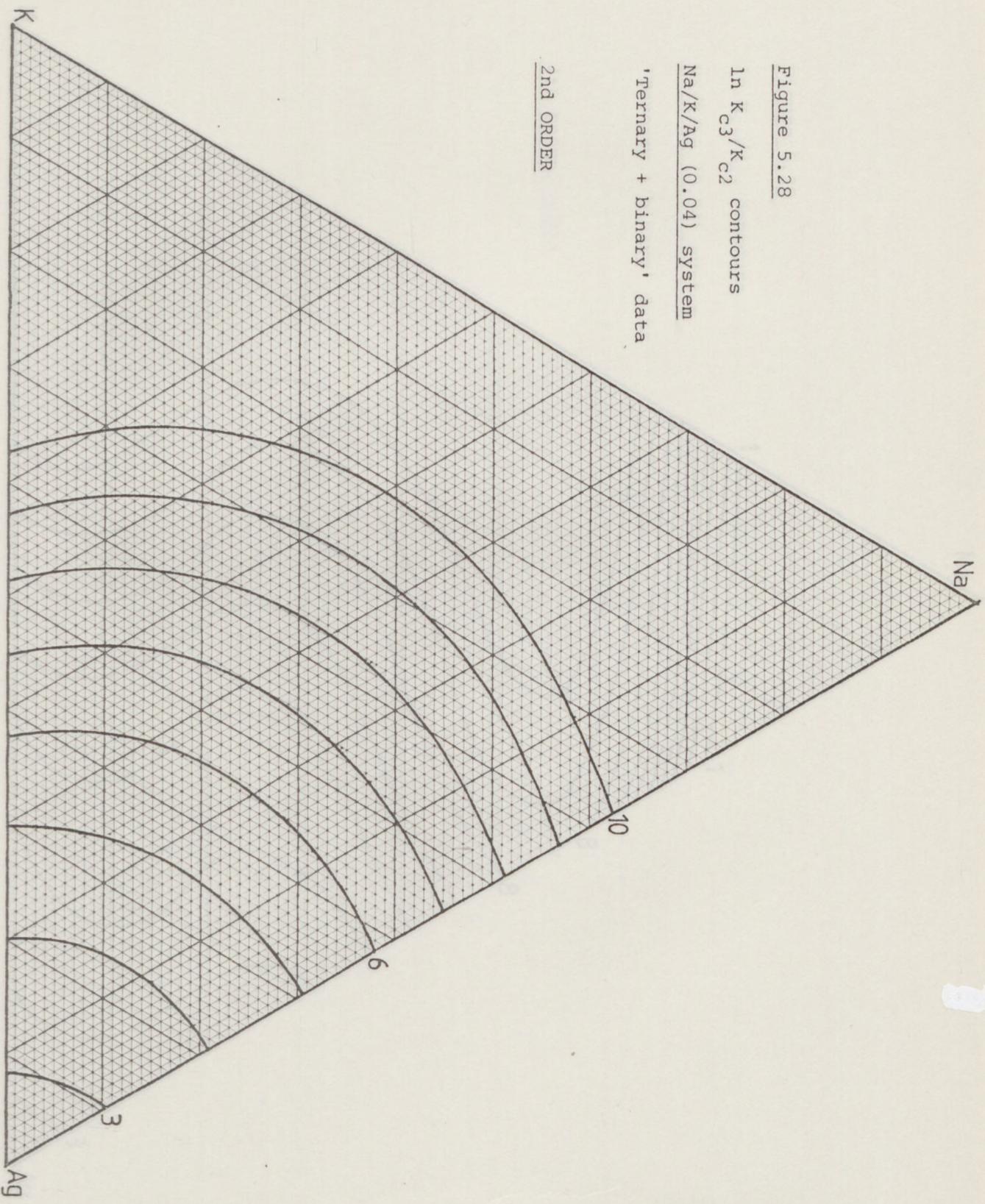
Figure 5.29
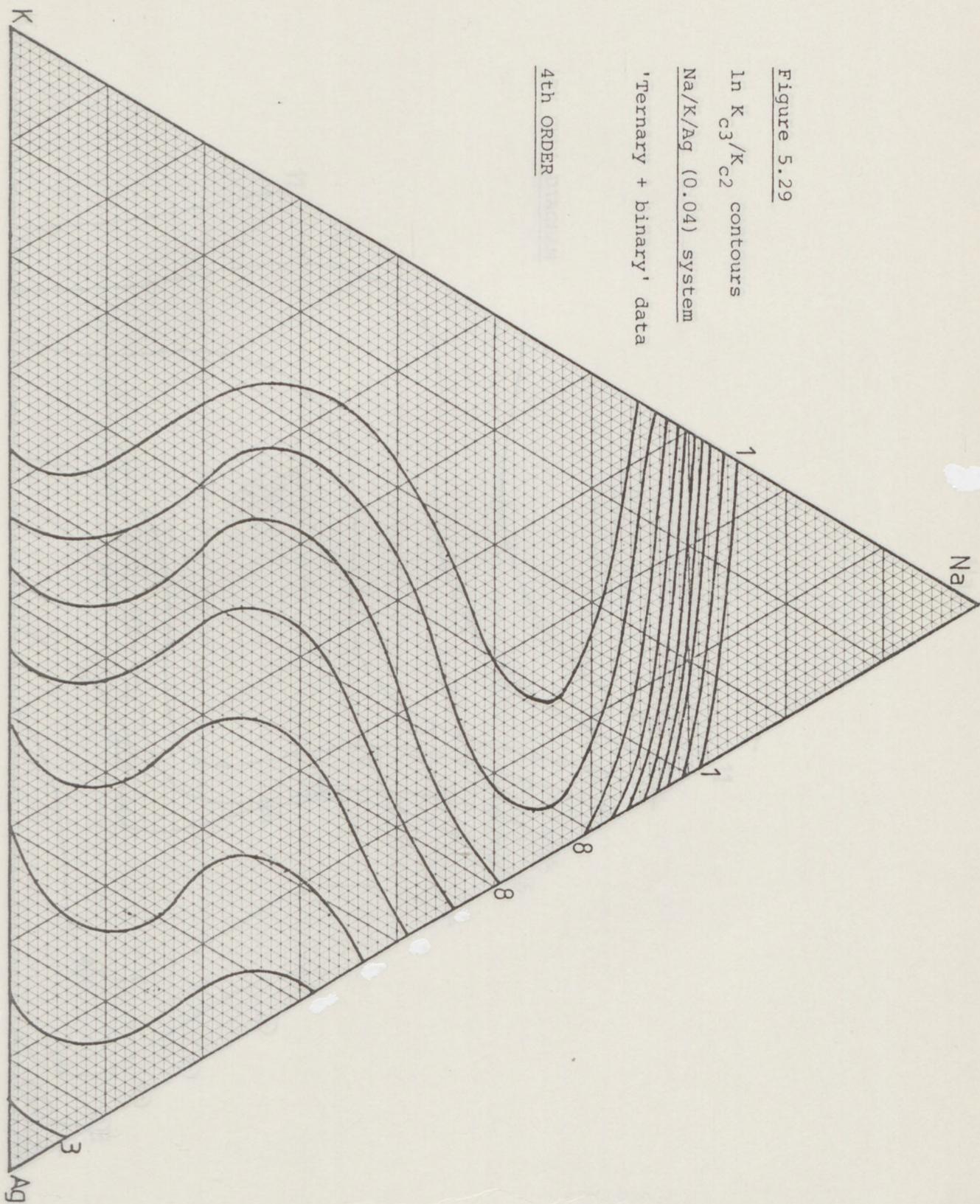
ln K_{c3}/K_{c2} contours

Na/K/Ag (0.04) system

'Ternary + binary' data

4th ORDER

Figure 5.30
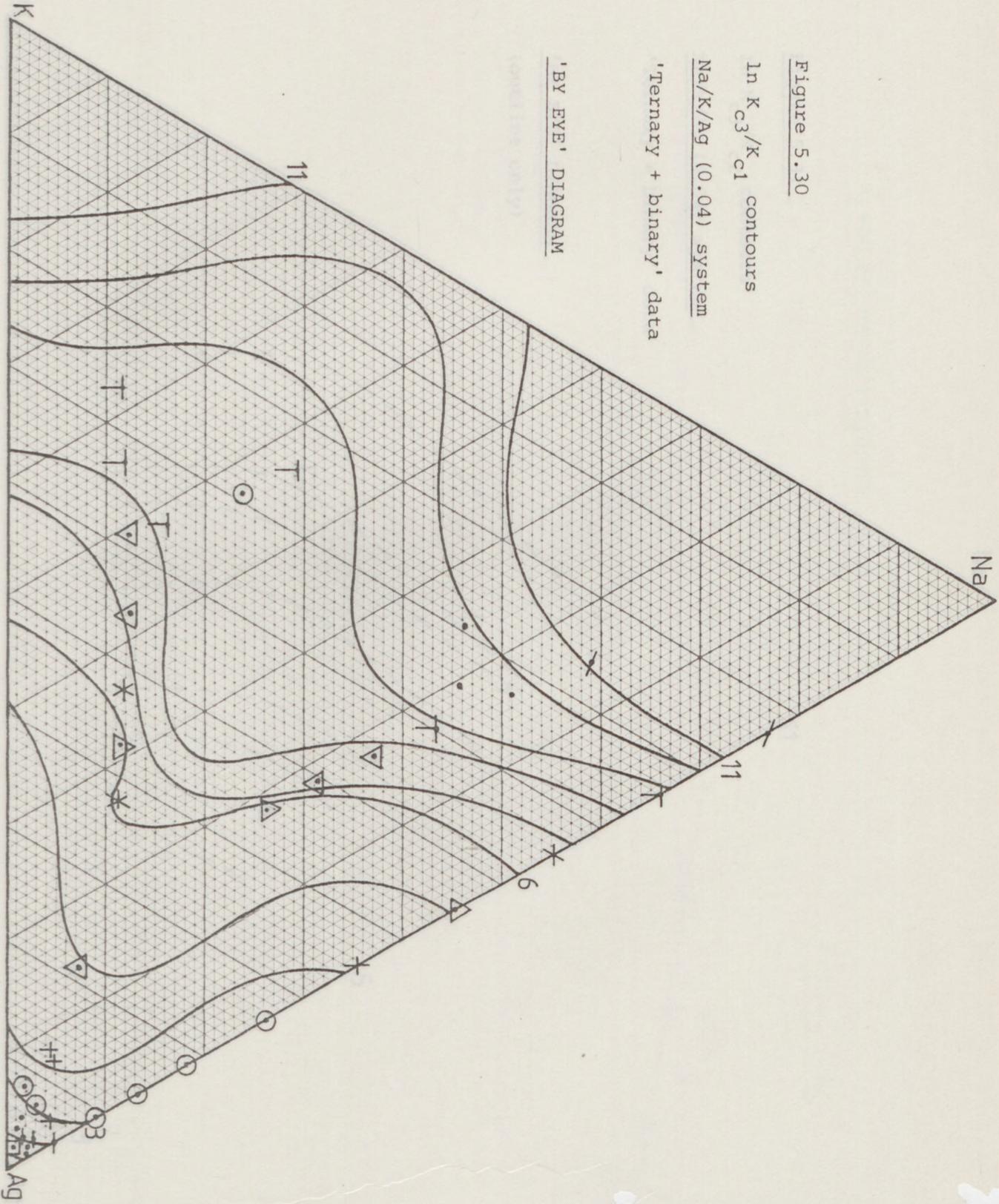
ln K_{c3}/K_{c1} contours

Na/K/Ag (0.04) system

'Ternary + binary' data

'BY EYE' DIAGRAM

Figure 5.31

ln K_{c3}/K_{c2} contours

Na/K/Ag (0.04) system

'Ternary + binary' data

'BY EYE' DIAGRAM

(outline only)
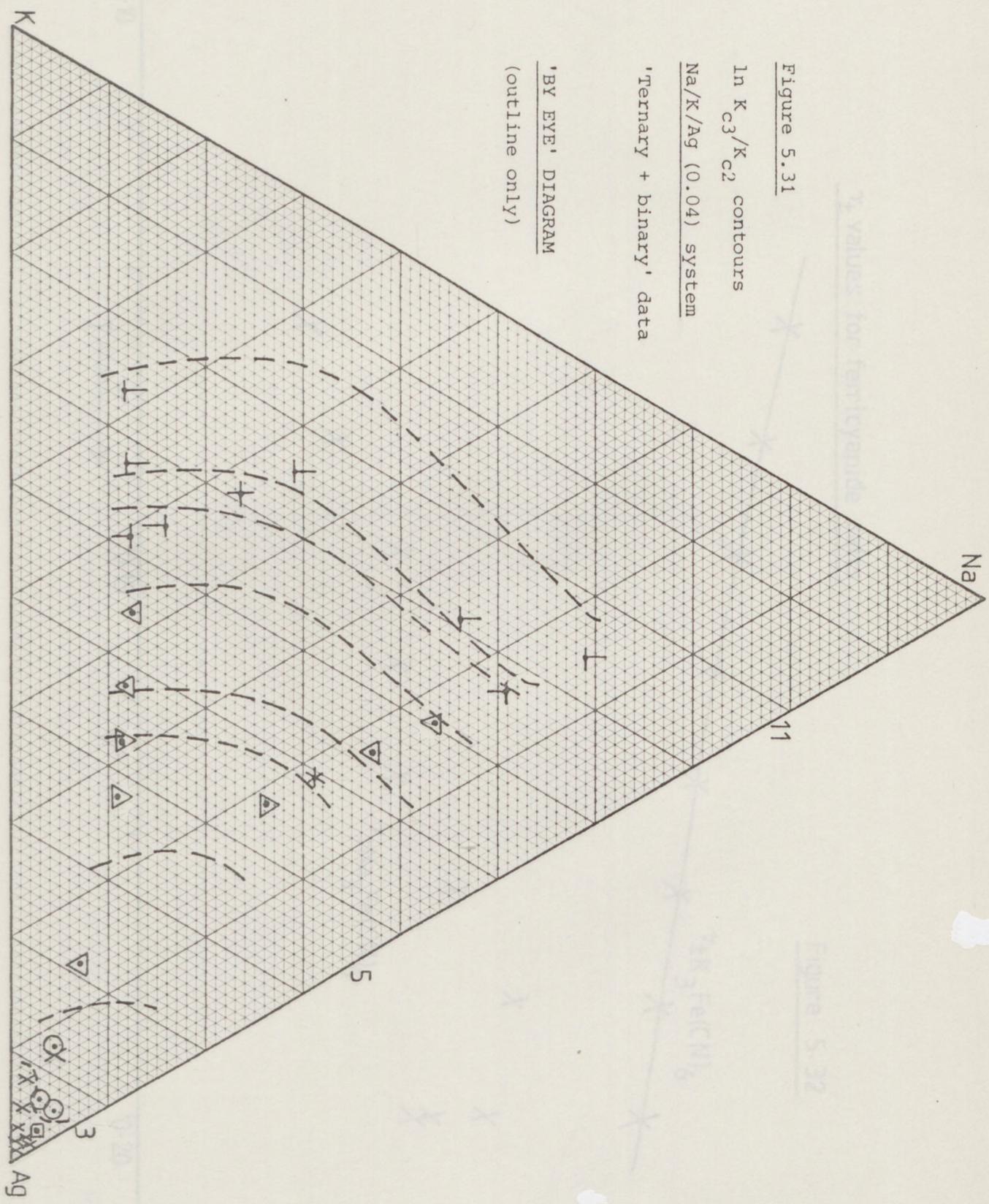
$\gamma_{\pm}$ values for ferricyanide salts
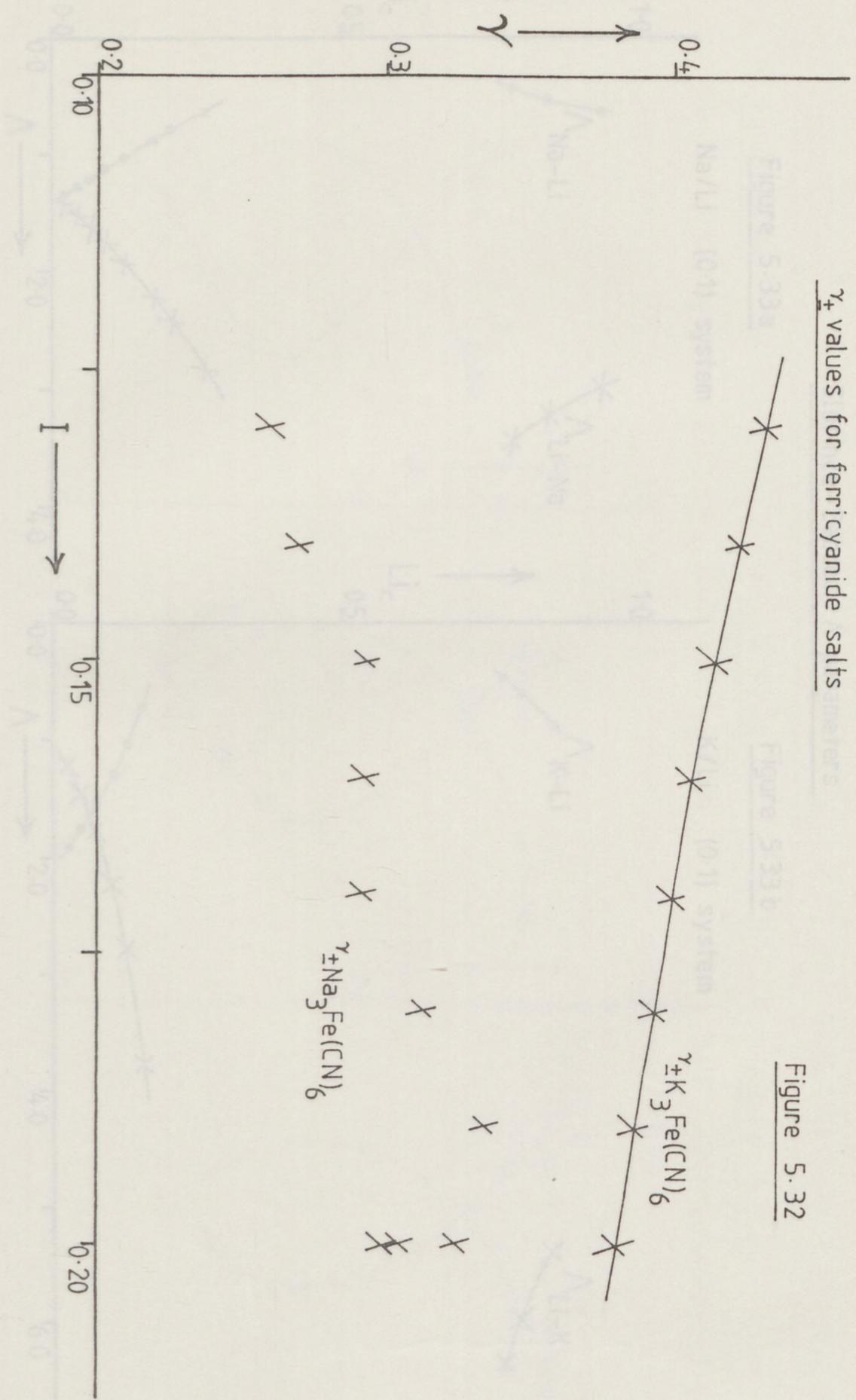
Figure 5.32

Elprince–Babcock Λ parameters

Figure 5.33a
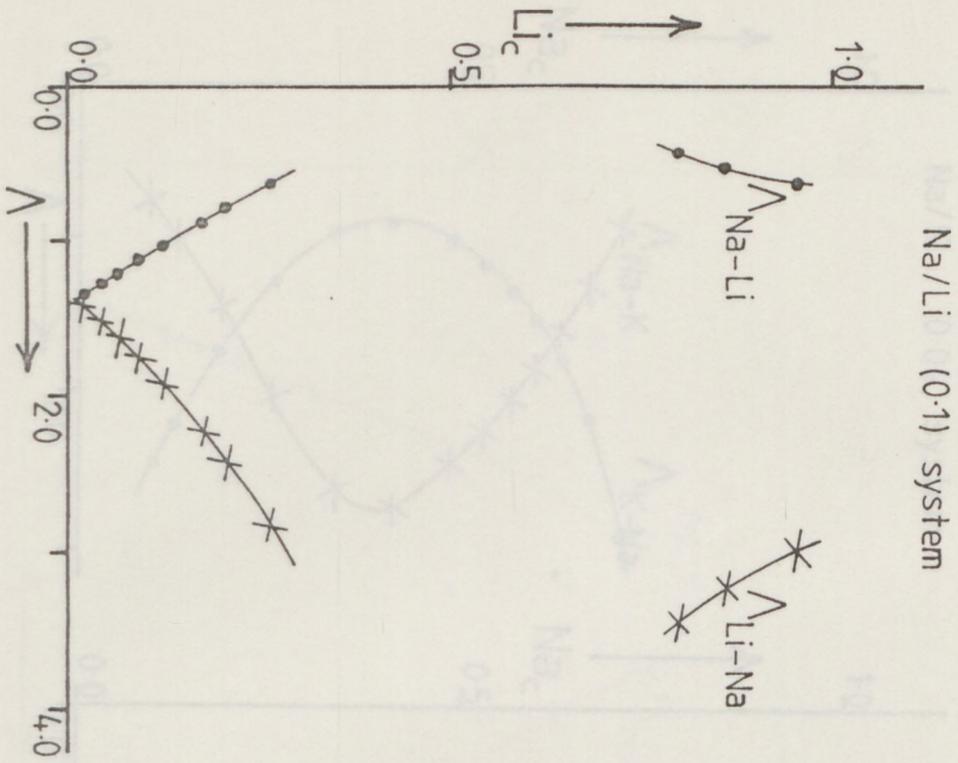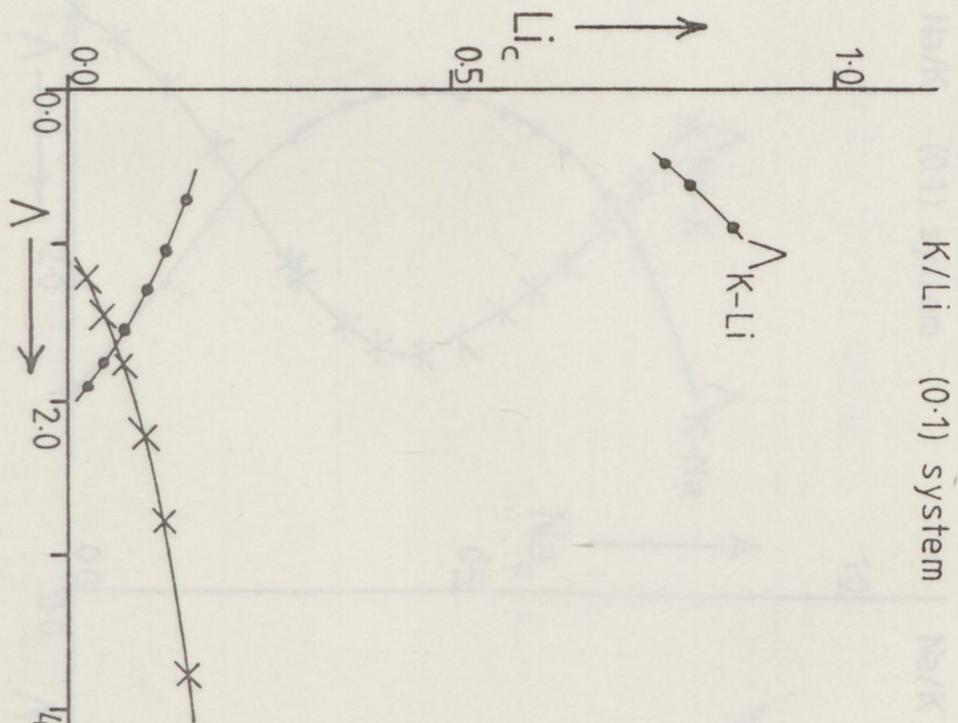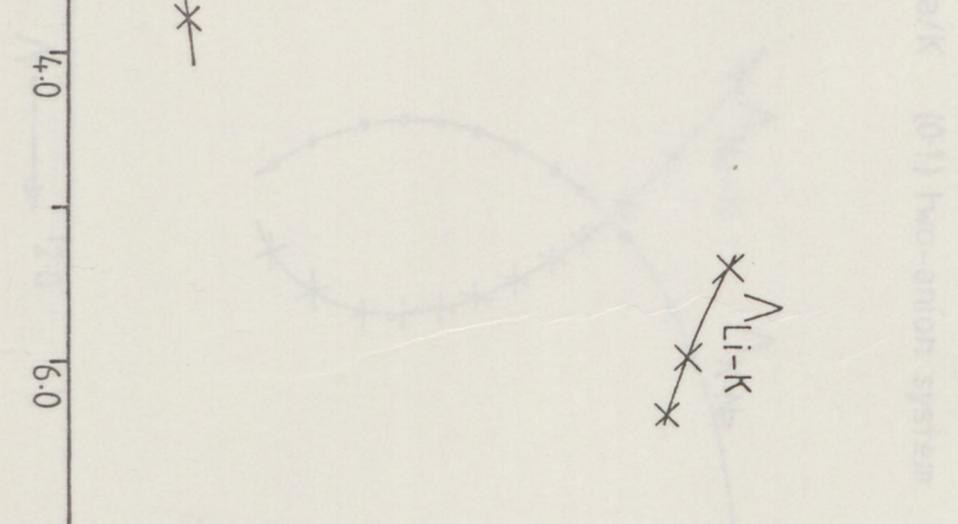
Na/Li (0·1) system

Figure 5.33b

K/Li (0·1) system

Elprince–Babcock Λ parameters

Figure 5.34a — Na/K (0·04) system

Figure 5.34b — Na/K (0·1) system

Figure 5.34c — Na/K (0·1) two-anion system
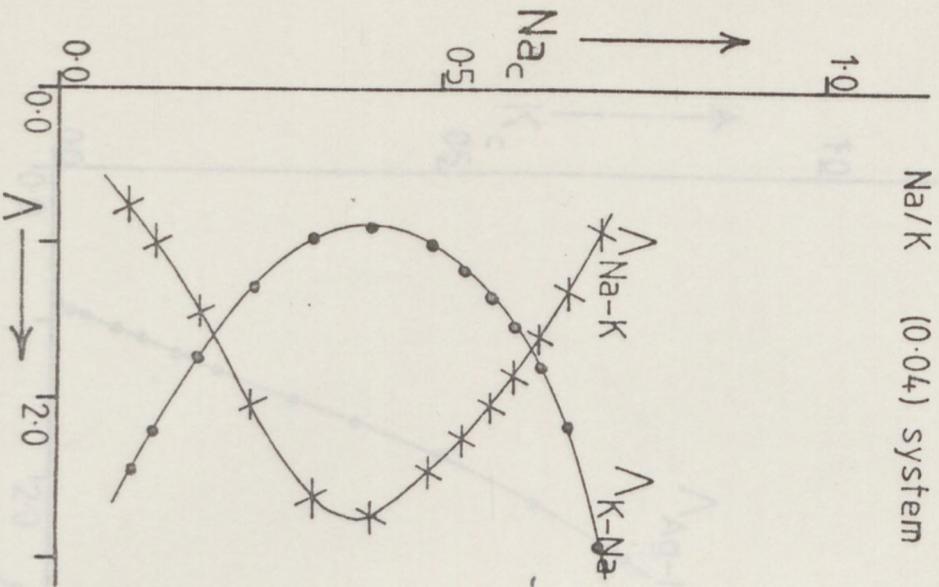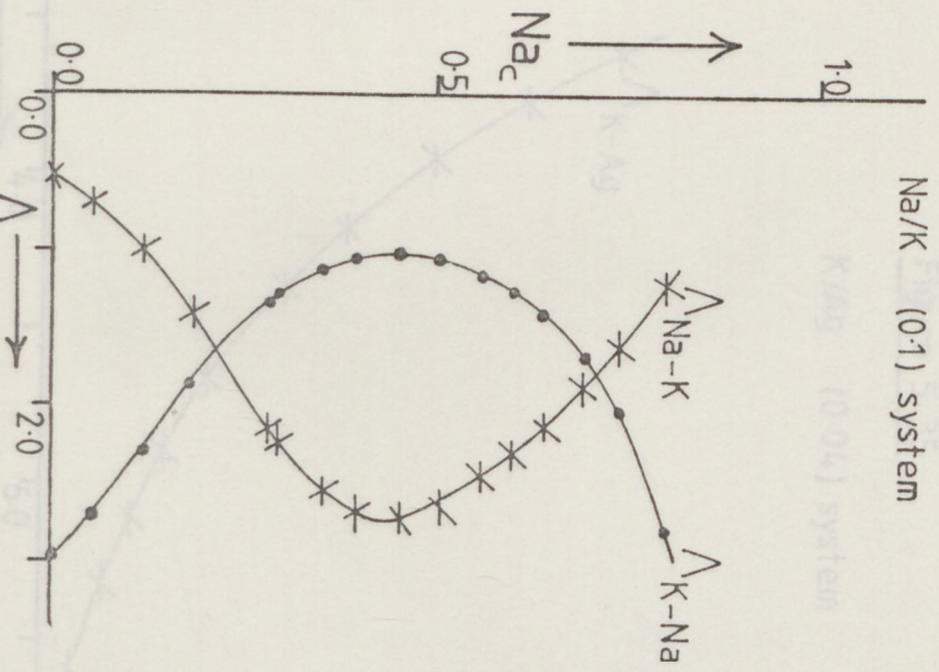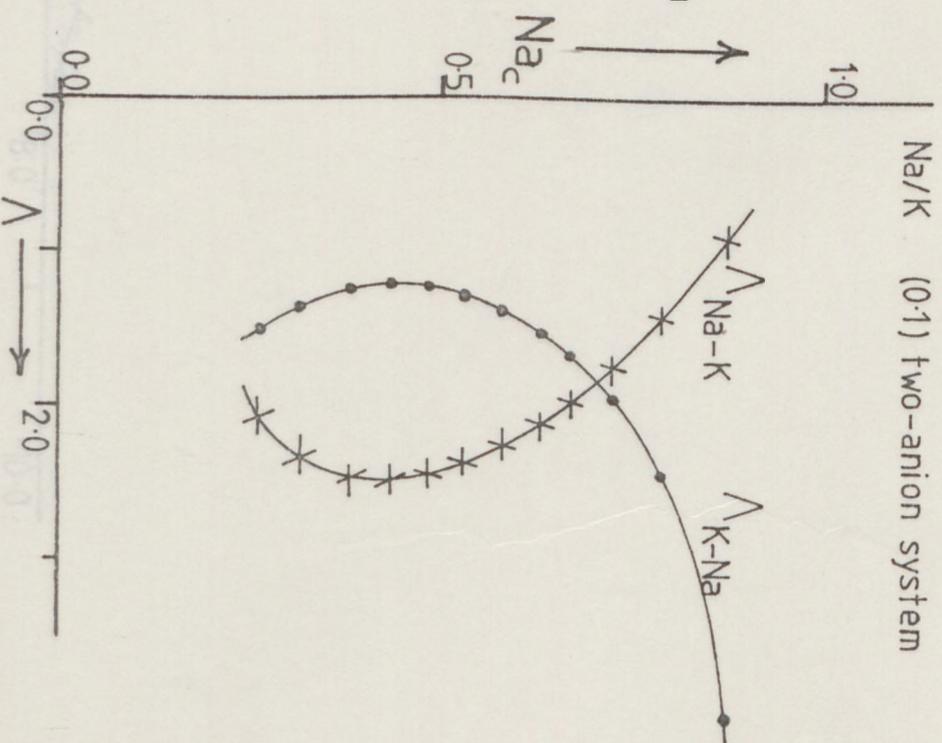
Elprince–Babcock Λ parameters
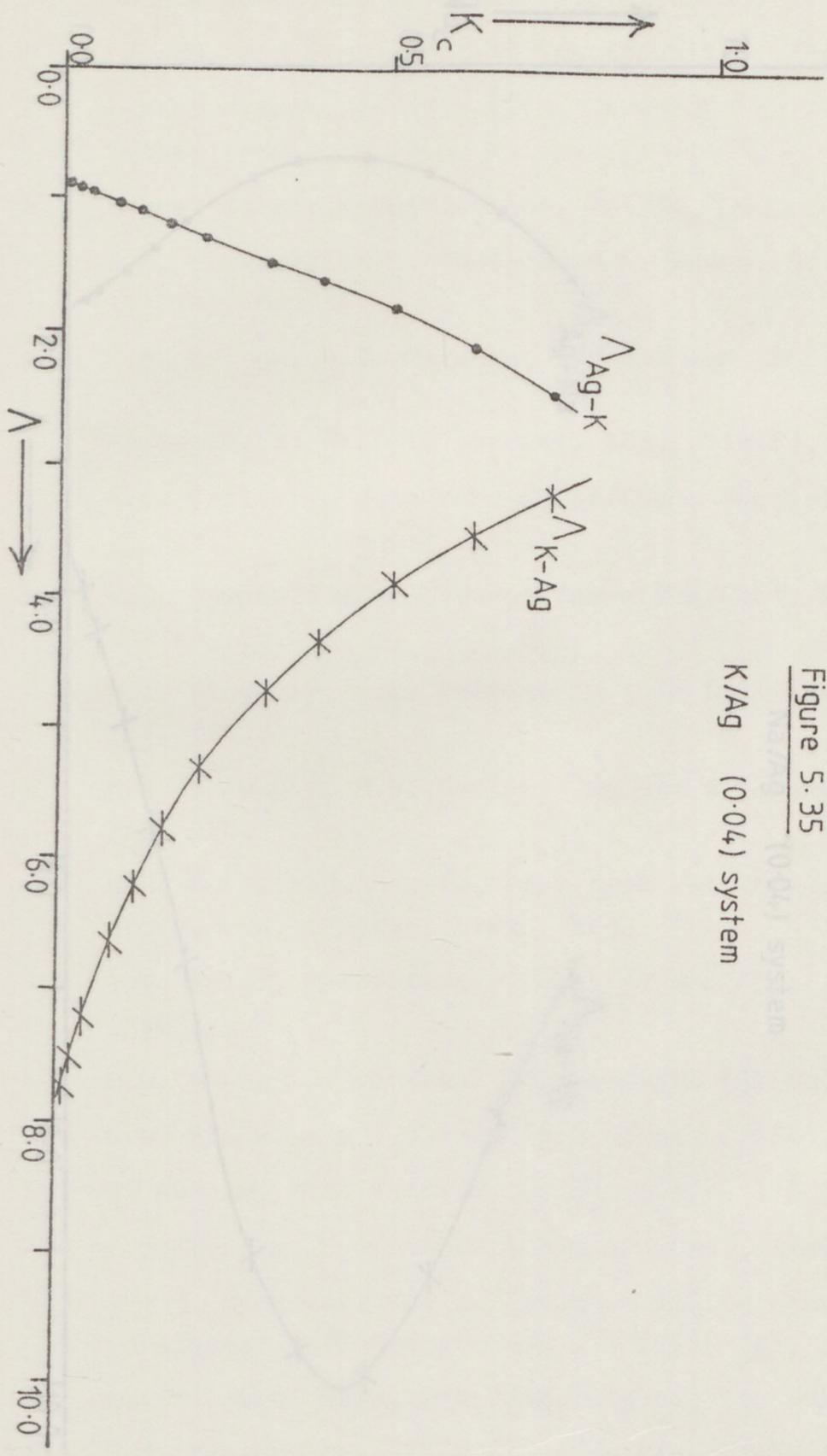
Figure 5.35

K/Ag   (0·04) system

Figure 5.36

Elprince–Babcock Λ parameters

Na/Ag (0·04) system

Ag–Na

Na–Ag

Na_c

Λ

REFERENCES

P1   Procter and Gamble Patent Specification, 1505/74, Ireland.

P2   Procter and Gamble Patent Specification, 74/450266, USA.

P3   Henkel Patent Specification, 74/003381 to 74/003384,
      Netherlands.

P4   Henkel Patent Specification, 789/74, Ireland.

P5   J.M. Corkhill, B.L. Madison, M.E. Burns, British Patents,
      1429143, May 1976.

P6   R.M. Milton, U.S. Patents, 2882243 and 2882244, April 1959.

1   P. Berth, J. Am. Oil Chemists Soc., (1978), 55, 52.

2   A.C. Savitsky, Soaps/Cosmetics/Chem. Specialities, (1977)
      53, 29.

3   T.C. Campbell et al , Soaps/Cosmetics/Chem. Specialities,
      (1978), 55, 33.

4   M.J. Schwuger, H.G. Smolka, Colloid & Polymer Sci., (1976)
      254, 1062.

5   M.J. Schwuger, H.G. Smolka, Colloid & Polymer Sci., (1978)
      256, 270.

6   G.H. Kuhl, H.S. Sherry, Proc. 5th Int. Conf. Zeolites, Ed.
      L.V.C.Rees, (Heyden, 1980), 813.

7   J.V. Smith, Minerological Soc. of Am., Special Paper No.1,
      (1963).

8   D.W. Breck, J. of Chem. Ed., (1964), 41, No. 12, 679.

9   D.W. Breck et al , J. Am. Chem. Soc., (1956), 78, 5963.

10   R. Rudham, M.K. Sanders, J. Catalysis, (1972), 27, 287.

11   P.B. Venuto, P.S. Landis, Adv. in Cat., (1968), 18, 259.

12   Kh. M. Minachev, Ya. I. Isakov "Zeolite Chemistry and
      Catalysis", ACS Monogr. Ser., (1976), 171, 451.

13   L.V.C. Rees, Chem. and Ind., (1977), 15, 647.

14   R.M. Barrer, "Zeolites and Clay Minerals", (Academic Press,
      1978).

15   J.A. Rabo, "Zeolite Chemistry and Catalysis", ACS Monogr.
      Ser., (1976) <u>171</u>, 332.

16   J.D. Sherman, A.I. Chem. E. Symp. Ser., No.179, (1978),
      <u>74</u>, 98.

17   D.W. Breck, "The Properties and Applications of Zeolites",
      Ed. R.P. Townsend, (The Chemical Society, 1980), 391.

18   P. Fletcher, Ph.D. Thesis, The City University, London,1979.

19   R.M. Barrer, J. Chem. Soc., (1948), 2158.

20   R.M. Barrer, Discussions Faraday Society, (1944), <u>40</u>, 206.

21   R.M. Barrer, D.A. Ibbitson, Trans. Faraday Soc., (1944),
      <u>40</u>, 195.

22   D.W. Breck *et al*, J. Am. Chem. Soc., (1956), <u>78</u>, 2338.

23   R.M. Barrer, L.V.C. Rees, M. Shamsuzzoha, J. Inorg. Nucl.
      Chem., (1966), <u>28</u>, 629.

24   R.M. Barrer, J.A. Davies, L.V.C. Rees, J. Inorg. Nucl. Chem.,
      (1968), <u>30</u>, 3333.

25   R.M. Barrer, J.A. Davies, L.V.C. Rees, J. Inorg. Nucl. Chem.,
      (1969), <u>31</u>, 2599.

26   R.M. Barrer, W. Busser, W.F. Grütter, Helv. Chim. Acta,
      (1956), <u>39</u>, 518.

27   A.C. Savitsky, Household and Personal Products Industry,
      (1977), <u>14</u>, 52.

28   P. Shimizu, Soaps/Cosmetics/Chem. Specialities, (1977),
      <u>53</u>, 33.

29   S.A.I. Barri, L.V.C. Rees, J. Chromatogr., (1980), <u>201</u>, 21.

30   H.S. Sherry, J. Phys. Chem., (1966), <u>70</u>, 1158.

31   H.S. Sherry, J. Phys. Chem., (1968), <u>72</u>, 4086.

32   D.H. Olson, H.S. Sherry, J. Phys. Chem., (1968), <u>72</u>, 4095.

33   H.S. Sherry, "Molecular Sieve Zeolites - I", (Adv. Chem.
      Ser. 101), Am. Chem. Soc., (1971), 350.

34   H.S. Sherry, "Ion Exchange in the Process Industries",
      (Soc. of Chem. Ind., 1969), 329.

35   G. Schweiker, J. Am. Oil Chemists Soc., (1978), 55, 36.

36   A. Cremers, ACS Symp. Ser., (1977), 40, 179.

37   P.P. Lai, L.V.C. Rees, J.C.S. Faraday I, (1976), 72, 1809.

38   P.P. Lai, L.V.C. Rees, J.C.S. Faraday I, (1976), 72, 1818.

39   P.P. Lai, L.V.C. Rees, J.C.S. Faraday I, (1976), 72, 1827.

40   A. Dyer *et al*, J. Inorg. Nucl. Chem., (1966), 28, 615.

41   G. Jakobi, M.J. Schwuger, Chemiker-Zeitung, (1975), 98, 182.

42   P. Berth *et al*, Angewandte Chemie, (1975), 87, 115.

43   P. Krings, M.J. Schwuger, C.H. Krauch, Naturwissenschaften,
      (1974), 61, 75.

44   P. Fletcher, R.P. Townsend, J.C.S. Faraday I, (1982),
      78, 1741.

45   H.S. Sherry, H.F. Walton, J. Phys. Chem., (1967), 71, 1457.

46   D.W. Breck, "Zeolite Molecular Sieves", (Wiley-Inter-
      science, 1973).

47   W. Loewenstein, Amer. Min., (1954), 39, 92.

48   W.M. Meier, "Molecular Sieves", (Soc. Chem. Ind., 1968).

49   W.J. Mortier, "Compilation of Extra Framework Sites in
      Zeolites", (Butterworths, 1982).

50   J.V. Smith, "Molecular Sieve Zeolites - I", (Adv. Chem.
      Ser., 101), Am. Chem. Soc., (1971), 109.

51   L. Broussard, D.P. Shoemaker, J. Am. Chem. Soc., (1960),
      82, 1041.

52   B. Beagley, J. Dwyer, T.K. Ibrahim, J.C.S. Chem. Comm.,
      (1978), 12, 493.

53   D.H. Olson, J. Phys. Chem., (1970), 74, 2758.

54   B.K.G. Theng, E. Vansant, J.B. Uytterhoeven, Trans.
      Faraday Soc., (1968), 64, 3370.

55   W.J. Mortier, H.J. Bosmans, J. Phys. Chem., (1971), 75
      3327.

56   Kyong Tai No *et al*, J. Phys. Chem., (1981), 85, 2065.

57   H. Herden *et al*, J. Inorg. Nucl. Chem., (1981), 43, 2533.

58   R. Schöllner, H. Herden, ACS Symp. Ser., (1977), 40, 357.

59   R.M. Barrer, B.M. Munday, J. Chem. Soc., (A), (1971), 2904.

60   R.M. Barrer, J. Klinowski, J.C.S. Faraday I, (1974),
      70, 2080.

61   R.P. Townsend, D.I.C. Thesis, Imperial College, London,1977.

62   R.M. Barrer, J.D. Falconer, Proc. Roy. Soc., (1956),
      A236, 227.

63   R.M. Barrer, Bull. Soc. Fr. Mineral Cristollogr., (1974),
      92, 89.

64   R.M. Barrer, W.M. Meier, Trans. Faraday Soc., (1958),
      54, 1074.

65   R.M. Barrer, W.M. Meier, Trans. Faraday Soc., (1959),
      55, 130.

66   R.M. Barrer, J. Klinowski, J.C.S. Faraday I, (1974),
      70, 2362.

67   A. Maes, A. Cremers, J.C.S. Faraday I, (1975), 71, 265.

68   R.M. Barrer, R. Papadopoulos, L.V.C. Rees, J. Inorg. Nucl.
      Chem., (1967), 29, 2047.

69   R.M. Barrer, J. Klinowski, Phil. Trans. Roy. Soc., (1977)
      285, 637.

70   I.J. Gal, P. Radovanov, J.C.S. Faraday I, (1975), 71, 1671

71   R.M. Barrer, R.P. Townsend, J.C.S. Faraday I, (1976), 72, 661.

72   R.M. Barrer, R.P. Townsend, J.C.S. Faraday I, (1976), 72
      2650.

73   P. Fletcher, R.P. Townsend, J.C.S. Faraday I, (1981), 77
      497.

74   A. Dyer, H. Enamy, R.P. Townsend, Sep. Sci. & Tech., (1981)
      16, 173.

75   G.L. Gaines, H.C. Thomas, J. Chem. Phys., (1953), 21, 714.

76   R.M. Barrer, A.J. Walker, Trans. Faraday Soc., (1964)
      60, 171.

77   R.A. Robinson, R.H. Stokes, "Electrolyte Solutions",
      (Butterworths, 1970).

78   P.W. Atkins, "Physical Chemistry", (Oxford, 1978).

79   J. Kielland, J. Soc. Chem. Ind., (1953), 54, 232.

80   E. Glueckauf, Nature, (1949), 163, 414.

81   R.M. Barrer, J. Klinowski, J.C.S. Faraday I, (1972), 68
      1956.

82   C.J.F. Böttcher, "Theory of Electric Polarisation",
      (Elsevier, 1952).

83   F.A. Cotton, G. Wilkinson, "Advanced Inorganic Chemistry",
      (Interscience, 1966).

84   P. Fletcher, R.P. Townsend, J. Chromatogr., (1980),201, 93.

85   P. Fletcher, R.P. Townsend, J.C.S. Faraday II, (1981),
      77, 955.

86   P. Fletcher, R.P. Townsend, J.C.S. Faraday II, (1981),
      77, 965.

87   P. Fletcher, R.P. Townsend, J.C.S. Faraday II, (1981),
      77, 2077.

88   P. Fletcher, R.P. Townsend, J.C.S. Faraday II, (1983),
      79, 419.

89   M.L.McGlashan, "Chemical Thermodynamics", (Academic Press,
      1979).

90   R.M. Barrer, J. Klinowski, J.C.S. Faraday I, (1972), 68, 73.

91   E.A. Guggenheim, Philos. Mag., (1935), 19, 588.

92   P. Debye, E. Hückel, Phys. Z., (1925), 25, 97.

93   G. Scatchard, Chem. Rev., (1939), 19, 309.

94   G. Scatchard, J. Am. Chem. Soc., (1961), 83, 2636.

95   G. Scatchard et al, J. Phys. Chem.,(1970), 74, 3786.

96   K.S. Pitzer, J. Phys. Chem., (1973), 77, 268.

97   M.H. Lietzke, R.W. Stoughton, J. Phys. Chem., (1962),
      66, 508.

98   R.M. Barrer, Proc. 5th Int. Conf. Zeolites, Ed. L.V.C. Rees,
      (Heyden, 1980), 275.

99   F. Helfferich,"Ion Exchange", (McGraw Hill, 1962).

100   L.V.C. Rees, "The Properties and Applications of Zeolites"
      Ed. R.P. Townsend, (The Chemical Society, 1980), 218.

101   V.S. Soldatov, V.A. Bichkova, Sep. Sci. Technol., (1980)
      15, 89.

102   A.M. Elprince, K.L. Babcock, Soil Sci., (1975), 120, 332.

103   W.J. Argersinger *et al*, Trans. Kansas Acad. Sci., (1950),
      53, 404.

104   G.M. Wilson, J. Am. Chem. Soc., (1964), 86, 127.

105   G. Scatchard, Chem. Rev., (1949), 44, 7.

106   C.V. McDaniel, P.K. Maher, A.C.S. Monograph (Zeolite Chem.
      Catal.), (1976), 171, 285.

107   F.D. Snell, "Photometric and Fluorometric Methods of Analysis
      - Metals Part 2", (Wiley-Interscience, 1978).

108   A.I. Vogel, "Quantitative Inorganic Analysis", (Longmans
      Green & Co., 1964).

109   D.J. Malcolme-Lawes, "Introduction to Radio Chemistry",
      (Macmillan, 1979).

110   T.A.H. Peacocke, "Radiochemistry: Theory and Experiment",
      (Wykeham, 1978).

111   P. Fletcher, R.P. Townsend, Proc. Roy. Soc., *in print*.

112   H. Herden *et al*, Z. Chem.,(1980), 20, 272.

113   K.R. Franklin, Private Communication.

114   R.P. Townsend *et al*, Proc. 6th Int. Conf. Zeolites,
      Nevada, (1983).

115   R.M. Barrer, J. Klinowski, J.C.S. Faraday I, (1975), 71, 690.

116   T.C. Golden, R.C. Jenkins, J. Chem. Eng. Data, (1981),
      26, 366.

117   M. Loizidou, Ph.D. Thesis, The City University, London,1982.

118   R.M. Barrer, B.M. Munday, J. Chem. Soc. (A), (1971), 2914.

119 V.P. Kol'nenkov, G.V. Bogomolov, Dokl. Akad. Nauk SSSR,
     (1977), 236, 1144.

120 T. Kata○ka, H. Yashida, J. Chem. Eng. Japan,(1980), 13,328.

121 A.M. Elprince, K.L. Vanslow, G. Sposito, Soil Sci. Soc.
     Amer. J., (1980), 44, 964.

122 S.Y. Chu, G. Sposito, Soil Sci. Soc. Amer. J., (1981),
     45, 1084.

123 H.K. Hardy, Acta. Metall., (1953), 1, 202.

124 R.M. Barrer, J. Klinowski, H.S. Sherry, J.C.S. Faraday II,
     (1973), 67, 2961.

125 M. Constenoble, A. Maes, J.C.S. Faraday I, (1978), 74,131.

APPENDIX I

Treatment of integrals obtained in Section 2.2.4.

Consider the third integral in equation (2.112);

$$\frac{1}{3} \int_{K_{c3}(C_c=0)}^{K_{c3}(C_c)} C_c \, d\ln K_{c3} \qquad \ldots\ldots(A1)$$

There are two problems to overcome in the direct evaluation of this. Firstly in the Fletcher-Townsend model, K_{c3} is a function of both A_c and B_c (where $C_c = 1 - A_c - B_c$), and therefore for any given value of $\ln K_{c3}$ there can be several different values of A_c. Secondly, one cannot determine the lower limit of the integral, i.e. K_{c3} at $C_c = 0$ [see equation (2.97)]. This latter problem also applies to the other integrals in equation (2.112). These difficulties can be by-passed by resorting to transforming the integrals[86] using the standard equation for integration by parts, *viz*

$$\frac{1}{3} \int_{K_{c3}(C_c=0)}^{K_{c3}(C_c)} C_c \, d\ln K_{c3} = \frac{1}{3} \int_{0,K_{c3}(C_c=0)}^{C_c,K_{c3}(C_c)} d(C_c . \ln K_{c3}) - \frac{1}{3} \int_{0}^{C_c} \ln K_{c3} d(C_c)$$

$$\ldots\ldots(A2)$$

$$= \frac{1}{3}(1 - A_c - B_c)\ln K_{c3} + \frac{1}{3} \int_{1}^{A_c} \ln K_{c3} dA_c + \frac{1}{3} \int_{0}^{B_c} \ln K_{c3} dB_c \qquad \ldots\ldots(A3)$$

This shows that the value of $\ln K_{c3}$ in the first term on the r.h.s. of equation (A3) is indeed $\ln K_{c3}$ at A_c, B_c.

Part I :-   Preparation of K-X (KNO_3 solution used)

Part II:-   Preparation of Li-X (Li NO_3 solution used)

Exchange No.	Duration (hrs)	Solution concentration (mol.dm^{-3})	Na$^+$ concentration in wash liquor (ppm)	(m equiv.dm^{-3})	Decrease in concentration (ppm)
I 1	3.5	1	-	-	
2	18.5	1	-	-	
3	3.5	1	-	-	
4	2.25	1	-	-	
5	17.5	1	-	-	
6	2.25	1	157	4.02	
7	72	1	109	2.79	48
8	69	1	90	2.30	19
9	71	1	50	1.28	40
10	75.5	1	40	1.02	10
11	43	1	25	0.64	15
12	99	1	19	0.49	6
13	69	1	14	0.36	5
14	94.5	0.5	10	0.26	4
II 1	3.5	1	-	-	
2	18.5	1	-	-	
3	3.5	1	-	-	
4	2.25	1	-	-	
5	17.5	1	-	-	
6	2.25	1	-	-	
7	72	1	198	28.70	
8	69.5	1	158	22.90	40
9	71	1	144	20.87	14
10	76	1	129	18.70	15
11	43	1	91	13.19	38
12	99	1	60	8.70	31
13	69	1	62	8.99	} 23
14	95	0.5	37	5.36	
15	45	0.5	30	4.35	7

APPENDIX III a

Flame Photometer Calibration for Na

Instrument scale

Na concentration (ppm)
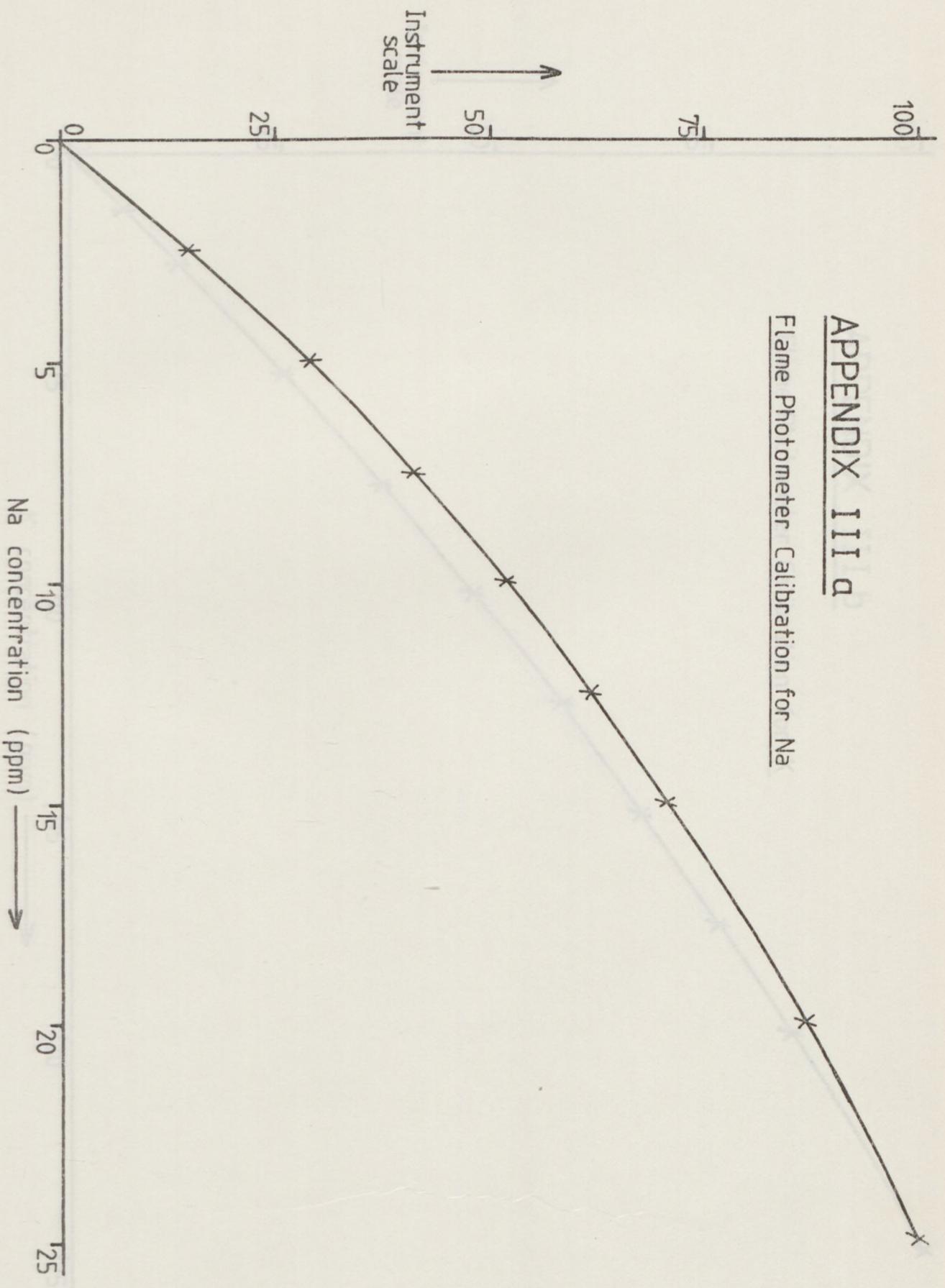
APPENDIX III b

Flame Photometer Calibration for K

Instrument scale

K concentration (ppm)

Computer Flow Diagram

Binary Thermodynamic Treatment

(A special form of this program was used for the two-anion binary system. See Program No. 1)
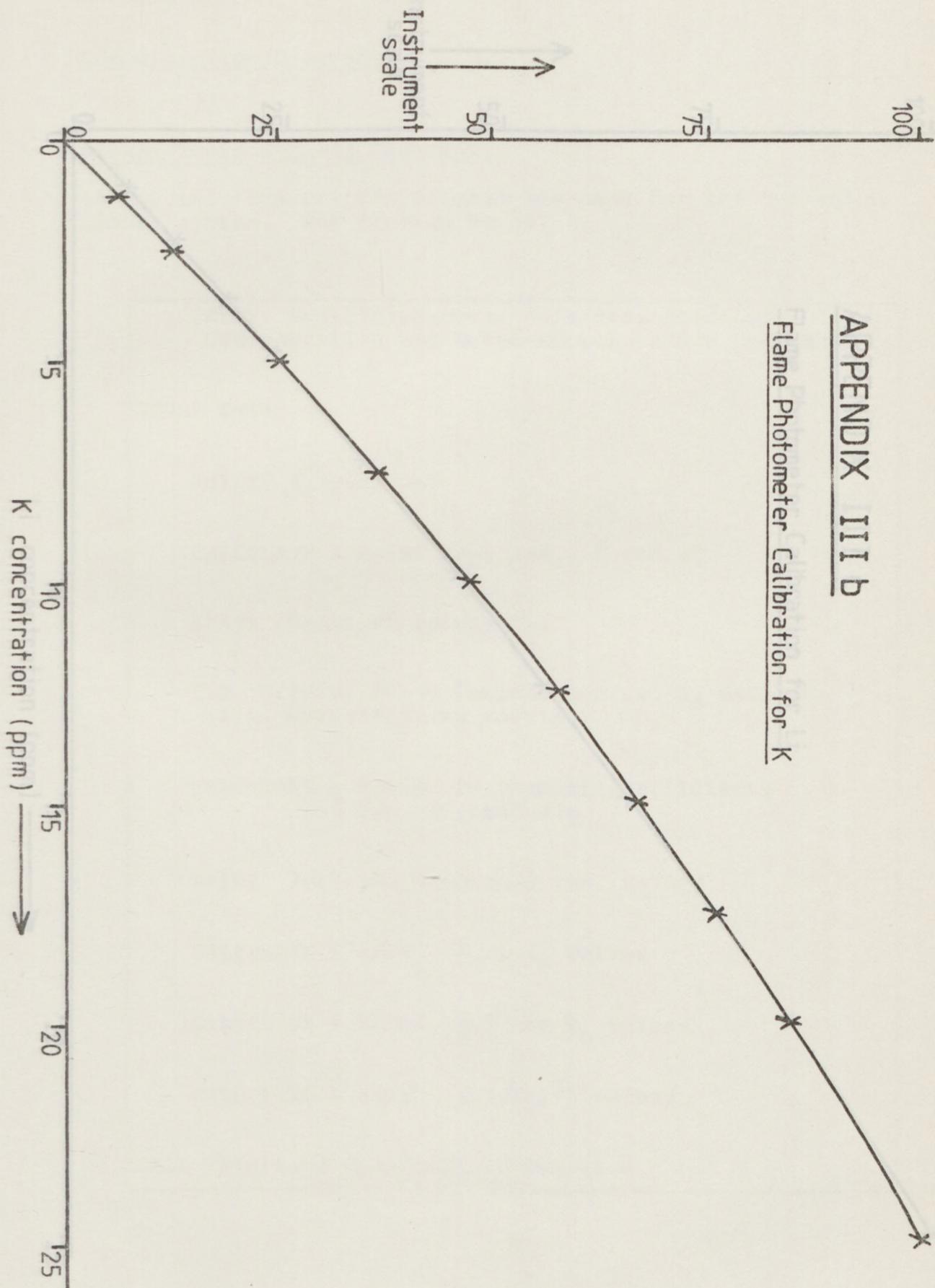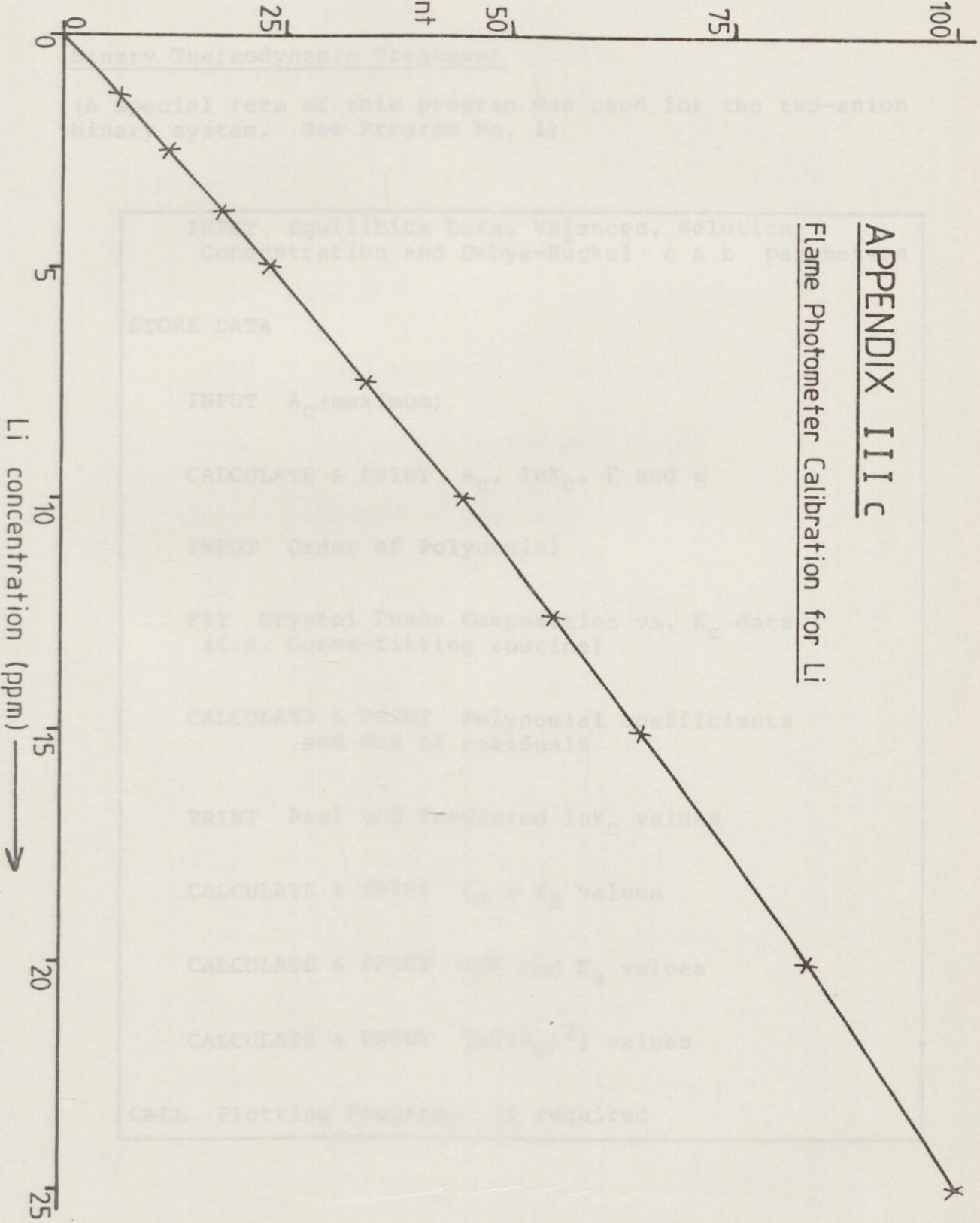
APPENDIX IIIc

Flame Photometer Calibration for Li

Instrument scale

Li concentration (ppm)

INPUT Equilibrium Data, Valences, Solution
       Concentration and Debye-Huckel a & b parameters

STORE DATA

INPUT A_c (maximum)

CALCULATE & PRINT A_c, lnK_c, P and a

INPUT Order of Polynomial

FIT Crystal Phase Composition vs. K_c data
     (i.e. Curve-fitting routine)

CALCULATE & PRINT Polynomial Coefficients
                   and Sum of residuals

PRINT Real and Predicted lnK_c values

CALCULATE & PRINT C_o & F_o values

CALCULATE & PRINT K_o values

CALCULATE & PRINT values

CALL Plotting Program if required

APPENDIX IV

Computer Flow Diagram

Binary Thermodynamic Treatment

(A special form of this program was used for the two-anion binary system. See Program No. 1)

INPUT   Equilibium Data, Valences, Solution
        Concentration and Debye-Hückel a & b parameters

STORE DATA

    INPUT A_c (maximum)

    CALCULATE & PRINT A_c, $\ln K_c$, Γ and α

    INPUT   Order of Polynomial

    FIT   Crystal Phase Composition vs. K_c data
          (i.e. Curve-fitting routine)

    CALCULATE & PRINT Polynomial coefficients
                and Sum of residuals

    PRINT   Real and Predicted $\ln K_c$ values

    CALCULATE & PRINT f_A & f_B values

    CALCULATE & PRINT $\Delta G^{\ominus}$ and K_a values

    CALCULATE & PRINT $\ln[(K_c)^3]$ values

CALL   Plotting Programs if required

APPENDIX IV

Computer Flow Diagram

Calculation of a Mean Molal Stoichiometric Activity
Coefficient of a Pure Salt

(See Program No. 2)

INPUT A_c and Concentration of Anion X

INPUT A_s and T_N for One-anion Binary System

INPUT A_s and T_N for Two-anion Binary System

INPUT Γ for One-anion Binary System

INPUT Valences of all ions

CALCULATE Γ for Two-anion Binary System
(i.e. for mixed salt solution)

INPUT Debye-Hückel a & b parameters for
three (known) salts

STORE SELECTED DATA

CALCULATE Concentrations, K_m and I

CALCULATE $\gamma_{\pm}$ values for the 3 (known) pure salts

CALCULATE $\gamma_{\pm}$ value (unknown) for the 4th salt

PRINT $\gamma_{\pm}$ and log $\gamma_{\pm}$ for all salts and I

CONTINUE WITH NEW DATA

Computer Flow Diagram

Calculation of Elprince & Babcock Λ Parameters

(See Program No. 3)

```
┌─────────────────────────────────────────────────────────────┐
│                                                              │
│      INPUT    Fraction of Ion A in Crystal and Solution      │
│               and Estimated Starting Value of Λ              │
│                                                              │
│                                                              │
│      CALCULATE & PRINT   gᴱ                                  │
│                                                              │
│                                                              │
│      CALCULATE   Λ₂₁ from Λ₁₂  (using input Λ value)         │
│       Then   CALCULATE   Λ₁₂ from Λ₂₁                        │
│                                                              │
│                                                              │
│      COMPARE  Starting Λ₁₂ and Calculated Λ₁₂               │
│                                                              │
│                                                              │
│      IF  (Starting Λ – Calculated Λ) > 0.00001  THEN         │
│       make a step change to Starting Λ and  REPEAT           │
│                                                              │
│                                                              │
│      IF  Λ₁₂ and Λ₂₁ values are diverging  THEN              │
│         reverse data and  REPEAT  from beginning             │
│                                                              │
│                                                              │
│       When Starting and Calculated Λ values cross-over,      │
│      REVERSE  direction of calculation and  REPEAT           │
│      using a smaller step change.  This procedure            │
│      is repeated until the Starting and Calculated           │
│      values come within 0.00001 of one another.              │
│                                                              │
│                                                              │
│      PRINT   Λ₁₂ and Λ₂₁                                     │
│                                                              │
│                                                              │
│      CALCULATE & PRINT  Errors  if required                  │
│                                                              │
│                                                              │
│      CALCULATE & PRINT  gᴱ from Λ values                     │
│                                                              │
│                                                              │
│      CALCULATE & PRINT  Binary Equilibrium Constants         │
│                                                              │
│                                                              │
│  CONTINUE  with next set of data                             │
└─────────────────────────────────────────────────────────────┘
```

APPENDIX IV

Computer Flow Diagrams

Prediction of Crystal Phase Activity Coefficients and
Solution Phase Compositions using the Elprince-Babcock
Model

(See Program No. 4)

```
        INPUT   K_a values for the 3 conjugate binary
                systems

        INPUT   Elprince-Babcock Λ terms and Ternary
                Crystal Phase Compositions

        CALCULATE & PRINT  Crystal Phase Activity
          Coefficients and Solution Phase Compositions


CONTINUE  with new data
```

Plotting A_C vs. lnK_C, f_A & f_B and α

```
        INPUT   Maximum & minimum values of parameter(s)

        FEED  data from Binary Thermodynamic Treatment

        PLOT  Points

        PLOT  Curve represented by Polynomial Equation
              used to fit lnK_C
```

APPENDIX IV

Computer Flow Diagram

Ternary Thermodynamic Treatment

(3 Programs were used consecutively)

```
┌─────────────────────────────────────────────────────────────┐
│        INPUT    Equilibrium Data                             │
│                                                              │
│        INPUT    Ion valences and $T_N$ value                 │
│                                                              │
│        INPUT    Debye-Hückel  a & b  parameters              │
│  STORE DATA                                                  │
│                                                              │
│        CALCULATE   Cation Concentrations, $K_m$ values and I │
│                                                              │
│        CALCULATE   Γ values for mixed solution               │
│                                                              │
│        CALCULATE   Γ ratios                                  │
│                                                              │
│        PRINT   $K_m$ values and Γ ratios                     │
│                                                              │
│  STORE CALCULATED DATA   (for next program)                  │
└─────────────────────────────────────────────────────────────┘


┌─────────────────────────────────────────────────────────────┐
│  FEED DATA                                                   │
│                                                              │
│        CALCULATE   $K_c$ ratios                              │
│                                                              │
│        ADD  Binary $K_c$ data  (in cubed form)              │
│                                                              │
│        INPUT   Number of Polynomial Coefficients             │
│                (i.e. select the order of fitting equation)   │
└─────────────────────────────────────────────────────────────┘
```

(continued overleaf)

Ternary Thermodynamic Treatment   (continued)

```
┌─────────────────────────────────────────────────────────┐
│      FIT  Crystal Phase Composition vs. K_C ratio data    │
│           (i.e. Surface-fitting routine)                  │
│                                                           │
│                                                           │
│      PRINT  Polynomial Coefficients                       │
│                                                           │
│                                                           │
│      PRINT  calculated data  if required                  │
│       (i.e. Real & Predicted lnK_C ratio values)          │
│                                                           │
│                                                           │
│  STORE CALCULATED DATA   (for next program)               │
│                                                           │
│  N.B. Cubed Binary Data are discarded at this stage.      │
│   These data are used only to improve the fitting         │
│   procedure, and not in subsequent calculations.          │
└─────────────────────────────────────────────────────────┘
```

```
┌─────────────────────────────────────────────────────────┐
│  FEED DATA                                                │
│                                                           │
│      RE-FORM  Polynomial Equations                        │
│                                                           │
│      PRINT  Real & Predicted lnK_C ratio values           │
│                                                           │
│      PRINT  Polynomial Coefficients and Order of          │
│             Fitting                                       │
│                                                           │
│                                                           │
│      PRINT  Sum of residuals for each K_C ratio           │
│                                                           │
│                                                           │
│      CALCULATE & PRINT  Crystal Phase Activity            │
│              Coefficients                                 │
│                                                           │
│                                                           │
│      CALCULATE & PRINT  ΔG^⊖ and K_a ratio values         │
└─────────────────────────────────────────────────────────┘
```

APPENDIX IV

Computer Flow Diagram

Generation of Data for Distorted Solution Phase Diagrams

(2 Programs were used consecutively)

```
┌─────────────────────────────────────────────────────────┐
│     INPUT   Equilibrium Data and Number of Points        │
│                                                          │
│ STORE DATA                                               │
│                                                          │
│     CALCULATE   Parameters q₁ and q₂                     │
│                                                          │
│     INPUT   Order of Polynomial Equation                 │
│                                                          │
│     FIT   Solution Phase Composition vs. q data          │
│       (i.e. Surface-fitting routine)                     │
│                                                          │
│     CALCULATE   Crystal Phase Composition Data           │
│       corresponding to self-generated Solution Phase     │
│       Composition Data using the Fitting Equations       │
│                                                          │
│     SELECT   Crystal Phase Data which are near the       │
│       Experimental Crystal Phase Compositions            │
│                                                          │
│ STORE SELECTED DATA    (for next program)                │
└─────────────────────────────────────────────────────────┘
```

```
┌─────────────────────────────────────────────────────────┐
│ FEED DATA                                                │
│                                                          │
│     PLOT   Distorted Curves within the Triangles for     │
│            each Cation                                    │
│                                                          │
│     PRINT   Data for Manual Plotting                     │
└─────────────────────────────────────────────────────────┘
```

APPENDIX IV

Computer Flow Diagram

Generation of Contour Data

```
INPUT   Order of Polynomial and Coefficients

INPUT   High and Low values of K_C ratio

CALCULATE   Range of K_C ratio values and Band
            widths

CALCULATE & PRINT   Crystal Phase Compositions that
                    fall within each band

REPEAT   for other orders and for other K_C ratio
```

Computer Program No. 1

```
10  REM  - A PROGRAM TO CALCULATE THE THERMODYNAMIC PARAMETERS OF A TWO-ANION BINARY SYSTEM
20  HOME
30  DIM X(15),Y(15),A(11),IX(15),IY(15),Z(15),F(5,5,5),PI(6,6),F(15),E(15),NX(15)
40  DIM AL(15),IZ(15)
50  D$ = CHR$ (4)
60  PRINT " IS DATA FROM FILE OR TERMINAL? FILE NAME MUST BE DATA": PRINT
70  PRINT "TYPE F OR T": INPUT QUEST$: IF QUEST$ = "F" THEN  GOTO 310
80  PRINT : PRINT "INPUT NUMBER OF POINTS": INPUT ITEMS
90  PRINT "INPUT VALUES OF AC THEN AS THEN INITIAL NORMALITY (EQ/L) OF ANION X (FROM SALT AX)
100 FOR N = 1 TO ITEMS
110 INPUT X(N),Y(N),NX(N): NEXT N
120 PRINT " ": PRINT "INPUT ZA,ZB,ZX,ZY,TN": INPUT ZA,ZB,ZX,ZY,TN
130 PRINT "DO YOU NEED TO INPUT DEBYE HUCKEL TERMS": INPUT QUES$: IF QUES$ = "NO" THEN  GOTO 180
140 PRINT "INPUT DEBYE-HUCKEL PARAMETERS": PRINT : PRINT "INPUT A&B FOR SALT AX"
150 INPUT AA,BA: PRINT "INPUT A&B FOR SALT BY": INPUT AB,BB
160 PRINT : PRINT "INPUT A&B FOR SALT AY": INPUT AY,BY
170 PRINT : PRINT "INPUT A&B FOR SALT BX": INPUT AX,BX
180 PRINT D$"OPEN DATA,L15"
190 PRINT D$;"WRITE DATA"
200 PRINT ITEMS
210 FOR N = 1 TO ITEMS
220 PRINT X(N): PRINT Y(N): PRINT NX(N)
230 NEXT N
240 PRINT ZA: PRINT ZB: PRINT ZX: PRINT ZY: PRINT TN
250 PRINT AA: PRINT BA: PRINT AB: PRINT BB
260 PRINT AY: PRINT BY: PRINT AX: PRINT BX
270 PRINT D$"CLOSE DATA"
280 PRINT " "
290 PRINT "THE DATA IS NOW IN A FILE NAMED DATA"
300 GOTO 430
310 REM  OUTPUT DATA FROM FILE
320 PRINT D$;"OPEN DATA,L15"
330 PRINT D$;"READ DATA"
340 INPUT ITEMS
350 FOR N = 1 TO ITEMS
360 INPUT X(N): INPUT Y(N): INPUT NX(N)
370 NEXT N
380 INPUT ZA: INPUT ZB: INPUT ZX: INPUT ZY: INPUT TN
390 INPUT AA: INPUT BA: INPUT AB: INPUT BB
400 INPUT AY: INPUT BY: INPUT AX: INPUT BX
410 PRINT D$;"CLOSE DATA"
420 REM  - IS GAMMA RATIO KNOWN?
430 PRINT : PRINT "CAN YOU INPUT THE GAMMA RATIO ?": INPUT GAM$
440 IF GAM$ = "NO" THEN  GOTO 470
450 PRINT : PRINT "INPUT GAMMA RATIO FOR EACH AC VALUE"
460 FOR I = 1 TO ITEMS: PRINT "INPUT  I , GAMMA (I)": INPUT I,F(I): NEXT I
470 HOME
480 PRINT "": PRINT "NUMBER OF POINTS = ";ITEMS: PRINT " "
490 PRINT "AC","AS","NX (EQ/L)": PRINT
500 FOR I = 1 TO ITEMS: PRINT X(I),Y(I),NX(I),I
510 NEXT I
520 PRINT " ": PRINT "DO YOU WISH TO CHANGE OR ADD POINTS"
530 INPUT QUE$: IF QUE$ = "NO" THEN  GOTO 620
540 PRINT " ": PRINT " INPUT TOTAL NUMBER OF DATA POINTS": INPUT ITEMS
550 PRINT " ": PRINT "INPUT THE NUMBER OF POINTS TO BE CHANGED OR ADDED": INPUT CNOS
```

(continued overleaf)

```
560  IF CNOS = 0 THEN  GOTO 120
570  FOR I = 1 TO CNOS: PRINT " ": PRINT "INPUT  I ,X(I) ,Y(I) ,NX(I)"
580  INPUT J,X(J),Y(J),NX(J)
590  NEXT I
600  GOTO 120
610  REM  - IS ZEOLTE FULLY OR PARTIALLY EXCHANGED ?
620  PRINT "INPUT ACMAX": INPUT AM
630  NY = TN - NX:MX = NX / ZX:MY = NY / ZY
640  AX = 4.9677E - 10:BX =  - 0.02675
650  PRINT "AC","LNKC","G.R.(X)","G.R.(Y)","ALPHA": PRINT
660  REM  - CALCULATE THE MOLAR CONCENTRATIONS, AND HENCE, THE MASS ACTION QUOTIENT
670  FOR I = 1 TO ITEMS
680  AC = X(I) / AM:BC = 1 - AC:AS = Y(I):BS = 1 - AS
690  MA = (AS * TN) / ZA:MB = (BS * TN) / ZB
700  ALP = (ZA / ZB) * (AC * BS / (AS * BC))
710  AL(I) =  INT (ALP * 100000) / 100000
720  KM = ((AC ^ ZB) * (MB ^ ZA)) / ((BC ^ ZA) * (MA ^ ZB))
730  REM  - IF GAMMA RATIO IS KNOWN, DEBYE-HUCKEL AND MODIFIED GLUECKAUF MODELS ARE BYPASSED
740  IF GAM$ = "NO" THEN  GOTO 760
750  GAM = F(I): GOTO 1360
760  REM  -          DEBYE-HUCKEL MODEL
770  REM  - CALCULATE THE IONIC STRENGTH
780  IS = 0.5 * ((MA * ZA * ZA) + (MB * ZB * ZB) + (MX * ZX * ZX) + (MY * ZY * ZY))
790  RIS = (IS ^ 0.5)
800  REM  - CALCULATE THE MEAN MOLAL STOICHIOMETRIC ACTIVITY COEFFICIENTS OF THE PURE SALTS
810  P1 = ( - 0.5115) * (ZA * ZX) * RIS
820  P2 = (3.291E9) * AA * RIS
830  P3 = ( - 0.5115) * (ZA * ZY) * RIS
840  P4 = (3.291E9) * AY * RIS
850  Q1 = ( - 0.5115) * (ZB * ZX) * RIS
860  Q2 = (3.291E9) * AX * RIS
870  Q3 = ( - 0.5115) * (ZB * ZY) * RIS
880  Q4 = (3.291E9) * AB * RIS
890  L1 = (P1 / (P2 + 1)) + (BA * IS)
900  L2 = (P3 / (P4 + 1)) + (BY * IS)
910  L3 = (Q1 / (Q2 + 1)) + (BX * IS)
920  L4 = (Q3 / (Q4 + 1)) + (BB * IS)
930  REM - MODIFIED GLUECKAUF MODEL
940  K1 = (0.5115) * RIS / (RIS + 1) .
950  K2 = ((ZA + ZX) * (ZA + ZX)) * (ZA * MA + ZX * MX)
960  K3 = ((ZB + ZX) * (ZB + ZX)) * MB
970  K4 = ((ZA + ZY) * (ZA + ZY)) * MY
980  G1 = K2 + (ZB * K3) + (ZY * K4)
990  G1 = G1 * K1 * (ZA * ZX)
1000 G1 = G1 + (K2 * L1) + (K3 * L3 * ZA) + (K4 * L2 * ZX)
1010 G1 = G1 / (4 * IS * (ZA + ZX))
1020 G1AX = G1 - K1 * (ZA * ZX)
1030 K5 = ((ZA + ZY) * (ZA + ZY) * (ZA * MA + ZY * MY))
1040 K6 = ((ZB + ZY) * (ZB + ZY)) * MB
1050 K7 = ((ZA + ZX) * (ZA + ZX)) * MX
1060 G2 = K5 + (ZB * K6) + (ZX * K7)
1070 G2 = G2 * K1 * (ZA * ZY)
1080 G2 = G2 + (K5 * L2) + (K6 * L4 * ZA) + (K7 * L1 * ZY)
1090 G2 = G2 / (4 * IS * (ZA + ZY))
1100 G2AY = G2 - K1 * (ZA * ZY)
1110 J1 = K1
1120 J2 = ((ZB + ZX) * (ZB * ZX)) * (ZB * MB + ZX * MX)
1130 J3 = ((ZA + ZX) * (ZA + ZX)) * MA
1140 J4 = ((ZB + ZY) * (ZB + ZY)) * MY
1150 G3 = J2 + (ZA * J3) + (ZY * J4)
```

(continued overleaf)

- 339 -

```
1160 G3 = G3 * J1 * (ZB * ZX)
1170 G3 = G3 + (J2 * L3) + (J3 * L1 * ZB) + (J4 * L4 * ZX)
1180 G3 = G3 / (4 * IS * (ZB + ZX))
1190 G3BX = G3 - J1 * (ZB * ZX)
1200 J5 = ((ZB + ZY) * (ZB + ZY)) * (ZB * MB + ZY * MY)
1210 J6 = ((ZA + ZY) * (ZA + ZY)) * MA
1220 J7 = ((ZB + ZX) * (ZB + ZX)) * MX
1230 G4 = J5 + (ZB * J6) + (ZY * J7)
1240 G4 = G4 * J1 * (ZB * ZY)
1250 G4 = G4 + (J5 * L4) + (J6 * L2 * ZB) + (J7 * L3 * ZY)
1260 G4 = G4 / (4 * IS * (ZB + ZX))
1270 G4BY = G4 - J1 * (ZB * ZY)
1280  REM - LOG MEAN ACTIVITY COEFFICIENTS OF MIXED SALTS READY
1290 G1 = G1 * (ZA + ZX) * ZB:G3 = G3 * (ZB + ZX) * ZA
1300 G2 = G2 * (ZA + ZY) * ZB:G4 = G4 * (ZB + ZY) * ZA
1310 G5 = (G3 - G1) / ZX:G6 = (G4 - G2) / ZY
1320  REM - CALCULATE GAMMA RATIOS
1330 G5 = 2.303 * G5:G5 =  EXP (G5):GAM = G5
1340 G6 = 2.303 * G6:G6 =  EXP (G6)
1350  REM   GAMMA VALUES READY
1360 KC = KM * GAM:KC =  LOG (KC):KC =  INT (KC * 100000) / 100000
1370  PRINT AC,KC,G5,G6,ALP
1380 X(I) = AC:Y(I) = KC: NEXT I
1390  IF GAM$ = "YES" THEN  GOTO 1420
1400  PRINT : PRINT : PRINT "GAMMA RATIO BASED ON ANION X IS ";GAM
1410  PRINT : PRINT : PRINT "GAMMA RATIO BASED ON ANION Y IS ";G6
1420  PRINT : PRINT "INPUT ORDER OF POLYNOMIAL"
1430  INPUT POWER
1440 NTERMS = POWER + 1
1450  FOR I = 1 TO NTERMS
1460  FOR J = 1 TO NTERMS
1470  FOR K = 1 TO NTERMS
1480 P(I,J,K) = 0.0
1490  NEXT K
1500  NEXT J
1510  NEXT I
1520  FOR I = 1 TO NTERMS
1530  FOR J = 1 TO NTERMS
1540  FOR M = 1 TO ITEMS
1550 P(I,J,1) = P(I,J,1) + (X(M) ^ (I + J - 2))
1560  NEXT M
1570  NEXT J
1580  NEXT I
1590 P(1,1,1) = ITEMS
1600  FOR I = 1 TO NTERMS
1610  FOR M = 1 TO ITEMS
1620 PI(I,1) = PI(I,1) + (Y(M) * (X(M) ^ (I - 1)))
1630  NEXT M
1640  NEXT I
1650  FOR K = 2 TO NTERMS
1660  FOR I = K TO NTERMS
1670  FOR J = K - 1 TO NTERMS
1680 P(I,J,K) = ((P(I,J,K - 1) * P(K - 1,K - 1,K - 1)) / P(I,K - 1,K - 1)) - P(K - 1,J,K - 1)
1690  NEXT J
1700  NEXT I
1710  NEXT K
1720 M = NTERMS + 1
1730  FOR K = 2 TO NTERMS
1740  FOR I = K TO NTERMS
1750 PI(I,K) = ((PI(I,K - 1) * P(K - 1,K - 1,K - 1)) / P(I,K - 1,K - 1)) - PI(K - 1,K - 1)
```

```
1760  NEXT I
1770  NEXT K
1780  M = NTERMS
1790  A(M) = PI(M,M) / P(M,M,M)
1800  FOR I = 1 TO M - 1
1810  KNO = M - I
1820  SUM = 0.0
1830  FOR J = KNO + 1 TO M
1840  L = J
1850  SUM = SUM + (A(L) * P(KNO,L,KNO))
1860  NEXT J
1870  A(KNO) = (PI(KNO,KNO) - SUM) / P(KNO,KNO,KNO)
1880  NEXT I
1890  FOR I = 1 TO NTERMS: IF  ABS (A(I)) ( 1E - 5 THEN A(I) = 0.0: NEXT I
1900  HOME
1910  FOR I = 1 TO NTERMS: PRINT " A";I;" = ";A(I): NEXT I
1920  FOR L = 1 TO ITEMS
1930  FOR N = 1 TO 9
1940  Z(L) = Z(L) + (A(N) * (X(L) ^ (N - 1)))
1950  NEXT N
1960  NEXT L
1970  FOR N = 1 TO ITEMS
1980  XSUM = ((Y(N) - Z(N)) ^ 2) + XSUM
1990  NEXT N
2000  SR =  SQR (XSUM / (ITEMS - POWER - 1))
2010  PRINT : PRINT "SUM OF RESIDUALS = ";SR
2020  PRINT " ": PRINT "DO YOU REQUIRE THE CALCULATED DATA"
2030  INPUT QUEST$: IF QUEST$ = "NO" THEN  GOTO 2100
2040  HOME
2050  PRINT : PRINT "X          Y          Y CALC": PRINT
2060  FOR I = 1 TO ITEMS: PRINT X(I);"        ";Y(I);"          ";Z(I)
2070  NEXT I
2080  INPUT ANY$
2090  REM  - CALCULATE THE STANDARD FREE ENERGY
2100  FOR N = 1 TO 9
2110  INX = INX + (A(N) / N): NEXT N
2120  LNKA = (ZB - ZA) + INX
2130  LED = (( - 8.314 * 298 / (ZA * ZB)) * LNKA) / 1000:LNKA =  EXP (LNKA)
2140  HOME
2150  PRINT "CRYSTAL PHASE CORRECTION"
2160  PRINT : PRINT "","FA","FB"
2170  FOR I = 1 TO ITEMS
2180  BC = 1 - X(I):IY = 0
2190  FOR N = 1 TO NTERMS
2200  IY = IY + (A(N) * (X(I) ^ N) / N)
2210  NEXT N
2220  IZ = INX - IY:FA = ((ZB - ZA) * BC) - Z(I) + (X(I) * Z(I)) + IZ
2230  FB = (X(I) * Z(I)) - ((ZB - ZA) * X(I)) - IY
2240  FA =  EXP (FA):FA = FA ^ (1 / ZB):FB =  EXP (FB):FB = FB ^ (1 / ZA)
2250  PRINT I,FA,FB:F(I) = FA:E(I) = FB
2260  NEXT I
2270  PRINT : PRINT "DELTA G = ";LED;"     KA = ";LNKA
2280  PRINT : PRINT "DO YOU REQUIRE A PLOT OF AC VS. LNKC?": INPUT PLO$
2290  IF PLO$ = "YES" THEN  GOTO 2340
2300  PRINT : PRINT "DO YOU REQUIRE PLOTS OF AC VS. FA & FB OR AC VS. ALPHA?": INPUT CUR$
2310  IF CUR$ = "NO" THEN  GOTO 2360
2320  PRINT  CHR$ (4);"BLOAD CHAIN,A520"
2330  CALL 520"THERM3"
2340  PRINT  CHR$ (4);"BLOAD CHAIN,A520"
2350  CALL 520"THERM2"
2360  END
```

Computer Program No. 2

```
10  REM - A PROGRAM TO CALCULATE THE MEAN MOLAL STOICHIOMETRIC ACTIVITY COEFFICIENT OF A PURE SALT
20  P = 0
30  POKE  - 12524,0
40  HOME
50  HGR
60  POKE  - 16303,0
70  D$ =  CHR$ (4)
80  P = P + 1
90  PRINT : PRINT "INPUT AC AND NORMALITY OF ANION X WHERE X IS ASSOCIATED WITH THE INGOING ION A"
100  INPUT AC,N2X
110  PRINT : PRINT "INPUT AS & TN FOR SYSTEM 1 (COMMON ANION) AND AS & TN FOR SYSTEM 2 (TWO ANIONS)"
120  INPUT A1S,T1N,A2S,T2N
130 AS = A2S
140  PRINT : PRINT "DO YOU NEED TO INPUT GAMMA RATIO FOR SYSTEM 1?": INPUT GAM$
150  IF GAM$ = "NO" THEN  GOTO 170
160  PRINT : PRINT "INPUT GAMMA RATIO FOR SYSTEM 1": INPUT G1
170  PRINT : PRINT "DO YOU NEED TO INPUT THE Z VALUE  (VALENCE)  OF ANY ION?": INPUT Z$
180  IF Z$ = "NO" THEN  GOTO 210
190  PRINT : PRINT "INPUT ZA , ZB , ZX , ZY": INPUT ZA,ZB,ZX,ZY
200  REM  - CALCULATE THE GAMMA RATIO FOR SYSTEM 2
210 G =  LOG (G1)
220 TN = T1N / T2N:TN =  LOG (TN)
230 B1S = 1 - A1S
240 B1S =  LOG (B1S):A1S =  LOG (A1S)
250 B2S = 1 - A2S
260 B2S =  LOG (B2S):A2S =  LOG (A2S)
270 G2 = ZA * B1S + ZB * A2S - ZA * B2S - ZB * A1S + G
280  IF ZA = ZB THEN  GOTO 300
290 G2 = G2 + (ZA - ZB) * TN
300 GAM =  EXP (G2)
310 TN = T2N:NX = N2X
320  PRINT : PRINT "ARE DEBYE-HUCKEL DATA ON FILE?": INPUT QUE$
330  IF QUE$ = "YES" THEN  GOTO 450
340  PRINT : PRINT "INPUT DEBYE-HUCKEL PARAMETERS": PRINT : PRINT "INPUT A&B FOR SALT AX"
350  INPUT AA,BA: PRINT "INPUT A&B FOR SALT BY": INPUT AB,BB
360  PRINT : PRINT "INPUT A&B FOR SALT AY": INPUT AY,BY
370  PRINT D$;"OPEN DHFILE,L15"
380  PRINT D$;"WRITE DHFILE"
390  PRINT AA: PRINT BA
400  PRINT AB: PRINT BB
410  PRINT AY: PRINT BY
420  PRINT D$;"CLOSE DHFILE"
430  PRINT : PRINT "THE DEBYE-HUCKEL DATA ARE NOW IN A FILE NAMED DHFILE"
440  GOTO 520
450  REM  - OUTPUT DATA FROM FILE
460  PRINT D$;"OPEN DHFILE,L15"
470  PRINT D$;"READ DHFILE"
480  INPUT AA: INPUT BA
490  INPUT AB: INPUT BB
500  INPUT AY: INPUT BY
510  PRINT D$;"CLOSE DHFILE"
520  REM  - DEBYE HUCKEL DATA READY
```

(continued overleaf)

```
530 GM = GM + GAM
540 MG = GM / P
550 PRINT : PRINT
560 PRINT : PRINT "SYSTEM 2 (TWO ANIONS)"
570 PR£ 1
580 PRINT : PRINT
590 PRINT "AC","AS","NX (EQ/L)","GAMMA RATIO","MEAN GAMMA R"
600 PRINT AC,AS,NX,GAM,MG
610 REM  - CALCULATE THE MOLAR CONCENTRATIONS, AND HENCE, THE MASS ACTION QUOTIENT
620 NY = TN - NX
630 MX = NX / ZX:MY = NY / ZY
640 PRINT ""
650 BC = 1 - AC:BS = 1 - AS
660 MA = (AS * TN) / ZA:MB = (BS * TN) / ZB
670 KM = ((AC ^ ZB) * (MB ^ ZA)) / ((BC ^ ZA) * (MA ^ ZB))
680 REM -         THE DEBYE-HUCKEL MODEL
690 REM  - CALCULATE THE IONIC STRENGTH
700 IS = 0.5 * ((MA * ZA * ZA) + (MB * ZB * ZB) + (MX * ZX * ZX) + (MY * ZY * ZY))
710 RIS = (IS ^ 0.5)
720 P1 = ( - 0.5115) * (ZA * ZX) * RIS
730 P2 = (3.291E9) * AA * RIS
740 P3 = ( - 0.5115) * (ZA * ZY) * RIS
750 P4 = (3.291E9) * AY * RIS
760 Q3 = ( - 0.5115) * (ZB * ZY) * RIS
770 Q4 = (3.291E9) * AB * RIS
780 REM  - CALCULATE THE MEAN MOLAL STOICHIOMETRIC ACTIVITY COEFFICIENTS OF THE PURE SALTS
790 L1 = (P1 / (P2 + 1)) + (BA * IS)
800 L2 = (P3 / (P4 + 1)) + (BY * IS)
810 L4 = (Q3 / (Q4 + 1)) + (BB * IS)
820 K1 = MX * ((ZA + ZX) * (ZA + ZX))
830 K1 = K1 * L1:M1 = 2.303 * L1:M1 =  EXP (M1)
840 K2 = ZB * ((ZA + ZY) * (ZA + ZY))
850 K2 = K2 * L2:M2 = 2.303 * L2:M2 =  EXP (M2)
860 K3 = ZA * ((ZB + ZY) * (ZB + ZY))
870 K3 = K3 * L4:M4 = 2.303 * L4:M4 =  EXP (M4)
880 K4 = (K2 - K3) * MY
890 K5 = 4 * IS * (G2 / 2.303)
900  IF ZA = ZB THEN  GOTO 950
910 K6 = ZA * ZB / (1 + (1 / RIS))
920 K6 = K6 * ((ZA - ZB) * (ZA - ZB)) * (0.5115)
930 K6 = K6 * ((MA * ZA) - (MB * ZB))
940  GOTO 960
950 K6 = 0
960 KK = K4 + K1 + K5 - K6
970 KK = KK / MX
980 L3 = KK / ((ZB + ZX) * (ZB + ZX))
990 L = 2.303 * L3
1000 L =  EXP (L)
1010 PRINT : PRINT : PRINT "LOG GAMMA(AX) = ";L1,"GAMMA(AX) = ";M1
1020 PRINT : PRINT "LOG GAMMA(AY) = ";L2,"GAMMA(AY) = ";M2
1030 PRINT : PRINT "LOG GAMMA(BY) = ";L4,"GAMMA(BY) = ";M4
1040 PRINT : PRINT
1050 PRINT : PRINT "LOG GAMMA(BX) = ";L3,"GAMMA(BX) = ";L
1060 PRINT : PRINT "IONIC STRENGTH OF SOLUTION = ";IS
1070 PR£ 0
1080 PRINT : PRINT : PRINT
1090 PRINT : PRINT "DO YOU WISH TO REPEAT THE PROGRAMME?": INPUT YE$
1100  IF YE$ = "NO" THEN  GOTO 1120
1110  GOTO 80
1120  END
```

Computer Program No. 3

```
10  REM  - A PROGRAM TO CALCULATE ELPRINCE AND BABCOCK LAMDA PARAMETERS FOR BINARY ION EXCHANGE
20  HOME
30  REM  - ESTABLISH NATURE OF EXCHANGING IONS
40  PRINT "INPUT ION 1 (INGOING ION) AND ION 2
50  INPUT K1$,K2$: PRINT
60  PRINT "INPUT GAMMA RATIO  GA"
70  INPUT GA: PRINT " "
80  PRINT " ": PRINT "INPUT N1,F1,X1,F2,L WHERE L IS THE ESTIMATED STARTING VALUE OF LAMDA
90  INPUT N1,F1,X1,F2,L
100  PRINT " ": PRINT " "
110  Q = L:G = GA
120  REM  - SET STEP CHANGE
130  ST = 0.1
140  REM   - CALCULATE N2 FROM N2=1-N1 AND X2 FROM X2=1-X1
150  N2 = 1 - N1:X2 = 1 - X1
160  REM   - CALCULATE DELTA G EXCESS FROM INPUT DATA
170  DG = N1 *  LOG (F1) + N2 *  LOG (F2)
180  DG = DG * 8.314 * 298 / 1000
190  SN = 0:I = 1:CV$ = "0":L = Q
200  I1$ = K1$:I2$ = K2$
210  L12 = L
220  IF CV$ = "FINISH" THEN A2 = L21
230  REM  - CALCULATE L21 FROM L12
240  A = N1 + L12 * N2
250  X =  -  LOG (F1) -  LOG (A) + N2 * L12 / A
260  L21 = N2 * X / (N2 - N1 * X)
270  IF CV$ = "FINISH" THEN A1 = L12
280  REM  - CALCULATE L12 FROM L21
290  B = N2 + L21 * N1
300  Y =  -  LOG (F2) -  LOG (B) + N1 * L21 / B
310  L12 = N1 * Y / (N1 - N2 * Y)
320  SN = SN + 1
330  IF SN = 100 THEN  PRINT "THE SERIES MAY NOT BE CONVERGING"
340  IF SN = 200 THEN  GOTO 370
350  GOTO 440
360  REM  - REVERSE DATA
370  DUM = N1:N1 = N2:N2 = DUM
380  DUM = F1:F1 = F2:F2 = DUM
390  DUM = X1:X1 = X2:X2 = DUM
400  DUM$ = I1$:I1$ = I2$:I2$ = DUM$
410  G = 1 / G
420  PRINT : PRINT "DATA IS NOW REVERSED": PRINT
430  GOTO 190
440  LCAL = L12
450  IF CV$ = "FINISH" THEN C1 = L12:C2 = L21: GOTO 5100
460  IF LCAL ) L THEN L = L - ST:D$ = "POSITIVE"
470  IF LCAL ( L THEN L = L + ST:D$ = "NEGATIVE"
480  IF  ABS (L - LCAL) ( 0.00001 THEN  GOTO 590
490  IF I = 1 THEN  GOTO 560
500  IF DD$ = D$ THEN  GOTO 560
510  K = K + 1
520  IF K = 2 THEN  GOTO 550
```

(continued overleaf)

```
530 ST = ST / 10
540   GOTO 560
550 K = 0
560 I = 2
570 DD$ = D$
580   GOTO 210
590 CV$ = "FINISH": GOTO 210
600   PRINT : PRINT
610   PRINT "ION 1 IS ";I1$,"ION 2 IS ";I2$: PRINT : PRINT
620   PRINT "N1=";N1;"   F1=";F1;"   X1=";X1: PRINT " "
630   PRINT "N2=";N2;"   F2=";F2;"   X2=";X2: PRINT " ": PRINT " "
640   REM - CALCULATE AND PRINT MEAN LAMDA VALUES
650   PRINT "L12 = ";(A1 + C1) / 2;" +/- "; ABS ((A1 - C1) * 100 / (2 * A1));" %": PRINT " "
660   PRINT "L21 = ";(A2 + C2) / 2;" +/- "; ABS ((A2 - C2) * 100 / (2 * A2));" %": PRINT " "
670   PRINT "DELTA G EXCESS = ";DG;" KJ/MOL  AT 298 K  (FROM INPUT N & F VALUES)": PRINT
680 L21 = (A2 + C2) / 2:L12 = (A1 + C1) / 2
690   REM - CALCULATE DELTA G EXCESS FROM CALCULATED LAMDA VALUES
700 A = N1 + L12 * N2:B = N2 + L21 * N1
710 DG = N1 *  LOG (A) + N2 *  LOG (B)
720 DG =  - DG * 8.314 * 298 / 1000
730   PRINT "DELTA G EXCESS = ";DG;" KJ/MOL  AT 298 K (FROM CALCULATED LAMDA VALUES)": PRINT
740   PRINT "DO YOU REQUIRE ERRORS": INPUT QW$
750   PRINT QW$
760   IF QW$ = "NO" THEN  GOTO 1010
770   PRINT "INPUT STARTING % ERROR AND STEP": INPUT PE,EP
780   HOME : PRINT " F1       F2       L12      L21    % ERROR"
790 S1 = L12:S2 = L21
800   FOR J = 1 TO 6
810   PRINT "   "
820   FOR I = 1 TO 2
830 L12 = S1 * (100 + PE) / 100:L21 = S2 * (100 - PE) / 100
840 F1 =  -  LOG (N1 + (L12 * N2))
850 F1 = F1 + N2 * ((L12 / (N1 + (L12 * N2))) - (L21 / (N2 + (N1 * L21))))
860 F2 =  -  LOG (N2 + (L21 * N1))
870 F2 = F2 + N1 * ((L21 / (N2 + (N1 * L21))) - (L12 / (N1 + (N2 * L12))))
880 F1 =  EXP (F1):F2 =  EXP (F2)
890 F1 = F1 * 1E5:F2 = F2 * 1E5:L12 = L12 * 1E5:L21 = L21 * 1E5
900 F1 =  INT (F1) / 1E5:F2 =  INT (F2) / 1E5:L12 =  INT (L12) / 1E5:L21 =  INT (L21) / 1E5
910   IF I = 2 GOTO 930
920   PRINT F1; TAB( 09);F2; TAB( 18);L12; TAB( 27);L21; TAB( 37);PE: GOTO 940
930   PRINT F1; TAB( 09);F2; TAB( 18);L12; TAB( 27);L21; TAB( 37);
940 PE =  - PE: NEXT I
950 PE = PE + EP
960   NEXT J
970   HTAB 45
980   PRINT "DO YOU REQUIRE MORE ERRORS"
990   INPUT RT$
1000   IF RT$ = "YES" THEN  GOTO 770
1010  REM  - CALCULATE BINARY EQUILIBRIUM CONSTANTS
1020  PR£ 1
1030 K12 = N1 * X2 * F1 * G / (N2 * X1 * F2)
1040 K21 = 1 / K12: PRINT " "
1050   PRINT "K12=";K12,"K21=";K21,"   IF GAMMA RATIO=";GA
1060  REM   - LET GAMMA RATIOS BE UNITY
1070 G = 1: PRINT " "
1080 K12 = N1 * X2 * F1 * G / (N2 * X1 * F2)
1090 K21 = 1 / K12
1100   PRINT "K12=";K12,"K21=";K21,"   IF GAMMA RATIO=1"
1110   PRINT
1120   PRINT " ": PRINT "PRESS RETURN TO ENTER NEXT SET OF DATA"
1130   INPUT QUEST$
1140   HOME
1150   GOTO 80
```

APPENDIX IV

Computer Program No. 4


```
10  REM    - A PROGRAM TO CALCULATE TERNARY CRYSTAL PHASE COEFFICIENTS AND
20  REM   - PREDICTED SOLUTION PHASE COMPOSITIONS USING THE ELPRINCE-BABCOCK MODEL
30  HOME : PRINT "INPUT BINARY EQUILIBRIUM CONSTANTS"
40  PRINT "K21 , K32 , K31  FOR THE THREE"
50  PRINT "CONJUGATE BINARY SYSTEMS"
60  INPUT K2,K4,K5
70  K1 = 1 / K2:K3 = 1 / K4:K6 = 1 / K5
80  REM  - ESTABLISH NATURE OF IONS
90  PRINT : PRINT "INPUT ION 1 , ION 2 , ION 3"
100  INPUT I1$,I2$,I3$
110  PR£ 1
120  PRINT : PRINT "ION 1 = ";I1$;"    ION 2 = ";I2$;"    ION 3 = ";I3$
130  PRINT : PRINT : PRINT "CRYSTAL PHASE ACTIVITY COEFFICIENTS AND"
140  PRINT "SYSTEM COMPOSITIONS ARE:-": PRINT
150  PR£ 0
160  PRINT : PRINT "INPUT TERNARY CRYSTAL PHASE"
170  PRINT "COMPOSITIONS  N1 , N2"
180  PRINT : PRINT "AND ELPRINCE-BABCOCK LAMDA TERMS"
190  PRINT "L12 , L21 , L23 , L32 , L31 , L13"
200  INPUT N1,N2,L1,L2,L3,L4,L5,L6
210  REM   - CALCULATE N3 FROM N1 AND N2
220  N3 = 1 - N1 - N2
230  A = N1 + N2 * L1 + N3 * L6
240  B = N1 * L2 + N2 + N3 * L3
250  C = N1 * L5 + N2 * L4 + N3
260  REM  - CALCULATE CRYSTAL PHASE COEFFICIENTS
270  F1 = N1 / A + N2 * L2 / B + N3 * L5 / C
280  F1 = 1 -  LOG (A) - F1
290  F1 =  EXP (F1)
300  F2 = N1 * L1 / A + N2 / B + N3 * L4 / C
310  F2 = 1 -  LOG (B) - F2
320  F2 =  EXP (F2)
330  F3 = N1 * L6 / A + N2 * L3 / B + N3 / C
340  F3 = 1 -  LOG (C) - F3
350  F3 =  EXP (F3)
360  REM  - CALCULATE SOLUTION PHASE COMPOSITIONS
370  X2 = N1 * F1 / (K1 * N2 * F2)
380  X2 = X2 + N3 * F3 / (K4 * N2 * F2)
390  X2 = X2 + 1
400  X2 = 1 / X2
410  X1 = N2 * F2 / (K2 * N1 * F1)
420  X1 = X1 + N3 * F3 / (K5 * N1 * F1)
430  X1 = X1 + 1
440  X1 = 1 / X1
450  X3 = 1 - X1 - X2
460  PR£ 1
470  PRINT : PRINT : PRINT "N1 = ";N1;"   F1 = ";F1;"   X1 = ";X1
480  PRINT : PRINT "N2 = ";N2;"   F2 = ";F2;"   X2 = ";X2
490  PRINT : PRINT "N3 = ";N3;"   F3 = ";F3;"   X3 = ";X3
500  PR£ 0
510  PRINT : PRINT : PRINT "PRESS RETURN TO FEED IN MORE DATA "
520  PRINT "FOR THE SAME SYSTEM"
530  INPUT ANY$
540  HOME
550  GOTO 160
```

(i) Li/Na-X exchange (0.1 equiv. dm^{-3})

Li$_c$	Li$_s$	α	lnK$_c$	lnK$_c$ calc	f$_{Li}$	f$_{Na}$
.02	.092	0.201	-1.635	-1.646	0.513	1.000
.044	.185	0.203	-1.629	-1.677	0.529	0.999
.065	.276	0.182	-1.735	-1.703	0.542	0.997
.094	.372	0.175	-1.776	-1.734	0.557	0.995
.126	.46	0.169	-1.810	-1.766	0.574	0.991
.181	.542	0.187	-1.711	-1.814	0.597	0.984
.208	.62	0.161	-1.860	-1.835	0.608	0.980
.263	.7	0.153	-1.911	-1.876	0.627	0.971
.345	.769	0.158	-1.877	-1.940	0.656	0.952
.412	.834	0.139	-2.004	-2.000	0.681	0.931
.462	.871	0.127	-2.096	-2.053	0.701	0.909
.505	.9	0.113	-2.211	-2.108	0.722	0.885
.647	.941	0.114	-2.197	-2.366	0.804	0.762
.717	.967	0.086	-2.482	-2.550	0.852	0.672
.798	.986	0.056	-2.914	-2.823	0.910	0.546
.858	.993	0.043	-3.190	-3.072	0.949	0.444
.952	.998398	0.032	-3.481	-3.556	0.993	0.286

$\Gamma = 0.967$

3rd Order Fitting Parameters:-

A1	A2	A3	A4
-1.618	-1.463	2.758	-3.529

APPENDIX V   Binary Isotherm Data & Derived Thermodynamic Data

(ii) Li/K-X exchange (0.1 equiv. dm^{-3})

Li_c	Li_s	α	lnK_c	lnK_c calc	f_{Li}	f_K
.024	.093	0.240	-1.411	-1.360	0.323	0.998
.049	.187	0.224	-1.479	-1.510	0.373	0.992
.073	.282	0.201	-1.590	-1.618	0.413	0.986
.103	.375	0.191	-1.636	-1.712	0.450	0.978
.129	.457	0.176	-1.720	-1.763	0.471	0.972
.16	.558	0.151	-1.874	-1.791	0.482	0.969
.202	.638	0.144	-1.923	-1.787	0.481	0.969
.315	.701	0.196	-1.612	-1.662	0.439	1.002
.424	.76	0.232	-1.442	-1.582	0.416	1.031
.483	.822	0.202	-1.581	-1.624	0.426	1.011
.499	.833	0.200	-1.594	-1.650	0.432	0.998
.515	.866	0.164	-1.789	-1.682	0.439	0.982
.516	.859	0.175	-1.726	-1.684	0.439	0.981
.578	.901	0.150	-1.877	-1.881	0.479	0.880
.631	.946	0.098	-2.310	-2.141	0.531	0.752
.706	.971	0.072	-2.618	-2.661	0.631	0.531
.781	.989	0.040	-3.210	-3.353	0.752	0.317
.808	.994	0.025	-3.656	-3.640	0.798	0.252
.864	.998	0.013	-4.347	-4.291	0.888	0.146

$\Gamma = 1.017$

4th Order Fitting Parameters:-

A1	A2	A3	A4	A5
-1.178	-8.454	37.149	-54.947	21.353

APPENDIX V   Binary Isotherm Data & Derived Thermodynamic Data

(iii) K/Na-X exchange (0.1 equiv. dm^{-3})

K_c	K_s	α	$\ln K_c$	$\ln K_c$ calc	f_K	f_{Na}
.108	.056	2.041	0.744	0.798	0.338	0.997
.2	.125	1.750	0.590	0.574	0.407	0.962
.26	.2	1.405	0.371	0.370	0.477	0.918
.306	.279	1.139	0.161	0.202	0.538	0.875
.359	.348	1.049	0.079	0.008	0.612	0.821
.398	.435	0.859	-0.122	-0.128	0.666	0.780
.438	.521	0.717	-0.303	-0.258	0.718	0.739
.494	.601	0.648	-0.403	-0.419	0.783	0.685
.548	.67	0.597	-0.485	-0.550	0.834	0.640
.603	.752	0.501	-0.661	-0.658	0.873	0.601
.644	.808	0.430	-0.814	-0.725	0.895	0.577
.701	.836	0.460	-0.746	-0.804	0.919	0.547
.711	.86	0.400	-0.884	-0.817	0.922	0.542
.813	.92	0.378	-0.942	-0.961	0.954	0.486
.878	.957	0.323	-1.098	-1.097	0.974	0.433
.942	.983	0.281	-1.239	-1.308	0.992	0.357
.98763	.997498	0.200	-1.577	-1.526	1.000	0.289
.05712	.02698	2.185	0.812	0.840	0.325	1.001
.05207	.02322	2.311	0.868	0.840	0.325	1.001
.04513	.02005	2.310	0.868	0.838	0.325	1.001

$\Gamma = 1.031$

4th Order Fitting Parameters:-

A1	A2	A3	A4	A5
0.783	2.158	-22.259	34.559	-16.840

APPENDIX V   Binary Isotherm Data & Derived Thermodynamic Data

(iv) K/Na-X exchange (Two-anion system)   (0.1 equiv. dm^{-3})

K_C	K_S	α	$\ln K_C$	$\ln K_C$ calc	f_K	f_{Na}	m_X (mol dm^{-3})
.13	.051	2.780	0.763	0.771	0.336	0.988	0.01
.211	.119	1.980	0.561	0.542	0.406	0.950	0.02
.276	.195	1.573	0.320	0.320	0.480	0.900	0.03
.331	.271	1.331	0.135	0.124	0.551	0.848	0.04
.371	.351	1.091	-0.059	-0.016	0.603	0.807	0.05
.421	.431	0.960	-0.191	-0.185	0.668	0.755	0.06
.469	.509	0.852	-0.323	-0.334	0.725	0.706	0.07
.516	.592	0.735	-0.434	-0.467	0.776	0.662	0.08
.564	.677	0.617	-0.569	-0.587	0.820	0.620	0.09
.619	.756	0.524	-0.752	-0.708	0.862	0.577	0.10
.682	.808	0.510	-0.822	-0.828	0.899	0.534	0.10
.737	.858	0.464	-0.921	-0.925	0.925	0.499	0.10

For Γ values
see Table 5.1

4th Order Fitting Parameters:-

A1	A2	A3	A4	A5
0.889	0.860	-16.748	25.785	-12.449

Additional Equilibrium Points

K_C	K_S	T_N (mol dm^{-3})	m_X (mol dm^{-3})
.401	.444	0.25	0.125
.409	.467	0.5	0.25

Binary Isotherm Data & Derived Thermodynamic Data

(v) K/Na-X exchange (0.04 equiv. dm^{-3})

K_C	K_S	α	$\ln K_C$	$\ln K_C$ calc	f_K	f_{Na}
.06114	.03379	1.862	0.635	0.623	0.432	1.008
.132	.07	2.020	0.716	0.724	0.394	1.017
.192	.114	1.847	0.626	0.660	0.415	1.006
.246	.162	1.688	0.536	0.526	0.461	0.976
.293	.226	1.419	0.363	0.373	0.515	0.937
.334	.282	1.277	0.257	0.225	0.570	0.894
.371	.34	1.145	0.148	0.089	0.623	0.852
.403	.413	0.959	-0.028	-0.028	0.669	0.815
.436	.483	0.827	-0.176	-0.144	0.716	0.776
.471	.545	0.743	-0.284	-0.258	0.762	0.737
.516	.625	0.640	-0.434	-0.389	0.814	0.691
.589	.708	0.591	-0.513	-0.558	0.878	0.629
.742	.862	0.460	-0.763	-0.766	0.943	0.549
.811	.912	0.414	-0.869	-0.842	0.960	0.517
.87	.943	0.405	-0.892	-0.938	0.974	0.477
.901	.963	0.350	-1.038	-1.012	0.982	0.447
.665	.799	0.499	-0.681	-0.680	0.920	0.583

$\Gamma = 1.013$

4th Order Fitting Parameters:-

A1	A2	A3	A4	A5
0.318	7.002	-35.946	49.962	-22.763

APPENDIX V   Binary Isotherm Data & Derived Thermodynamic Data

(vi) Ag/Na-X exchange (0.04 equiv. dm^{-3})

Ag_c	Ag_s	α	lnK_c	lnK_c calc	f_{Ag}	f_{Na}
.9729	.571	26.972	3.312	3.399	0.999	0.126
.951	.364	33.911	3.541	3.472	0.996	0.135
.909	.203	39.218	3.686	3.594	0.987	0.151
.868	.143	39.409	3.691	3.694	0.977	0.165
.817	.097	41.561	3.744	3.800	0.960	0.181
.730	.055	48.649	3.901	3.946	0.930	0.202
.645	.031	56.793	4.056	4.140	0.876	0.231
.545	.012	98.619	4.608	4.437	0.776	0.276
.449	.006	134.999	4.922	4.880	0.620	0.343
.34	.00213	241.340	5.503	5.659	0.385	0.465
.231	.000312	962.488	6.886	6.828	0.169	0.647

$\Gamma = 1.017$

3rd Order Fitting Parameters:-

A1	A2	A3	A4
11.044	-24.383	29.513	-12.877

- 352 -

(vii) Ag/K-X exchange (0.04 equiv. dm^{-3})

Ag_c	Ag_s	α	lnK_c	lnK_c calc	f_{Ag}	f_K
.977	.585	30.134	3.410	3.383	1.000	0.151
.957	.407	32.427	3.483	3.418	0.998	0.157
.917	.247	33.681	3.521	3.496	0.993	0.169
.881	.174	35.145	3.563	3.578	0.985	0.181
.838	.12	37.934	3.640	3.688	0.970	0.199
.782	.066	50.764	3.931	3.852	0.940	0.228
.683	.035	59.405	4.088	4.198	0.857	0.293
.603	.016	93.412	4.541	4.527	0.761	0.362
.492	.005635	170.904	5.145	5.053	0.600	0.483
.369	.002040	286.103	5.660	5.724	0.409	0.644
.249	.000512	646.863	6.476	6.462	0.245	0.808
.99557	.889	28.058	3.338	3.354	1.000	0.147
.98841	.759	27.076	3.303	3.365	1.000	0.149

$\Gamma = 1.004$

3rd Order Fitting Parameters:-

A1	A2	A3	A4
8.222	-7.635	2.104	0.657

APPENDIX VI

(I)   Ternary Isotherm Data

(i) Na/K/Li (0.1 equiv. dm^{-3}) system

Na_c	K_c	Na_s	K_s	K_{m1}	K_{m2}	K_{m3}
.938	.052	.928	.025	2.309	20.117	0.022
.86	.122	.855	.052	2.228	28.274	0.016
.799	.172	.771	.087	2.660	18.468	0.020
.749	.215	.694	.118	3.338	16.064	0.019
.699	.253	.615	.156	3.800	11.040	0.024
.648	.291	.532	.189	4.407	8.902	0.025
.598	.334	.45	.227	5.701	7.738	0.023
.552	.365	.373	.263	6.921	5.708	0.025
.504	.404	.304	.293	8.732	5.023	0.023
.45	.447	.226	.321	12.522	4.283	0.019
.063	.924	.034	.92	12.096	1.926	0.043
.142	.835	.062	.845	21.464	1.724	0.027
.212	.757	.091	.77	24.754	1.860	0.022
.264	.694	.125	.685	19.917	2.199	0.023
.308	.638	.163	.601	14.699	2.606	0.026
.363	.576	.194	.522	14.772	3.030	0.022
.395	.531	.229	.43	11.102	4.074	0.022
.433	.483	.271	.357	8.356	5.073	0.024
.476	.433	.308	.276	6.960	7.280	0.020
.518	.382	.344	.201	5.429	10.914	0.017
.157	.092	.0154	.0075	11.024	19.203	4.7E-3
.227	.173	.04	.026	7.535	12.144	0.011
.28	.238	.07	.051	6.253	9.929	0.016
.355	.299	.105	.086	7.687	8.359	0.016
.389	.328	.136	.115	7.592	7.527	0.017
.417	.357	.18	.152	6.754	7.038	0.021
.442	.374	.222	.196	6.571	5.785	0.026
.461	.391	.267	.24	6.095	5.121	0.032
.475	.415	.293	.285	6.924	5.018	0.029
.492	.427	.349	.336	6.082	4.455	0.037
.304	.089	.058	.01	4.739	23.203	9.1E-3
.414	.086	.116	.012	3.100	25.098	0.013
.532	.074	.177	.013	3.263	22.163	0.014
.35	.158	.092	.029	4.746	13.940	0.015
.462	.15	.155	.032	3.971	15.447	0.016
.54	.157	.215	.034	3.386	21.042	0.014
.609	.151	.29	.037	3.030	22.240	0.015
.477	.23	.19	.06	4.209	14.982	0.016
.566	.183	.26	.045	3.227	21.035	0.015
.126	.234	.021	.05	11.166	5.299	0.017
.122	.327	.023	.113	15.246	2.476	0.026
.176	.448	.036	.199	21.601	2.109	0.022

(continued overleaf)

(i) Na/K/Li (0.1 equiv. dm^{-3}) system   (continued)

Na$_c$	K$_c$	Na$_s$	K$_s$	K$_{m1}$	K$_{m2}$	K$_{m3}$
.051	.074	.003	.006	26.539	10.134	3.7E-3
.048	.192	.004	.02	19.263	9.863	5.3E-3
.05	.578	.007	.283	47.678	1.115	0.019
.049	.657	.007	.343	56.558	1.159	0.015
.656	.123	.129	.041	32.374	6.647	4.6E-3
.61	.102	.192	.024	6.465	15.477	0.001
.648	.077	.221	.02	6.163	13.952	0.012
.685	.066	.247	.016	5.519	18.160	0.001
.75	.066	.396	.018	3.116	22.608	0.014
.797	.064	.486	.019	2.843	24.639	0.014
.83	.063	.567	.021	2.750	23.673	0.015
.859	.061	.663	.022	2.384	23.364	0.018
.89	.06	.75	.022	2.354	28.582	0.015
.914	.056	.838	.023	2.264	25.183	0.018
.803	.135	.678	.048	2.204	29.516	0.015
.698	.207	.509	.075	2.984	24.325	0.014
.608	.246	.348	.104	4.844	12.020	0.017
.482	.31	.204	.13	7.496	7.706	0.017
.734	.237	.702	.159	3.515	10.185	0.028
.674	.295	.629	.234	4.025	6.555	0.038
.619	.35	.553	.311	4.884	4.964	0.041
.566	.403	.475	.389	6.013	3.952	0.042
.517	.45	.395	.47	7.320	2.865	0.048
.468	.496	.317	.549	8.980	2.058	0.054
.397	.471	.174	.359	14.038	2.669	0.027
.346	.511	.131	.395	17.874	2.100	0.027
.228	.602	.074	.436	19.817	1.783	0.028
.183	.614	.041	.459	36.682	0.987	0.028
.025	.458	.003	.198	46.397	0.992	0.022
.048	.442	.006	.193	43.891	1.030	0.022
.071	.46	.009	.195	44.776	1.197	0.019
.096	.452	.013	.192	40.742	1.320	0.019
.117	.428	.016	.197	42.571	1.116	0.021
.018	.877	.004	.703	45.296	0.965	0.023
.032	.874	.009	.694	31.717	1.409	0.022
.047	.848	.013	.694	29.850	1.152	0.029
.079	.818	.023	.682	28.172	1.200	0.030

$\Gamma_3 / \Gamma_1 = 0.904$

$\Gamma_3 / \Gamma_2 = 0.825$

APPENDIX VI

(I) Ternary Isotherm Data

(ii) Na/K/Li (0.04 equiv. dm^{-3}) system; 6-day exchange

Na_c	K_c	Na_s	K_s	K_{m1}	K_{m2}	K_{m3}
.957	.033	.948	.014	1.643	20.915	0.029
.921	.062	.886	.038	2.961	11.449	0.029
.878	.099	.842	.04	2.254	30.139	0.015
.825	.145	.78	.061	2.494	28.313	0.014
.787	.174	.727	.078	2.627	22.985	0.017
.75	.202	.659	.1	3.219	18.001	0.017
.709	.235	.602	.123	3.565	15.220	0.018
.668	.267	.546	.139	3.776	14.615	0.018
.631	.296	.483	.163	4.558	12.241	0.018
.59	.324	.421	.187	5.167	9.764	0.020
.05871	.93108	.02014	.93857	34.642	1.365	0.021
.09179	.88946	.0399	.8769	23.152	1.985	0.022
.135	.84	.059	.831	22.790	1.965	0.022
.182	.782	.076	.758	25.632	2.049	0.019
.227	.729	.096	.695	25.320	2.210	0.018
.26	.688	.106	.645	27.009	2.221	0.017
.299	.639	.132	.585	21.441	2.404	0.019
.334	.598	.158	.513	18.547	3.110	0.017
.361	.567	.184	.447	15.552	4.202	0.015
.381	.53	.212	.377	10.610	5.078	0.019
.111	.037	.0074	.0025	17.361	17.431	3.3E-3
.157	.081	.0171	.0063	8.403	23.075	5.2E-3
.203	.126	.0272	.0136	8.594	16.441	7.1E-3
.243	.166	.0441	.0237	6.837	14.043	0.010
.279	.202	.06	.0365	6.801	11.466	0.013
.315	.24	.077	.055	7.481	9.079	0.015
.359	.279	.099	.074	7.968	8.955	0.014
.392	.31	.124	.098	8.248	8.264	0.015
.418	.341	.151	.123	8.327	8.364	0.014
.438	.351	.184	.157	7.916	6.558	0.019

$$\Gamma_3 / \Gamma_1 = 0.961$$

$$\Gamma_3 / \Gamma_2 = 0.924$$

APPENDIX VI

(I) Ternary Isotherm Data

(iii) Na/K/Li (0.04 equiv. dm^{-3}) system; long-term exchange

Na_c	K_c	Na_s	K_s	K_{m1}	K_{m2}	K_{m3}
.9565	.0347	.95157	.01185	1.434	35.460	0.020
.9168	.0686	.9075	.0235	1.652	39.864	0.015
.8926	.087	.851	.037	2.569	28.940	0.013
.829	.144	.792	.057	2.425	34.100	0.012
.787	.179	.745	.073	2.436	30.467	0.013
.749	.21	.686	.094	2.863	24.528	0.014
.709	.242	.626	.112	3.174	22.041	0.014
.673	.269	.567	.134	3.618	17.503	0.016
.633	.298	.515	.148	3.664	16.110	0.017
.593	.325	.45	.18	4.340	11.163	0.021
.06508	.92268	.0241	.9385	22.664	1.094	0.040
.1002	.8809	.059	.867	11.115	2.380	0.038
.1545	.8192	.075	.818	17.239	1.981	0.029
.195	.77	.087	.756	22.125	2.076	0.022
.242	.713	.108	.691	21.735	2.122	0.022
.274	.669	.117	.644	22.137	1.932	0.023
.313	.621	.14	.592	19.349	1.998	0.026
.36	.57	.169	.527	18.220	2.385	0.023
.38	.543	.199	.451	13.766	3.451	0.021
.409	.506	.227	.385	11.275	.4.376	0.020
.206	.038	.023	.00335	9.108	18.502	5.9E-3
.25	.079	.0333	.00714	7.285	23.319	5.9E-3
.302	.131	.0451	.0132	7.504	24.428	5.9E-3
.331	.175	.077	.027	5.171	17.725	0.011
.366	.211	.097	.04	5.506	15.045	0.012
.397	.243	.116	.057	6.312	12.199	0.013
.426	.277	.145	.077	6.285	11.539	0.014
.449	.307	.181	.101	5.957	10.960	0.015
.468	.331	.206	.118	6.188	11.648	0.014
.487	.352	.235	.149	6.955	10.304	0.014

$$\Gamma_3/\Gamma_1 = 0.961$$

$$\Gamma_3/\Gamma_2 = 0.924$$

APPENDIX VI

(I) Ternary Isotherm Data

(iv) Na/K/Ag (0.04 equiv. dm^{-3}) system

Na_c	K_c	Na_s	K_s	K_{m1}	K_{m2}	K_{m3}
.59	.151	.90315	.09636	5.2E-4	0.007	2.7E5
.509	.163	.86621	.13232	0.001	0.012	68312
.436	.169	.83046	.16708	1.7E-3	0.012	48353
.371	.176	.79024	.20585	0.002	0.013	33578
.312	.182	.74498	.24865	0.003	0.016	20630
.261	.185	.696	.292	0.005	0.023	8971
.117	.622	.1152	.88382	0.005	0.002	99233
.119	.557	.15957	.83896	0.004	0.003	98251
.121	.492	.20985	.78719	0.004	0.005	47561
.124	.423	.26140	.73369	0.004	0.008	31200
.119	.362	.3162	.67604	0.004	0.011	22197
.115	.313	.365	.62	0.005	0.021	9142
.11	.269	.415	.567	0.004	0.025	9465
.013	.043	.125	.498	0.050	0.029	698
.046	.082	.439	.445	0.008	0.043	2927
.462	.245	.73218	.26683	0.001	0.004	1.5E5
.029	.014	.504	.119	0.011	0.095	952
.047	.071	.477	.388	0.008	0.052	2367
.238	.472	.33151	.66153	0.017	0.017	3391
.291	.466	.37349	.62554	0.003	0.003	1.1E5
.071	.142	.459	.52	0.002	0.013	33249
.16	.481	.28355	.71401	0.003	0.005	56575
.457	.197	.78342	.2151	0.002	0.006	1.0E5
.00431	.00341	.115	.113	0.036	0.019	1461
.0128	.00573	.334	.106	0.015	0.043	1483
.01132	.0119	.225	.206	0.025	0.039	1014
.00983	.01834	.114	.302	0.074	0.026	.529
.02405	.01319	.494	.155	0.010	0.054	1816
.01741	.02272	.328	.291	0.014	0.046	1532
.01134	.03138	.168	.439	0.026	0.031	1230
.04596	.0242	.642	.192	0.007	0.040	3477
.02986	.04247	.433	.359	0.009	0.045	2438
.01942	.06453	.225	.557	0.015	0.037	1766

$$\Gamma_3/\Gamma_1 = 1.052$$

$$\Gamma_3/\Gamma_2 = 1.012$$

APPENDIX VI

(I) Ternary Isotherm Data

(v) Na/K/Li (Variable Solution Concentration) system

Na$_c$	K$_c$	Na$_s$	K$_s$	T$_N$	K$_{m1}$	K$_{m2}$	K$_{m3}$
.645	.295	.549	.209	0.25	3.944	6.840	0.037
.631	.302	.517	.233	0.5	4.288	5.136	0.045
.614	.305	.515	.237	0.75	3.382	4.253	0.070
.61	.308	.515	.237	1.0	3.265	4.312	0.071
.607	.308	.512	.241	1.5	3.196	4.003	0.078
.609	.308	.511	.244	2.0	3.321	3.947	0.076
.353	.588	.208	.552	0.25	10.999	2.720	0.033
.369	.572	.231	.521	0.5	9.769	3.172	0.032
.383	.557	.235	.518	0.75	10.169	2.921	0.034
.378	.547	.241	.509	1.0	7.631	2.454	0.053
.381	.542	.252	.501	1.5	6.778	2.483	0.059
.386	.536	.249	.502	2.0	7.185	2.348	0.059
.414	.372	.201	.19	0.25	6.166	5.296	0.031
.424	.369	.224	.218	0.5	5.706	4.080	0.043
.426	.368	.228	.226	0.75	5.682	3.761	0.047
.426	.368	.24	.23	1.0	5.066	3.711	0.053
.426	.368	.241	.234	1.5	5.063	3.566	0.055

(vi) Na/K/Li (NO$_3$/SO$_4$/Fe[CN]$_6$) system

Na$_c$	K$_c$	Na$_s$	K$_s$	T$_N$	K$_{m1}$	K$_{m2}$	K$_{m3}$
.79	.171	.711	.08	0.04	3.095	22.036	0.015
.703	.254	.613	.152	0.1	4.301	13.307	0.017
.233	.725	.094	.693	0.04	29.784	2.239	0.015
.325	.629	.16	.6	0.1	20.534	2.823	0.017
.267	.203	.055	.038	0.04	7.549	10.060	0.013
.391	.331	.131	.12	0.1	8.702	6.868	0.017

APPENDIX VI

(II) Thermodynamic Data

(i) Na/K/Li (0.1 equiv. dm^{-3}) system

Orders of Fitting:- 4 for K_{c3}/K_{c1}, 5 for K_{c3}/K_{c2}

$-Ln(K_{c3}/K_{c1})$		$-Ln(K_{c3}/K_{c2})$		Crystal Phase Coeffs.		
Real	Calc	Real	Calc	ϕ_{Na}	ϕ_K	ϕ_{Li}
4.775	4.779	7.032	7.143	1.100	0.458	0.547
5.045	4.930	7.678	7.793	1.228	0.433	0.642
4.973	5.021	7.003	7.411	1.280	0.528	0.689
5.288	5.075	6.951	6.861	1.285	0.649	0.705
5.172	5.147	6.331	6.346	1.258	0.772	0.707
5.253	5.227	6.048	5.898	1.206	0.883	0.696
5.628	5.319	6.026	5.480	1.130	0.980	0.672
5.712	5.427	5.611	5.297	1.063	1.017	0.656
6.049	5.565	5.588	5.094	0.980	1.050	0.633
6.610	5.758	5.629	4.929	0.890	1.074	0.613
5.742	5.860	3.997	3.381	0.771	1.613	0.550
6.778	6.659	4.348	3.711	0.704	1.722	0.655
7.139	6.820	4.643	4.126	0.666	1.498	0.654
6.872	6.739	4.760	4.343	0.656	1.334	0.626
6.434	6.561	4.796	4.451	0.669	1.237	0.602
6.595	6.274	5.102	4.545	0.714	1.163	0.584
6.320	6.081	5.409	4.617	0.762	1.137	0.585
5.971	5.870	5.564	4.745	0.832	1.108	0.595
5.966	5.670	6.103	4.947	0.922	1.074	0.617
5.874	5.514	6.664	5.262	1.022	1.018	0.649
7.856	7.718	8.503	7.695	0.740	0.683	0.980
6.636	6.884	7.206	7.789	0.936	0.633	0.938
6.062	6.396	6.616	7.327	1.021	0.685	0.870
6.303	5.979	6.479	6.712	1.053	0.755	0.781
6.173	5.844	6.256	6.327	1.042	0.812	0.739
5.872	5.757	6.005	5.920	1.017	0.882	0.700
5.621	5.694	5.586	5.657	1.003	0.930	0.676
5.349	5.657	5.267	5.406	0.984	0.980	0.655
5.584	5.647	5.354	5.111	0.950	1.040	0.631
5.205	5.623	4.986	4.932	0.937	1.081	0.617
6.357	6.885	8.037	8.442	0.917	0.500	0.920
5.586	6.518	7.769	8.541	0.990	0.462	0.878
5.564	6.286	7.572	8.021	1.019	0.523	0.837
5.850	6.383	7.019	8.436	1.056	0.488	0.896
5.596	6.085	7.046	8.350	1.118	0.481	0.859
5.586	5.871	7.505	7.960	1.162	0.530	0.831
5.420	5.734	7.505	7.692	1.181	0.563	0.807
5.682	5.763	7.044	7.465	1.173	0.609	0.809
5.490	5.708	7.456	7.610	1.198	0.582	0.811
6.594	7.395	5.940	6.668	0.784	0.914	0.932
6.456	7.283	4.730	5.381	0.722	1.247	0.827

(continued overleaf)

(i) Na/K/Li (0.1 equiv. dm^{-3}) system   (continued)

| $-Ln(K_{c3}/K_{c1})$ | | $-Ln(K_{c3}/K_{c2})$ | | Crystal Phase Coeffs. | | |
Real	Calc	Real	Calc	ϕ_{Na}	ϕ_{K}	ϕ_{Li}
6.992	6.948	4.758	4.214	0.670	1.526	0.686
8.974	8.787	8.103	8.062	0.534	0.623	1.009
8.306	8.288	7.728	7.769	0.617	0.671	0.987
7.938	8.338	4.274	4.141	0.405	1.503	0.659
8.319	8.430	4.523	4.218	0.398	1.483	0.668
8.949	5.738	7.458	7.667	1.156	0.556	0.791
6.572	5.960	7.538	7.814	1.101	0.544	0.812
6.374	5.989	7.283	7.571	1.065	0.575	0.792
6.416	5.941	7.699	7.398	1.055	0.594	0.772
5.492	5.722	7.566	7.398	1.076	0.564	0.733
5.395	5.540	7.646	7.453	1.088	0.526	0.697
5.288	5.388	7.533	7.505	1.096	0.496	0.667
4.989	5.244	7.364	7.516	1.101	0.472	0.639
5.166	5.064	7.754	7.488	1.107	0.452	0.605
4.961	4.929	7.462	7.359	1.104	0.449	0.577
5.066	5.160	7.753	7.667	1.231	0.489	0.695
5.478	5.276	7.669	6.947	1.263	0.662	0.741
5.743	5.414	6.743	6.659	1.226	0.741	0.753
6.171	6.605	6.291	6.335	1.117	0.802	0.731
4.936	5.068	6.092	6.563	1.279	0.711	0.700
4.766	5.150	5.346	5.785	1.212	0.898	0.681
4.875	5.265	4.983	5.193	1.112	1.043	0.650
5.062	5.421	4.735	4.811	1.003	1.126	0.618
5.134	5.601	4.288	4.633	0.910	1.151	0.595
5.212	5.807	3.831	4.568	0.829	1.148	0.581
6.366	5.949	4.798	8.878	0.831	1.087	0.610
6.609	6.200	4.560	4.661	0.756	1.156	0.603
6.652	6.919	4.336	4.011	0.610	1.473	0.619
7.293	7.218	3.770	3.762	0.564	1.634	0.632
7.767	8.381	4.014	5.091	0.430	1.178	0.710
7.693	8.087	4.033	4.714	0.481	1.356	0.720
7.884	7.872	4.354	4.260	0.504	1.539	0.703
7.793	7.611	4.455	4.121	0.551	1.614	0.704
7.713	7.381	4.164	4.247	0.608	1.581	0.719
7.692	7.304	3.935	4.743	0.549	1.181	0.633
7.358	7.185	4.336	4.403	0.574	1.329	0.636
7.035	7.399	3.872	4.246	0.557	1.458	0.663
6.959	7.413	3.895	3.934	0.567	1.655	0.678

Fitting Parameters for Kc3/Kc1 :-

A1	A2	A3	A4	A5	A6	A7
-9.787	13.010	5.094	-20.599	4.605	14.105	-38.727

A8	A9
-1.272	34.431

Fitting Parameters for Kc3/Kc2 :-

A1	A2	A3	A4	A5	A6
-7.902	36.778	-33.546	-241.344	210.523	606.911

A7	A8	A9	A10	A11
-404.447	-647.107	311.211	247.747	-79.450

APPENDIX VI

(II) Thermodynamic Data

(ii) Na/K/Li (0.04 equiv. dm^{-3}) system; 6-day exchange

Orders of Fitting:- 4 for K_{c3}/K_{c1}, 1 for K_{c3}/K_{c2}

$-Ln(K_{c3}/K_{c1})$		$-Ln(K_{c3}/K_{c2})$		Crystal Phase Coeffs.		
Real	Calc	Real	Calc	ϕ_{Na}	ϕ_{K}	ϕ_{Li}
4.073	4.529	6.656	7.138	1.139	0.439	0.523
4.649	4.576	6.040	7.053	1.225	0.493	0.572
5.071	4.650	7.703	6.938	1.286	0.551	0.616
5.211	4.795	7.680	6.795	1.290	0.609	0.649
5.106	4.922	7.314	6.714	1.261	0.638	0.661
5.269	5.053	7.029	6.637	1.217	0.660	0.667
5.305	5.214	6.795	6.541	1.152	0.681	0.666
5.380	5.384	6.772	6.450	1.082	0.697	0.662
5.578	5.547	6.605	6.367	1.016	0.710	0.656
5.603	5.717	6.279	6.299	0.952	0.721	0.651
7.442	7.280	4.247	4.031	0.379	1.029	0.436
7.010	7.222	4.592	4.194	0.410	1.033	0.462
6.968	7.150	4.556	4.379	0.444	1.028	0.489
7.245	7.158	4.759	4.604	0.469	1.009	0.518
7.296	7.143	4.897	4.805	0.490	0.983	0.539
7.430	7.136	4.971	4.964	0.505	0.958	0.554
7.048	7.098	4.899	5.156	0.527	0.926	0.571
7.015	7.014	5.268	5.311	0.553	0.897	0.583
6.964	6.927	5.695	5.427	0.578	0.875	0.591
6.389	6.864	5.691	5.593	0.604	0.848	0.605
8.607	8.926	8.650	8.986	0.485	0.437	0.966
7.436	7.959	8.485	8.635	0.647	0.475	0.934
7.142	7.251	7.830	8.278	0.785	0.512	0.895
6.527	6.819	7.286	7.963	0.868	0.545	0.857
6.314	6.551	6.875	7.679	0.910	0.574	0.822
6.271	6.385	6.503	7.384	0.920	0.606	0.785
6.383	6.250	6.539	7.065	0.912	0.639	0.745
6.372	6.208	6.413	6.816	0.889	0.667	0.716
6.403	6.227	6.446	6.583	0.852	0.696	0.690
6.058	6.189	5.909	6.482	0.847	0.706	0.678

Fitting Parameters for Kc3/Kc1 :-

A1	A2	A3	A4	A5	A6	A7
-11.247	18.865	14.367	-16.584	-69.609	-8.254	101.222

A8	A9
12.738	-42.336

Fitting Parameters for Kc3/Kc2 :-

A1	A2	A3
-9.441	2.211	5.672

APPENDIX VI

(II) Thermodynamic Data

(iii) Na/K/Li (0.04 equiv. dm^{-3}) system; long-term exchange

Orders of Fitting:- 3 for K_{c3}/K_{c1}, 1 for K_{c3}/K_{c2}

$-Ln(K_{c3}/K_{c1})$		$-Ln(K_{c3}/K_{c2})$		Crystal Phase Coeffs.		
Real	Calc	Real	Calc	ϕ_{Na}	ϕ_{K}	ϕ_{Li}
4.330	4.764	7.576	7.804	1.062	0.347	0.523
4.730	4.845	7.952	7.660	1.102	0.388	0.558
5.292	4.903	7.753	7.586	1.115	0.410	0.575
5.341	5.043	8.024	7.337	1.122	0.470	0.607
5.238	5.149	7.803	7.190	1.105	0.504	0.619
5.344	5.248	7.531	7.061	1.080	0.531	0.626
5.443	5.358	7.420	6.929	1.045	0.557	0.628
5.474	5.459	7.090	6.822	1.011	0.577	0.628
5.417	5.575	6.936	6.709	0.971	0.598	0.627
5.388	5.696	6.372	6.609	0.930	0.617	0.625
6.371	5.983	3.379	3.748	0.537	1.019	0.398
5.724	6.283	4.221	3.951	0.518	1.014	0.423
6.418	6.557	4.293	4.247	0.515	0.992	0.457
6.964	6.716	4.637	4.488	0.510	0.965	0.482
6.950	6.798	4.663	4.767	0.523	0.926	0.508
6.893	6.834	4.493	4.990	0.537	0.893	0.528
6.658	6.777	4.426	5.226	0.567	0.854	0.546
6.714	6.630	4.720	5.466	0.612	0.812	0.562
6.523	6.567	5.178	5.603	0.636	0.790	0.572
6.361	6.455	5.454	5.786	0.675	0.759	0.585
7.376	7.996	8.124	9.148	0.620	0.380	0.898
7.161	7.369	8.363	8.805	0.733	0.409	0.861
7.267	6.801	8.486	8.379	0.840	0.446	0.816
6.201	6.559	7.472	8.044	0.877	0.481	0.786
6.163	6.345	7.207	7.751	0.903	0.509	0.755
6.226	6.204	6.924	7.490	0.913	0.535	0.727
6.162	6.113	6.809	7.220	0.906	0.563	0.702
6.004	6.066	6.652	6.986	0.891	0.590	0.678
6.140	6.036	6.812	6.798	0.876	0.611	0.660
6.252	6.009	6.683	6.629	0.861	0.630	0.643

Fitting Parameters for Kc3/Kcl :-

A1	A2	A3	A4	A5	A6	A7
-11.686	22.794	6.293	-31.849	-24.284	16.076	24.464

Fitting Parameters for Kc3/Kc2 :-

A1	A2	A3
-9.765	1.818	6.393

APPENDIX VI

(II)   Thermodynamic Data

(iv) Na/K/Ag (0.04 equiv. dm^{-3}) system

Orders of Fitting:- 3 for K_{c3}/K_{c1}, 2 for K_{c3}/K_{c2}

Ln(K_{c3}/K_{c1})		Ln(K_{c3}/K_{c2})		Crystal Phase Coeffs.		
Real	Calc	Real	Calc	ϕ_{Na}	ϕ_{K}	ϕ_{Ag}
20.132	19.358	17.468	17.536	1.103	0.887	0.503
17.858	18.032	15.599	16.341	0.921	0.773	0.652
17.214	17.132	15.207	15.343	0.791	0.643	0.757
16.581	16.551	14.745	14.563	0.708	0.538	0.822
15.790	16.138	14.075	13.928	0.648	0.458	0.863
14.490	15.824	12.877	13.420	0.602	0.398	0.890
16.758	17.228	17.820	17.611	0.471	0.790	0.437
17.119	16.095	17.429	16.607	0.395	0.691	0.533
16.326	15.503	16.045	15.678	0.382	0.597	0.629
15.865	15.287	15.241	14.780	0.409	0.509	0.723
15.591	15.240	14.494	14.002	0.444	0.433	0.798
14.438	15.238	12.985	13.425	0.472	0.381	0.850
14.657	15.189	12.871	12.935	0.486	0.338	0.889
9.594	11.829	10.113	10.570	0.178	0.173	0.998
12.869	13.044	11.137	10.986	0.265	0.197	0.990
18.502	17.833	17.338	16.378	0.910	0.827	0.689
11.411	11.135	9.226	10.483	0.141	0.168	0.998
12.633	12.823	10.737	10.919	0.246	0.193	0.992
12.234	16.126	12.214	16.366	0.470	0.752	0.629
17.376	16.435	17.472	16.814	0.513	0.859	0.619
16.521	14.191	14.777	11.561	0.380	0.234	0.970
16.731	15.696	16.161	15.815	0.412	0.633	0.637
18.030	17.580	16.638	15.870	0.872	0.728	0.719
10.655	10.540	11.267	10.307	0.116	0.159	1.000
11.519	10.706	10.448	10.359	0.123	0.161	1.000
10.640	10.895	10.187	10.385	0.131	0.163	1.000
8.930	11.085	9.943	10.413	0.139	0.164	1.000
12.145	11.062	10.430	10.454	0.138	0.166	0.999
11.630	11.296	10.434	10.474	0.149	0.167	0.999
10.808	11.491	10.597	10.494	0.159	0.169	0.999
13.130	11.606	11.394	10.629	0.165	0.176	0.996
12.558	11.978	10.900	10.650	0.187	0.177	0.997
11.706	12.423	10.785	10.734	0.217	0.182	0.995

Fitting Parameters for Kc3/Kc1 :-

A1	A2	A3	A4	A5	A6	A7
10.377	10.582	34.889	-21.761	-103.192	34.335	100.056

Fitting Parameters for Kc3/Kc2 :-

A1	A2	A3	A4	A5
10.2699	4.490	5.221	10.419	8.856

APPENDIX VI

(II) Thermodynamic Data

(iv) Na/K/Ag (0.04 equiv. dm^{-3}) system

Orders of Fitting:- 4 for K_{c3}/K_{c1}, 4 for K_{c3}/K_{c2}

Ln(K_{c3}/K_{c1})		Ln(K_{c3}/K_{c2})		Crystal Phase Coeffs.		
Real	Calc	Real	Calc	ϕ_{Na}	ϕ_{K}	ϕ_{Ag}
20.132	19.893	17.468	17.096	1.865	0.707	0.454
17.858	18.175	15.599	16.936	1.461	0.930	0.630
17.213	16.954	15.207	15.609	1.184	0.728	0.768
16.582	16.235	14.745	14.315	1.030	0.523	0.848
15.790	15.854	14.076	13.400	0.949	0.403	0.887
14.490	15.674	12.877	12.913	0.909	0.349	0.903
16.758	17.157	17.820	18.030	0.701	0.903	0.425
17.119	16.242	17.429	16.868	0.649	0.770	0.533
16.326	15.681	16.065	15.839	0.644	0.654	0.638
15.865	15.422	15.241	14.907	0.681	0.552	0.736
15.591	15.348	14.494	14.217	0.728	0.481	0.806
14.438	15.354	12.985	13.743	0.771	0.434	0.851
14.656	15.344	12.872	13.363	0.798	0.397	0.884
9.594	11.689	10.113	10.625	0.266	0.179	0.996
12.869	13.261	11.137	11.549	0.442	0.241	0.981
18.502	17.611	17.338	16.730	1.334	0.957	0.694
11.410	11.137	9.226	10.583	0.221	0.177	0.996
12.633	13.053	10.737	11.455	0.414	0.234	0.984
12.234	15.939	12.214	15.617	0.720	0.623	0.655
17.376	16.068	17.472	15.925	0.751	0.690	0.654
16.521	14.483	14.776	12.270	0.648	0.298	0.956
16.731	15.799	16.161	15.652	0.682	0.625	0.650
18.030	17.421	16.638	16.262	1.303	0.852	0.722
10.655	10.189	11.267	9.947	0.162	0.144	1.000
11.519	10.486	10.448	10.174	0.178	0.155	0.999
10.640	10.674	10.187	10.221	0.190	0.157	0.999
8.930	10.859	9.943	10.269	0.202	0.160	0.999
12.145	11.006	10.430	10.490	0.212	0.172	0.997
11.630	11.183	10.434	10.483	0.225	0.171	0.998
10.809	11.313	10.597	10.458	0.235	0.170	0.997
13.130	11.788	11.394	10.938	0.273	0.198	0.992
12.558	12.041	10.900	10.932	0.298	0.198	0.993
11.706	12.379	10.785	10.981	0.333	0.201	0.991

Fitting Parameters for Kc3/Kc1 :-

A1	A2	A3	A4	A5	A6	A7
9.945	26.908	38.562	-129.547	-139.730	267.586	196.293

A8	A9
-157.302	-78.334

Fitting Parameters for Kc3/Kc2 :-

A1	A2	A3	A4	A5	A6
9.792	26.488	13.460	-206.016	-33.318	616.453

A7	A8	A9
71.770	-534.082	-37.954